Characterisation of a Novel Caspase STRICA and the Bcl-2 Homologues BUFFY and DEBCL in *Drosophila melanogaster*

by

Joanna Doumanis, B.Sc (Hons)

Enrolled through the Department of Medicine,
Faculty of Health Science, The University of Adelaide

Research conducted at the Institute of Medical and Veterinary Science,
Department of Haematology, Hanson Institute, Adelaide

**A thesis submitted for the degree of Doctor of Philosophy,
in the Faculty of Health Science, The University of Adelaide**

July 2004

Abstract

Apoptosis, or Programmed Cell Death (PCD) is characterised by a number of morphological features including chromatin condensation, nuclear envelope breakdown, cytoplasmic shrinkage and plasma membrane blebbing. Cells are specified to die in order to remove excess, unwanted, or harmful cells, and to delete cells once their function has been fulfilled. Dysfunction of the apoptotic pathway can have disastrous effects on the viability of the organism as a whole. Too little cell death can result in cancer, whereas too much apoptosis is the cause of some neurodegenerative diseases. In addition to maintaining optimal cell numbers in the adult organism, apoptosis is critical during development where it plays a role in organ sculpting and immunity.

Apoptosis is mediated by a family of caspases (**c**ysteinyl **asp**artate-specific protein**ases**) that cleave their substrates following an aspartate residue. Once caspases are activated, the cell is committed to die, cellular substrates are cleaved and the morphological features characterising apoptosis are observed. Caspases are present in healthy cells as inactive zymogens containing a large and small active subunit, and an N-terminal prodomain. Caspases often require proteolytic cleavage at precise residues for activation. Mature caspases are dimers comprised of two large and two small subunits. Caspases are commonly categorised into two main groups. Class I, upstream or initiator caspases have long prodomains containing protein-protein interaction domains including caspase-recruitment domains (CARDs) or death effector domains (DEDs). Recruitment of adaptor molecules brings several procaspase molecules together to facilitate proximity-induced activation. Class II, downstream or effector caspases have very short prodomains or lack a prodomain entirely, and are activated by initiator caspases. Activated effector caspases target many cellular proteins for degradation by recognising and cleaving specific aspartate residues.

Mechanisms are in place to regulate the activity of caspases to prevent aberrant cell death. Inhibitor of apoptosis molecules physically interact with procaspases to prevent activation by adaptor-mediated oligomerisation. Additionally, the Bcl-2 family of proteins,

containing both prosurvival and proapoptotic members, control initiation of the intrinsic, mitochondrial pathway of caspase activation. The core apoptotic machinery is conserved between the worm, fly and mammals. The fruitfly, *Drosophila melanogaster* is a useful model organism in the study of complex genetic pathways such as apoptosis and has homologues for most of the components of the apoptotic machinery.

At the commencement of the studies described in this thesis, six caspases were described in *Drosophila*. Two of these, DRONC and DREDD are classified as initiator caspases based on the presence of a long prodomain, while DCP-1, DRICE, DECAY and DAMM, lack long prodomains and are therefore considered to be downstream caspases. Results presented in this thesis report the cloning of a novel *Drosophila* caspase, STRICA, and demonstrate the ability of this molecule to function as a caspase. The *strica* gene consists of 1581 coding nucleotides and encodes a protein product of 527 amino acids. STRICA is a long-prodomain-containing caspase that has all the conserved features that characterise the caspase family but lacks a CARD or DEDs. Indeed, the prodomain of STRICA is unique and bears no significant homology to other caspase prodomains. STRICA is a cytoplasmic protein expressed throughout *Drosophila* development and is expressed in larval tissues that histolyse during fly metamorphosis. Additionally, as with most caspases identified to date, STRICA is able to induce apoptosis when overexpressed in mammalian and insect cell lines. STRICA-induced apoptosis is suppressed by DIAP1 and p35 and to a lesser extent by DIAP2. The prodomain of STRICA is processed when overexpressed in cells and this processing requires the catalytic cysteine residue in the active site of STRICA. Active STRICA is also shown to cleave the key *Drosophila* survival molecule, DIAP1.

Overexpression of STRICA in the fly eye results in ectopic cell death of pigment cells with a more severe small, rough eye phenotype observed in homozygous *GMR-strica* flies. This apoptotic phenotype is suppressed by DIAP1 and p35, and partially suppressed by DIAP2. Physical interaction between STRICA and DIAP1 and DIAP2 is demonstrated. Unlike DRONC, STRICA-induced apoptosis in the fly eye is not affected by halving the

dosage of *reaper*, *hid* and *grim*. A potential AKT phosphorylation site was identified in the prodomain of STRICA. The *Drosophila* AKT homologue, DAKT, inhibits STRICA-induced cell death in cultured cells and in the fly eye, to some extent.

Characterisation of the *Drosophila* Bcl-2 homologues, BUFFY and DEBCL, with particular emphasis on the differential localisation of these two proteins, is presented in this thesis. DEBCL is a proapoptotic Bcl-2 homologue that localises to mitochondria in transfected cells. BUFFY has been reported to be the prosurvival Bcl-2 homologue in *Drosophila*, and resides on the ER membrane and nuclear envelope in transfected cells. Results demonstrate the residues that are important for intracellular targeting of BUFFY and DEBCL, and indicate that residues in the transmembrane domain (TMB) itself, in addition to TMB flanking residues, are required for appropriate localisation. The importance of the membrane anchor is demonstrated and a functional nuclear localisation signal (NLS) in the N-terminus of BUFFY identified.

This thesis contributes to the understanding of programmed cell death in *Drosophila* by characterising a novel, *Drosophila* caspase, STRICA, and analysing the differential localisation of the *Drosophila* Bcl-2 homologues, BUFFY and DEBCL. A framework for further investigation is established. Some of the results presented have been published.

Statement

This thesis contains no material which has been accepted for any other degree or diploma in any university or other tertiary institution and, to the best of my knowledge, contains no material previously published or written by any other person, except where due reference has been made. I give consent for this thesis to be made available for loan and photocopying.

8·7·04

Dr. Leonie Quinn, from the laboratory of Dr. Helena Richardson (Peter MacCallum Institute, Melbourne) carried the *in situ* analysis of *strica* during *Drosophila* development, presented in figure 3.3 B. Dr. Loretta Dorstyn performed the *in vitro* cleavage experiment shown in figure 3.9 B.

Acknowledgements

I must begin by thanking Jesus, my strength, without whom I would have neither begun nor completed this challenge. I am thankful to Prof. Sharad Kumar for the opportunity to carry out my PhD studies under his supervision and for the privilege of working in such a dynamic lab. Many thanks to the Royal Adelaide Hospital Research fund and the DAWES committee for granting me a scholarship. I am grateful to Prof. Hay and Prof. Manoukian for providing me with transgenic flies, and Prof. Christoph Borner for providing me with control expression constructs for the analysis of BUFFY and DEBCL. Many thanks to members of the Molecular Regulation Lab, past and present, particularly Tash for her friendship and support when I first began working in the lab. Thankyou to 'the boys', Andrew for the occasional funny joke and Jim for his willingness to participate in feisty debates. Thanks to Tas, not only for introducing me to the wonderful world of *Drosophila*, but also for his friendship. I am grateful to Ingrid and Loretta for valuable input into my thesis. Thanks to Elaine, for proof-reading at the eleventh hour, and the Sydney Street Boutique girls for many laughs at work.

Where would I be without my family and friends? To Justin, for putting up with me trying to find an acryonym for my beloved caspase, while trying to watch the Australia Day cricket match. His love, support and encouragement over the years are greatly valued. My wonderful Mum, for her endless patience and support, I can't adequately express my gratitude. For my late father (Baba), who always wanted to see me "take the hat." My sisters, Trisia, Rena, Yiots and Bernice (Bunny) who can always be counted on for a laugh. Thanks to Rene, not only a dear sister, but also the best of friends. Yiots and Bunny, mwa! My beautiful nieces and nephew, Sarah, Blake, Jade and Amber, two of whom have entered the world since the start of my PhD. Thanks also to my friends, for their patience and encouragement. For all who have helped me get to this point, directly or indirectly, thankyou.

Publications

Kumar, S. and Doumanis, J. (2000) The fly caspases. Cell Death Diff. *7*(11), 1039-44

Doumanis, J., Quinn, L., Richardson, H. and Kumar, S. (2001) STRICA, a novel *Drosophila melanogaster* caspase with an unusual serine/threonine-rich prodomain, interacts with DIAP1 and DIAP2. Cell Death Differ. *8*(4), 387-94

Shearwin-Whyatt, L., Baliga, B., Doumanis, J. and Kumar, S. (2001) Chimeric caspase molecules with potent cell killing activity in apoptosis-resistant cells. Biochem Biophys Res Commun. *282(5)*, 1114-9

Abbreviations

aa	amino acid
Apaf-1	Apoptotic protease activating factor
Bcl-2	B-cell lymphoma
BH	Bcl-2 Homology
BIR	Baculoviral Inhibitory Repeat
bp	base pair
BSA	Bovine Serum Albumin
CARD	Caspase Recruitment Domain
Caspase	Cysteinyl aspartate-specific protease
ced	*C.elegans* cell death defective gene
CrmA	Cytokine response modifier
DAMM	Death Associated Molecule related to Mch2
Dapaf-1	*Drosophila* Apaf-1 homologue
DARK	*Drosophila* Apaf-1-Related Killer
dBORG	*Drosophila* Bcl-2 ortholog
DD	Death Domain
DEBCL	Death Executioner Bcl-2 homologue
DECAY	Death Executioner Caspase related to Apopain/Yama
DED	Death Effector Domain
DEPC	diethyl pyrocarbonate
DIAP	*Drosophila* inhibitor of apoptosis (1 and 2)
DISC	Death inducing signalling complex
DCP-1/-2	*Drosophila* caspase-1 /-2
DR	Death Receptor
DRICE	*Drosophila* ICE
DREDD	Death related Ced-3/Nedd2-like protein
DROB	*Drosophila* ortholog of Bcl-2
DRONC	*Drosophila* Nedd2-like caspase
DTT	1,4-dithiothreitol
ECL	Enhanced chemiluminescence
EcR	Ecdysone Receptor
EDTA	ethylenediaminetetra-acetic acid
EGFP	Enhanced Green Fluorescent Protein
Egl-1	egg-laying defective gene

EST	expressed sequence tag
FADD	Fas associated death domain
FasL	Fas ligand
FBS	Fetal bovine serum
FITC	Fluorescein isothiocyanate
FLIP	FLICE inhibitory protein
GFP	Green fluorescent protein
GMR	Glass minimal region
GST	Glutathione S-transferase
HA	haemaglutinin
HAC-1	Homologue of Apaf-1/Ced-4
HEPES	N-2-hydroxyethylpiperazine N'2-ethane sulphonic acid
hid	head involution defective
HRP	horseradish peroxidase
Hsp	heat shock promoter
IAP	Inhibitor of apoptosis protein
ICE	Interleukin 1-β converting enzyme
IgG	Immunoglobulin G (heavy and light)
IP	immunoprecipitation
IVT	*In vitro* translated
JNK	Jun N-terminal Kinase
kb	kilobase
kDa	kilo Dalton
LB	Luria broth
MA	membrane anchor
MOPS	3-[N-morpholino] propanesulfonic acid
MPD	minus prodomain
NAIP	neuronal apoptosis inhibitory protein
nedd2	neural precursor cell expressed developmentally downregulated gene
NP40	Nonidet P40
PAGE	polyacrylamide gel electrophoresis
PARP	Poly (ADP-ribose) polymerase
PBS-T	Phosphate Buffered Saline-Tween 20
PCD	Programmed Cell death
PCR	polymerase chain reaction
RNAi	RNA interference

RT	Room Temperature
RT-PCR	Reverse transcribed PCR
SEM	standard error of the mean
SD	standard deviation
SDS	sodium dodecyl sulphate
STRICA	Serine/Threonine-Rich Caspase
TAE	Tris acetate EDTA
TMB	transmembrane domain
TEMED	N, N, N', N'-tetramethylethylenediamine
TGF	Transforming Growth Factor
TGFR	TGF Receptor
TNF	Tumor Necrosis Factor
TNFR	TNF Receptor
TRAF	TNFR associating factor
WB	Western Blot

Table of Contents

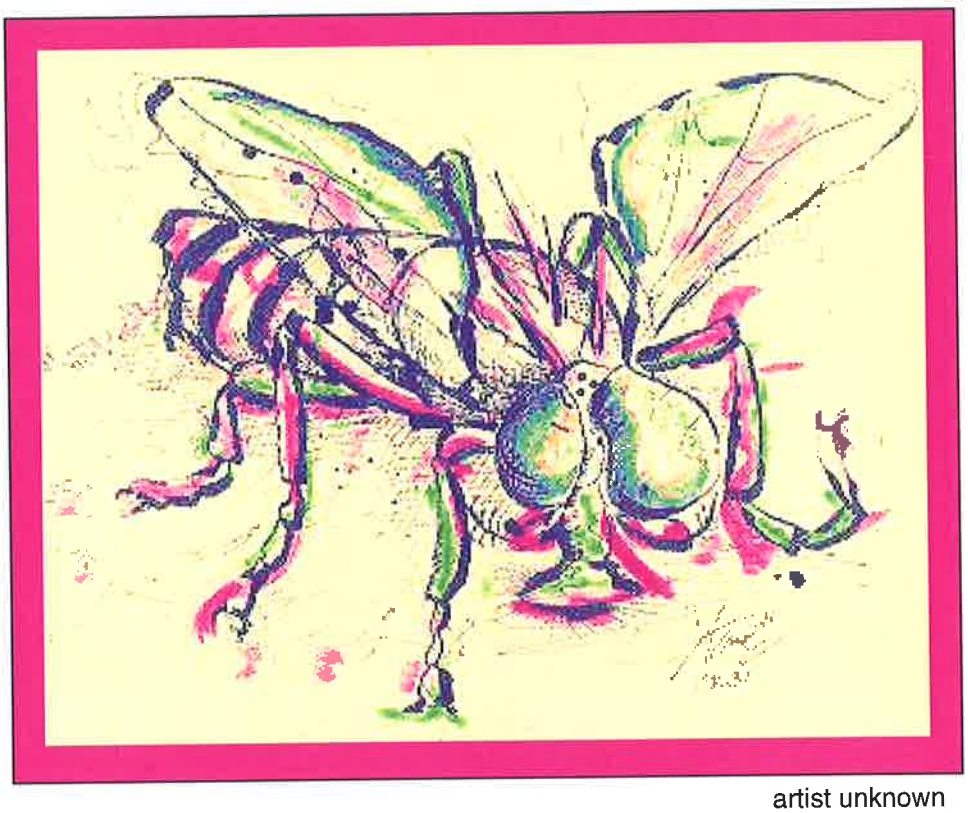

artist unknown

Chapter 1

Introduction

1.1 Apoptosis

Early observations of developmental cell death were first described by Vogt in 1842 but it was not until 1951 that cell death was described as a normal facet of development (Glucksmann, 1951). Later, Lockshin and Williams (1965) coined the term Programmed Cell Death (PCD) to describe the fate of some cells during insect and tadpole metamorphosis. The term 'apoptosis' was introduced by Kerr, Currie and Wyllie (1972) to describe cell death events accompanied by a number of common morphological features.

The signalling pathways leading to apoptosis and the molecular basis of such events are now better understood. At the molecular level, apoptosis is characterised by the cleavage of cellular proteins such as nuclear lamins, and cytoskeletal proteins fodrin and gelsolin (Utz and Anderson, 2000). Such changes underlie the observable morphological features associated with apoptosis such as chromatin condensation, nuclear envelope breakdown, cytoplasmic shrinkage and plasma membrane blebbing (Wyllie *et al.*, 1980). Apoptotic cells expose phosphatidylserine on the plasma membrane surface which acts as an 'eat me' signal for phagocytes, allowing the rapid removal of the dying cell without triggering an inflammatory response, otherwise associated with necrotic cell death (Fadok *et al.*, 1992; Martin *et al.*, 1995).

Cells of vastly different types undergo apoptosis in response to a variety of stimuli including UV irradiation, growth factor withdrawal, DNA damage, steroid hormone release and other factors. Cells are specified to die in order to remove excess, unwanted or harmful cells, and to delete cells that have fulfilled their function. Dysfunction of the apoptotic pathway can have disastrous effects on the viability of the organism as a whole. Too little cell death can result in autoimmune disease and cancer, whereas too much apoptosis is the cause of some neurodegenerative diseases (Green and Evan, 2002; Kaufmann and Gores, 2000; Chun *et al.*, 2002; Martin *et al.*, 1999). In addition to maintaining optimal cell numbers in the adult organism, apoptosis is critical during development where it plays a role in organ sculpting and immunity.

1.2 Apoptotic machinery

Pioneering studies in apoptosis using the nematode *Caenorhabditis elegans* provided valuable insights into the basic machinery required for cell death, and recently awarded a Nobel Prize to the researchers who carried out these early studies (Ellis and Horvitz, 1986). In *C.elegans*, 131 cells generated during development are programmed to die in a precise manner (Sulston and Horvitz, 1977). The products of four genes, *ced-3*, *ced-4*, *ced-9* and *egl-1*, are responsible for these death events (Ellis and Horvitz, 1986; Hengartner *et al.*, 1992; Conradt and Horvitz, 1998). EGL-1, CED-3 and CED-4 act to promote cell death, while CED-9 functions to protect cells destined for survival. Mutations in either *ced-3* or *ced-4* prevent all cell deaths in the worm (Ellis *et al.*, 1986).

ced-3 was first cloned by Yuan and colleagues (1993) and subsequently characterised. CED-3 is a serine-rich protein and its C-terminal region was found to be homologous to human Interleukin 1β–Converting Enzyme (ICE) and mouse Nedd2, indicating that CED-3 induces cell death through protease activity (Hugunin *et al.*, 1996). CED-3 was later shown to exhibit autocatalytic processing *in vitro*, following an aspartate residue (Hugunin *et al.*, 1996). The CED-3-like proteases, now known as caspases, are highly conserved proteins, which act as principal instigators of the cell death programme. Comparison of the substrate specificity of CED-3 with mammalian caspases revealed that CED-3 is more similar to mammalian Caspase-3/CPP32, than Caspase-1/ICE or Caspase-2/Nedd2 (Xue *et al.*, 1996).

The product of the *ced-4* gene was found to be a novel protein primarily expressed during embryogenesis (Yuan and Horvitz, 1992). CED-4 functions as an adapter molecule, inducing cell death by interacting with, and activating, the caspase CED-3 (Chinnaiyan *et al.*, 1997a, 1997b; Seshagiri and Miller, 1997; Wu *et al.*, 1997).

The survival molecule CED-9 is a homologue of mammalian Bcl-2 (B cell lymphoma-2) and contains a C-terminal hydrophobic membrane anchor. Like Bcl-2, CED-9 localises to membranes of the mitochondria, endoplasmic reticulum and the nuclear envelope (Hengartner and Horvitz, 1994a, 1994b; Wu *et al.*, 1997). CED-9 prevents cell death by sequestering

CED-4 away from CED-3, thereby preventing its activation (Chinnaiyan *et al.*, 1997a, 1997b; James *et al.*, 1997; Spector *et al.*, 1997; Wu *et al.*, 1997). EGL-1 is a death-inducing molecule containing a single Bcl-2 homology domain 3 (BH3). EGL-1 induces apoptosis in *C.elegans* by interacting with CED-9, preventing CED-9 from binding to CED-4, allowing for CED-4-dependent CED-3 activation (Shaham and Horvitz, 1996; Chinnaiyan *et al.*, 1997a, 1997b; Conradt and Horvitz, 1998). The cell death pathway in *C. elegans* is demonstrated schematically in figure 1.1.

1.3 Mammalian Apoptotic Machinery

Caspases are **c**ysteinyl **asp**artate-specific protein**ases** that cleave their substrates following an aspartate residue (Margolin *et al.*, 1997). Once caspases are activated, the cell is committed to die, cellular substrates are cleaved and the morphological features characterising apoptosis, such as DNA fragmentation, cytoplasmic shrinkage and membrane blebbing, are observed. Caspases are present in healthy cells as inactive zymogens that usually require proteolytic cleavage at precise residues to activate the enzyme. Procaspase molecules are made up of two catalytic subunits and an N-terminal prodomain. A highly conserved active site is present in the large subunit with a cysteine residue essential for enzymatic activity (Stennicke and Salvesen, 1999). Active caspases are dimers comprised of two large and two small subunits. Caspases are commonly categorised into two main groups based on the length of the prodomain at the N-terminus of the protein (Degterev *et al.*, 2003). Class I, upstream or initiator caspases have long prodomains which function as protein interaction domains. Such protein-protein interaction motifs include caspase-recruitment domains (CARDs) or death effector domains (DEDs) (figure 1.2), which function to recruit adaptor molecules, bringing several precursors together to facilitate proximity-induced caspase activation (Weber and Vincenz, 2001; Tibbetts *et al.*, 2003).

Class II, downstream or effector caspases have very short prodomains or lack a prodomain entirely (figure 1.2), and are activated by ClassI/initiator caspases. Activated

Figure 1.1 Cell Death machinery in *C. elegans*

The protein products of four genes, *egl-1*, *ced-3*, *ced-4* and *ced-9*, are essential for cell death and survival in the nematode, *C. elegans*. *ced-3* encodes a CARD domain-containing caspase that remains dormant in the cell until activated by the adaptor molecule CED-4, through proximity-induced activation. CED-4 also contains a CARD and is held inactive by the Bcl-2 homologue, CED-9. Activation of EGL-1, a BH3-only molecule, results in the binding of CED-9, thereby sequestering CED-9 away from CED-4. CED-4 is then released to bind and activate CED-3, cellular substrates are cleaved and cell death occurs. The p53 pathway responds to DNA damage, resulting in the upregulation of *egl-1* by the *C.elegans* p53 homologue, CEP-1.

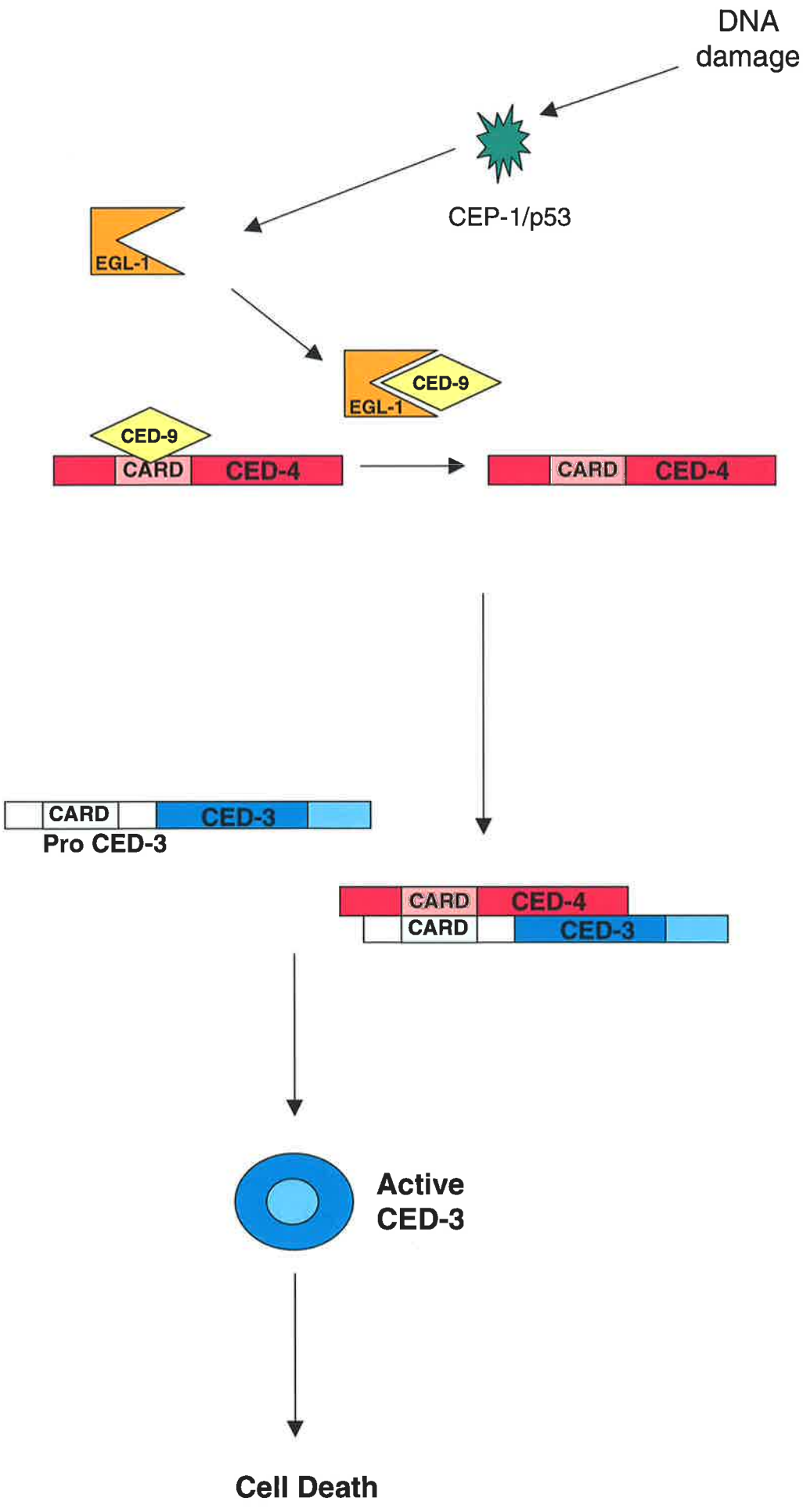
DNA
damage
CEP-1/p53
EGL-1
CED-9
EGL-1
CED-9
CARD
CED-4
CARD
CED-4
CARD
CED-3
Pro CED-3
CARD
CED-4
CARD
CED-3
Active
CED-3
Cell Death

Figure 1.2 The mammalian Caspase family

There are 13 caspases encoded by the mammalian genome. Caspases are divided into two main groups, based on the length of the N-terminal prodomain. Class I caspases contain long prodomains and possess either death effector domains (DEDs) or a caspase recruitment domain (CARD). DEDs and CARDs function as protein-protein interaction motifs and mediate the recruitment and activation of Class I caspases. Such caspases function upstream in the cell death pathway and are referred to as initiator caspases. Class II caspases lack protein interaction motif-containing prodomains and require the ClassI/initiator caspases for their processing and activation. Class II caspases cleave cellular substrates that are critical for cell viability and infrastructure and therefore execute cell death. All caspases share a homologous active site with an essential catalytic cysteine residue, demonstrated in column two. Caspases cleave their target substrates following an aspartate residue. The substrate specificity of most mammalian caspases has been determined (column 3). (Adapted from Degterev *et al.*, 2003 with data based on Thornberry *et al.*, 1997).

Class I

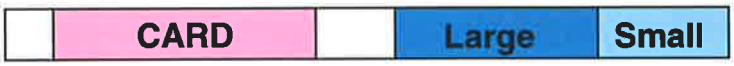

Caspase	Active site	Substrate specificity
Caspase-1	QACRG	WEHD
Caspase-2	QACRG	VDVAD
Caspase-4	QACRG	(W/L)EHD
Caspase-5	QACRG	(W/L)EHD
Caspase-9	QACGG	LEHD
Caspase-11	QACRG	(I/L/V/P)EHD
Caspase-12	QACRG	-

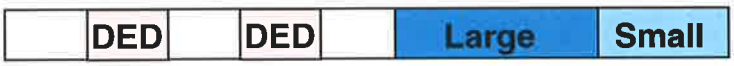

Caspase	Active Site	Substrate Specificity
Caspase-8	QACQG	LETD
Caspase-10	QACQG	-

Class II

Caspase	Active Site	Substrate Specificity
Caspase-3	QACRG	DEVD
Caspase-6	QACRG	VEHD
Caspase-7	QACRG	DEVD
Caspase-14	QACRG	-

effector caspases target many cellular proteins for degradation by recognising and cleaving specific aspartate residues (Degterev *et al.*, 2003).

1.3.1 The Caspase family

Caspase-1 or ICE (interleukin-1β converting enzyme) was the first caspase identified, based on its ability to process interleukin 1β, involved in the inflammatory response (Howard *et al.*, 1991; Thornberry *et al.*, 1992; Li *et al.*, 1995). Since the discovery that *C.elegans* CED-3 bears sequence homology to mammalian ICE (Yuan *et al.*, 1993), the caspase family has grown to include 13 members in mammals, 11 of which belong to the human species (Degterev *et al.*, 2003). Mammalian caspases have been numbered in order of their identification. Although several mammalian caspases have been implicated in the inflammatory response (Degterev *et al.*, 2003), only those involved in programmed cell death are discussed here.

Nedd2 (**N**eural precursor cell-**e**xpressed, **d**evelopmentally **d**own-regulated), one of a number of genes developmentally down-regulated in the mouse brain, was identified as an ICE/CED-3 homologue able to induce apoptosis in cultured cells, that could be suppressed by Bcl-2 (Kumar *et al.*, 1992; Kumar *et al.*, 1994). Nedd2, now referred to as Caspase-2, contains a CARD domain in its prodomain, which is required for procaspase oligomerisation and autoactivation (Butt *et al.*, 1998). There are two splice variants of Caspase-2, however the short form ($Nedd2_S$) was not found to play a significant role in cell death (Kumar *et al.*, 1997). Somewhat surprisingly, *caspase-2*$^{-/-}$ knockout mice develop normally but possess excess oocytes that are resistant to the chemotherapy agent doxorubicin (Bergeron *et al.*, 1998).

Caspase-3/CPP32 was cloned from human Jurkat T-lymphocytes as a 32 kDa molecule homologous to *C. elegans* CED-3 and mouse Nedd2 (Caspase-2) (Fernandes-Alnemri *et al.*, 1994). Mice deficient for *caspase-3* die at 1-3 weeks (Kuida *et al.*, 1996) and have enlarged brains due to increased numbers of neurons (Kuida *et al.*, 1996; Kuida *et al.*, 1998; Hakem *et*

al., 1998), indicating the importance of Caspase-3 for normal brain development. Caspases similar to Caspase-3 include Caspase-6 and -7 and act as downstream effectors that cleave many cellular proteins involved in cell viability, infrastructure and repair (Degterev *et al.*, 2003).

The prodomain of Caspase-8 contains two DEDs, which mediate binding to the adaptor molecule FADD. FADD is the intermediate between the death receptor in the cell's outer membrane, and Caspase-8. Signalling by extracellular factors like tumour necrosis factor (TNF) and Fas, triggers the recruitment of FADD and Caspase-8 into a receptor-mediated DISC (death inducing signalling complex). DISC formation results in Procaspase-8 processing and activation and initiates a cell death signalling cascade. Deficiency of *caspase-8* in Jurkat cells renders these cells resistant to death induced by Fas and TRAIL, indicating the requirement for Caspase-8 in death-receptor signalling (Juo *et al.*, 1998; Bodmer *et al.*, 2000; Sprick *et al.*, 2000). Moreover, mouse embryonic fibroblasts (MEFs) from *caspase-8*-deficient embryos are completely resistant to Fas, TNF and DR3 receptor-mediated apoptosis but remain sensitive to stimuli such as UV irradiation which signals through the intrinsic apoptotic pathway within the cell (Varfolomeev *et al.*, 1998). *caspase-8*$^{-/-}$ mice are embryonic lethal with decreased myeloid progenitor cells, impaired cardiac muscle formation and abdominal haemorrhage (Varfolomeev *et al.*, 1998). *fadd*$^{-/-}$ knockout mice display similar phenotypes, consistent with the requirement for this molecule in the activation of Caspase-8 (Yeh *et al.*, 1998).

Caspase-8 activation is regulated by FLICE-like inhibitory proteins (FLIPs). Cellular FLIP (c-FLIP), also known as Casper, is a catalytically inactive molecule similar to Caspase-8 (Yeh *et al.*, 2000). Two c-FLIP isoforms have been described (Irmler *et al.*, 1997). The short isoform encodes the prodomain of Caspase-8 and prevents Procaspase-8 recruitment to the DISC by competing for FADD binding (Kirchhoff *et al.*, 2000). The long isoform contains a pseudocatalytic domain, lacking the cysteine residue, in addition to the prodomain and

although this isoform can cause initial Procaspase-8 processing, further activation is inhibited by c-FLIP$_L$ (Krueger *et al.*, 2001).

Caspase-9 is a CARD-containing caspase with a long prodomain. In contrast to Caspase-2, Caspase-9 does not oligomerise and autoactivate, instead relying on the release of cytochrome c from mitochondria and interaction with the CED-4 homologue, Apaf-1, as part of the apoptosome (Srinivasula *et al.*, 1998). *caspase-9*$^{-/-}$ knockout mice are embryonic lethal, displaying enlarged brains due to a lack of Caspase-3 activation and apoptosis (Hakem *et al.*, 1998; Kuida *et al.*, 1998). The similarities in the phenotypes of *caspase-3*$^{-/-}$ and *caspase-9*$^{-/-}$ mice demonstrate the relationship between these two caspases. Compensatory activation of other caspases has been reported in cells deficient for *apaf-1* or *caspase-9*, suggesting that apoptosome-independent cell death occurs in these cells (Marsden *et al.*, 2002).

1.3.2 Caspase Substrate Specificity

The substrate specificities for individual caspases have shed light on their various functions in the apoptotic pathway (Degterev *et al.*, 2003). The preferred substrates for caspases 1-11 have been determined (Thornberry *et al.*, 1997; Talanian *et al.*, 1997; Kang *et al.*, 2000) (figure 1.2). The optimal substrate cleavage site is referred to as the P4,P3,P2,P1 tetrapeptide sequence, where P1 represents the aspartate residue where cleavage takes place. Based on their cleavage specificity and the preferred P4 residue in the substrate, caspases can be divided into 3 groups. Group I caspases, Caspase-1, -4 and -5, recognise cleavage sites with a bulky residue such as tryptophan (W) in the P4 position preferring a WEHD tetrapeptide, whereas group II caspases, Caspase-6, -8, -9 and -11, prefer leucine or valine in this position and cleave (L/V)EXD sites. Caspase-2, -3 and -7 form group III caspases and cleave DEXD sites, where X can be valine, threonine or histidine. Thus, with some exceptions, downstream, effector caspases have distinct substrate specificities from their upstream relatives. This is consistent with the observation that effector caspases require

processing by activated initiator caspases and their preferred sites of cleavage should be distinct from their own substrate specificities to prevent inappropriate autoactivation. Interestingly, the cleavage site between the active subunits of upstream caspases conforms to their own substrate specificity allowing for autoprocessing at this site. Caspase-2 is unusual as it can both autoprocess by means of CARD-mediated oligomerisation, but also recognises Caspase-3-like tetrapeptide substrates and therefore may be able function downstream in the apoptotic pathway in some contexts (Butt *et al.*, 1998; Lassus *et al.*, 2002; Paroni *et al.*, 2002; Robertson *et al.*, 2002). Although Caspase-2, like Caspase-3, has a preference for aspartate in the P4 position, the optimal substrate for Caspase-2 is a pentapeptide, VDVAD (Talanian *et al.*, 1997). It should be noted, however, that synthetic short peptides were used to determine caspase substrate specificity while the *in vivo* cleavage sites may not always confer to these published classifications.

1.4 Caspase activation

Upon activation, caspases cause massive and rapid destruction in the cell resulting in death and phagocytosis of the cell corpse without triggering an inflammatory response. Because of the rapid and efficient execution of cell death caused by active caspases, their activation must be tightly controlled. In healthy cells, measures are in place to inhibit caspase activation and also prevent active caspase molecules from functioning inappropriately. In the worm, caspase inhibition and activation are seen in their simplest form. In healthy cells, the Bcl-2 homologue, CED-9, is bound to CED-4 (Chinnaiyan *et al.*, 1997; James *et al.*, 1997; Spector *et al.*, 1997). When the death signal is received, the BH3-only molecule, EGL-1, binds to CED-9, releasing CED-4 and allowing it to bind to CED-3 (Conradt and Horvitz, 1998). CED-4, acting as an adaptor, physically interacts with CED-3, causing the recruitment and subsequent activation of CED-3 zymogens (Yang *et al.*, 1998; Chinnaiyan *et al.*, 1997; Irmler *et al.*, 1997). Thus, adaptor-mediated oligomerisation of procaspase molecules leads to caspase activation in the worm.

Oligomerisation is also one of the main mechanisms of caspase activation in higher eukaryotes. The initiator caspase, Caspase-8, interacts with the Fas receptor through an adaptor intermediary, FADD. These associations occur through death domains (DDs) and death effector domains (DEDs) present in Fas, FADD and Caspase-8. Formation of the DISC brings multiple Procaspase-8 molecules into close proximity with each other, leading to the autoactivation of Caspase-8. Active Caspase-8 can activate downstream Caspases-3 -4 and -7 and also cleaves the BH3-only molecule, Bid. Truncated Bid (tBid) exerts its proapoptotic function by acting on mitochondria, causing the release of cytochrome c (Li *et al.*, 1998; Luo *et al.*, 1998).

The mammalian apoptosome is a high molecular weight complex that forms in apoptotic cells, where the intrinsic cell death pathway is activated causing cytochrome c release from mitochondria. Apoptosome formation requires the adapter molecule Apaf-1, cytochrome c and dATP (Liu *et al.*, 1996; Goldstein *et al.*, 2000). Apaf-1 contains an N-terminal CARD domain that is able to interact with the CARD of Procaspase-9. In addition to its N-terminal CARD domain and the CED-4 homology motif that binds dATP, Apaf-1 contains a series of WD40 repeats in its C-terminal region (Zou *et al.*, 1997, 1999; Li *et al.*, 1997; Hu *et al.*, 1998). This WD40 repeat domain binds to cytochrome c released from mitochondria when apoptosis is triggered. Although the *C.elegans* homologue of Apaf-1, CED-4, lacks any WD40 repeats, this region is critical in the regulation of Apaf-1 activity, as demonstrated by the constitutive nature of Apaf-1 lacking this region (Srinivasula *et al.*, 1998; Hu *et al.*, 1999). This suggests that the WD40 repeats not bound to cytochrome c perform an inhibitory role upon Apaf-1. Binding of cytochrome c induces a conformational change in Apaf-1 that allows recruitment of Procaspase-9, which is subsequently activated to cleave downstream caspases (Qin *et al.*, 1999). Mice lacking cytochrome c are embryonic lethal, demonstrating the necessity for this small molecule in programmed cell death (Li *et al.*, 2000). The crystal structure of the apoptosome was determined and revealed a wheel-like structure with seven spokes that suggests that active Caspase-9 molecules are continuously

generated which in turn activate Caspase-3 leading to the rapid demise of the cell (Acehan *et al.*, 2002).

In the case of Caspase-2, oligomerisation occurs between procaspase molecules via the N-terminal CARD domain. Upon oligomerisation, Caspase-2 autoprocesses, liberating the active enzyme (Butt *et al.*, 1998). Additionally, the prodomain of Caspase-2, when chimerically fused to Caspase-3, results in the constitutive autoactivation of Caspase-3 (Colussi *et al.*, 1998b), further demonstrating the potency of prodomain-mediated oligomerisation. This feature makes Caspase-2 unique and may be exploited to induce cell death in normally resistant cancer cell lines (Shearwin-Wyatt *et al.*, 2001).

Downstream, or executioner caspases, including Caspase-3, Caspase-6 and Caspase-7 in mammals, cleave cellular substrates vital for the maintenance of cell viability. The requirement for cleavage and activation of the downstream caspases by their upstream counterparts prevents apoptosis until cell death is appropriately initiated and the upstream caspases activated. Processing between the large and small subunits is necessary for enzyme activation. Downstream caspases harbour processing sites that conform to the substrate specificities of the upstream caspases and are, therefore, substrates for these activated class I caspases (Degterev *et al.*, 2003).

1.5 Caspase Regulation

Given the potency of active caspases and the resulting death of the cell, inhibition of caspase activity in healthy cells is clearly critical to the life of the cell and the function of the organism as a whole. Prevention of caspase activation as well as inhibiting prematurely activated caspases, is required to prevent inappropriate cell death.

1.5.1 Viral caspase inhibitors

Initiation of apoptosis is widely used by an organism to prevent the persistence of harmful cells that cause organ dysfunction and disease, including virus-infected cells. Many

viruses have developed apoptosis-inhibitory mechanisms to prevent host cell death upon infection, allowing for viral replication and survival. The baculoviral protein p35 was initially identified as a molecule able to suppress apoptosis in cells infected with viruses (Clem *et al.*, 1991) and has since been shown to inhibit a wide range of caspases (Bump *et al.*, 1995; Xue and Horvitz, 1995). p35 possesses a DQMD caspase cleavage site (Bump *et al.*, 1995) and structural analysis of Caspase-8/p35 complexes show that a conformational change is induced in p35 by caspase cleavage (Xu *et al.*, 2001) exposing a cysteine residue that forms a stable complex with the active site of Caspase-8, thereby preventing its activity (Fisher *et al.*, 1999; Riedl *et al.*, 2001; Xu *et al.*, 2001).

Following the identification of p35, two proteins similar to each other but different to p35 were identified in a screen to isolate baculoviral proteins able to suppress cell death in insect cells following infection by a p35-deficient virus (Crook *et al.*, 1993; Birnbaum *et al.*, 1994; Clem and Miller, 1994). Cp-IAP and Op-IAP were characterised by the presence of one or more baculoviral IAP repeats (BIRs). Since the identification of viral inhibitors of apoptosis, the IAP family of BIR domain-containing proteins has expanded and includes cellular counterparts in organisms as distant as yeast and humans.

CrmA, a **c**ytokine **r**esponse **m**odifier gene, is a cowpox viral protein that inhibits caspases (Ray *et al.*, 1992). CrmA preferentially suppresses Caspase-1 and -8, therefore inhibiting IL-1β processing and TNF-α- and Fas- triggered apoptosis (Enari *et al.*, 1995; Los *et al.*, 1995; Miura *et al.*, 1995). Like p35, CrmA inhibits caspases by acting as a pseudosubstrate that undergoes a conformational change upon caspase cleavage, preventing the cleavage of *bona fide* substrates (Ekert *et al.*, 1999; Renatus *et al.*, 2000).

Prior to the identification of the Caspase-8 inhibitor, cellular FLIP/Casper, FLIPs, structurally similar to Caspase-8 containing two tandem DEDs, were isolated from γ-herpes virus (Muzio *et al.*, 1996; Tschopp *et al.*, 1998). Viral FLIPs inhibit apoptosis induced by CD95 by interacting with, and inhibiting, the DISC, allowing for viral replication and survival (Bertin *et al.*, 1997; Hu *et al.*, 1997; Thome *et al.*, 1997).

1.5.2 Endogenous caspase inhibitors – The IAP family

Mammalian cells express caspase inhibitors similar to baculovirus OpIAP. Inhibitor of Apoptosis Proteins (IAPs) belong to a large family of proteins that contain one or more BIR domains (figure 1.3). Not all BIR-containing proteins (BIRps) function as inhibitors of apoptosis (Silke and Vaux, 2001; Verhagen *et al.*, 2001), as discussed below. IAPs form one of two BIRp subfamilies and function to inhibit apoptosis. The second subfamily has been implicated in cell cycle regulation. For example, *survivin* gene expression is cell cycle regulated (Kobayashi *et al.*, 1999; Li and Altieri, 1999) and Survivin-related molecules in yeast and *C.elegans* are involved in cytokinesis and chromosome segregation (Uren *et al.*, 1999; Gerring *et al.*, 1990; Yoon and Carbon, 1999; Fraser *et al.*, 1999).

In mammals, the first IAP discovered was NAIP (neuronal apoptosis inhibitory protein) isolated through positional cloning in the search for the gene involved in spinal muscular atrophy (SMA), a degenerative muscular disease caused by motor neuron loss (Roy *et al.*, 1995). Although NAIP was later discounted as the causative gene in SMA, loss of NAIP reportedly increases disease severity (Lefebvre *et al.*, 1995; Liu *et al.*, 1997; Orrell *et al.*, 1997). NAIP contains three BIR domains and although deletion of *naip* in the mouse has no effect on development, reduced survival of some neuronal subsets is observed following seizure induction (Holcik *et al.*, 2000).

Further members were added to the IAP family following NAIP identification, including cellular IAP1 (cIAP1), cIAP2 and X-linked IAP (XIAP), all containing three BIR domains and a C-terminal RING finger domain (Rothe *et al.*, 1995; Duckett *et al.*, 1996; Liston *et al.*, 1996; Uren *et al.*, 1996). Survivin (Ambrosini *et al.*, 1997), Livin (Lin *et al.*, 2000; Vucic *et al.*, 2000; Kasof and Gomes, 2001) and testis-specific IAP (Ts-IAP; Lagace *et al.*, 2001; Richter *et al.*, 2001) were identified as IAP-family members, but contain only one BIR domain while Survivin lacks a C-terminal RING domain.

IAPs suppress cell death by binding to caspases and preventing their activity. XIAP, cIAP1 and cIAP2 bind Procaspase-9 molecules directly to prevent its processing and

Figure 1.3 The Inhibitor of Apoptosis Proteins (IAPs)

IAPs were first isolated from viruses, with cellular homologues subsequently identified in most species ranging from yeast to mammals. IAPs are characterised by the presence of one or more baculoviral inhibitory repeats (BIRs) that are required for interaction with caspases. IAPs interact with activated caspases to prevent inappropriate cell death. Many IAPs contain a C-terminal RING domain that can function as an E3 ubiquitin ligase. (Adapted from Hay, 2000 and Liston *et al.*, 2003).

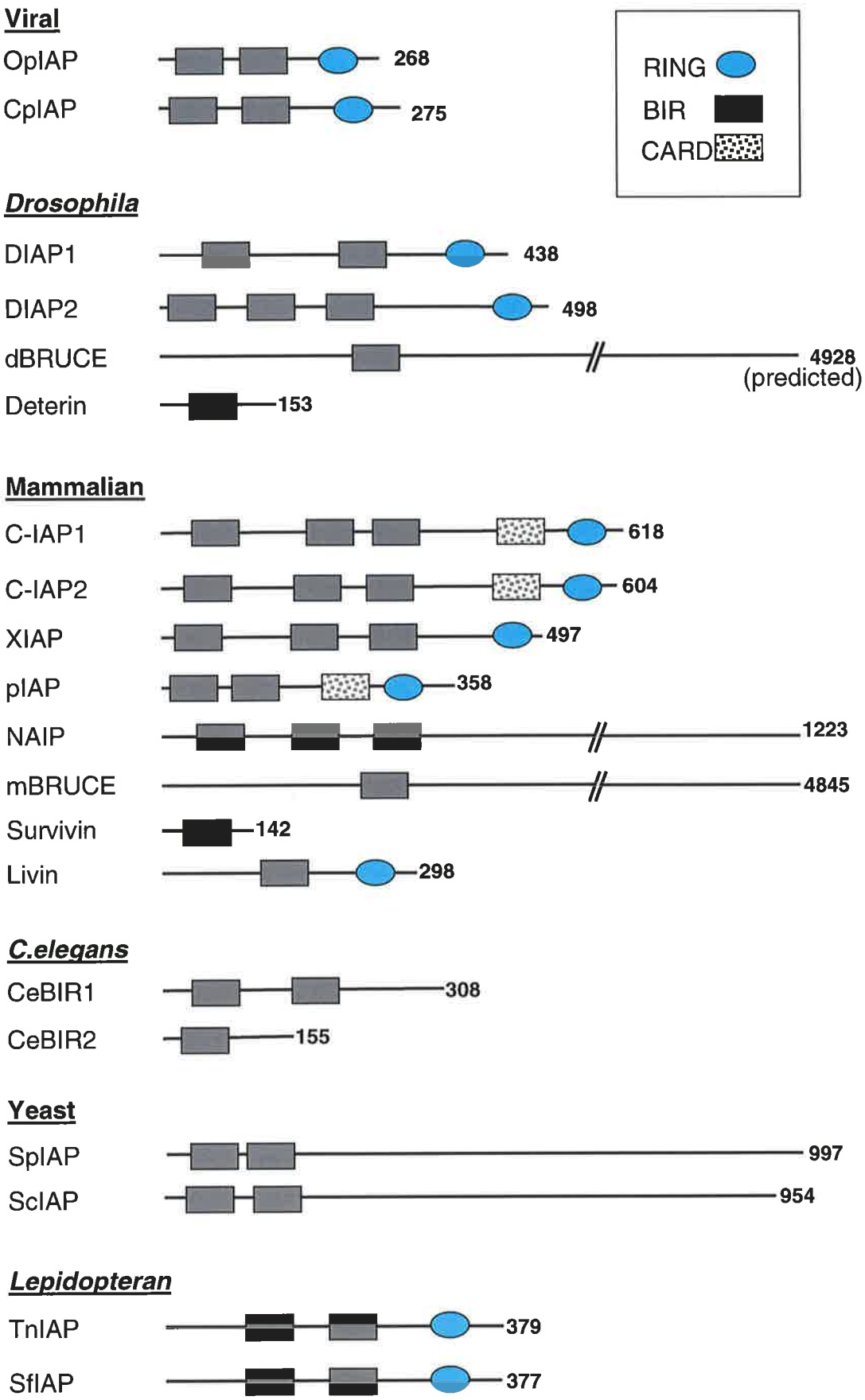
Viral
OpIAP
268
CpIAP
275
RING
BIR
CARD
Drosophila
DIAP1
438
DIAP2
498
dBRUCE
4928
(predicted)
Deterin
153
Mammalian
C-IAP1
618
C-IAP2
604
XIAP
497
pIAP
358
NAIP
1223
mBRUCE
4845
Survivin
142
Livin
298
C.elegans
CeBIR1
308
CeBIR2
155
Yeast
SpIAP
997
ScIAP
954
Lepidopteran
TnIAP
379
SfIAP
377

activation (Deveraux *et al.*, 1998; Takahashi *et al.*, 1998). Furthermore, XIAP has an inhibitory effect on active Caspase-9, and processing of Procaspase-3 by Caspase-9 is inhibited by all three IAPs (Deveraux *et al.*, 1998).

Structural studies have shed much light on the role of individual BIR domains in caspase inhibition. BIR domains fold into functionally independent structures that chelate a zinc ion by means of BIR cysteine and histidine residues (Hinds *et al.*, 1999). The zinc ion is held in the C-terminal portion of the domain. Overall, it appears that IAPs utilise their third BIR domain, BIR3 to inhibit Caspase-9, while BIR2 is critical for suppression of Caspase-3 and -7 (Roy *et al.*, 1997; Takahashi *et al.*, 1998; Sun *et al.*, 2000). In the case of Caspase-7, the crystal structure of the linker-BIR2 of XIAP bound to Caspase-7 reveals that the BIR2 domain itself is hidden within the crystal, whereas the linker region interacts with Caspase-7 by occupying the caspase substrate groove in a reverse orientation to that of substrate (Huang *et al.*, 2001). Similarly, the XIAP BIR2 was found to make limited contacts with Caspase-3, with the linker occluding the substrate-binding pocket (Riedl *et al.*, 2001). Thus, the linker region plays a prominent role in the interaction and inhibition of Caspase-3 and -7 (Chai *et al.*, 2001).

IAPs are themselves regulated by the mitochondrial apoptosis-inducing molecule Smac/Diablo, which sequesters IAPs away from interacting with caspases (Du *et al.*, 2000; Verhagen *et al.*, 2000) and, in the case of XIAP, occupies a pocket on the BIR3 domain of XIAP (Liu *et al.*, 2000; Wu *et al.*, 2000). Modelling suggests that although Smac/Diablo occupies a different site on XIAP to Caspase-3, steric hindrance caused by the binding of BIR3 by Smac/Diablo would prevent the binding of Caspase-3 to BIR2 (Riedl *et al.*, 2001). In the case of Caspase-9, BIR3 of XIAP interacts with monomeric Caspase-9, keeping it in an inactive conformation (Shiozaki *et al.*, 2003). Direct competition between Smac and Caspase-9 for the same BIR3 binding site in XIAP has been suggested due to the similarity between the N-terminal IAP-binding motif of Smac and the cleavage site in the linker region between the large and small subunits of Caspase-9 (Sun *et al.*, 2000; Liu *et al.*, 2000; Wu *et*

al., 2000). Indeed, Caspase-9 processing mutants, although active, cannot be inhibited by XIAP (Ekert *et al.*, 2001; Srinivasula *et al.*, 2001). Thus, XIAP exerts differential inhibitory activity on Caspase-3 and -9.

Besides binding to caspases and antagonists such as Smac/Diablo, IAPs have been reported to bind other molecules, although the significance of such interactions remains unclear. cIAP1 and cIAP2 interact with the signalling molecules TRAF1 and TRAF2 (Rothe *et al.*, 1995), XIAP binds a TGF-β-associated protein, TAB1 (Yamaguchi *et al.*, 1999), and *Drosophila* IAPs, DIAP1 and DIAP2 reportedly interact with Thick Veins, a protein that interacts with the Decapentaplegic (DPP) type I receptor (Oeda *et al.*, 1998). Thus, IAPs may function in cellular pathways other than apoptotic signalling pathways.

Interestingly, IAPs are potential caspase substrates. Consistent with this notion, zVAD-inhibitable cIAP1 cleavage products are detected in apoptotic cells and similarly sized fragments are generated by Caspase-3 (Clem *et al.*, 2001). One of the fragments consists of the spacer-RING carboxyl terminal fragment that reportedly induces apoptosis in transfected cells. XIAP has been shown to be cleaved during Fas-induced apoptosis to produce two fragments, BIR1-BIR2 and BIR3-RING (Deveraux *et al.*, 1999). BIR1-2 overexpression suppresses Fas-induced cell death inefficiently when compared with the full-length molecule suggesting caspase cleavage as a possible mechanism for cells to overcome the inhibition exerted by IAPs. Recently, the *Drosophila* IAP, DIAP1 has been shown to be cleaved by the *Drosophila* caspase, DRONC (discussed in section 1.11.1 below).

The role of the IAP RING domain has received much attention in recent times. The RING domains of cIAP1 and *Drosophila* DIAP1 have been suggested to have an inhibitory effect on the anti-apoptotic function of these molecules (Clem *et al.*, 2001; Hay *et al.*, 1995). Furthermore, ubiquitin ligase activity of RING domains has also been reported (Huang *et al.*, 2000), implicating IAPs in the degradation or modification of cellular proteins.

1.6 Apoptotic pathways in Mammals

In mammals, activation of the core apoptotic machinery occurs via two pathways, a receptor mediated extrinsic pathway, and an intrinsic pathway that is sensitive to the permeability of the outer mitochondrial membrane. Both pathways activate distinct initiator caspases and converge at the point of executioner caspase activation (figure 1.4).

1.6.1 Extrinsic pathway

The TNF receptor superfamily in mammals, including Fas, TNFR1, and death receptors (DR)-3, -4 and -5, contain death domains (DDs) in their intracellular region allowing for interaction with downstream apoptotic molecules (Barnhart *et al.*, 2003). Extracellular ligands, such as Fas, bind their receptors and a cascade of signalling events, leading to caspase activation and apoptosis, is initiated. The receptor-mediated pathway converges on the mitochondrial pathway with the cleavage and translocation of the BH3-only protein, Bid, by activated Caspase-8. Truncated Bid (tBid) causes the release of cytochrome c from mitochondria, which leads to formation of the apoptosome (Wei *et al.*, 2000).

1.6.2 Intrinsic pathway

The intrinsic cell death pathway in mammals revolves around the integrity of the mitochondrial membranes. Upon receipt of a death trigger such as UV-irradiation, cytotoxic drug treatment or serum-deprivation, a loss in the inner mitochondrial transmembrane potential ($\Delta\psi m$) results in permeabilisation of the outer mitochondrial membrane, allowing the release of small death-inducing molecules such as cytochrome c, Smac/Diablo and HtrA2 (van Gurp *et al.*, 2003). The release of cytochrome c from mitochondria allows apoptosome formation for the continuous activation of Caspase-9 and Caspase-3.

Besides cytochrome c, mitochondria harbour other small death-inducing molecules. Smac/Diablo often referred to as the little devil of death, contains a mitochondrial targeting sequence that is cleaved off once it reaches its destination to reveal an N-terminal AVPIA

Figure 1.4 The two main apoptotic pathways in mammals

Apoptosis occurs in mammals via two main pathways. An extrinsic or receptor-mediated pathway is triggered by the binding of extracellular factors to membrane-bound receptors. Binding of ligand to its receptor initiates the recruitment of Procaspase-8 into the death inducing signalling complex (DISC). Caspase recruitment is mediated through the adaptor molecule FADD, that contains both death domains (DD) for interaction with the receptor, and death effector domains (DEDs) for interaction with Procaspase-8. Formation of the DISC results in Caspase-8 activation and the subsequent activation of Caspase-3. An intrinsic pathway also exists in the cell that responds to death triggers such as UV irradiation, growth factor deprivation and cytotoxic drug treatment. In this pathway, proapoptotic Bcl-2 homologues, recruited to the outer mitochondrial membrane, oligomerise to form channels through which small death-inducing molecules, such as cytochrome c and Smac/Diablo, are released. Cytochrome c binds to Apaf-1 and initiates the formation of a high molecular weight complex known as the apoptosome. Procaspase-9 becomes activated by recruitment to the apoptosome, mediated by a CARD-dependent interaction with Apaf-1. XIAP, normally bound to active Caspase-3, is sequestered away by Smac/Diablo, releasing Caspase-3 to cleave cellular substrates and execute cell death. The two pathways are largely independent of each other but converge at the point of Caspase-3 activation. Additionally, active Caspase-8 cleaves the cytosolic BH3-only molecule, Bid. Truncated Bid (tBid) translocates to mitochondria and binds Bcl-2, allowing Bax oligomers to form resulting in cytochrome c release. (Adapted from Bratton and Cohen, 2003 and Degterev *et al.*, 2003)

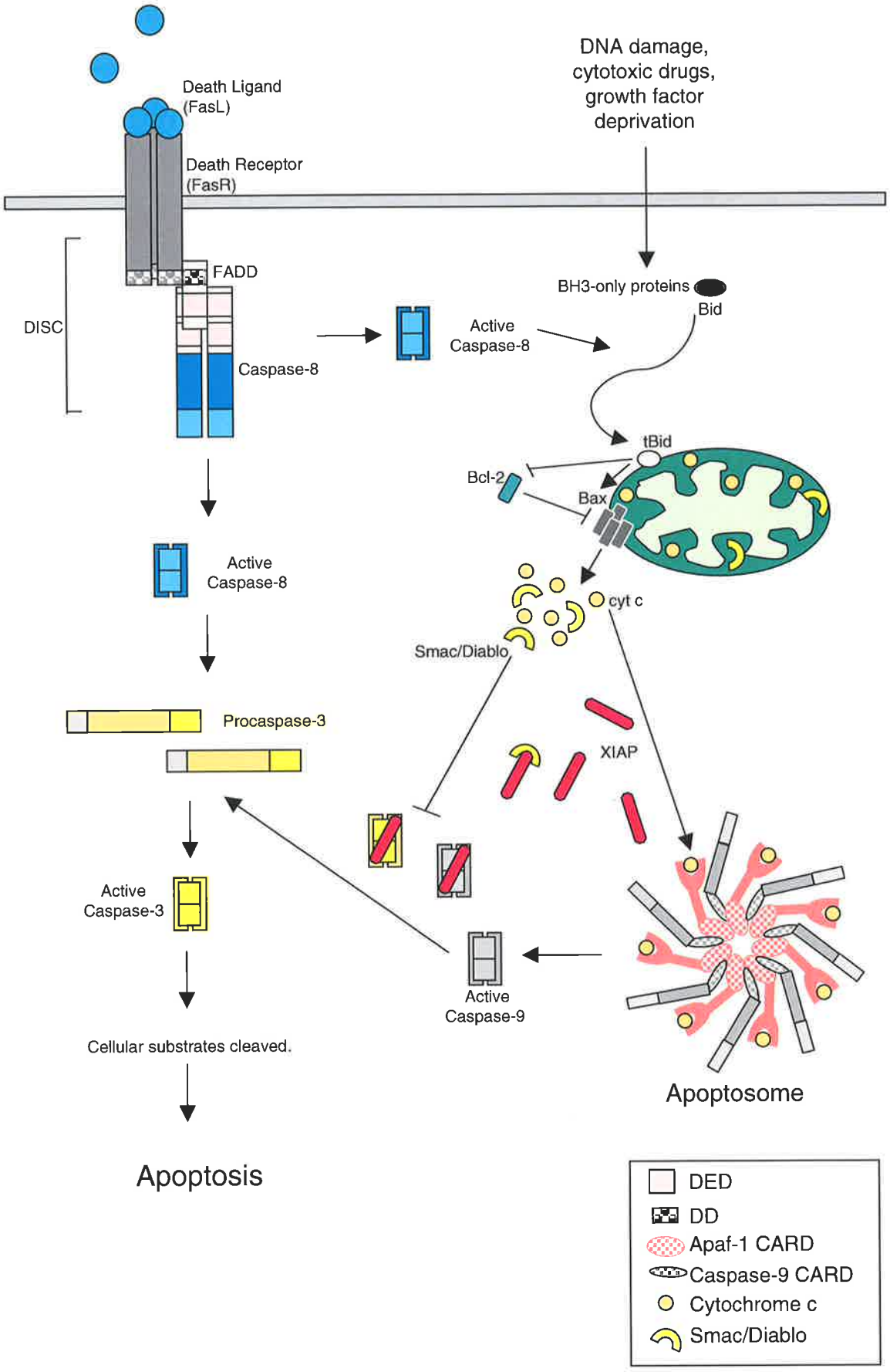
Death Ligand
(FasL)
Death Receptor
(FasR)
FADD
DISC
Caspase-8
Active
Caspase-8
DNA damage,
cytotoxic drugs,
growth factor
deprivation
BH3-only proteins
Bid
tBid
Bcl-2
Bax
cyt c
Smac/Diablo
XIAP
Active
Caspase-8
Procaspase-3
Active
Caspase-3
Cellular substrates cleaved.
Apoptosis
Active
Caspase-9
Apoptosome
DED
DD
Apaf-1 CARD
Caspase-9 CARD
Cytochrome c
Smac/Diablo

motif (Du *et al.*, 2000; Verhagen *et al.*, 2000). This motif is similar to the N-terminus of the *Drosophila* apoptosis activators, REAPER, HID and GRIM, and is required for interaction with the inhibitor of apoptosis protein XIAP (Deveraux *et al.*, 1999). Mutation of these N-terminal residues results in loss of IAP-binding thereby rendering Smac/Diablo inactive (Chai *et al.*, 2000). Structurally, the four N-terminal residues of Smac/Diablo occupy a hydrophobic pocket in both the BIR2 and BIR3 domains of XIAP, with greater affinity, however, for BIR3 (Srinivasula *et al.*, 2001; Chai *et al.*, 2000; Wu *et al.*, 2000; Liu *et al.*, 2000). Addition of Smac/Diablo to extracts releases XIAP-inhibited caspase activity (Du *et al.*, 2000). Thus, Smac/Diablo relieves the inhibition exerted by IAPs by releasing already activated, as well as dormant, caspase molecules such as Caspase-3 and Caspase-9 (Ekert *et al.*, 2001; Chai *et al.*, 2000).

Deletion of *smac/diablo* in mice does not result in severe phenotypic abnormalities besides slightly delayed Caspase-3 activation (Okada *et al.*, 2002) suggesting possible redundancy. Indeed, another Smac-like molecule, HtrA2/Omi, a serine protease, is released from mitochondria during apoptosis and reportedly inhibits XIAP through direct binding (Suzuki *et al.*, 2001a; Martins *et al.*, 2002a, 2002b; van Loo *et al.*, 2002; Verhagen *et al.*, 2002). As with Smac/Diablo, HtrA2 is mitochondrially-targeted when the targeting sequence is removed to reveal a Smac- and REAPER/HID/GRIM-like IAP-binding motif. Mutation of the N-terminal alanine renders HtrA2 incapable of binding XIAP (Verhagen *et al.*, 2002). The bacterial homologue of HtrA2 aids in the refolding of misfolded proteins (Spiess *et al.*, 1999) and, given the broad conservation of this molecule, a similar function has been suggested in mammals (Spiess *et al.*, 1999). Whether mechanisms exist to selectively release specific, individual IAP antagonists, and the apoptosome cofactor cytochrome c, remains to be determined. Regardless of the mechanism of release, mitochondria conceal potent weapons that rapidly cause cell death upon release.

Regulation of the intrinsic pathway is two-fold. While active caspases as well as procaspase molecules are bound by IAPs to prevent apoptosis and maintain cell viability, the Bcl-2 family of proteins regulate cytochrome c release at the point of mitochondria.

1.7 Bcl-2 family proteins

Bcl-2 was the first protein identified at the molecular level as an apoptosis regulator for its involvement in a chromosome translocation resulting in human B-cell lymphoma (Tsujimoto *et al.*, 1984). Vaux *et al.* (1988) demonstrated that the upregulation of Bcl-2 in cancer is not due to increased proliferation, but rather the promotion of cell survival. Moreover, the fundamental importance of this molecule is shown by its ability to promote cell survival in *C.elegans* (Vaux *et al.*, 1992). Bcl-2 was characterised shortly after as a structural and functional homologue of the *C.elegans* survival molecule CED-9 (Hengartner and Horvitz, 1994a).

To date, there are at least 20 Bcl-2 family members in mammals, and most species have at least one Bcl-2 homologue (figure 1.5). Family members all possess a Bcl-2 Homology (BH)3 domain and are classified into distinct groups based upon the presence or absence of BH1, BH2 and BH4 domains. The prosurvival molecules, including Bcl-2 itself, Bcl-X_L, Bcl-w, A1 and Mcl-1, act to protect cells from death-inducing signals such as deprivation of cytokines, irradiation and cytotoxic drugs (Cory *et al.*, 2003). These molecules possess BH1-BH3 domains as well as a BH4 domain only present in prosurvival family members. Knockout studies have shown that *bcl-2*-deficient mice are viable but die within a few months of birth due to polycystic kidney-induced renal failure (Veis *et al.*, 1993). Lymphocytes from these mice are susceptible to apoptotic stimuli due to loss of Bcl-2 activity. Mice deficient in *bcl-X_L* are embryonic lethal with extensive ectopic apoptosis observed in differentiating neurons, spinal cord and dorsal root ganglia (Motoyama *et al.*, 1995). The differences in knockout phenotypes of *bcl-2* and *bcl-X_L* demonstrate the importance of these molecules in distinct pathways of survival. Knockout mice lacking *bcl-*

Figure 1.5 The mammalian Bcl-2 family

A schematic representation of the Bcl-2 family in mammals, with their *C. elegans* homologues shown in italics. Members of the Bcl-2 family all contain a Bcl-2 homology 3 (BH3) domain. Members of the prosurvival faction also contain BH1, BH2 and BH4 domains, while proapoptotic Bcl-2 homologues lack the N-terminal BH4 domain. The proapoptotic molecules are further subdivided into two main groups. The Bax-like proteins have BH1-BH3 domains while the BH3-only subgroup only contain a BH3 domain, as their name suggests. Additionally, most Bcl-2 homologues contain a C-terminal, hydrophobic membrane anchor that targets Bcl-2 proteins to intracellular membranes of the mitochondria, endoplasmic reticulum and nuclear envelope.

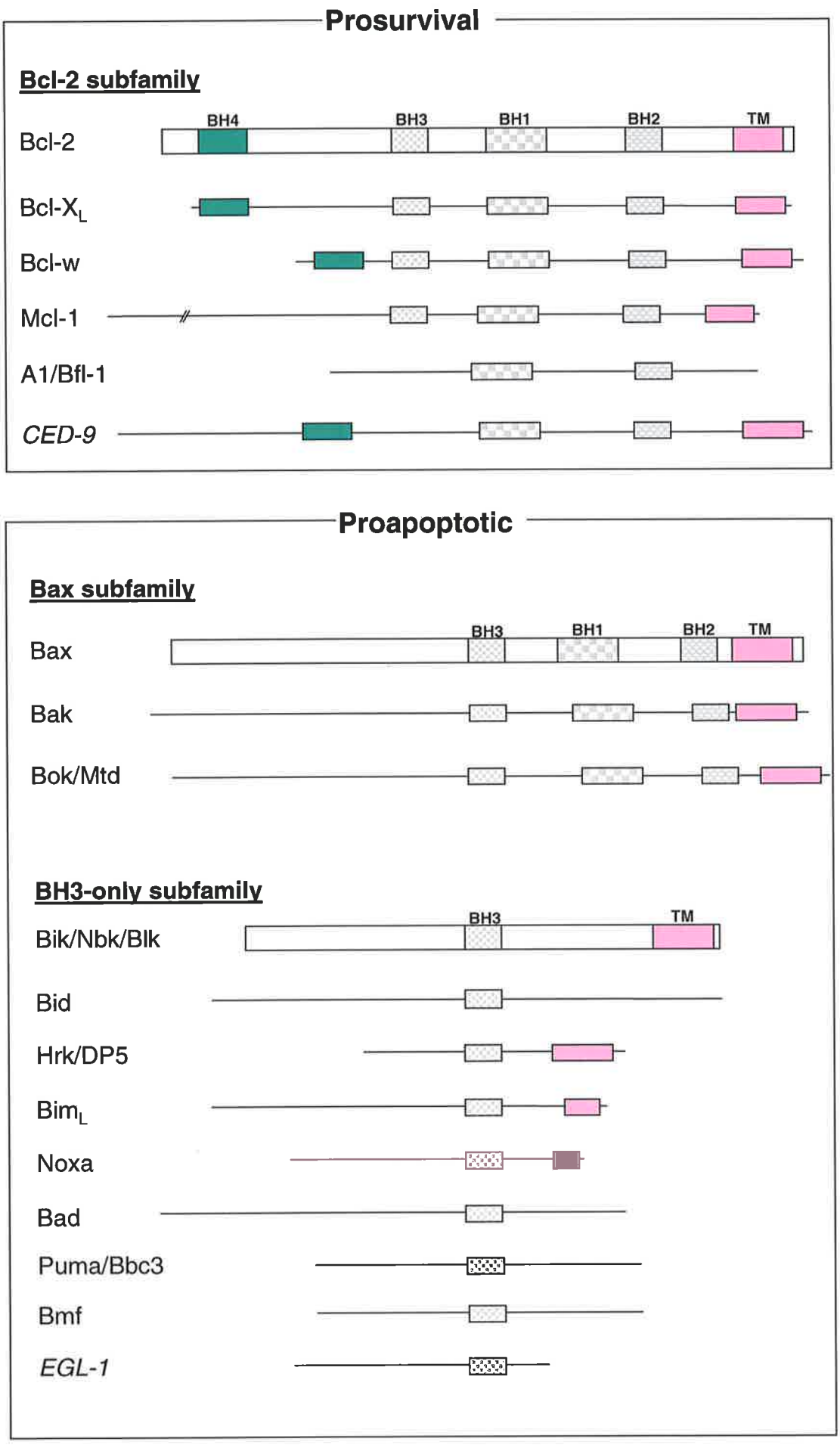
Prosurvival
Bcl-2 subfamily
BH4
BH3
BH1
BH2
TM
Bcl-2
Bcl-X$_L$
Bcl-w
Mcl-1
A1/Bfl-1
CED-9
Proapoptotic
Bax subfamily
BH3
BH1
BH2
TM
Bax
Bak
Bok/Mtd
BH3-only subfamily
BH3
TM
Bik/Nbk/Blk
Bid
Hrk/DP5
Bim$_L$
Noxa
Bad
Puma/Bbc3
Bmf
EGL-1

w, *A1* or *mcl-1* reveal specific roles for these prosurvival molecules. Bcl-w and Mcl-1 affect fertility in distinct ways. Bcl-w is implicated in spermatogenesis (Print *et al.*, 1998; Ross *et al.*, 1998) whereas *mcl-1*-deficient mice are embryonic lethal due to implantation defects (Rinkenberger *et al.*, 2000). *A1*-deficient mice are defective in neutrophil apoptosis (Hamasaki *et al.*, 1998).

Bax-like molecules are proapoptotic in nature and are structurally similar to their prosurvival counterparts, except for the absence of a BH4 domain. They include Bax, Bak and Bok. The role of Bak and Bax clearly overlap since knocking out one or the other has little effect on the viability of the mouse. *bax*-deficient mice have abnormalities in haematopoietic and neuronal development (Knudson *et al.*, 1995; Knudson and Korsmeyer, 1997). Bax has been implicated in neuronal cell death since apoptosis in the central nervous system is decreased in mice lacking Bax (White *et al.*, 1998; Deckwerth *et al.*, 1996; Miller *et al.*, 1997). In addition, *bax*-deficient males are sterile (Knudson and Korsmeyer, 1997) while females exhibit prolonged ovarian function due to a lack of apoptosis in primordial follicles (Perez *et al.*, 1999). *bak*-deficient mice are viable without developing age-related disorders (Lindsten *et al.*, 2000).

Strikingly, crossing the progeny of each knockout line to produce offspring lacking both *bax* and *bak* has a dramatic effect on animal viability with 90% of the progeny dying at birth (Lindsten *et al.*, 2000). Surviving mice display apoptosis-related abnormalities including the persistence of interdigital webbing, accumulated cells of the central nervous and haematopoietic systems and an imperforate vaginal canal (Lindsten *et al.*, 2000). These knockout studies reveal the redundant function of each individual molecule, with a requirement for at least Bax or Bak in the mammalian cell death pathway.

The third group of Bcl-2 family members contain only a BH3 domain and otherwise share minimal sequence homology with other family members. Hence, this group is referred to as the BH3-only group of proapoptotic proteins that includes Bid, Bim, Bad, Noxa, Bmf

and Puma (Puthalakath and Strasser, 2002). BH3-only proteins are homologues to the *C.elegans* death-inducer, EGL-1. BH3-only molecules are discussed in more detail below.

Structural studies have shown that BH1, BH2 and BH3 domains form a hydrophobic groove in both the prosurvival and proapoptotic molecules (Suzuki *et al.*, 2000; Petros *et al.*, 2001; Hinds *et al.*, 2003). In Bcl-X_L, this hydrophobic groove provides a docking site for the BH3 domain α-helix of the BH3-only molecule Bad (Petros *et al.*, 2001). The hydrophobic groove of Bcl-w houses its own C-terminal membrane anchor (Hinds *et al.*, 2003), which suggests a possible regulatory role for the transmembrane domain.

The mechanism by which the Bcl-2 family of proteins regulate the intrinsic/mitochondrial pathway of apoptosis is still a controversial issue (Cory *et al.*, 2003). One hypothesis is that the ratio of proapoptotic versus prosurvival Bcl-2 homologues is critical. Bcl-2 family members are able to form homo- and heterodimers. A high ratio of the prosurvival molecule, Bcl-2, sequesters propapoptotic molecules, such as Bax, preventing Bax homodimerisation on the mitochondrial outer membrane. Bax oligomers are proposed to form channels in the lipid membrane that allow the efflux of cytochrome c from the inner mitochondrial matrix (Antonsson *et al.*, 2000; Saito *et al.*, 2000; Roucou *et al.*, 2002b). Indeed, Bax has been shown to be present in high molecular weight complexes associated with the mitochondrial outer membrane in HeLa cells induced to undergo apoptosis (Antonsson *et al.*, 2001). Such oligomers are prevented from forming by Bcl-2 (Antonsson *et al.*, 2001; Mikhailov *et al.*, 2001).

Another hypothesis is that Bcl-2 family members interact with the voltage-dependent anion channel (VDAC) and either promote or prevent its opening and release of death inducing factors residing within the mitochondrial membranes (Shimizu *et al.*, 1999; 2001). VDAC and adenine nucleotide translocator (ANT), located on the outer and inner mitochondrial membranes respectively, function together to form the permeability transition (PT) pore, which acts as a non-selective channel for small molecules. However, this proposal has not been widely accepted, with reports demonstrating that high molecular weight

complexes comprised of Bax homodimers do not contain either VDAC or ANT (Antonsson *et al.*, 2001; Mikhailov *et al.*, 2001). What is clear is that activated Bax-like molecules cause membrane damage and the release of apoptosis inducers like cytochrome c, Smac/Diablo and Omi/HtrA2 (Liu *et al.*, 1996; Du *et al.*, 2000; Verhagen *et al.*, 2002; Suzuki *et al.*, 2001a).

1.7.1 BH3-only proteins

It is currently thought that the BH3-only proteins confer tissue-specificity by triggering apoptosis in response to specific cellular stresses in different cell types. BH3-only molecules are differentially expressed, and respond to different death-inducing stimuli (Puthalakath and Strasser, 2002). While *bim*-deficient lymphocytes are resistant to certain Bcl-2-antagonised death stimuli such as cytokine deprivation and calcium flux, sensitivity to other stimuli, like DNA damage and glucocorticoid treatment, remains (Bouillet *et al.*, 1999). Bim is required for the cell death of lymphocytes (Bouillet *et al.*, 2002) and T cell apoptosis (Hildeman *et al.*, 2002) in response to growth factor withdrawal, calcium flux or treatment with the cytoxic drug paclitaxel, but not by γ-irradiation (Bouillet *et al.*, 1999) demonstrating the signal-specific response of Bim.

Other BH3-only proteins are upregulated at the level of transcription to exert their proapoptotic function in specific ways. Expression of *noxa* and *puma* increases in response to the tumour suppressor p53 (Oda *et al.*, 2000; Han *et al.*, 2001; Nakano and Vousden, 2001), similar to their *C.elegans* counterpart *egl-1* that is upregulated by CEP-1, a p53-homologue, in response to DNA damage in germline cells (Hofmann *et al.*, 2002). *bid* is also reportedly upregulated by p53 and is involved in the p53 pathway of tumour suppression (Sax *et al.*, 2002). *bim* is upregulated transcriptionally by the Forkhead transcription factor (Dijkers *et al.*, 2000; Shinjyo *et al.*, 2001), which lies downstream of AKT/PKB in the phosphatidylinositol 3-kinase (PI3-K) survival pathway. Phosphorylated Forkhead, present in healthy cells, is excluded from the nucleus, preventing its function as a transcription factor.

Other BH3-only proteins undergo post-translational modifications that alter the localisation and function of these molecules (discussed below).

Activated BH3-only proteins rely upon Bax and Bak, which mediate the downstream assault on mitochondria. The requirement for Bax and Bak in apoptosis triggered by the BH3-only molecules is demonstrated in *bax*$^{-/-}$*bak*$^{-/-}$ cells that are resistant to tBid-induced cytochrome c release and apoptosis (Wei *et al.*, 2001). Moreover, cells deficient for *bax* and *bak* are resistant to apoptosis induced by all BH3-only members including Bad, Bim and Noxa (Cheng *et al.*, 2001). Hence, it is clear that the proapoptotic Bcl-2 homologues Bax and Bak are required for induction of cytochrome c release and apoptosis triggered by the BH3-only proteins.

1.7.2 Localisation of Bcl-2 family proteins

With some exceptions, most Bcl-2 family members contain a hydrophobic C-terminal domain required for targeting the molecule to intracellular membranes of the mitochondria, endoplasmic reticulum and nuclear envelope. Appropriate subcellular localisation is critical for the function of both prosurvival and proapoptotic Bcl-2-like molecules (Schinzel *et al.*, 2004). The anti-apoptotic Bcl-2 homologue Mcl-1 is normally localised to mitochondria in transfected cells but becomes diffuse in the cytosol when the C-terminal membrane anchor is removed (Akgul *et al.*, 2000). The transmembrane anchor of Bcl-rambo, a proapoptotic molecule, is required for its localisation to mitochondria and for its death-inducing activity (Kataoka *et al.*, 2001). Bax is predominantly present in the cytosol in healthy mouse thymocytes, but becomes membrane-bound upon induction of apoptosis by dexamethasone or γ-irradiation (Hsu *et al.*, 1997), with a requirement for the membrane anchor in mediating its mitochondrial targeting (Nechushtan *et al.*, 1999). A similar shift in Bax localisation in tumour cell lines treated with etoposide or staursporine was reported by Murphy *et al.* (2000). Overexpression of Bcl-2 prevents Bax translocation to mitochondrial membranes, thereby preventing cytochrome c release, caspase activation and apoptosis (Murphy *et al.*, 2000),

highlighting the importance of intracellular localisation in the control of apoptosis by Bcl-2 family proteins. Some researchers have also postulated that the C-terminal membrane anchor acts as a negative regulatory domain. Indeed, an intramolecular interaction between the C-terminal membrane anchor of Bax with an N-terminal epitope maintains Bax as a cytosolic molecule. Induction of apoptosis induces a conformational change that exposes the membrane anchor allowing it to insert into the mitochondrial outer membrane (Nechushtan *et al.*, 1999). Structural analysis of Bax later showed that, similar to Bcl-w, the hydrophobic membrane anchor occupies the receptor groove formed by the BH1-3 domains, considered to mediate heterodimerisation with prosurvival family members (Suzuki *et al.*, 2000; Hinds *et al.*, 2003).

Bcl-2 and Bcl-X_L reside on membranes in healthy cells. Recently, mutagenesis was employed to analyse the differential localisation of Bcl-2 and Bcl-X_L (Kaufmann *et al.*, 2003). Bcl-2 targets to the endoplasmic reticulum (ER), mitochondria and nuclear envelopes (Lithgow *et al.*, 1994; Kaufmann *et al.*, 2003), whereas Bcl-X_L is almost exclusively mitochondrial (Kaufmann *et al.*, 2003). Multiple positively charged amino acids flanking the transmembrane domain (TMB) of Bcl-X_L are responsible for mitochondrial targeting, whereas the absence of such a strong basic charge in Bcl-2 allows its distribution to other membranous organelles like the ER and nuclear envelope (Kaufmann *et al.*, 2003). Membrane localisation mediated by the TMB is critical for the function of Bcl-2 as deletion of this domain renders the molecule incapable of protecting Jurkat cells from apoptotic insults such as radiation (Rudner *et al.*, 2001). Moreover, a chimeric, ER-targeted Bcl-2 protects cells against radiation-induced apoptosis similarly to mitochondrially-targeted Bcl-2 (Rudner *et al.*, 2001).

The importance of intracellular localisation is also demonstrated in members of the BH3-only protein group. In healthy cells, where survival factors such as AKT and PKA are active, Bad is phosphorylated and detained in the cytosol via interaction with 14-3-3 (Zha *et al.*, 1996, 1997; Datta *et al.*, 1997; Harada *et al.*, 1999). Phosphorylation prevents the binding

of Bad to Bcl-X_L allowing it to exert its prosurvival function in the cell (Datta *et al.*, 2000). Dephosphorylation releases Bad from its cytosolic detention, allowing it to translocate to mitochondria, bind prosurvival Bcl-2 proteins, and initiate the intrinsic pathway of cell death (Wang, H.G. *et al.*, 1999).

Bim and Bmf are associated with the dynein motor complex and the myosin V motor complex respectively and are released in response to different signals (Puthalakath *et al.*, 1999; Puthalakath *et al.*, 2001). Bid normally resides in the cytoplasm but once cleaved by Caspase-8 to become tBid, becomes a potent death-inducer, translocating to mitochondria, causing cytochrome c release and apoptosis (Li *et al.*, 1998; Luo *et al.*, 1998). Thus, it is clear that post-translational modifications and transcriptional upregulation control the expression and activity of BH3-only proteins.

1.8 *Drosophila melanogaster* as a model organism for studying apoptosis

The fruitfly, *Drosophila melanogaster*, has always been utilised to study complex pathways, including apoptosis. The fly has many advantages in the delineation of genetic pathways including the availability of the sequence of the entire genome, its amenability to genetic manipulation and the ease with which sophisticated genetic approaches can be implemented. While redundancy in mammals can confuse knockout mouse phenotypes, the simpler *Drosophila* system can be used to elucidate the role of functional homologues in specific biological pathways.

Drosophila has been used in the study of human disease, especially human neurodegenerative diseases. There is a high level of genetic conservation between flies and humans (Rubin *et al.*, 2000) and *Drosophila* have a complex central nervous system that is amenable to the study of neurodegenerative behaviours. Models for Alzheimer's disease, Parkinson's disease, and polyglutamine repeat diseases such as Huntington's disease, have been established in *Drosophila* and are used to study the pathogenesis of these disorders (Chan and Bonini, 2000).

1.9 Apoptotic machinery in *Drosophila*

The cell death pathway in *Drosophila* is highly conserved. The *Drosophila* genome encodes homologues for most of the key molecules characterised from *C.elegans* and mammals (Table 1.1). Additionally, three genes encoding IAP-binding proteins, REAPER, HID and GRIM, functionally similar to Smac/Diablo, were first isolated in *Drosophila* and found to be essential for developmental cell death in the fly.

C. elegans	**Mammals**	***Drosophila***
	Smac/Diablo	REAPER, HID, GRIM
EGL-1	BH3-only proteins	?
CED-3	Caspase family	DRONC, DREDD, STRICA, DRICE, DCP-1, DECAY, DAMM
CED-4	Apaf-1	DARK
CED-9	Bcl-2 family	DEBCL, BUFFY
	XIAP, cIAP1, cIAP2	DIAP1, DIAP2
	FADD	dFADD
	TNF	Eiger
	TNFR	Wengen

Table 1.1 Conservation of the apoptotic machinery

The main components of the apoptotic pathway in worms, flies and mammals are shown. The *Drosophila* genome encodes homologues for almost all the key apoptotic molecules.

1.9.1 The H99 locus –*reaper*, *grim* and *hid*

The H99 deficiency, identified in genetic screens, spans a region responsible for all developmental cell death events in the fly (White *et al.*, 1994). Although apoptosis can be induced by x-irradiation, suggesting that the execution of apoptosis is preserved, the initiation

of apoptosis is severely abrogated in developing H99 deletion embryos, implicating the H99 gene products in the activation of apoptosis.

reaper was the first gene identified within this region (White *et al.*, 1994). *reaper* encodes a protein of 65 amino acids, and is expressed in cells prior to apoptotic cell death. Furthermore, overexpression of REAPER in the eye induces massive cell death resulting in a small eye phenotype (White *et al.*, 1996). REAPER-induced cell death in *Drosophila* schneider (S2) cells is accompanied by the classic morphological features of apoptosis and is caspase-dependent (Pronk *et al.*, 1996). *reaper* null flies display enlarged central nervous systems and male sterility, implicating REAPER in normal central nervous system apoptosis and gametogenesis in the fly (Peterson *et al.*, 2002). *reaper* is upregulated by the E93 transcription factor in response to the steroid hormone ecdysone, which mediates normal metamorphic changes in the fly (Lee *et al.*, 2002a, 2002b). The promoter region of *reaper* contains consensus binding sites for the *Drosophila* p53 homologue, Dmp53, demonstrating the involvement of REAPER in the p53 pathway in the fly (Brodsky *et al.*, 2000).

Two other activators of cell death were subsequently identified in the H99 region. The 410 amino acid protein product of the *head involution defective* (*hid*) gene behaves similarly to REAPER with the ability to induce apoptosis when expressed in both wildtype and H99 mutant embryos (Grether *et al.*, 1995). Ectopic expression of HID in the *Drosophila* eye shows a severe small eye phenotype as a result of ectopic programmed cell death. The caspase inhibitor, p35, can suppress this phenotype when coexpressed with HID in the eye. Homozygous *hid* mutants are embryonic lethal with extensive defects in apoptosis (Haining *et al.*, 1999). HID induces apoptosis in mammalian cells and localises to mitochondria via a C-terminal hydrophobic region (Haining *et al.*, 1999). HID is downregulated by the Ras/MAPK survival pathway (Bergmann *et al.*, 1998; Kurada and White, 1998). MAPK phosphorylation sites in HID are critical for downregulation, linking a phosphorylation signalling pathway to the regulation of apoptosis.

The third gene in the H99 region, *grim*, encodes a polypeptide of 138 amino acids. Like REAPER and HID, GRIM is able to induce apoptosis in H99 embryos and cultured cells, and localises to both the cytoplasm and mitochondria in mouse fibroblasts (Chen *et al.*, 1996; Claveria *et al.*, 1998). REAPER, HID and GRIM share a similar 14 amino acid N-terminus known as the RHG (REAPER/HID/GRIM) motif (Wing *et al.*, 1998). The peptide sequences outside of this motif share little similarity.

REAPER, HID and GRIM are functionally similar to Smac/Diablo in mammals, and exert their proapoptotic function by acting on *Drosophila* IAPs, such as DIAP1, to relieve their inhibition over caspases. IAPs can suppress REAPER-induced cell death by physical association between REAPER and the BIR domains of the IAP (Vucic *et al.*, 1997a). DIAP1 gain-of-function mutants suppress REAPER-, HID- and GRIM-induced cell death *in vivo*, however suppression is abolished when the BIR domains of DIAP1 are mutated (Goyal *et al.*, 2000). The crystal structure of DIAP1-BIR2 complexed to the N-terminal peptides of GRIM and HID reveal that the peptides bind to a groove on DIAP1 (Wu *et al.*, 2001). REAPER, HID and GRIM cause the downregulation of DIAP1 protein levels and, in the case of HID, downregulation requires the ubiquitin ligase activity of the DIAP1 RING domain (Yoo *et al.*, 2002). Conflicting results exist however, with Hays *et al.* (2002) reporting that REAPER and GRIM, but not HID, promote DIAP1 degradation *in vivo*. The identification of enhancers of GRIM- and REAPER-induced apoptosis that are involved in the ubiquitin pathway strengthens the evidence that the binding of DIAP1 by GRIM and REAPER leads to proteasomal degradation of DIAP1 (Wing *et al.*, 2002b).

Mapping just outside the H99 region, *sickle* encodes another IAP antagonist in *Drosophila*, capable of inducing cell death when overexpressed in cell lines and *Drosophila* embryos (Christich *et al.*, 2002; Srinivasula *et al.*, 2002; Wing *et al.*, 2002a). SICKLE possesses the N-terminal amino acids shared by other IAP-binding molecules including REAPER, HID and GRIM, and Smac/Diablo in mammals, and binds the BIR2 domain of DIAP1. Another molecule possessing the N-terminal IAP-binding motif, Jafrac2, localises to

the endoplasmic reticulum until its release into the cytosol when apoptosis is induced (Tenev *et al.*, 2002). Jafrac2, a thioredoxin peroxidase induces apoptosis in the fly eye and cultured cells and interacts with DIAP1. IAP antagonists share little sequence homology, with the exception of several N-terminal amino acids, making the identification of further IAP antagonists dependent on functional assays.

1.9.2 *Drosophila* Caspases

There are seven caspases in *Drosophila melanogaster*. Two of these, DRONC and DREDD are classified as upstream/initiator caspases based on the presence of long prodomains. Four of these caspases, DCP-1, DRICE, DECAY and DAMM, lack long prodomains and are therefore considered to be downstream/executioner caspases, requiring activation by initiator caspases before executing cell death. The characterisation of the seventh caspase, STRICA, is presented in this thesis.

a) DCP-1

The first caspase identified in *Drosophila*, DCP-1, contains a short prodomain with a strong caspase cleavage site marking the end of the prodomain. This caspase shares substrate specificity with mammalian Caspase-3 and therefore functions as a downstream caspase (Song *et al.*, 1997).

A null mutant of *dcp-1* initially suggested a critical role for DCP-1 in the apoptosis of nurse cells during normal oogenesis (McCall and Steller, 1998). However, it came to light that an adjacent gene was also deleted in these flies and contributed to the mutant phenotypes reported (Laundrie *et al.*, 2003). The adjacent gene, *pita*, deleted by P-element insertions in the *dcp-1* gene has recently been shown to encode a C2H2 zinc-finger protein. Loss of both of these genes was found to contribute to the lethality and defective nurse cell death previously attributed to DCP-1 (Laundrie *et al.*, 2003). While DCP-1 is essential for

apoptosis during mid-oogenesis, homozygous *pita* mutants are lethal and display dumpless egg chambers and premature apoptosis of nurse cells.

b) DRICE

The *Drosophila* caspase DRICE is an effector caspase similar to DCP-1 and is expressed at all developmental stages where programmed cell death occurs (Fraser and Evan 1997). Overexpression of DRICE sensitises *Drosophila* S2 cells to apoptotic triggers and DRICE is processed when apoptosis is induced by REAPER or cycloheximide (Fraser *et al.*, 1997). Activation of DRICE in lysates induced to die by overexpression of REAPER is due to the activity of DRONC, since processing of DRICE is dependent on DRONC activation (Dorstyn *et al.*, 2002). Like *reaper* and *dronc*, *drice* has been reported to be upregulated by the steroid hormone ecdysone during *Drosophila* development (Lee *et al.*, 2002a, 2002b). Overexpression of DRICE in the *Drosophila* retina shows no significant abnormalities, perhaps due the inability of DRICE to autoprocess (Song *et al.*, 1997). DRICE has recently been implicated in germline development. DRICE is activated in mid and late stage oogenesis with higher expression of DRICE observed during mid oogenesis and limited expression in late oogenesis (Peterson *et al.*, 2003). The process of spermatid individualisation also appears to require the activity of DRICE (Huh *et al.*, 2004).

c) DECAY

The fifth *Drosophila* caspase to be identified was called DECAY (*Drosophila* Executioner Caspase related to Apopain/Yama) (Dorstyn *et al.*, 1999b). Lacking a long prodomain, and with high homology to Caspase-3 and Caspase-7, DECAY is classified as a downstream, effector caspase. Overexpression of DECAY in cultured *Drosophila* S2 cells induces apoptosis. Recombinant DECAY was also shown to be active on fluorogenic substrates DEVD and VDVAD and can cleave *in vitro* translated PARP (Poly ADP-ribose polymerase). *decay* transcript is expressed at low levels throughout *Drosophila* development

and no upregulation is observed during metamorphosis in response to ecdysone. *decay* is expressed in tissues such as midgut, salivary gland and ovaries, where apoptosis occurs at various developmental stages (Dorstyn *et al.*, 1999b). The significance of DECAY in programmed cell death in *Drosophila* has not been fully elucidated.

e) DAMM

Harvey *et al.* (2001) identified the short prodomain caspase DAMM as a Death Associated Molecule related to Mch2 (Caspase-6). DAMM is able to induce apoptosis when overexpressed in mammalian and insect cells albeit at low levels. DAMM-induced cell death is inhibited by DIAP1, DIAP2 and p35. The functional significance of this caspase remains to be elucidated but it may be involved in a HID-mediated cell death pathway (Harvey *et al.*, 2001).

e) DRONC

The apical caspase, DRONC, is the only CARD-containing caspase in *Drosophila* (Dorstyn *et al.*, 1999a). *dronc* is differentially expressed throughout development, with upregulation of the *dronc* transcript observed at the late third instar larval and early pupal stages. Expression of *dronc* at these stages corresponds to two pulses of the steroid hormone ecdysone and mediates the changes associated with metamorphosis (Dorstyn *et al.*, 1999a). The ecdysone receptor binds the *dronc* promoter directly (Cakouros et al., 2004). The *dronc* promoter also contains binding sites for several transcription factors that govern the transcriptional expression of *dronc* in different larval tissues undergoing cell death such as midgut and salivary gland (Cakouros *et al.*, 2002). In flies that are mutant for the transcription factor, Broad complex (BR-C), expression of DRONC is reduced or ablated. Additionally, apoptosis induced by ecdysone in a responsive *Drosophila* cell line, *l(2)*mbn, is absolutely dependent on the presence of DRONC (Cakouros *et al.*, 2002).

dronc null mutants are pupal lethal and have midgut and salivary glands that persist beyond the normal temporal histolysis of these tissues (Daish *et al.*, unpublished data). RNAi ablation of the *dronc* transcript in early embryos results in a decrease in embryonic cell death, further demonstrating an essential role for DRONC in developmental apoptosis (Quinn *et al.*, 2000).

Overexpression of DRONC in the fly eye results in a small, rough eye phenotype due to ectopic cell death. Inappropriate apoptosis induced by DRONC is inhibited by DIAP1 and p35 (Quinn *et al.*, 2000). Interestingly, DIAP1 fails to rescue the apoptotic phenotype induced by ectopic expression of DRONC lacking the prodomain, consistent with the observation that the DRONC prodomain is required for the interaction with DIAP1 (Meier *et al.*, 2000).

Halving the dosage of the H99 genes enhances apoptosis induced by DRONC in the eye, placing DRONC downstream of REAPER, HID and GRIM, in the major apoptotic pathway in flies (Quinn *et al.*, 2000). . DRONC has been shown to genetically interact with many apoptotic molecules, including DIAP1 and the Apaf-1 homologue DARK (Quinn *et al.*, 2000). The C-terminal RING domain of DIAP1 functions as an E3 ubiquitin ligase and reportedly targets DRONC for degradation via the proteasome (Muro *et al.*, 2002). This inhibition is relieved by REAPER, which binds directly to DIAP1 (Chai *et al.*, 2003).

DRONC is unique amongst other caspases in some regards. The active sites of most caspases conform to the QAC R/Q/K G consensus whereas DRONC has an active site PFCRG (Dorstyn *et al.*, 1999a). Unlike other caspases, DRONC has been shown to cleave substrates following a glutamate residue and has been reported to cleave DIAP1 following a glutamate residue (Yan *et al.*, 2004). DRONC has also been shown to autoprocess itself following a glutamate residue but processes the downstream caspase DRICE at the classic aspartate residue (Hawkins *et al.*, 2000). In a positive feedback mechanism, DRICE is able to cleave DRONC, preventing the inhibition of DRONC by DIAP1 (Kaiser *et al.*, 1998).

DRONC is structurally and functionally similar to mammalian Caspase-9. The interaction between DRONC and DARK suggests that a high molecular weight complex resembling an apoptosome may form to activate DRONC and subsequently activate the effector caspase DRICE. Although DRONC is recruited to a high molecular weight complex *in vitro* (Dorstyn *et al.*, 2002), this complex is active in the absence of a release of cytochrome c from the mitochondria (Dorstyn *et al.*, unpublished data). A significant proportion of DRONC and DRICE localises near mitochondria suggesting the possibility that an apoptosome-like complex may form at mitochondria without the need for cytochrome c release (Dorstyn *et al.*, 2002).

f) DREDD

The *Drosophila* caspase, DREDD (Death-Related ced-3/NEDD2-like gene) was isolated from an embryonic cDNA library (Chen *et al.*, 1998). DREDD is a long prodomain-containing caspase that contains two death effector domains (DEDs), making DREDD the likely homologue of mammalian Caspase-8. Consistent with this, DREDD interacts with the *Drosophila* homologue of the adapter molecule FADD, dFADD via a unique death-inducing domain (DID) present in both molecules (Hu and Yang 2000). This interaction enhances the death-inducing activity of DREDD and induces DREDD processing.

The *dredd* transcript is present in early embryos prior to the onset of zygotic expression, and accumulates in *Drosophila* tissues that undergo extensive developmental cell death, including the brain and ventral nerve cord (Chen *et al.*, 1998). *dredd* also accumulates to high levels during oogenesis, at a time when extensive apoptosis of nurse cells occurs. However, *dredd* fails to accumulate in embryos homozygous for the H99 deficiency in which the cell death activators, REAPER, HID and GRIM are absent (Chen *et al.*, 1998). Furthermore, targeted ectopic expression of *reaper*, *hid* and *grim* individually using the UAS/Gal4 system results in the accumulation of *dredd* transcripts in tissues where *dredd* is

not normally widely expressed, emphasising the direct relationship between REAPER-, HID- and GRIM-induced apoptosis and *dredd* accumulation (Chen *et al.*, 1998).

Unlike most caspases, overexpression of full-length DREDD or prodomain-deleted DREDD in *Drosophila* S2 cells does not induce apoptosis and processing is not observed (Chen *et al.*, 1998). However processing of DREDD is observed when coexpressed with REAPER, HID or GRIM. In addition, cell killing induced by REAPER and GRIM is suppressed by heterozygosity at the *dredd* locus (Chen *et al.*, 1998), placing DREDD downstream of REAPER and GRIM in the apoptotic pathway.

The involvement of DREDD in the innate immune response in *Drosophila* demonstrates a unique, non-apoptotic, role for this caspase. Specific anti-microbial peptide-encoding genes are induced in response to microbial infection (Imler and Hoffmann, 2000; Khush and Lemaitre, 2000). Flies carrying loss-of-function mutations in *dredd* were found to be susceptible to infection by gram-negative bacteria, with expression of antibacterial peptides suppressed in these flies, demonstrating that DREDD regulates the immune response in the fly (Leulier *et al.*, 2000). Mutations in *dredd* prevent induction of antibacterial genes and also prevents signalling through the NF_KB homologue, Relish (Elrod-Erickson *et al.*, 2000). The importance of DREDD in the antibacterial immune response in the fly demonstrates the role of a caspase in a physiological pathway distinct from apoptosis.

1.10 Apoptotic pathways in the fly

Although most key players in programmed cell death are conserved, some differences exist between *Drosophila* and mammals that suggest these organisms utilise molecules differently. The main apopotic pathways in the fly are represented in figure 1.6.

1.10.1 A *Drosophila* Apoptosome?

In mammals, Apaf-1 is essential for the activation of Caspase-9 via the mitochondrial pathway (Zou *et al.*, 1999). Release of cytochrome c from mitochondria, triggers the

Figure 1.6 Pathways of apoptosis in *Drosophila*

Three activators of apoptosis, REAPER, HID and GRIM, respond to apoptotic stimuli and initiate apoptosis by binding to IAPs, thereby relieving the inhibition of DIAP1 over both upstream and downstream caspases. DRONC activation is essential for cell death and requires the adaptor molecule, DARK. Activated DRONC processes and activates the downstream caspase DRICE, and cell death is executed. The steroid hormone ecdysone is required for organ sculpting during *Drosophila* metamorphosis and transcriptionally upregulates *dark*, *dronc* and *drice* temporally and spatially during fly development. The p53, DNA damage-response pathway functions in the fly with upregulation of *reaper* by the *Drosophila* p53 homologue, Dmp53. A TNF-like, receptor mediated pathway exists in the fly with the binding of Wengen by its extracellular TNF-homologous ligand, Eiger, to initiate apoptosis through JNK in a DARK/DRONC-dependent manner. Adapted from Nordstrom and Abrams, 2000.

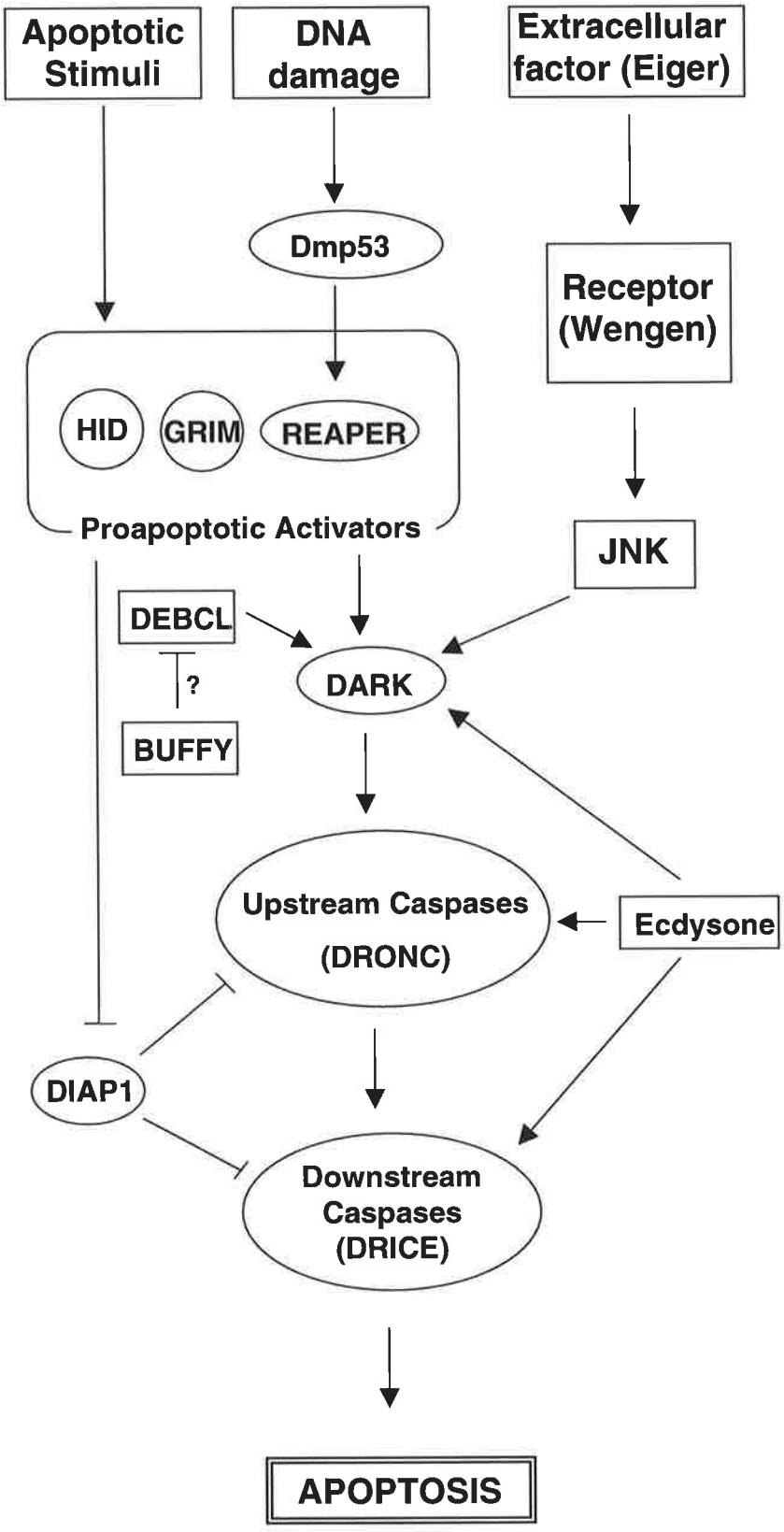
Apoptotic Stimuli
DNA damage
Extracellular factor (Eiger)
Dmp53
Receptor (Wengen)
HID
GRIM
REAPER
Proapoptotic Activators
JNK
DEBCL
?
DARK
BUFFY
Upstream Caspases (DRONC)
Ecdysone
DIAP1
Downstream Caspases (DRICE)
APOPTOSIS

formation of the apoptosome, a large complex comprised of Apaf-1 molecules associated with Procaspase-9, cytochrome c and dATP (Degterev *et al.*, 2003).

Drosophila melanogaster possess a CED-4/Apaf-1 homologue molecule named DARK/Dapaf-1/HAC-1 (Kanuka *et al.*, 1999; Rodriguez *et al.*, 1999; Zhou *et al.*, 1999). *dark* encodes a 1440 amino acid polypeptide containing an N-terminal CARD domain, a CED-4 homology domain and, in similarity with Apaf-1, WD40 repeats that can bind cytochrome c *in vitro*.

dark is expressed in regions that normally undergo apoptosis during embryonic development (Zhou *et al.*, 1999) and is transcriptionally upregulated in pregastrulation embryos in response to UVB and UVC (Zhou *et al.*, 2003). DARK induces apoptosis in cultured *Drosophila* SL2 cells with increased activity observed when the WD repeat region is removed, suggesting a possible inhibitory role for this region (Rodriguez *et al.*, 1999; Kanuka *et al.*, 1999). *dark* loss-of-function mutations cause reduced cell death in the central nervous system (CNS) in embryos, enlarged nervous systems in larvae, and pleiotrophic effects including melanotic tumours, wing defects and impaired viability in adults (Rodriguez *et al.*, 1999; Kanuka *et al.*, 1999; Zhou *et al.*, 1999). Mutations in *dark* were reported by Rodriguez *et al.* (1999) to suppress apoptosis induced by REAPER, HID and GRIM *in vivo*. Furthermore, *dark* ablation by RNAi in insect cells inhibits stress-induced apoptosis (Zimmermann *et al.*, 2002). DRONC, which functions downstream of REAPER, GRIM and HID, requires DARK for its activation (Quinn *et al.*, 2000; Dorstyn *et al.*, 2002).

Given the requirement for DARK in the activation of the apical caspase DRONC, and the presence of CARD domains in both of these molecules, it seems logical to assume that a similar mechanism of apoptosome formation and caspase activation exists in the fly. However, Dorstyn *et al.* (2002) have shown that apoptotic cells in which active DRICE is present, display mitochondrially localised cytochrome c, demonstrating that caspase activation and apoptosis proceed without the release of cytochrome c. This finding indicates

functional differences in the mechanism of caspase activation in the fly compared with the intrinsic mammalian pathway (Dorstyn *et al.*, 2002).

1.10.2 An extrinsicTNF pathway in the fly

Recently, a receptor-mediated pathway in the fly has been characterised. A gain-of-function screen was employed to identify a tumour necrosis factor (TNF) superfamily ligand named Eiger, which can induce apoptosis, causing a small eye phenotype in the *Drosophila* compound eye (Igaki *et al.*, 2002a). Eiger-induced cell death occurrs through activation of the JNK pathway and is suppressed by DIAP1 (Igaki *et al.*, 2002a; Moreno *et al.*, 2002). Eiger has been reported to act independently of the Caspase-8 homologue, DREDD, while requiring the activity of DRONC and DARK (Moreno *et al.*, 2002).

The receptor to which Eiger binds and signals through, Wengen, belongs to the TNF receptor superfamily and is characterised by the presence of a conserved TNFR homology domain in the extracellular region. *wengen* is expressed throughout development and downregulation of *wengen* by RNAi suppresses cell death caused by overexpression of Eiger (Kanda *et al.*, 2002; Kauppila *et al.*, 2003). In addition to interacting genetically, Eiger and Wengen have been shown to physically interact (Kanda *et al.*, 2002). Thus, while a TNF receptor pathway exists in the fly, the significance of this remains to be fully elucidated.

1.11 Regulation of Apoptosis in *Drosophila*

Regulation of caspases is critical for the maintenance of cell integrity and the health of the organism. While the viral protein p35 is an effective inhibitor of caspase-induced cell death in *Drosophila*, endogenous IAPs exist in the fly and play a critical role in cell survival. *Drosophila* also possesses two Bcl-2 homologues, the roles of which are not fully understood.

1.11.1 *Drosophila* IAPs

Hay *et al.*, (1995) screened for genetic mutations that could enhance or suppress REAPER-induced apoptosis in the *Drosophila* eye and identified a lethal mutation in *thread* that enhanced the small eye phenotype resulting from REAPER overexpression. *thread* was found to encode an IAP, named DIAP1 (*Drosophila* IAP1). A second IAP, DIAP2 was also identified (Hay *et al.*, 1995). DIAP1 contains two BIR domains while DIAP2 has three. Both molecules have a C-terminal RING domain (Hay *et al.*, 1995) (figure 1.3) later found to possess ubiquitin ligase activity (Yoo *et al.*, 2002; Hays *et al.*, 2002; Ryoo *et al.*, 2002).

DIAPs exert their function by physically interacting with the N-terminal domains of the *Drosophila* death activators REAPER, HID and GRIM (Vucic *et al.*, 1997, 1998; Kaiser *et al.*, 1998). DIAP1 inhibits the activation of the *Drosophila* effector caspase, DRICE and suppresses the activity of active DRICE (Kaiser *et al.*, 1998). In *Drosophila*, DIAP1 appears to be essential for cell survival. Depletion of *diap1* by RNAi causes massive caspase-dependent cell death in *Drosophila* cell lines that is suppressed by cosilencing *dronc* or *dark* (Muro *et al.*, 2002). *In vivo*, DIAP1 mutants exhibit severe defects associated with unrestrained caspase activity, in a DARK-dependent fashion (Rodriguez *et al.*, 2002).

For apoptosis to proceed in *Drosophila*, the degradation of DIAP1 is critical and results in the rapid activation of caspases in a DARK-dependent manner (Igaki *et al.*, 2002b; Rodriguez *et al.*, 2002). REAPER has been reported to cause the degradation of DIAP1, dependent on the RING domain of DIAP1 (Ryoo *et al.*, 2002). Degradation of DIAP1 via the ubiquitin-mediated proteasomal pathway was confirmed by the interaction of DIAP1 with Morgue, a *Drosophila* protein related to a ubiquitin conjugase (Hays *et al.*, 2002). DIAP1 protein is also stabilised by the proteasome inhibitor, MG132 (Dorstyn *et al.*, unpublished results). The degradation of DIAP1 is mediated by the N-end rule pathway, whereby caspase cleavage at the N-terminus renders DIAP1 highly unstable (Ditzel *et al.*, 2003; Varshavsky, 2003). Somewhat controversial is the report that the RING finger of DIAP1 mediates the

ubiquitination and subsequent degradation of DRONC (Wilson *et al.*, 2002). It appears that although DRONC may be ubiquitinated by DIAP1, this does not result in DRONC degradation.

Structural analyses of DIAP1-BIR2 complexed with N-terminal peptides from GRIM and HID show that the first four amino acids bind a surface groove on DIAP1, similar to the binding of the mammalian death activator Smac/Diablo to XIAP (Wu *et al.*, 2001). This surface groove can also be bound by DRONC, indicating that GRIM, REAPER and HID compete for DIAP1 binding to allow for DRONC activation (Chai *et al.*, 2003). Recently, it was demonstrated that different BIR domains of DIAP1 interact with specific caspases. The effector caspases DRICE and DCP-1 bind the BIR1 domain of DIAP1, while the BIR2 domain is required for the binding and inhibition of DRONC (Zachariou *et al.*, 2003; Meier *et al.*, 2000). In the former case, proteolytic cleavage of DRICE and DCP-1 is a necessary prerequisite to DIAP1 binding (Zachariou *et al.*, 2003). Thus, BIR domains can perform distinct roles in caspase inhibition to prevent cell death.

Structural studies have recently revealed that DRICE is inhibited by DIAP1 through an interaction involving a conserved surface groove on BIR1 of DIAP1 (Yan *et al.*, 2004). The amino terminal 20 amino acids play an autoinhibitory role by occupying the surface groove, thereby preventing BIR1 from binding and inhibiting DRICE. Removal of these amino acids is required to allow inhibition (Yan *et al.*, 2004). Furthermore, REAPER, HID and GRIM competitively bind the BIR1 domain of DIAP1, relieving DIAP1-mediated inhibition of DRICE (Yan *et al.*, 2004). Interestingly, DRONC has been shown to cleave DIAP1 between the BIR1 and BIR2 domains, following a glutamate residue, *in vitro* (Yan *et al.*, 2004). Such cleavage reportedly occurs constitutively in *Drosophila* cells (personal communication cited by Yan *et al.*, 2004), although published data is awaited.

The role of DIAP2 in apoptosis is more enigmatic. Despite the ability of DIAP2 to inhibit DRONC-induced death *in vivo*, it does not physically interact with DRONC (Quinn *et al.*, 2000). DIAP1 and DIAP2 interact with the *Drosophila* Decapentaplegic (DPP) type I

receptor, Thick Veins, possibly implicating these IAPs in TGF-β superfamily kinase signalling pathways (Oeda *et al.*, 1998).

Two other inhibitors of apoptosis in *Drosophila* have been published. Deterin contains a single BIR repeat and a C-terminal RING domain and inhibits apoptosis in cultured insect cells (Jones *et al.*, 2000). The *Drosophila* homologue of BRUCE, dBRUCE inhibits REAPER and GRIM but not HID-induced apoptosis (Vernooy *et al.*, 2002).

1.11.2 *Drosophila* Bcl-2 homologues

Two Bcl-2 homologues exist in the fly, DEBCL/dBORG-1/DROB-1 and BUFFY/dBORG-2 (Colussi *et al.*, 2000; Brachmann *et al.*, 2000; Igaki *et al.*, 2000). Given that cytochrome c is not required for DRONC activation, the role of the Bcl-2 homologues in *Drosophila* remains to be fully understood (Igaki and Miura, 2004). To date, no EGL-1 homologue has been identified in the fly.

a) DEBCL

debcl encodes a 300 amino acid protein containing BH1, BH2, BH3 and a hydrophobic C-terminal membrane anchor for targeting to membranous organelles within the cell. DEBCL is most similar to the proapoptotic Bcl-2 family member Bok and, consistent with this, induces apoptosis in cultured *Drosophila* cells and in transgenic flies (Colussi *et al.*, 2000; Igaki *et al.*, 2000). *debcl* expression correlates with developmental cell death in various *Drosophila* tissues consistent with a proapoptotic role for this molecule. Additionally, *debcl* RNAi implicates DEBCL in normal cell death events during embryogenesis (Colussi *et al.*, 2000). While DEBCL genetically interacts with DIAP1 and DARK, halving the dose of *reaper*, *hid* and *grim* does not affect DEBCL-induced apoptosis (Colussi *et al.*, 2000). Like many Bcl-2 family members, upon overexpression, DEBCL localises to the mitochondrial outer membrane, dependent on the transmembrane anchor at the C-terminus of the protein (Igaki *et al.*, 2000). Interestingly, *Drosophila* S2 cells expressing DEBCL have been reported

to be protected against apoptosis induced by CED-3 expression or serum deprivation, suggesting that DEBCL may play a prosurvival role in some contexts (Brachmann *et al.*, 2000). Overexpression of DEBCL in *Drosophila* cells does not trigger the release of cytochrome c from mitochondria (Dorstyn *et al.*, 2002) suggesting that Bcl-2 family members in *Drosophila* may induce apoptosis in a cytochrome c-independent manner.

b) BUFFY

BUFFY is highly homologous to DEBCL, and is more similar in primary structure to the proapoptotic mammalian Bcl-2 homologues Bax and Bok than to Bcl-2. BUFFY lacks the conserved BH4 domain that characterises prosurvival Bcl-2 homologues. However, ablation of *buffy* by RNAi in embryos results in increased apoptotic cell deaths (Quinn *et al.*, 2003). Additionally, BUFFY overexpression protects *Drosophila* tissues against apoptosis induced by γ- irradiation. Genetically, BUFFY functions downstream of REAPER, HID and GRIM and upstream of DRONC (Quinn *et al.*, 2003). BUFFY interacts with DEBCL both genetically in the fly eye and physically in cultured cells and has also been implicated in cell cycle regulation (Quinn *et al.*, 2003). Despite the characterisation of BUFFY as a prosurvival Bcl-2 homologue, the roles of BUFFY and DEBCL in *Drosophila* apoptosis remain to be fully understood. Part of this thesis further investigates the mechanisms by which these molecules function in programmed cell death.

1.12 Aims

At the time of commencement of this study into cell death molecules in *Drosophila*, the field of apoptosis was becoming more and more dynamic with multitudes of publications released, demonstrating the complexity of this essential signalling pathway. It became apparent that maintaining homeostasis relies on the tight regulation of the pathways of apoptosis and that many different factors play a role in the temporal and spatial cell death events that occur both in development and adulthood. Using *Drosophila* as a model system simplifies, to some extent, the study of cell death. At the commencement of this study, five *Drosophila* caspases had been cloned and characterised, and a sixth caspase was being characterised in our laboratory. With the sequence of the *Drosophila* genome completed, one *Drosophila* caspase remained to be cloned and characterised. The two Bcl-2 homologues in *Drosophila* were also in the infant stage of characterisation. This project encompassed the following aims:

1) To clone a predicted *Drosophila* caspase and establish its ability to function as a caspase.

2) To assess the role of this caspase *in vivo*, and establish its position in the apoptotic pathway by assessing its relationship with other apoptotic molecules.

3) To analyse the role of amino acid residues flanking the transmembrane domain in the differential intracellular localisation of the *Drosophila* Bcl-2 homologues, BUFFY and DEBCL.

Chapter 2

Materials and Methods

2.1 DNA Manipulation

2.1.1 Quantification of DNA

The concentration of a DNA sample was determined using a spectrophotometer to measure the absorption at 260nm, assuming that an $O.D_{260nm}$ reading of 1.0 is equivalent to 50µg/ml of DNA. Alternatively, DNA was separated on agarose minigels and the concentration estimated by comparison of the intensities of ethidium bromide-stained bands with markers of known concentration.

2.1.2 Separation of DNA fragments by electrophoresis

0.8%-2% agarose was dissolved in TAE buffer (Tris-acetate-EDTA – 40mM Tris-acetate, 1mM EDTA) to resolve DNA fragments of varying molecular weights. DNA samples were prepared for loading into TAE-immersed gels by the addition of 10x DNA loading buffer (0.25% bromophenol blue, 0.25% xylene cyanol, 30% glycerol) to a final concentration of 1x. Routinely, gels were electrophoresed at 80 – 110 volts, monitoring the migration of the dye front as a guide. Gels were stained in ethidium bromide (2µg/ml) for 10-30 min and visualised by viewing under a short-wavelength UV transilluminator (254nm) and photographed. Alternatively, gels were scanned using a Fluorimager 595 (Molecular Dynamics) with a 610nm filter. Standard molecular weight markers used were EcoRI-digested fragments of bacteriophage SPP1 and HindIII-digested bacteriophage lamba DNA (Geneworks).

2.1.3 Restriction endonuclease digestion

DNA was digested with the required restriction enzyme (Amersham Biosciences or New England Biolabs) in a 20-50µl total volume. Each reaction contained the target DNA, 1 unit enzyme/µg DNA, 1x digestion buffer (varying compositions depending on the enzyme) and sterile H_2O. To prevent non-specific digestion, bovine serum albumin (BSA) was added to 0.1mg/ml where required. Digests were incubated at 37°C for 1–3 h. Reactions were

terminated either by heat inactivation at 65°C for 10 min, or by the addition of loading dye and subsequent electrophoresis.

2.1.4 Purification of DNA fragments

a) ULTRA-CLEAN™

Digested DNA fragments were routinely purified for further procedures using the ULTACLEAN™ kit from Geneworks, as per the manufacturer's instructions. Following agarose gel electrophoresis, DNA fragments were excised from the gel using an actual size fluorimager printout. The gel slice was weighed and dissolved in 3 volumes of ULTRA-MELT™ solution at 55°C. ULTRA-BIND™ beads were added to the DNA/melt mix (5µl plus 1µl/µg DNA) and incubated at room temperature for 5 min with frequent gentle inversion. The DNA-bound ULTRA-BIND™ beads were pelleted by centrifugation at 13000 rpm for 10 sec and washed twice in ULTRA-WASH™ solution in the same volume used for the addition of ULTRA-MELT™. The beads were dried in a 55°C heating block after the final wash. DNA was eluted from the beads by resuspending in 10- 20 µl sterile H_2O or TE buffer. Following centrifugation for 1 min at 13000rpm, the supernatant containing the DNA was carefully removed and transferred to a clean microfuge tube.

b) Phenol/Chloroform extraction

To purify a dirty DNA sample or as part of a routine purification, the DNA solution was made up to 200µl in sterile H_2O. An equal volume of 1:1 phenol/chloroform was added and the tube vortexed thoroughly for 30 sec. The aqueous and solvent layers were separated by centrifugation at 13000 rpm for 3 min. The upper aqueous phase was carefully removed and traces of phenol were extracted with an equal volume of chloroform followed by centrifugation as above. DNA was precipitated, from the aqueous phase, with 2 volumes of absolute ethanol and 0.1 volumes 3M sodium acetate (NaAc) pH 4.6 and incubated on ice for 30 min–1 h. DNA was pelleted by centrifugation at 13000 rpm for 10 min and the resulting

pellet washed in 70% ethanol. The air-dried pellet was resuspended in 10 – 30µl sterile H_2O. With low concentration of DNA, 1µl glycogen (Roche) was added prior to ethanol precipitation, to aid visualisation of the pellet and minimise loss of DNA.

2.1.5 End-filling DNA fragments

Restriction-digested DNA with 3' overhangs was end-filled using Klenow (Amersham Biosciences). A reaction mixture containing 1 unit of Klenow and 0.2mM dNTP mix in 1x One-Phor-All Buffer Plus (Amersham Biosciences) diluted in sterile H_2O was incubated at 37°C for 30 min. DNA was then purified by ULTRA-CLEAN™ or phenol/chloroform extraction as described above.

2.1.6 Dephosphorylation of DNA

5' phosphate groups were removed from DNA fragments by treatment with 1 unit of calf intestinal phosphatase (CIP) (New England Biolabs (NEB)) in buffer 3 (NEB) at 37°C for 30 min and purified as above.

2.1.7 Ligation of DNA fragments

20µl ligation reactions containing 1 Weiss unit of T4 DNA ligase (USB), 1x ligation buffer (50mM Tris-HCl pH 7.6, 10mM $MgCl_2$, 10mM DTT, 50µg/ml BSA, 1mM ATP), vector and insert DNA (in a 1:5 ratio), were prepared and incubated at 4°C for 24 h, or 1–3 h at room temperature. An aliquot was transformed into competent DH5α as described in the following section.

2.2 Transformation of Chemically Competent Bacterial Cells

2.2.1 Preparation of competent *E.coli* cells

5ml ψ broth (ψb (20g/L Bacto-tryptone [Difco], 5g/L Bacto-yeast extract [Difco], 5g/L $MgSO_4$, and pH7.6 with KOH)) was inoculated with a single bacterial colony or a

glycerol stab and grown overnight overnight at 37°C with shaking. This culture was subcultured 1:20 into 100ml of ψb and grown at 37°C with shaking until $O.D_{600nm}$ reached 0.4-0.5. Cells were chilled on ice for 15 min and then pelleted at 6000rpm for 5 min at 4°C. Medium was aspirated and the cell pellet was resuspended in 40ml ice-cold Tfb I buffer (30mM KOAc, 100mM KCl, 10mM $CaCl_2.2H_2O$, 50mM $MnCl_2.4H_2O$, 15% glycerol adjusted to pH 5.8 with 0.2M acetic acid and filter sterilised). Cells were incubated for 5 min on ice before being pelleted by centrifugation as above and resuspended in 4ml Tfb II buffer (10mM MOPS, 75mM $CaCl_2.2H_2O$, 10mM KCl, 15% glycerol adjusted to pH 6.5 with 0.5M KOH and filter sterilised). Cells were incubated on ice for 15 min. 50µl aliquots of competent cells were transferred into 1.5ml microfuge tubes snap-frozen on dry ice. Aliquots were stored at -70°C.

2.2.2 Transformation of chemically competent cells

Aliquots of chemically competent bacterial cells were thawed on ice. 5-10µl of ligation reaction or 5-10ng uncut plasmid was added to cells, mixed gently, and incubated on ice for 20 min. Cells were heat shocked at 42°C for 2 min and cooled on ice for 5 min. The transformed cells were cultured in 1ml SOC medium(2% (w/v) bacto-tryptone [Difco], 0.5% (w/v) bacto-yeast extract [Difco], 0.05% (w/v) NaCl 0.25 mM KCl pH7, 10mM $MgCl_2$, 200mM glucose, pH 7.0) at 37°C for 1 h. Cells were pelleted by centrifugation and resuspended in 100µl SOC medium before being plated onto agar plates (Luria broth + 15g/L Bacto-agar [Difco]) containing the appropriate antibiotics for plasmid-encoded resistance (ampicillin 100µg/ml, kanamycin 25µg/ml or chloramphenicol 34µg/ml). For blue/white colour selection, cells transformed with plasmids encoding the *LacZ* reporter gene were plated onto agar plates spread with 4µl of 1M IPTG (isopropylthio-β-D-galactoside (Progen)) and 40µl of 20mg/ml X-gal (5-bromo-4-chloro-3-indolyl-β-D-galactoside (Progen)). Plates were incubated at 37°C overnight.

2.2.3 Colony cracking for screening transformants

Screening for colonies containing the cloned gene of interest, where blue/white colour selection could not be employed, was carried out using the colony cracking method. Single colonies growing on selection plates were picked using a pipette tip, spotted onto a gridded agar plate and then transferred to a microfuge tube containing 15µl cracking solution (50µM NaOH, 0.5% SDS, 5µM EDTA, 0.1% bromophenol blue). Bacterial cells were lysed by heating to 65°C for 15 min. Samples were loaded dry into wells of 1% agarose gels and electrophoresed at 40 volts. Once the samples had migrated into the gel, the gel was fully submerged in TAE buffer and electrophoresis continued at 100 volts. Colonies containing positive clones were identified as plasmid species migrating slower than empty vector alone.

2.3 Purification of plasmid DNA from bacterial cultures

2.3.1 Small scale plasmid purification

2ml LB containing the appropriate antibiotic (see section 2.2.2 for antibiotic concentrations) were inoculated with single transformed bacterial colonies and grown overnight at 37°C with shaking. 1.5ml of each overnight culture was transferred to a microfuge tube and pelleted for 1 min at 13000 rpm. Cell pellets were resuspended in 150µl ice cold Qiagen buffer P1 (50mM Tris-HCl pH 8.0, 10mM EDTA, 100µg/ml RNase A). Cells were lysed by the addition of 150µl buffer P2 (200mM NaOH, 1% SDS). Chromosomal DNA and proteins were precipitated by mixing the lysate with 150µl buffer P3 (3M KAc pH 5.5). Lysates were cleared by centrifugation at 13000 rpm for 5 min. Supernatants were transferred to clean microfuge tubes and plasmid DNA was precipitated by the addition of 2 volumes (900µl) 100% ethanol and 0.1 volume (45µl) sodium acetate pH 4.6 and incubated on ice for 20 min. DNA was then pelleted at 13000 rpm for 10 min and resuspended in 50µl sterile H_2O.

2.3.2 Large scale plasmid purification

Purification of plasmid DNA on a larger scale was carried out using the QIAGEN plasmid Midi Kit (QIAGEN). 50-100ml cultures were grown at 37°C overnight. Cells were pelleted at 3000 rpm in a BECKMAN Avanti^{TM} J-25 centrifuge and pellets resuspended in 4ml ice-cold buffer P1 (as above). Bacterial cells were lysed by the addition of 4ml buffer P2 (as above) and incubated at room temperature for 5 min. Chromosomal DNA and protein was precipitated by the addition of 4ml buffer P3 (as above) and mixed by gentle inversion several times. Lysates were centrifuged at 15000 rpm for 20 min at 4°C. Supernatants were transferred to QIAGEN columns pre-equilibrated with 4ml QIAGEN equilibration buffer QBT (750mM NaCl, 50mM MOPS pH7, 15% isopropanol, 0.15% Triton X-100). The columns were washed twice with 10ml wash buffer QC (1M NaCl, 50mM MOPS pH7, 15% isopropanol) and DNA was eluted in 5ml elution buffer QF (1.25M NaCl, 50mM Tris-Cl, pH8.5, 15% isopropanol). DNA was precipitated by the addition of 0.7 volumes of isopropanol and pelleted by centrifugation at 15000rpm for 30 min at 4°C. After careful removal of the supernatants, DNA pellets were air-dried and resuspended in 400µl sterile H_2O. The DNA solution was transferred to a 1.5ml microfuge tube and precipitated by the addition of 0.1 volume 3M NaAc, pH 4.6 and 2 volumes of 100% ethanol and incubated on ice for at least 30 min. DNA was pelleted by centrifugation at 13000 rpm for 10 min, washed with 70% ethanol and resuspended in 100µl sterile 1x TE buffer. The concentration of plasmid DNA in solution was measured by absorbance spectroscopy as described in section 2.1.1.

2.4 Amplification and Sequencing of DNA

2.4.1 Primer design

The following are primers designed for the cloning of *strica*:

DCP75'KpnI 5' – GCC*GGTACC*ATGGCCATAACTTGCACATCTCCC – 3'

5'DCP7NdeNEW 5' – GGC*CATATG*GGTTGGTGGAGCAAGAAAAGCG – 3'

DCP75'KpnNEW 5' – GCC*GGTACC*ATGGGTTGGTGGAGCAAGAAAAGCG – 3'

DCP73'FLAG 5' – CGC*TCTAGA*TCACTTGTCATCGTCCTTGTAGTCAA

TATAATCTCCAAAAACG – 3'

3'dcp7R3 5' – CTTGGTGCCTCCTGACGATCC – 3'

5'DCP7- C429G 5' – GCTGATTTTCGTTCAGGCC**G**GCAAGGGCGACTGCCAACTAGGG – 3'

3'DCP7- C429G 5' – CCCTAGTTGGCAGTCGCCCTTGC**C**GGCCTGAACGAAAATCAGC – 3'

5'StMPDKpn 5' – GCC*GGTACC*ATGGCGAAGCCGCTCAGTTCGACCGC – 3'

3'STRICA-PRO 5' – GCG*GGATCC*CGGTCAACTTGCTTGGGAGCG – 3'

3'DCP7BamHI 5' – GCG*GGATCC*CGAATATAATCTCCAAAAACG – 3'

5'STRICA-Nco 5' – GGG*CCATGG*CCATGGGTTGGTGGAGCAAGAAAAGC – 3'

5'STDPD-NcoI 5' – GGG*CCATGG*CCAAGCCGCTCAGTTCTACCGC – 3'

5'Str(S119G) 5' – CGCTCCCGACCGCCCGGTTTGAACGGCGTCTCC – 3'

3'Str(S119G) 5' – GGAGACGCCGTTCAAACCGGGCGGTCGGGAGCG – 3'

5'pIE-STΔPD-BamHI 5' – CCC*GGATCC*GCCATGGCGAAGCCGCTCAGTTCTACCGC – 3'

The following are primers designed for the cloning of *buffy* and *debcl*:

E42B-HAF1 5' – CG*GAATTC*ATGTACCCATACGACGTCCCAGACTACGCT

GCTCCCACCACCAGTCCGCCACCC – 3'

E42B-R3 5' – CCG*CTCGAG*CTAGAACAGCAGCGAATACAG – 3'

B48E5'FLAG 5' – GCG*GGATCCCTCGAG*ATGGACTACAAGGACGACGATGACAAG

CCCGGCACCTCGTATCCCACGAATAACGATAAT – 3'

BuffyR2 5' – GGC*CTCGAG*TTAGGAATTCGTAAATCGTTG – 3'

3'Buffy-MA 5' – TCAAGGATTCAGGCTGTTGGTAGTGGG – 3'

5'GFP-DebXho 5' – CCG*CTCGAG*CATGGCTCCCACCACCAGTCCG – 3'

5'GFP-BuffyXho 5' – CCG*CTCGAG*TCCCGGCACCTCGTATCCC – 3'

E48BRKpn 5' – GC*GGTACC*TTAGGAATTCGTAAATCGTTGG – 3'

DebXBufTM-F 5' – GGAGTGGCATCAACAGACACATCA**GACCGAGA**GTTTTACCCACTACC –3'

DebXBufTM- R 5' – GGTAGTGGGTAAAAC**TCTCGGTC**TGATGTGTCTGTTGATGCCACTCC – 3'

F-BuffyRRK 5' – GGCCTAATTCTAGTTTTTATGATTCTGCGA**CGA**AA**A**ATTTAACTTGATTG

TACCAAAAATATACCAACG – 3'

R-BuffyRRK 5' – CGTTGGTATATTTTTGGTACAATCAAGTTAAAT**TTTCG**TCGCAGAATCA

TAAAAACTAGAATTAGGCC – 3'

DEBCL-mutX-F 5' – CCTGTCGCGGCACATC**GC**ACCC**GC**GGTCGGCGAATTTACG – 3'

DEBCL-mutX-R 5' – CGTAAATTCGCCGACC**GC**GGGT**GC**GATGTGCCGCGACAGG – 3'

DebclRR/AA-F 5' – GGTCTCAAACGTGTGT**GCG**GCCATTGGAGGTCAACTG – 3'

DebclRR/AA-R 5' – CAGTTGACCTCCAATGGCCGCACACACGTTTGAGACC – 3'

5'BufNLSmut 5' – GCCTGTGCGGTCATTATATC**GCGGCAGC**CCTCAGAAGATC TGGTTTGTTC – 3'

3'BufNLSmut 5' – GAACAAACCAGATCTTCTGAGG**GC**T**GCCGC**GATATAATGA CCGCACAGGC – 3'

The following primers were used to clone *dakt* into pcDNA3:

Dakt-Kpn-F 5' – CGG*GGTACC*ATGTCAATAAACACAACTTTCG – 3'

Dakt-MYCXhoR 5' – CCCG*CTCGAG*CTACAGGTCTTCCTCCGAGATCAGCTTCTGCTCTTGCATC GATGCGAGACTTGTGG – 3'

5'DAKT-int 5' – GTGATGCAGTACGTGAACGGTGGC – 3'

3'DAKT-int 5' – CGCTTCGTGGCTTAAATGCC – 3'

5' primers are forward (sense) and 3' primers are reverse (anti-sense) primers. N-terminal or C-terminal tags are underlined. Bases in bold indicate mutations giving rise to amino acid substitutions. MPD stands for Minus Prodomain. DCP7 stands for *Drosophila* Caspase-7 and was used prior to the naming of STRICA. MA is an abbreviation for membrane anchor. Restriction enzyme sites introduced for cloning purposes are italised as follows:

CATATG – NdeI

GGATCC – BamHI

GGTACC – KpnI

TCTAGA – XbaI

CCATGG – NcoI

CTCGAG – XhoI

2.4.2 Primer Purification

Oligonucleotide primers immersed in ammonium hydroxide were synthesised at the IMVS/HCCR, Department of Tissue Pathology by Mr. A. Mangos and were purified by butanol extraction. 100µl deprotected oligonucleotide/ ammonium hydroxide solution was mixed with 1ml butanol and vortexed vigorously for 30 seconds. Oligonucleotides were pelleted by centrifugation at 13000 rpm for 1 min. The supernatant was aspirated and the DNA pellet air-dried and resuspended in 100µl sterile H_2O. Primer concentration was determined by absorbance spectroscopy at 260nm (OD_{260} 1 = 20 µg/ml).

Primers were also purchased commercially through Geneworks. In this case oligonucleotides were received as dried pellets and were resuspended at 100ng/µl in sterile H_2O.

2.4.3 Amplification of DNA by PCR

a) Taq polymerase amplification

For detection of mRNA transcripts by RT-PCR and other methods where high fidelity amplification is not required, Taq DNA polymerase was used. Polymerase chain reaction (PCR) was performed in a 50µl reaction volume containing 1x AmpliTaq reaction buffer (Perkin Elmer), 200µM of each deoxynucleotide-triphosphate (dNTP) (dATP, dTTP, dCTP, dGTP), 2.5mM $MgCl_2$, DNA template (1-3µl first strand cDNA or 100ng plasmid DNA), 100ng each of forward and reverse primers, and 2.5 units AmpliTaq polymerase (Perkin Elmer) in sterile H_2O. Reactions were set up in 0.5ml PCR tubes (Treff), overlaid with 50µl mineral oil if required, and DNA synthesised in a DNA Thermal Cycler (Hybaid) or PCR Sprint. Standard conditions for amplification consisted of template denaturation at 95°C for 1min, followed by 25-35 cycles of 1min denaturation at 94°C, primer annealing at 50°C-55°C 1 min, and primer extension at 72°C for 2-5 min (depending on the size of DNA fragment to

be amplified). A 10 min extension at 72°C was performed after completion of the last cycle to ensure completion of DNA synthesis. Reactions were held at 4 °C.

b) DyNAzyme™ amplification

DyNAzyme™ DNA polymerase (Finnzymes) was used to PCR amplify DNA sequences for cloning into pGEMTEasy™ by T/A cloning. PCR reactions containing 1 x Optimised Buffer (10mM Tris-HCl, pH 8.8, 1.5 mM $MgCl_2$, 50 mM KCl, 0.1 % Triton® X-100), 2mM dNTP mix (diluted 1:10 for a final concentration of 200µM each dNTP), 100ng of forward and reverse primers, 1 unit of Dynazyme DNA polymerase and 100ng template DNA, were set up in 0.5ml PCR tubes in a 50µl final volume. Standard PCR conditions were used for amplification as described above.

c) Amplification using Pfu polymerase

For cloning of DNA into vectors, Pfu DNA polymerase (Stratagene) was used to reduce the risk of incorporating erroneous bases leading to mutations. Pfu is a high fidelity DNA polymerase with proof-reading activity. DNA was synthesised using 100ng DNA template, 2mM dNTP mix, 100ng forward and reverse primers, 100ng template DNA, 1x reaction buffer (20mM Tris-HCl pH 8.75, 10mM KCl, 10mM $(NH_4)_2$ SO_4, 2mM $MgCl_2$, 0.1% Triton X-100, 0.1mg/ml BSA) and 2.5 units Pfu polymerase in a total volume of 50µl sterile H_20. Reactions were overlaid with mineral oil where required and synthesis was carried out in a DNA thermal cycler (Hybaid) or PCR sprint under standard amplification conditions.

d) Pwo polymerase amplification

Another option for high fidelity amplication of DNA was the use of Pwo (*Pyrococcus woesei*) polymerase (Roche). DNA was synthesised in a 50µl reaction essentially as

described above, using the reaction buffer recommended for Pwo (10mM Tris-HCl pH 8.85, 25mM KCl, 5mM $(NH_4)_2SO_4$, 2mM $MgSO_4$).

2.4.4 Site directed mutagenesis

Single point mutations of a target DNA sequence were generated using the Quikchange Site-Directed Mutagenesis Kit (Stratagene). 100ng plasmid DNA template was amplified in a 50µl reaction containing 1x reaction buffer (10mM KCl, 10mM $(NH_4)SO_4$, 20mM Tris-HCl pH 8.8, 2mM $MgSO_4$, 0.1% Triton X-100, 0.1mg/ml nuclease-free BSA), 150ng of each mutagenic primer, 2mM each dNTP, 2.5U *Pfu* Turbo DNA polymerase in sterile H_2O. Reactions were amplified by one cycle of denaturation at 95°C for 30 sec, followed by 12-18 cycles of denaturation at 95°C for 30 sec, primer binding at 55°C for 1 min and extension at 68°C for 2 min/kb of plasmid length. Template DNA was digested with 1µl *Dpn*I restriction enzyme in Buffer 4 (NEB) at 37°C for 1 h, which only digests methylated, parental DNA, leaving the newly synthesised mutant plasmid intact. 1µl - 5µl of this product was transformed into chemically competent bacterial cells as described in section 2.2.2. Plasmid DNA was prepared as described in section 2.3.2 and sequenced to confirm the presence of the desired mutation.

2.4.5 Sequencing of cloned DNA

Plasmid DNA prepared using the QIAGEN midiprep kit was sequenced using the ABIPRISM Dye Terminator Cycle Sequencing Reaction Kit. Sequencing reactions consisting of 100ng primer, 5µl BigDye Terminator Ready Reaction Mix Version 3(A/C/G/T-Dye Terminator, dGTP, dATP, dCTP, dTTP, Tris-HCl pH9.0, $MgCl_2$, thermal stable pyrophosphatase, AmpliTaq polymerase) were added to 200-500ng template DNA and the volume made up to 20 µl with sterile H_2O. The following conditions were used to sequence plasmid DNA in a DNA thermal cycler (Hybaid): [96°C -10 sec, 50°C -5 sec, 60°C -4 min] x 25 cycles, followed by a 4°C hold. DNA was precipitated by the addition of 20µl sterile

water and 60µl of isopropanol, vortexed and incubated at room temperature for 15 min. Sequencing products were pelleted by centrifugation at 13000 rpm for 20 min at 4°C. The resulting pellet was washed in 75% isopropanol, pelleted for 5 min at 4°C, air-dried and sequenced using a Perkin Elmer automated sequencer. 1µl glycogen (Roche) was routinely added prior to isopropanol precipitation to visualise the DNA pellet.

2.5 Generation of plasmid DNA constructs

2.5.1 Purchased constructs

pOT2-STRICA: EST clone LP09213 (Research Genetics) contained an incomplete *strica* cDNA fused to the transferrin receptor sequence. The strica sequence lacked a portion of the 3'sequence.

pcDNA3.1 was purchased from Invitrogen (figure 2.1)

pBluescript II SK(+) was purchased from Stratagene (figure 2.2)

pGEMTEasy™: purchased from Promega

pEGFPc2: purchased commercially from Clontech (figure 2.3)

pGEX4T3: purchased from Amersham Biosciences

pAS2.1 and pACT2: Yeast two hybrid cloning vectors were purchased from Clontech.

pIE1.4 was purchased from Novagen (figure 2.5)

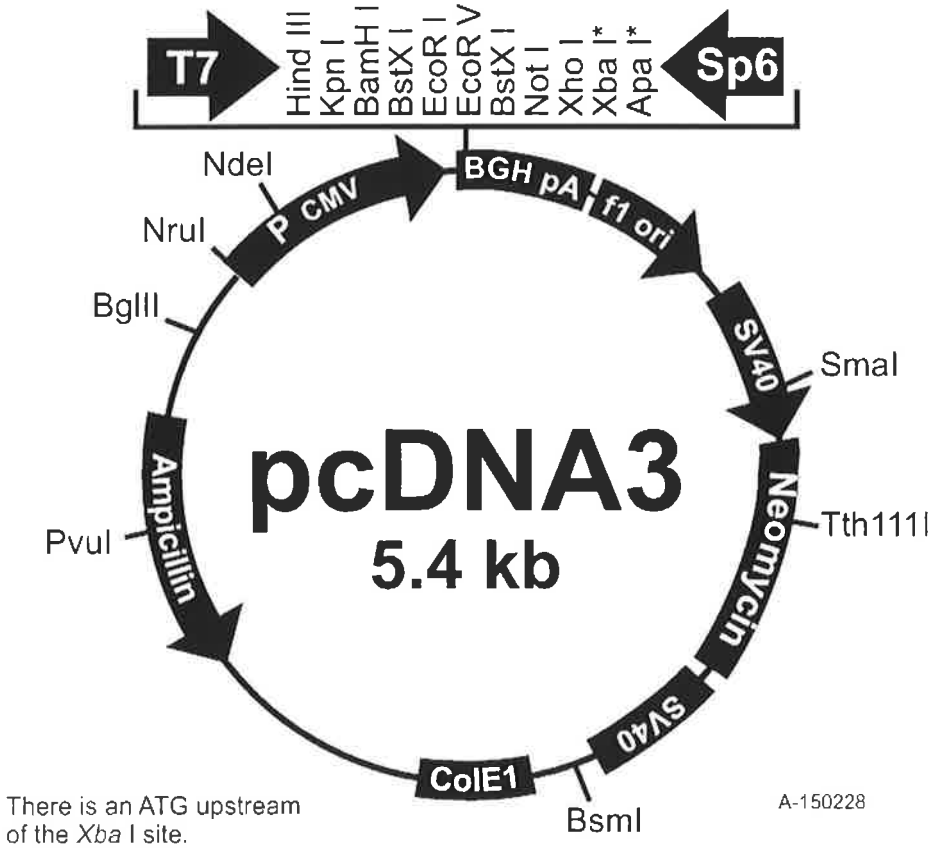

Figure 2.1 pcDNA3.1 was purchased from Invitrogen. Cloned inserts are expressed constitutively under the control of the CMV promoter.

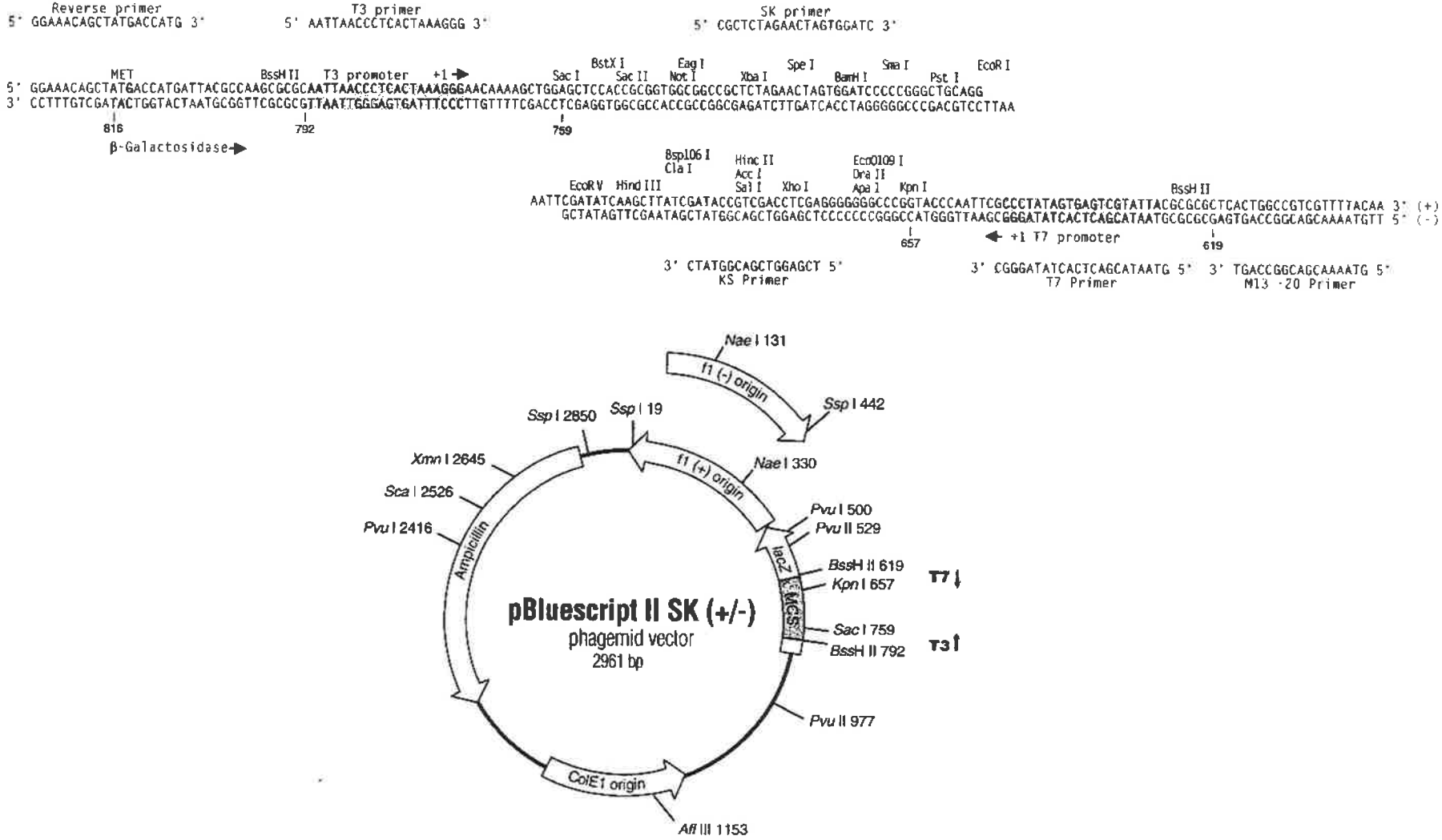

Figure 2.2 pBluescript II SK (+) cloning vector: purchased from Stratagene. The Multiple Cloning Site (MCS) is present within the LacZ reporter gene, allowing for blue/white colour selection of colonies carrying cloned inserts.

pEGFP-C2 Vector Information PT3051-5

GenBank Accession #: U57606 Catalog #6083-1

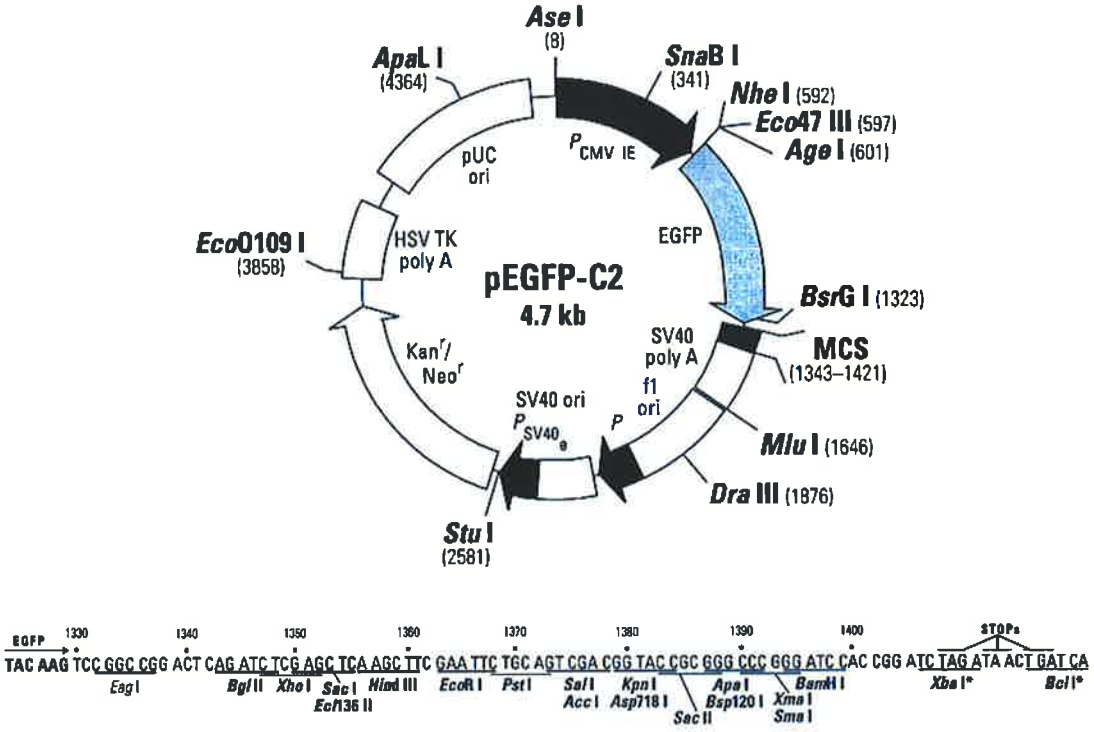

Figure 2.3 pEGFP-c2: was purchased from Clontech for the expression of EGFP fusion proteins in mammalian cell lines. Cloning inserts into the MCS fuses EGFP to the N-terminus of the protein. Fusion protein expression is visualised by fluorescent microscopy.

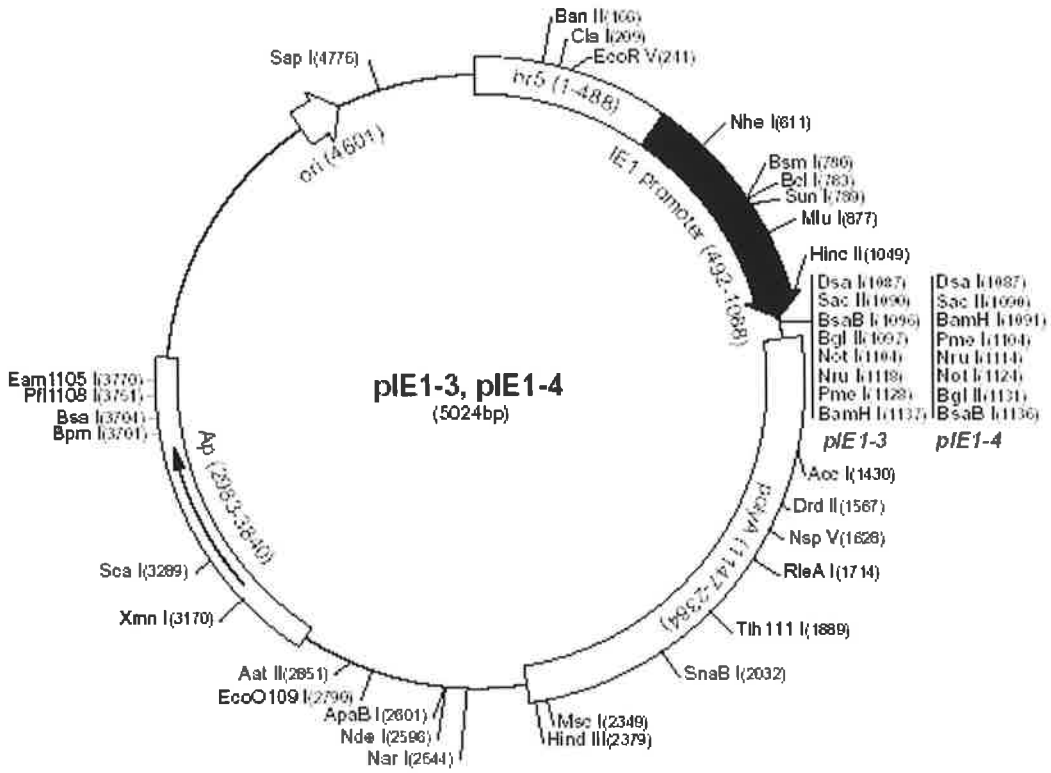

Figure 2.5 pIE1.4 vector: expression of cloned inserts is under the control of the IE 1 (immediate early) promoter, allowing for constitutitve protein expression in insect cells.

2.5.2 Mammalian expression constructs

pcDNA3-STRICA$_{FLAG}$: A 965bp strica PCR product, from bp612 to the 3' stop codon was amplified from a *Drosophila* larval yeast two-hybrid cDNA library using primers DCP7 5'KpnI and DCP73'FLAG, containing KpnI and XbaI restriction sites respectively. DCP73'FLAG also bore a FLAG tag-encoding sequence as indicated. This PCR product was directionally cloned into pcDNA3. The 5'-most 834bp of *strica* was amplified from pOT2-STRICA (EST clone LP09213) using primers DCP75'KpnNEW and 3'dcp7R3 and cloned into pcDNA3 directionally into KpnI/EcoRV sites (blunt PCR product was digested with KpnI only, leaving the 3' end blunt for cloning into the blunt EcoRV site of the vector). The full-length strica ORF was obtained by a 3-way ligation by means of a BanI site present in the region of overlap between each PCR product. The final pcDNA3-STRICA$_{FLAG}$ construct was sequenced. Two point mutations discovered were corrected.

pcDNA3-STRICA (C429G) $_{FLAG}$: The catalytic cysteine residue (C429) was mutated to a glycine residue by Quikchange site-directed PCR mutagenesis using primers 5'DCP7-C429G and 3'DCP7-C429G and pcDNA3-STRICA$_{FLAG}$ as a template.

pcDNA3-STRICA ΔPD$_{FLAG}$: removal of the putative prodomain of STRICA was achieved by PCR amplifying *strica ΔPD* with primers 5'StMPDKpn and DCP3'FLAG and directionally cloning into the KpnI and XbaI sites of pcDNA3.

pcDNA3-STRICA (S119G)$_{FLAG}$: A point mutation was introduced into the putative AKT phosphorylation consensus site by site-directed mutagenesis using primers 5'Str(S119G) and 3'Str(S119G)

pcDNA3-DRONC: the coding region of *dronc* was directionally subcloned from pBluescript (Stratagene) into pcDNA3 utilising HindIII/XbaI restriction sites by Dr. Loretta Dorstyn.

pcDNA3-$_{HA}$BUFFY: BUFFY tagged at the N-terminus with HA was constructed by Kathryn Mills.

pcDNA3-p35: provided by Dr Vishva Dixit (Genentech, San Fransisco, USA)

pcDNA3-DIAP1$_{MYC}$: pBluescript-DIAP1 $_{MYC}$, provided by Dr Bruce Hay (Caltech, USA) was used to subclone DIAP1 $_{MYC}$ into the EcoRI/BamHI sites of pcDNA3.

pcDNA3-DIAP2$_{HA}$: The DIAP2 coding region was PCR amplified from pBS-DIAP2 to generate a 3'HA tag. The cDNA was cloned blunt into the EcoRV of pcDNA3.

pcDNA3-Flag-Bcl-X$_L$, pcDNA3-Flag-Bcl-X$_L$ (RS), pcDNA3-Flag-Bcl-X$_L$ (SK), pcDNA3-Bcl-2 and **pcDNA3-Bcl-2 (HKRK):** were kindly provided by Prof. Christoph Borner.

pEGFP-X-TMB(Bcl-X$_L$), pEGFP-AFNA-TMB (Bcl-X$_L$), pEGFP-X/2-TMB(Bcl-2) and **pEGFP-X(Bcl-X$_L$)TMB(Bcl-2):** provided by Prof. Christoph Borner.

pEGFPc2-BUFFY and **pEGFPc2-BUFFYΔMA**: *buffy* was PCR amplified by Pfu DNA polymerase, using primers 5'EGFPBuffyXho and E48AKpn using pIE1.4-$_{FLAG}$BUFFY as a template. *buffyΔMA* was similarly amplified, using a different 3'primer, 3'Buffy-MA. PCR products were cloned blunt into the EcoRV site of pBluescript II SK+ (pBS-SK+). Clones in the reverse orientation were selected for subcloning by excision of the fragments with XhoI/BamHI, and directional cloning into pEGFP-c2. This created N-terminally EGFP-tagged BUFFY and BUFFYΔMA in the correct frame and orientation.

pEGFPc2-DEBCL: *debcl* was PCR amplified with Pfu DNA polymerase using 5'EGFPDebXho and E42B-R3, from a 21 h *Drosophila* embryonic cDNA library. PCR

product was cloned blunt into the EcoRV sites of pBSII SK+. Reverse-orientated clones were chosen for sequence excision by XhoI/BamHI digestion, and directional cloning into pEGFPc2.

pEGFPc2-DebXBufTM and **pEGFPc2-BUFFY RRK**: The X domain of DEBCL was introduced at the N-terminal transmembrane anchor flank of buffy by Pfu Turbo PCR mutagenesis using primers DebXBufTM-F and DebcXBufTM-R on pBSIISK+-BUFFY template. Mutations were introduced at the C-terminal flank by site-directed mutagenesis using primers F-BuffyRRK and R-BuffyRRK, also on pBSIISK+-BUFFY template. Clones carrying inserts in the reverse orientation were sequenced to determine the incorporation of the mutant nucleotide(s) and subcloned into the BamHI/XhoI sites of pEGFP-c2.

pEGFP-DEBCL mutX and **pEGFPc2-DEBCL RR/AA**: The X domain of DEBCL was mutated by PCR mutagenesis using primers DEBCLmutX-F and DEBCLmutX-R. The C-terminal arginines were mutated to alanines using primers DebclRR/AA-F and DebclRR/AA-R. Products were amplified from a pBSIISK+-DEBCL template and subcloned into pEGFPc2 as described for buffy mutants above.

pEGFPc2-DEBCL DM (double mutant): using pBS-DEBCL mut X as a template, mutagenesis primers DebclRR/AA-F and DebclRR/AA-R were used in a PCR reaction as described. Constructs containing both the mutX and RR/AA mutations were identified by sequencing and directionally subcloned into the BamHI/XhoI sites of pEGFP-c2.

pcDNA3-DAKT$_{MYC}$: *dakt* cDNA was amplified in two halves from a 21hr *Drosophila* embryo cDNA library using Pfu Turbo DNA polymerase. The 5' half was amplified with primers DaktKpn-F and 3'Dakt-int. The 3'half was amplified using 5'DAKT-int and DaktMycXhoR. A region of overlap between each PCR product was amplified and contained

a SacI site. Each PCR product was ligated into the blunt EcoRV site of pBluescript SKII+. The 5' *dakt* sequence was excised from Bluescript by digestion with KpnI and SacI. The 3' sequence was excised with SacI and XhoI. Full-length, C-terminally MYC-tagged *dakt* was cloned into the KpnI/XhoI sites of pcDNA3 by a 3-way ligation, using the internal SacI site present in both fragments.

2.5.3 Insect expression constructs

pRMHa3 was provided by Dr. Helena Richardson (figure 2.4)

pRMHa3-STRICA$_{FLAG}$/STRICA(C429G)$_{FLAG}$: *strica*$_{FLAG}$ and *strica(C429G)*$_{FLAG}$ were PCR amplified from pcDNA3 constructs using PwoI DNA polymerase (Roche) using primers DCP5'KpnINEW and DCP3'FLAG. Insect vector pRMHa3 was digested with BamHI and the site was end-filled using T4 DNA polymerase. Blunt-cut vector was subsequently digested with KpnI and purified. STRICA$_{FLAG}$ and STRICA(C429G)$_{FLAG}$ PCR products were digested with KpnI at the 5'end, leaving the 3' end blunt, and ligated into pRMHa3 KpnI/blunt.

pIE1.4-$_{HA}$DEBCL, pIE1.4-$_{HA}$DEBCL(L/G), and **pIE1.4-$_{HA}$DEBCL(E/G):** *debcl* and mutants were amplified using Dynazyme from pcDNA-$_{HA}$DEBCL/(L/G)/(E/G), constructed by Dr. Paul Colussi, with primers E42B-HAF1 and E42B-R3. The resulting PCR products were cloned into pGEMT-Easy™ subcloning vector and excised by NotI digestion. NotI-digested-*debcl* was cloned non-directionally into the NotI site in pIE1.4 and the final clones selected for correct orientation and sequenced.

pIE1.4-$_{FLAG}$BUFFY and **pIE1.4–$_{FLAG}$mBUFFY** (mutant buffy): $_{FLAG}$*buffy* and $_{FLAG}$*mbuffy* were PCR amplified using Dynazyme DNA polymerase with primers B48EFLAG5' and BuffyR2, and cloned directionally into the BamHI/NotI sites of pIE1.4, through a pGEMT-

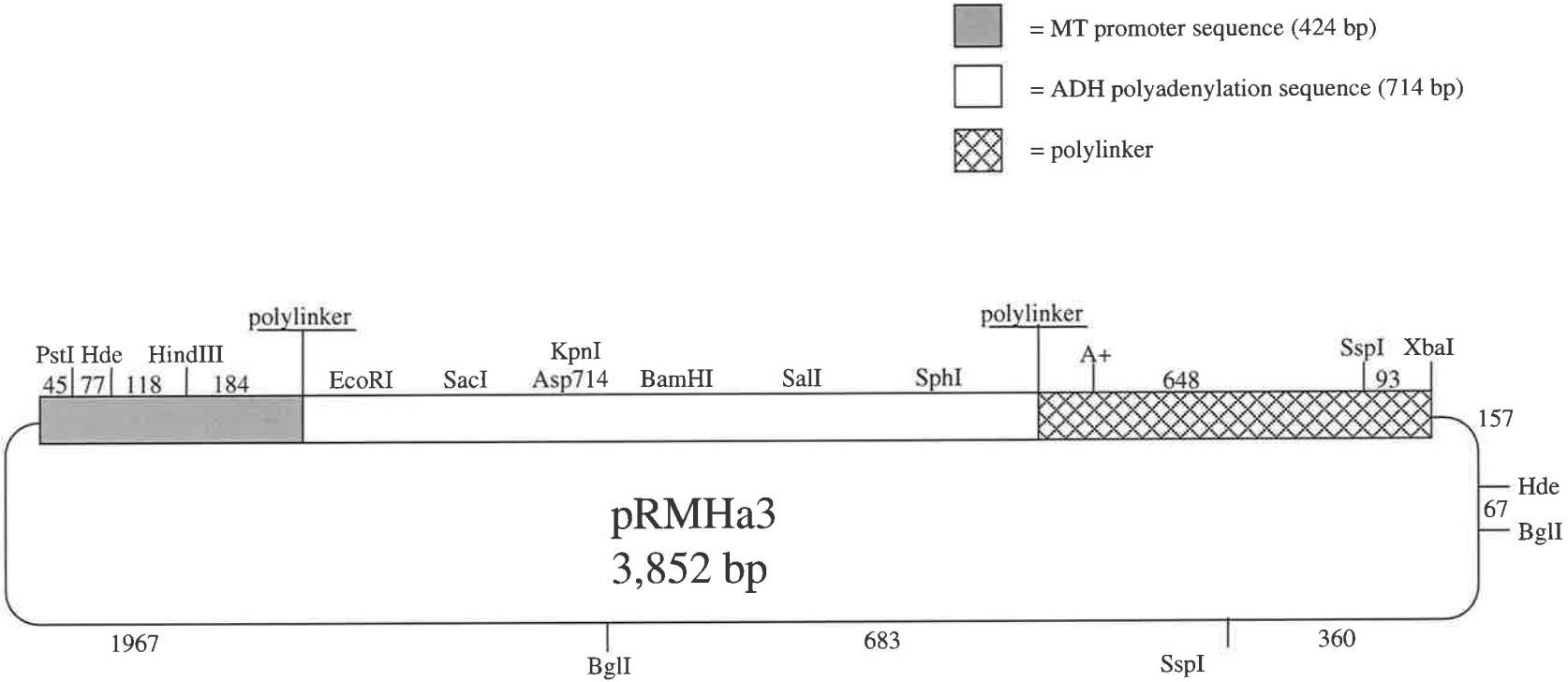

Figure 2.4 pRMHa3 insect expression vector. Cloned inserts are expressed under the control of the $CuSO_4$-inducible metallothionein promoter for expression in insect cells.

Easy™ cloning intermediate. Resulting clones were sequenced as described. pcDNA3-mBUFFY was used as a template to amplify mutant *buffy* encoding 3 amino acid substitutions in the BH3 domain, G143V, D144A and E145A.

pIE1.4-$_{FLAG}$BUFFYΔMA: $_{FLAG}$*buffy* lacking the C-terminal membrane anchor was amplified using primers B48EFLAG5' and 3'Buffy-MA, using Dynazyme, and cloned into pGEMT-Easy™. $_{FLAG}$*buffyΔMA* was subcloned directionally into the BamHI and NotI sites of pIE1.4.

pIE1.4-Buf1-118EGFP: pIE1.4-$_{FLAG}$BUFFY was digested with PstI and NotI, dropping out the last 546bp of *buffy* . The pIE1.4 backbone contained the first 354 bp (118amino acids) of *buffy*. The EGFP coding sequence was excised from pEGFP-N1 by digestion with PstI and NotI. The fragment was purified and ligated with the pIE1.4-Buf1-118 vector described above. The resulting plasmid fused the first 118 amino acids in frame to EGFP. This construct possessed several restriction sites between Buf1-118 and EGFP.

pIE1.4-EGFP: Digeston of pIE1.4-Buf1-118EGFP with BamHI dropped out the *buffy* sequence. The remaining pIE1.4-EGFP was religated.

pIE1.4-wtBuf1-118-StricaC-term: pGEMTEasy™-STRICA(C429G*)* was digested with SmaI (within the *strica* coding region) and NotI (in the MCS of the vector). *Buf1-118* was excised from pIE1.4-*Buf1-118EGFP* with BamHI and SmaI. Both fragments were purified and cloned by a 3-way ligation into the BamHI/NotI sites of pIE1.4.

pIE1.4-mutNLSBuf1-118-StricaC-term: The putative nuclear localisation signal (NLS) was mutated in the above construct by PCR site-directed mutagenesis using primers 5'BufNLSmut and 3'BufNLSmut.

pRMHa2, **pUAST** and **pGMR** plasmids were provided by Dr Helena Richardson (Peter MacCallum Cancer Institute, Melbourne). Vector descriptions can be found in Brand and Perrimon (1993) and Richardson et al. (1995).

pRM-DIAP1$_{HA}$: DIAP1 was HA-tagged by PCR amplification from pBS-DIAP1$_{MYC}$, and cloned directionally into the EcoRI/BamHI sites of pRMHa3 by Dr. Natasha Harvey.

pRM-DIAP2$_{HA}$: DIAP2 was amplified from a pBS-DIAP2 template introducing a 5' EcoRI site and 3' HA tag. The PCR product was EcoRI-digested and cloned into pRMHa3 EcoRI/blunt by Dr.Natasha Harvey.

pRM-p35$_{HA}$: pcDNA3-p35 was used as a template to amplify p35 with a 3'HA tag. The product was digested with EcoRI/BamHI and cloned into these sites in pRMHa3.

pCaSpeR.h-lacZ: provided by Prof. Masayuki Miura

2.5.4 Bacterial expression constructs

pGEX4T3-STRICA ΔPD: *strica ΔPD* was PCR amplified using primers 5'pIEStΔPD-BamHI and DCP7'3'FLAG using PwoI DNA polymerase and cloned into pGEMTEasy™. The insert was directionally subcloned into the BamHI/NotI sites of pGEX4T3 for expression of GST-STRICA ΔPD

2.5.5 Yeast expression constructs

pAS2.1-STRICA (C429G): *strica (C429G)* was amplified by PwoI DNA polymerase with primers 5'DCP7NdeINEW and 3'DCP7BamHI and directionally cloned into the NdeI/BamHI sites of pAS2.1. The resulting construct expresses a STRICA(C429G)-DBD (DNA binding domain) fusion protein.

pACT2-STRICA (C429G): For expression of an activation domain (AD)-STRICA (C429G) fusion protein, *strica (C429G)* was PCR amplified using primers 5'STRICA-Nco and 3'DCP7BamHI and directionally cloned into the NcoI/BamHI sites of pACT2.

pACT2-STRICA ΔPD: STRICA lacking the prodomain was PCR amplified with primers 5'StDPD-NcoI and 3'DCPBamHI and directionally cloned into pACT to create an AD-STRICA ΔPD fusion protein.

pAS2.1-STRICA PDO and **pACT2-STRICA PDO**: The prodomain of STRICA was PCR amplified with 3'STRICA-PRO and either 5'STRICA-NcoI or 5'DCPNdeINEW for directional cloning into pACT2 and pAS2.1 vectors respectively.

2.6 Yeast methods

2.6.1 Yeast Media

YPD growth medium was prepared by dissolving 20g Difco peptone and 10g yeast extract in 1L H_2O followed by autoclaving. For YPD agar plates, 20g agar was added to the mix. Following autoclaving, the media was allowed to cool to 55°C before adding dextrose (glucose) to 2%. For selection of transformants carrying plasmids with selectable growth markers, synthetic dropout (SD) medium was prepared by combining a minimal SD base with an amino acid dropout solution lacking the amino acid encoded by the plasmid cassette. In general, 6.7g yeast nitrogen base (Clontech) and 20g agar (for plates) was dissolved in 850ml H_2O and 100ml of the appropriate 10x concentrated dropout solution (Clontech) was added.

2.6.2 Yeast strains

Yeast strains were strored as glycerol stocks at -70°C in YPD medium with 25% glycerol. Frozen strains were recovered by streaking a portion of the glycerol onto a YPD plate and incubating at 30°C for 3-5 days until colonies appeared. Plates were sealed with parafilm and stored at 4°C for up to 2 months.

2.6.3 Protocols for culturing, transformation and library screening

All procedures were essentially as described in the Clontech yeast protocols handbook, including methods for transformation of yeast with plasmid constructs, screening of yeast two-hybrid libraries and extraction of protein from yeast for Western blotting.

2.7 Tissue Culture

Cell culture was carried out in Class II biohazard laminar flow hoods (Gelman Sciences)

2.7.1 Mammalian cell lines and culture conditions

NIH3T3, COS-7 and 293T cells were grown as monolayers in tissue culture dishes or flasks. The murine fibroblast cell line, NIH-3T3, was maintained in Dulbecco's modified Eagle's medium (DMEM) (GibcoBRL), supplemented with 10% FBS and 1% glutamine. The large T antigen-transformed human embryonic kidney (HEK) cell line, HEK-293T, and monkey cell line, COS-7, were grown in RPMI-1640 (Gibco BRL) supplemented with 10% FBS. Media also contained 2% sodium hydrocarbonate, 10% HEPES, 1% penicillin (Glaxo), 1% streptomycin sulphate (Glaxo) and adjusted to pH7 (DMEM) or pH7.4 (RPMI) with 1M HCl.

All cell lines were grown at 37°C in a humidified incubator containing 5% CO_2. Cells were maintained in log phase (1-10 X 10^5 cells/ml) with at least 95% viability. Cell density was calculated using a haemocytometer and viability determined by trypan blue 0.8% w/v in PBS) dye exclusion. To passage cells, medium was aspirated and the cells rinsed in phosphate-buffered-saline (PBS), and detached by incubation at 37°C in trypsin (0.054% w/v trypsin (Difco)/0.54mM EDTA in Hank's balanced salt solution (HBSS)). Following treatment with trypsin for several min, cells were removed to a 50ml tube in complete medium (medium supplemented with 10% FBS) and spun down in a centrifuge (Beckman

GS-6) for 5 min at 1200 rpm. The cell pellet was resuspended in complete medium and the cells seeded in fresh dishes or flasks.

2.7.2 Cryopreservation of cells

Cells in log phase were harvested, pelleted by centrifugation and resuspended in complete medium at 5-10 x 10^6 cells/ml. To a 500µl aliquot of cells in cyropreservation tubes (Nunc), an equal volume of cryoprotectant (30% FBS/ 20% dimethyl sulphoxide (DMSO) (BDH, Merck)/ 50% RPMI 1640) was added slowly. Cells were frozen by controlled rate freezing and stored in liquid nitrogen tanks.

2.7.3 Thawing cyropreserved cells

Cells were thawed rapidly in a 37°C water bath and transferred to a 10ml tube. 10 ml of complete medium was added slowly to cells, 1ml at a time. Cells were pelleted by centrifugation and washed a further 2 times in medium. Following the final wash, cells were seeded into tissue culture flasks or dishes.

2.7.4 Insect cell lines and culture conditions

The adherent *Drosophila* cell lines, Schneider L2 (SL2) and BG2-c2 were maintained in Schneider's culture medium (GibcoBRL) supplemented with 0.5% penicillin/streptomycin (GibcoBRL), 1% glutamine and 10% FBS, and incubated at 27°C. Additionally, BG2-c2 cell culture medium was supplemented with 10µg/ml insulin (Novartis). Cells were passaged by washing once in fresh medium and scraping cells off the bottom of the flask with a cell scraper (Costar). Cell density and viability was determined by trypan blue exclusion. Cells were maintained at 10^6 cells/ml in 75cm^2 tissue culture flasks. BG2 cells were provided by Dr. Ui-Tei (Nippon Medical School Japan).

2.7.5 Cryopreservation of *Drosophila* cell lines

Cells were harvested as described and resuspended in fresh medium containing 10% FBS at 5-10 x 10^6 cells/ml. An equal volume of freezing mix (20%FBS/ 10% DMSO/ 70% Schneider's medium) was added to cells in 2ml cryopreservation vials (Nunc). Cells were frozen by controlled rate freezing and stored in liquid nitrogen tanks.

2.7.6 Thawing cryopreserved *Drosophila* cells

Vials of SL2 or BG2 cells removed from liquid nitrogen tanks were thawed at room temperature and seeded into a 25cm^2 flask. Once cells had adhered to the flask after incubation at 27°C, they were washed twice in complete Schneider's medium and incubated in 5ml medium at 27°C.

2.8 Transient trasfection assays

2.8.1 Transfection of mammalian cells using FuGENE

The day prior to transfection, NIH-3T3, 293T or COS cells, were seeded at 2.5 x 10^5 cells per 35mm dish, each well of a 6-well plate, or 5-7 x 10^5 cells in 60mm dishes, in an appropriate volume of media. For immunoflourescence, cells were seeded onto glass coverslips, sterilised by flaming with ethanol, in 6 well plates. The following day, FuGENE 6 transfection reagent (Roche) was diluted in 100µl (35mm dishes) or 150µl (60mm dishes) of serum-free medium and incubated at room temperature for 5 min. The amount of FuGENE used was in a 3:1 ratio to the µg amount of DNA used. Generally, 2µg of DNA was transfected into cells in 35mm dishes and 4µg transfected into cells seeded in 60mm dishes. Diluted FuGENE was added to DNA and incubated at room temperature for 15-20 min. Following incubation, DNA/FuGENE complexes were added, dropwise, to cells and incubated at 37°C overnight. 18-24 h post-transfection, cells were either harvested for analysis by SDS-PAGE and western immunoblotting, or subject to assay conditions such as death assays.

2.8.2 Transfection of *Drosophila* BG2 and SL2 cells using CellFectin reagent

The day prior to transfection, 10^6 cells were seeded into 6 well plates or 35mm dishes, or 2 x 10^6 seeded into 60mm dishes. A total of 2µg or 4µg of plasmid DNA was transfected into 35mm or 60mm dishes respectively as follows: DNA was diluted in 100µl serum free Schneider's Sf-900II medium (SFM-GibcoBRL). In a separate tube, CellFectin reagent (GibcoBRL) was similarly diluted to a final volume of 100µl in SFM. The amount of CellFectin used was in a 4:1 ratio with respect to the µg amount of DNA used. Diluted CellFectin was added to the diluted DNA, mixed gently, and incubated for 20 min at room temperature. 800µl of SFM was added to the DNA/CellFectin mix following incubation. Pre-seeded cell monolayers were washed once with 2-3ml of SFM and then overlayed with the prepared transfection mix. In the case of 60mm dishes, an additional 500µl of SFM was added to ensure adequate cell coverage. Cells were incubated with transfection mix for 4 h at 27°C, after which the medium was aspirated and replaced with 2-3 ml of complete Schneider's medium. Cells were incubated for 16-24 h prior to harvest, or induced with 0.7mM $CuSO_4$ or by heat-shock as described below.

2.9 Immunofluorescence

Following transfection, cells were washed in PBS prior to fixation with 4% PFA (paraformaldehyde)/ 0.18% Triton X-100. After fixation, cells were washed in PBS three times. Primary antibody diluted in PBS containing 10% FBS was added to cells and incubated for 1-3 h at room temperature, shaking gently. Anti-tag antibodies for FLAG, MYC and HA were diluted 1:250 – 1:500. Mitochondria were stained with α-cytochrome c antibody (BD biosciences) and the endoplasmic reticulum with α-Calnexin (Cell Signalling). Cells were washed as above and incubated in secondary antibody for 30 min-1 h. Species-specific antibodies conjugated to fluorophores such as Alexa Fluor® 488 and Alexa Fluor® 568 (molecular probes), rhodomine (Chemicon), TexasRed and FITC (Chemicon) were used to detect transfected proteins of interest. Following incubation in secondary antibody, cells

were washed, coverslips were removed, air-dried and mounted, cells-side down, onto glass slides in a drop of anti-fade solution (1%propylgalate/ 87% glycerol). Fluorescent excitations were analysed using a fluorescent microscope and the appropriate filters. For staining nuclei, a drop of Hoechst DNA stain (diluted to 0.4μg/ml in PBS) was added to cells for 5 min and washed as above, just prior to mounting in anti-fade solution. Due to the FITC, Alexa Fluor® 488 and EGFP green being outside the printing gammut, the green was substituted with a reproducible green in some cases.

2.10 Apoptosis assays

2.10.1 Mammalian cell death assays

COS7 or 293T cells were transiently transfected with pcDNA3 vector expressing STRICA or mutants (C429G, S119G, ΔPD) together with pEF-LacZ in a 3:1 ratio, as described above. Where indicated, STRICA and mutants were cotransfected with DIAP1 or DAKT mammalian expression constructs in equal amounts. 24 h following transfection, cells were fixed and stained for β-galactosidase activity as described for insect cell death assays (see below). β-gal positive cells were analysed by light microscopy and counted as viable or apoptotic based on cellular morphology. Apoptosis was calculated as the percentage of apoptotic blue cells out of the total number of blue cells scored.

2.10.2 SL2 and BG2 cell death assays

Pre-seeded SL2 cells were transiently transfected in duplicate with 1.5μg metallothionein-inducible pRMHa3 vector containing STRICA or STRICA (C429G) together with 0.5μg of the heat shock inducible pCaSpeR.hs-LacZ reporter construct. STRICA was cotransfected with DIAP1, DIAP2 or p35 in equal amounts. A total of 3.5 μg was transfected in each case, made up with empty pRMHa3 vector where necessary. 16 h following transfection, β-galactosidase expression was induced by a 30 min heat shock at 37°C followed by a 30 min recovery at 27°C. This was repeated twice more prior to induction of gene

expression from the metallothionein promoter by the addition of $CuSO_4$ to a final concentration of 0.7mM. To calculate the percentage of cells that survive following protein expression, cells were fixed in 2% formaldehyde/0.2% glutaraldehyde in PBS for 5 min and washed twice in PBS. β-galactosidase activity was visualised by staining cells with X-gal stain (1mg/ml X-gal/ 5mM potassium ferrocyanide/ 5mM potassium ferricyanide/ 2mM MgCl2 in PBS) for 3 h at 37°C. β-gal positive cells were identified microscopically. Loss of cells 48 h after induction was determined as the ratio of β-gal positive cells in $CuSO_4$-induced dishes to the number in untreated dishes. A minimum of 200 cells was counted.

For BUFFY and DEBCL BG2 cell death assays, cells were seeded and transfected using CellFectin (as described above) with 0.5μg pIE-LacZ reporter plasmid and 1.5μg of each construct, to a total of 3.5μg DNA. 24 h after transfection, cells were fixed and stained with X-gal as described above. % survival was calculated by scoring the number of β-gal positive cells over a fixed number of fields of view, compared to the number observed in the vector alone control. In general, death assays were performed in duplicate and represented with ±SD or ±SEM error bars.

2.11 Cellular Fractionation

Cells were seeded into D60 dishes in 1.5ml culture medium, and transfected as described. 24-48 hours post-transfection, cells were detached from dishes in existing medium, using a cell scraper, and transferred to microfuge tubes. Cells were pelleted by centrifugation at 2000rpm for 4 min. Cell pellets were resuspended in 100μl Buffer A (20mM Hepes pH 7, 10mM KCl, 1.5mM $MgCl_2$, 1mM EDTA, 1mM EGTA, 1mM DTT, 250mM sucrose) supplemented with 1x protease inhibitor cocktail (Amersham Biosciences). Cells were incubated on ice for 15 minutes and lysed by passing through a 23-gauge needle 25 times. Lysed cells were centrifuged at 2500rpm for 10 minutes at 4°C to collect the P1 fraction containing undisrupted cells and nuclei. The supernatant was centrifuged at 13000rpm for 10 min at 4°C. The resulting pellet was the heavy membrane (HM) fraction,

containing mitochondria and intact golgi. The supernatant was centrifuged at 50 000rpm in a Beckman ultra centrifuge to pellet light membrane (LM) organelles such as the endoplasmic reticulum (ER) and golgi membranes. The final supernatant contained the soluble (S-100) fraction. The P1 fraction was generally resuspended in 200µl PBS, depending on the pellet size, and the HM and LM fractions were resuspended in 20µl PBS. 7µl 4x PLB (200mM Tris-HCl pH6.8, 400mM DTT, 8%SDS, 0.4% bromophenol blue, 40%glycerol) was added to 20µl aliquots of P1 and S-100, and the HM and LM fractions.

2.12 RNA Analysis

2.12.1 Quantification of total RNA preparations

Measuring the absorbance at 260nm on a spectrophotometer was used to determine the concentration of RNA in a prepared sample, assuming that an OD_{260nm} reading of 1.0 represents 40µg/ml of RNA. RNA integrity was confirmed by electrophoresis on 1% agarose/TAE gels, stained with ethidium bromide, and visualised under short wavelength UV. Alternatively, 5 µg RNA was run on mini-formaldehyde gels (described below) to ensure the integrity of the sample.

2.12.2 RNA extraction

a) Total RNA preparation

For extraction of total RNA from adherent cells, cells were scraped off the tissue culture dishes, pelleted by centrifugation in a microfuge and resuspended in 1 ml TRIzol reagent (Invitrogen). For *Drosophila* embryos, larvae, pupae, adult flies or dissected tissues, samples were homogenised using an microfuge plastic eppendorf homogenisor in 100µl TRIzol. The volume of TRIzol was made up to 1ml following homogenisation. 200µl chloroform per 1 ml homogenate was added, mixed vigorously for 15 seconds and incubated at RT for 2 min. The suspension was than centrifuged at 13 000 rpm for 15 min at 4°C. The aqueous phase containing RNA was transferred to an RNAse-free microfuge tube. RNA was

precipitated by the addition of 500µl isopropanol and incubated on ice for 20-30 min. RNA was pelleted by centrifugation at 13 000rpm for 20 min at 4°C, washed with 70% ethanol, air-dried and resuspended in 20-100µl diethylpyrocarbonate (DEPC) (SIGMA)-treated sterile H_2O, depending on pellet size. RNA concentration was determined by measuring the absorbance at 260nm as described.

b) Poly A^+ RNA purification

PolyA$^+$ RNA was isolated using Dynabeads® mRNA Purification kit (DYNAL). (1mg) Oligo-$(dT)_{25}$ dynabeads were prepared by washing once in 500µl Binding Buffer (20mM Tris-HCl pH7.5, 1M LiCl, 2mM EDTA) and resuspended in 500µl Binding buffer. 100µg of total RNA in100µl DEPC-treated water was heated to 65°C for 5 min in order to disrupt secondary RNA structures. Total RNA was mixed thoroughly with 100µl pre-washed oligo-$(dT)_{25}$ dynabeads. PolyA mRNA was allowed to anneal to the beads by incubation at room temperature for 30 min with gentle rotation. Using the DYNAL MPC-E-1 magnet, the mRNA-bound beads were concentrated to the side of the tube and washed twice in 200µl Washing Buffer (10mM Tris-HCl pH7.5, 0.15M LiCl, 1mM EDTA). mRNA was eluted from the beads by addition of 10µl Elution Buffer (10mM Tris-HCl pH7.5) and incubation at 65°C for 2-5 min. The tube was placed immediately onto the magnet and the eluted mRNA was transferred to a clean microfuge tube. Approximately 2µg mRNA was isolated from 100µg total RNA. Oligo-$(dT)_{25}$ dynabeads were stripped and reconstituted after each use up to 5 times, as follows: 1mg Oligo$(dT)_{25}$ beads were resuspended in 200µl reconditioning solution (0.1M NaOH) and incubated at 65°C for 2 min to rid of any excess bound mRNA. Beads were immediately separated from solution on the magnet and washed twice in reconditioning solution each at 65°C for 2 min. Beads were resuspended in 200µl storage buffer (250mM Tris-HCl pH8, 20mM EDTA, 0.1% Tween 20, 0.02% sodium azide) and washed 3-4 times in this solution until pH<8. Beads were stored in 200µl storage buffer at 4°C.

2.12.3 RNA gel electrophoresis

RNA samples were prepared as follows: 20µg total fly RNA or 2-5µg of PolyA$^+$ selected RNA was mixed with formaldehyde running buffer (4µl formaldehyde, 10µl formamide, 2.5µl 10x MOPS solution, 1µl ethidium bromide [400µg/ml]). Samples were denatured at 65°C for 10 min, chilled on ice and 2µl RNA loading dye (50% glycerol, 1mM EDTA pH8, 0.25% bromophenol blue, 0.25% xyelene cyanol) was added. 5µl RNA molecular weight markers (Boehringer Mannheim) were denatured and treated as above. Samples were loaded onto a 1.2% agarose gel containing 1x MOPS (20mM MOPS pH7, 1mM EDTA pH8, 8mM NaAc), 2.2M formaldehyde in DEPC-treated water, and electrophoresed dry (with buffer just below level of the gel) in 1xMOPS buffer. Gels were electrophoresed at 80 volts for 2h, or until bromophenol blue dye front had run ¾ way through the gel. The gel was washed several times in sterile water prior to scanning using a FluorImager 595 (Molecular Dynamics) with a 610nm filter.

2.12.4 Northern blotting

a) Synthesis of ^{32}P-labelled probes

DNA probes were labelled with ^{32}P using the Geneworks DNA-gigaprime labelling kit as per the manufacturer's instructions. Briefly, 500ng-1µg DNA fragment was denatured at 95°C for 10 min and snap cooled on ice. Denatured DNA was then added to a mix containing 4µl each of dCTP, dTTP, dGTP, 5µl ^{32}P-dATP (50µCi), 5µl reaction mix, 2 units Klenow and incubated at 37°C for 20 min. Labelled probes were purified through Bio-Gel P-6 columns (BIORAD) and then denatured by incubation at 95°C for 10 min. 50µl salmon sperm carrier DNA was heat denatured as above and added to the DNA probe. The labelled probe was finally added to hybridisation buffer and incubated with the membrane in a HYBAID oven overnight at 65°C.

b) RNA transfer

RNA fragments embedded in agarose following electrophoresis were transferred onto Biodyne nylon transfer membrane (Pall) by capillary action overnight (as described in Maniatis et al., 1989). The gel was placed well-side down onto 3mm Whatman paper soaked in 20x SSPE buffer (175.3g/L NaCl, 27.6g/L NaH_2PO_4, 7.4g/L EDTA pH7.4). Nylon membrane, cut to size was placed on top of the gel, followed by 3 sheets of Whatman filter paper and a stack of absorbant paper towel. A weight was placed on top and the transfer apparatus left overnight. The following day, the RNA was cross-linked at 254nm short wavelength UV using and Ultra-Lum UVC-515 Ultraviolet Multilinker at 1800 Joules/m^2.

c) Probe hybridisation and signal detection

The membrane was pre-hybridised in 10ml hybridisation buffer (50% formamide, 5 x SSPE, 1mM EDTA pH8, 5x Denhardts solution, 0.1% SDS, 100µg/ml denatured salmon sperm carrier DNA) at 42°C for 4-5 h in a HYBAID oven. The membrane was probed overnight with a DNA probe labelled using a DNA labelling kit purchased from Geneworks as described above. The following day, hybridisation buffer was discarded and the membrane washed 3 times in 2x SSC/0.1% SDS for 10min per wash, followed by 2-3 washes in 0.5x SSC/0.1% SDS at 65°C. The membrane was laid down between amplifying screens in a film cassette and exposed to X-ray film (KODAK) at -70°C over 1-5 days. Films were processed using an Ilford Ilfospeed 2240 X-ray processor.

2.12.5 *In situ* mRNA analysis

For *in situ* RNA analysis, antisense and sense digoxygenin labelled riboprobes were prepared using T7 and SP6 RNA polymerases from linearized pcDNA3-*strica* as a template. Digoxygenin labelling was performed according to the manufacturer's instructions (Roche Biochemicals). Briefly, 1µg linearised plasmid DNA was mixed with 2µl 10x DIG RNA labelling mix, 2µl 10x transcription buffer, 2µl appropriate RNA polymerase in a total volume

of 20µl. Reactions were incubated at 37°C for 2 h and stopped by the addition of 2µl 0.2M EDTA pH8 on ice. Hybridisation signals for *Drosophila* embryos and larval tissues were further amplified using Tyramide Signal Amplification (TSA™) Indirect system according to the protocol supplied by the manufacturer (NEN Life Science Products). Embryos and dissected larval tissue were fixed in 0.1M Hepes, 50mM EGTA, 0.01% Nonidet P40, 4% paraformaldehyde pH 6.9 for 20 min. Dissected ovaries from 3 day old adult females were fixed and treated with 50% ethanol/50% xylene for 30 min, washed in ethanol, then methanol and finally in PBS with 0.01% Triton X-100 (PBT). Ovaries were then refixed for 25 min in 4% paraformaldehyde and then treated with proteinaseK (5µg/ml) for 8 min at room temperature. Fixed sections were washed several times in PBS/0.05% Tween20 (PBST) and then in hybridisation buffer (50% deionized formamide, 5x SSC, 50µg/ml heparin, 100µg/ml denatured salmon sperm DNA, 0.1% Tween20) for 10 min each. Embryos and tissues sections were pre-hybridised in 400µl buffer, for 1 h at 55°C. Riboprobe was heat denatured and hybridised to sections overnight in 100µl hybridisation buffer. After hybridisation, non-specifically bound probe was removed by digestion with RNaseA (125µg/ml in PBST) for 1 h at 37°C. Hybridisation was detected using the secondary antibody detection system (Boehringer Mannheim) as follows: Sections were blocked in 10% skim milk in TBST (100mM Tris HCl, 150mM NaCl pH7.5, 0.05% Tween20) for 1 h and then incubated with anti-DIG antibody (1:2000 in 10% milk/TBST) for 1 h at room temperature. Unbound antibody was washed 5 times for 20 min each in PBST, followed by 3x 20 min washes in AP buffer (100mM NaCl, 50mM MgCl2, 100mM Tris HCl pH9.5, 0.1% Tween20). Colour development substrates nitro blue tetrazolium (NBT) and 5-bromo-1-chloro-3-indolyl phosphate (BCIP) were mixed in AP buffer and added to embryo/tissue sections and stained for at least 1 h in the dark to allow colour to develop. Reactions were stopped by rinsing several times in PBST/ 20mM EDTA and sections were mounted in 80% glycerol.

2.12.6 First strand cDNA synthesis and RT-PCR

cDNA was generated from total RNA for reverse transcribed (RT)-PCR using the First-strand cDNA Synthesis Kit (Amersham Biosciences) as per the manufacturer's instructions. Briefly, a standard reaction was prepared as follows: 1-5µg of total RNA, made up to 8µl with DEPC-treated H_2O, was heat denatured at 65°C for 10 min and snap-cooled on ice. 5µl Bulk first-strand rection mix, 1µl NotI-d$(T)_{18}$ primer at 0.2µg/µl (or pd$(N)_6$ primer for random primed amplification) and 1µl 200mM DTT solution were mixed in an microfuge tube and added to the denatured RNA sample. The reaction was mixed gently by pipetting and incubated at 37°C for 1 h. Samples were stored at -20°C. For RT-PCR, reactions were set up as described in section 2.4.3 using 1-2µl from a 15µl first-strand cDNA synthesis reaction.

2.12.7 RNA interference (RNAi) in insect cell lines

Using the Ambion MEGAscript™ kit, sense and antisense RNA transcripts were synthesised using linearised pCDNA3 or pGEMTEasy constructs as templates. In brief, linearised plasmid DNA was purified by phenol/chloroform extraction following restriction digestion and analysed by running 1µl on a mini-agarose gel. 1µg linearized plasmid DNA was used in a transcription reaction containing 10x reaction buffer, 75mM dNTPs (for T7 transcription) or 50mM dNTPs (SP6 transcription) and 2.5 units enzyme mix in a total volume of 25µl according to the manufacturer's directions. Synthesis reactions were incubated at 37°C for 5 h to overnight. Newly made RNA molecules were purified by phenol/chloroform extraction and ethanol precipitation. Equal amounts of sense and antisense transcripts were mixed together and secondary structures were removed by heating to 65°C for 20 min. RNA strands were cooled slowly to room temperature, allowing complementary strands to anneal forming double-stranded RNA. dsRNA integrity was analysed by running an aliquot on a mini-formaldehyde gel. Insect cells were seeded into tissue culture plates or

dishes in the presence of 37nM double-stranded RNA and agitated. Cells were incubated with dsRNA for 48-72 h prior to analysis by PCR, western blotting or death assays.

2.13 Protein Analysis

2.13.1 Determination of protein concentration

Protein concentration was calculated using Bicinchoninic acid (BCA) as described by the manufacturers (PIERCE). A standard curve was established by preparing serial dilutions of the protein standard, bovine serum albumin (BSA) in the range 0.1-1.0mg/ml. Reagents A and B were mixed in a 50:1 ratio and 100µl was added to each sample and incubated at 37°C for 30 min until a change in colour was observed. The optical density at 562nm of each standard was measured and plotted on a graph to obtain a standard curve. This graph was then used to determine the protein concentration of samples of interest prepared as above for which the absorbance at 562nm was measured.

2.13.2 Protein extract preparation

To determine expression of a transgene in the fly eye, 10 adult fly heads were dissected and placed in a microfuge tube. 1x Protein loading buffer (PLB, see below) was added and the heads homogenised using an microfuge tube homogenisor. Samples were boiled for 5-10 min prior to analysis by SDS-PAGE and Western blotting. Whole cell protein extracts were prepared by resuspending insect or mammalian cells in PBS, to which an equal volume of 2x PLB (100mM Tris-HCl pH 6.8, 200mM DTT, 4% SDS, 0.2 % bromophenol blue, 20% glycerol) was added. Samples were boiled and loaded on protein gels.

2.13.3 Expression of recombinant protein in *E.coli*

Colonies of *Escherichia coli* BL21 Star cells transformed with the pGEX4T3-STRICA ΔPD expression plasmid were used to inoculate overnight cultures. The following morning, cultures were subcultured 1:50 into 200ml LB and grown for 3 h at 37°C in a shaking

incubator. Protein expression was induced at 37°C for 3 h, or for 5-6 h at 30°C, by the addition of 0.5mM-1mM isopropyl β-D-thiogalactoside (IPTG). Cultures were pelleted by centrifugation at 6000 rpm for 15min and the bacterial pellets resuspended in PBS. Cells were lysed by sonication (5 x 1min bursts with 2min incubation of ice in between each pulse) and clarified by centrifugation at 13000rpm for 10min at 4°C. Solubility was ascertained by SDS-PAGE and Coomassie staining (described below). For lysates prepared for use in caspase cleavage assays, bacterial pellets were sonicated in Ice Assay Buffer (0.1mM Hepes pH7, 10%PEG4000, 0.1% CHAPS, 10mM DTT, 1X protease inhibitor cocktail).

2.13.4 *In vitro* translation

cDNAs were transcribed and translated using the Promega TNT™ Coupled Reticulocyte Lysate System. Protein was labelled with ^{35}S-methionine in a 50µl translation reaction containing 25µl TNT Rabbit Reticulocyte Lysate, 2µl TNT reaction buffer, 1µl T7 or SP6 polymerase, 1µl methionine-deficient amino acid mixture, 4µl ^{35}S-methionine, 1µl RNasin ribonuclease inhibitor, 1µg DNA template and sterile H_2O. Reactions were allowed to proceed by incubation at 30°C for 90min and were stored at -20°C for up to a week, if not used immediately.

2.13.5 Caspase cleavage assays

5µl of ^{35}S-methionine-labelled protein was incubated with either cytoplasmic extracts, purified caspases, bacterially expressed caspases or with 100µg of protein extracts prepared from whole flies, larvae or pupae, for 3 h at 37°C. Assays were prepared in caspase assay buffer in a 20µl total volume. 1x Complete™ protease inhibitor cocktail (Roche) was added where indicated. Reactions were terminated by the addition of an equal volume of 2x PLB and boiling for 5-10min. Samples were centrifuged for 5 min at 9000g and loaded onto SDS polyacrylamide gels for electrophoresis. Following electrophoresis, proteins were transferred

to polyvinylidine difluoride membrane (NEN Life Science Products) using a semi-dry apparatus (Biometra) and visualised by autoradiography.

2.13.6 Immunoprecipitation assays

5x 10^5 mammalian cells or 3x10^6 insect cells were seeded into 6cm dishes in 2ml of appropriate medium. The following day, cells were co-transfected with the plasmids of interest (as described in section 2.7). 24-48 h post-transfection, cells were harvested by rinsing once in ice-cold PBS, and lysed in 1.5ml lysis buffer A (50mM Tris-HCl pH 7.6, 150mM NaCl, 0.1% NP40) or lysis buffer B (20mM Tris-HCl pH 7.4, 135mM NaCl, 02-0.5% Triton X-100, 10% glycerol), supplemented with Complete™ protease inhibitor cocktail and 200µM NaVO3, 1mM NaF, 500µM Na pyrophosphate (Roche) for 30 min on ice. Cells were scraped and transferred to microfuge tubes and debris was pelleted by centrifugation at 13000rpm for 10 min at 4°C. Lysates were transferred to clean tubes and pre-cleared with 20µl protein G-sepharose (Amersham Biosciences), rotating for 2 h at 4°C. Samples were pelleted for 2 min at 13000rpm, 4°C and the supernatants removed to clean tubes. Proteins were immunoprecipitated by the addition 2-4µg of the appropriate antibody, rotating at 4°C overnight. 20µl protein G-sepharose was added either concominantly with antibody overnight, or the next morning for 2 h at 4°C. Antibody/sepharose complexes were collected by centrifugation at 13000rpm for 2 min and washed twice in lysis buffer and twice in PBS. Finally, 20µl 2x PLB was added and the samples prepared for SDS-PAGE.

2.13.7 SDS-PAGE and transfer of proteins to PVDF membrane

Resolving polyacrylamide gels of specific percentage were prepared with the following reagents: 10-15% polyacrylamide solution (BIORAD), 37.5 mM Tris pH8.8, 0.1% SDS, 0.1% ammonium persulfate, 0.05% TEMED (GIBCO). The resolving gels were cast with Hoefer plates and spacers, and overlayed with a 5% stacking gel (5% polyacrylamide, 0.125M Tris-HCl pH6.8, 0.1% SDS, 0.1% APS, 0.1% TEMED) into which a comb of 10-15

wells were inserted. The assembled gel was placed in a Hoefer minigel tank (Amersham Biosciences) and submerged in protein electrophoresis buffer (25mM Tris, 250mM glycine, 0.1% SDS). Samples were prepared for electrophoresis by boiling in an equal volume of 2 X PLB. Samples were loaded into the wells of the protein gel and run through the stacking gel at 100 volts, and through the resolving gel at 200 volts. When the dye front reached the bottom of the gel, separated proteins and prestained markers (Invitrogen) were transferred to a polyvinylidine difluoride (PVDF) (polyscreen Dupont) membrane using a Hoefer semi-dry transfer apparatus (Amersham Biosciences). The transfer apparatus was assembled as follows: two sheets of Whatman filter paper (2M) presoaked in protein transfer buffer (49mM Tris, 39mM glycine, 0.0375% SDS, 20% methanol) were placed on the cathode (+) of the apparatus. A same-sized piece of PVDF, similarly soaked in transfer buffer was placed on top of the Whatmann, followed by the gel and another 2 pieces of Whatmann. Separated proteins were transferred to the membrane for 90 min at 130mAmps.

2.13.8 Coomassie staining

Proteins were visualised directly on polyacrylamide gels by staining with Coomassie Brillian Blue R-250 (Biorad) (0.25% w/v Coomassie Blue in 5:4:1 H_20:MeOH:acetic acid) for a minimum of 1 h at room temperature. Following staining, gels were soaked in destain (5:4:1 H_20:MeOH:acetic acid) replaced several times over 2-3 h.

2.13.9 Western Blotting

Detection of tagged or endogenous protein was carried out following transfer to PVDF. Non-specific sites were blocked by incubating the membrane in a 5% skim milk (Diploma) solution made up in PBS-Tween20 (PBS-T) for 3h at room temperature, or overnight at 4°C, shaking gently. Primary antibodies were diluted in blocking solution at various dilutions. Mouse α-MYC, rat α-HA (Roche) and mouse α-FLAG (Sigma) were all diluted 1:1000. Membranes were blotted with primary antibodies for 2-3 h at room

temperature, or overnight at 4°C. Membranes were washed as follows: 3x 5 min, 2x 10 min in PBS-T. Secondary antibodies, anti-mouse/rat/rabbit conjugated with either horseradish peroxidase (HRP) or Alkaline Phosphatase (AP) (Amersham Biosciences) were diluted 1:2000 in blocking solution and incubated for 1 h at room temperature. Membranes were washed as described above and proteins visualised by the enhanced chemiluminescence (ECL) system (Amersham Biosciences) in the case of HRP-conjugated detection antibodies. In this instance, equal volumes of each ECL reagent were mixed and the blot incubated for 1 min in this mix, after which the membrane was exposed to Hyperfilm ECL (Amersham Biosciences) for 30sec to 5 min depending upon signal intensity. When alkaline phosphatase-conjuagated antibodies were employed, the blot was incubated for 1 min in Attophos reagent (Amersham Biosciences) and visulised on a Typhoon 9410 using ImageQuant software (Amersham Biosciences).

2.13.10 Stripping Western blots

To blot a membrane a second time with another antibody, the blot was rinsed first in PBS-T and then stripped in stripping buffer (100 mM β-mercaptoethanol, 2% SDS, 62mM Tris-hCl pH 6.8) for 5-10 min at 55°C, shaking gently. Following stripping, the blot was washed twice in PBS-T for 10 min and blocked in 5% skim milk/PBS-T as described previously, prior to incubation with primary antibody.

2.14 Manipulation of Drosophila *melanogaster*

2.14.1 Fly stocks

GMR-strica/Cyo	Prof. Bruce Hay, Caltech, CA.
GMR-diap1 (X chromosome)	Dr. Helena Richarson, Peter Mac, Vic
GMR-diap2	Dr. Helena Richarson, Peter Mac, Vic
GMR-p35	Dr. Helena Richarson, Peter Mac, Vic
thread^{5}*/Tm3*	Dr. Helena Richarson, Peter Mac, Vic

GMRGal4UAS-Buffy	Dr. Helena Richarson, Peter Mac, Vic.
UAS-dakt/Cyo	Prof. Armen Manoukian, Toronto
UAS-dpten (2^{nd})	Prof. Armen Manoukian, Toronto
UAS-pkb$_{HA}$ (2^{nd})	Prof. Armen Manoukian, Toronto
w; DAKT q1/Tm3Sb	Prof. Armen Manoukian, Toronto

2.14.2 Fly maintenance

Fly stocks were kept and maintained in vials containing a yeast-based food mix (10g/L agar, 100g/L polenta, 186g/L yeast, 143g/L treacle, 25ml/L tegosept (100g methyl parahydroxybenzoate, 2.5g/L tetracycline in 1L ethanol) and 15ml/L acid mix (orthophosphoric acid: propionic acid at a 1:10 ratio in water). Fly stocks were maintained at 18°C. Genetic crosses were carried out at 18°C, 25°C or 29°C depending on gene toxicity.

2.14.3 Embryo collection

Lay tubes placed over a grape juice agar plate (35g/L J Grade agar, 20g/L sucrose, 30ml tegosept) with a globule of yeast, were used to set up crosses. Flies were allowed to lay eggs on the agar plate. Resulting embryos were washed off the plate with PBS-T and brushed into microfuge tubes. Larvae and pupae were collected by direct separation from adult fly stocks. Larvae are light in colour, distinguishable from pupae with developed mandibula and formation of eye pigment during later pupal stages. Additionally, pupating larvae are sedimentary compared to wandering larvae.

2.14.4 Sexing adult flies

Flies were collected for analysis under carbon dioxide anaesthesia and visualised under a light microscope. Males and females were distinguished from each other in a number of ways. Females have larger, pointed abdomens compared with the smaller rounded

abdomen of males. Males also have black pigmentation on their posterior tergites. Males are easily discerned from females by their genitalia, due to the presence of torsal sex combs.

2.14.5 Collection of virgins

Virgins were collected from adult fly stocks under a light microscope, on CO2 pads. Virgins are very pale in colour and dark meconium is still visible in the underside of the abdomen. Virgins remain so until around 6 h post-eclosion. Vials are cleared first thing in the morning and virgins collected several times throughout the day.

2.14.6 Dechorionation and fixation of embryos

Embryos were aspirated in 50:50 bleach:PBS-T mixture for 2 min and washed thoroughly in PBS-T. Embryos were fixed in 0.5x Buffer A (1M Hepes, 0.5M EGTA, 0.1% NP40), 2% formaldehyde, 50% heptane for 20 min at room temperature with agitation. The bottom layer of solution was removed and replaced with an equal volume of methanol to remove the vitelline membrane. Embryos were shaken until they sunk to the bottom, indicating the removal of the vitelline membrane. Embryos were washed with 3 changes of 1ml methanol for 5 min each wash, at room temperature. Rehydration of embryos was carried out by replacement of half the solution with 50% methanol, 50% PBS-T, shaking for 5 min. 1ml of PBS-T was added and shaken for a further 5 min, followed by several washes in PBS-T. Embryos are then ready for *in situ* hybridisation as described in section 2.12.5. Alternatively, embryos can be stored in ethanol at 4°C and rehydrated, as described, prior to use.

2.14.7 Fly crosses and genetic interaction studies

GMR-strica flies were kindly provided by Prof. Bruce Hay, Caltech, USA. Crosses were set up at 25°C. Virgins were collected and crossed to males. To determine whether STRICA interacts genetically with various molecules *in vivo*, *GMR-strica* flies were crossed

to strains overexpressing DIAP1 (*GMR-diap1*), DIAP2 (*GMR-diap2*) or p35 (*GMR-p35*). To test for interaction between *strica* and the H99 genes, *GMR-strica* flies were crossed to a strain deficient for *reaper*, *hid* and *grim* (*Df(3L)H99*). A strain carrying a specific loss-of-function *diap1* allele (*thread5*) was crossed to *GMR-strica* to assess the progeny for phenotype enhancement. The eye phenotypes of the progeny were examined for suppression or enhancement of the STRICA phenotype by light microscropy, and photographed.

2.14.8 Establishment of balanced, eye-driven stocks

To drive expression of PKB, DAKT and dPTEN in the eye balanced over a phenotypic chromosome, *UAS-dakt*, *UAS-dpten* and *UAS-pkb* were crossed to the *GMR-Gal4* driver line. *GMRGal4/UAS-X* virgins were then crossed with a *Df(2)rougheye/Cyo* double balancer fly stock. Virgin progeny were screened for recombination events resulting in *GMRGal4-UASdakt/Cyo*, *GMRGal4-UASpkb/Cyo*, and *GMRGal4-UASdpten /Cyo* flies. The phenotype of flies overexpressing dPTEN were identified by light microscopy. Two *GMRGal4-UASdpten/Cyo* virgins were collected and crossed back to *Df(2)rougheye/Cyo* flies to generate stocks. Line 2 was used for further crosses. For DAKT and PKB, virgin progeny that appeared to have enlarged eyes and curly wings were selected and crossed back to *Df(2)rougheye/Cyo* to generate stocks. PKB was HA tagged, allowing for detection of overexpressing lines by Western blotting. Of three potential lines, one (line 2) was found to express PKB. A commercial AKT antibody (Cell Signaling) that cross-reacts with *Drosophila* AKT was used to detect lines overexpressing DAKT. Four lines were identified and two, lines 4 and 5, were used in subsequent crosses. Protein extracts were prepared from 10 fly heads (5 male and 5 female) and analysed by SDS-PAGE. Eye-driven lines were crossed to *GMR-strica* flies and the progeny assessed for enhancement or suppression of the STRICA overexpresion eye phenotype.

Chapter 3

The Cloning and Characterisation of a Novel Drosophila Caspase, STRICA

3.1 Introduction

Prior to the cloning of *strica*, five *Drosophila* caspases, DCP-1, DRONC, DECAY, DREDD and DRICE, were published in the literature (Song *et al.*, 1997; Dorstyn *et al.*, 1999a; Dorstyn *et al.*, 1999b; Chen *et al.*, 1998; Fraser and Evan 1997). The sixth caspase, DAMM (Harvey *et al.*, 2001) was cloned and characterised concomitantly with the cloning of STRICA (Doumanis *et al.*, 2001). The cloning of the caspase, STRICA, added the seventh and final member to the *Drosophila* caspase family (Kumar and Doumanis, 2001). With the sequence of the entire *Drosophila* genome released early in 2000 (Rubin *et al.*, 2000; Myers *et al.*, 2000), no other caspase molecules are predicted.

Upstream or initiator caspases are characterised based on the presence of a long prodomain. In some caspases, long prodomains are required for adaptor binding and subsequent caspase activation. In *Drosophila*, DRONC and DREDD contain long prodomains. The DRONC prodomain contains a CARD (**CA**spase **R**ecruitment **D**omain) which mediates the interaction between DRONC and the CED-4/Apaf-1-like adaptor molecule, DARK, making DRONC a likely functional homologue of mammalian Caspase-9. DREDD contains two Death Effector Domains (DEDs) and is able to bind to the *Drosophila* homologue of the mammalian Caspase-8 adaptor, dFADD (Hu and Yang, 2000).

The aim of this chapter was to clone a caspase predicted by the sequenced and annotated *Drosophila* genome and demonstrate the ability for this molecule to function as a caspase. This chapter reports the cloning of the *Drosophila* caspase STRICA from a *Drosophila* larval cDNA library and demonstrates that STRICA is a long prodomain-containing caspase that contains all the conserved features that characterise the caspase family. STRICA is expressed throughout *Drosophila* development. STRICA is able to induce apoptosis when overexpressed in both mammalian and insect cell lines. STRICA autoprocesses between the prodomain and large subunit when overexpressed, and is is shown to cleave DIAP. The potential function of the prodomain is discussed.

3.2 Identification and cloning of the *strica* cDNA

strica was identified using a TBLASTN search of the Berkeley *Drosophila* Genome Project database, as a region of genomic DNA displaying significant homology to mammalian caspases. From this region of homology, *strica*-specific primers were designed and used in conjunction with library-specific vector primers to amplify various sections of the *strica* coding region from a *Drosophila* larval cDNA library. The full-length *strica* open reading frame (ORF) could not be amplified as a single PCR product from this library. The 5' end of the *strica* ORF was obtained from EST clone LP09213 (Research Genetics). A region overlapping with the 5' fragment obtained in the EST to the 3' end of *strica* was amplified using library DNA as a template. The full-length sequence was cloned using a BanI site in the overlapping region. The cDNA sequence of *strica* has been deposited in the GenBank database under accession number AF242735.

The sequence of *strica* encodes an initiator methionine residue downstream of a predicted stop codon. The genomic sequence contains three exons separated by two short intronic regions. At the 3' end, a stop codon marks the end of the open reading frame. The *strica* ORF consists of 1581 coding nucleotides (figure 3.1) and encodes a protein product of 527 amino acids giving rise to a protein with a predicted molecular weight of 57 kilo Daltons (kDa) (figure 3.2B).

The primary sequence of STRICA contains all the conserved residues found in members of the caspase family including a catalytic cysteine residue within a QACKG active site (figure 3.2 A). Based on amino acid sequence comparison with other known mammalian and insect caspases, STRICA is most homologous to the long prodomain-containing caspases DREDD, and Caspase-8 (figure 3.2 C). Interestingly, the caspase domains of STRICA share the highest degree of identity with the short prodomain-containing caspase, DAMM (GenBank accession no. AF240763). The QACKG sequence surrounding the catalytic

Figure 3.1 Genomic organisation of the *strica* gene

A The genomic organisation of the *strica* gene is shown. The gene consists of three exons separated by two small introns. Numbers denote the coding region of the gene. **B** The complete coding sequence of *strica* is shown in blue. The initiation methionine and 3' stop codon are shown in pink. The two introns of approximately 60bp each are represented by inverted triangles.

A

B

```
1     tcacaaagcaactacagcgcagtgcgtgaaagccagtttaagacagaaagctcaacacac
61    gcaaaccggagtcattatgggttggtggagcaagaaaagcgagacggatcgcagtcagcc
121   cagccaggaactggtggcgcaggacccgcgcacacgagtccagactacgagtgcagccac
181   ggagacgaccaacacagccgtgcaaaactcgaccataacggacaacaacaagcagacggt
241   tacctttctcaccacccgccagacggtgacgcacacgcagcgggcgctgatcacggagac
301   gacaacgcgacgcacgcctagtcaggcggagttagaggctctcttcgcaaagataaagat
361   gggcggtgagggacccattggctccaccaccaccactacgacgaccacctcctcgcgctc
421   ccgaccgcccagtttgaacggcgtctcctttcgctccacacaacccttcaaagccacggc
481   aagcaatgctggcaaacggtcaagcaccttagtcaagaccgagcagacgacagtgaccca
541   aaagaatgggcgcacggtcacccagcacctggagactcatagagtggacctcaagggaag
601   tcgacctaaggcgacctgggcgtcatttgcgtccactgcaaacagctcaacatccagcta
661   cgtctcaccttatcgtcagaagccaagcatggccataacttgcacatctcccaacatcaa
721   gacaccaaaaaccactagctccacgtccagttccagtgccagctccattacgagtccgcc
781   caaaccatcatcatctgtatcctccatttcaagcattttcaagtccgctcccaagcaagt
841   tgacaagccgctcagttctaccgcaactcccaagcccttcattagtctgggatcgtcagg
901   aggcaccaagccgaaggtcactgccgtcgcgcaatcccaagatgcccagggcacgatttc
961   aacgagcctgggtatctcgaaatcaagcctgaccaagaacaaactcaagcccgcccgggt
1021  gtatatcttcaaccacgagcggttcgataacaagaacgaattccgaaagggaagtgccca
1081  ggatgtgaaggtcttgcgcgccacctttgagcagctgaagtgcaaagtggaagttattac
1141  agatgcaaccctggtcaccattaaaaaaacagtgcgaatgttgcaaaccaaggactttga
1201  ggacaaaagcgctctggtcctcgtgatcctcagtcatggaacgcgccacgaccagatcgc
1261  agcaaaggatgacgactactccctggacgacgacgttgtttttcccattttgcgcaatag
1321  gacgcttaaggacaagcccaagctgattttcgttcaggcctgcaagggcgactgccaact
1381  agggggctttatgaccgatgccgcgcagcccaatgggtctccgaatgaaatcctcaagtg
1441  ctatagcacgtacgagggatttgtatcttttcgcacggaggacggaactccttttattca
1501  gacactgtgtgaagctcttaatcgatcggggaagacttcagacatcgacaccataatgat
1561  gaatgtgcgtcaagtggttaaaatgcaatccaaagaccgccaaattccatctgtcactag
1621  cactcttacctctaagtacgtttttggagattatatttgaccatagatcttaaatataag
1681  acacgccattaaatatcaaaatttgaccatagatcttaaatctaagacacgccattaaat
1741  atcaaaatt
```

Figure 3.2 STRICA protein sequence

A The primary structure of STRICA is shown, with the catalytic cysteine and surrounding residues highlighted in black. The putative prodomain of STRICA is rich in serine (S) and threonine (T) residues as highlighted in grey. **B** FLAG-tagged STRICA expressed in cultured mammalian cells demonstrates a protein consistent with the predicted molecular weight of 57kDa. **C** A phylogenetic tree representing relationships between the *Drosophila* caspase family members and various mammalian caspases. Human caspases are indicated by an 'h' and Sf Caspase-1 is a baculoviral caspase.

A

```
MGWWSKKSETDRSQPSQELVAQDPRTRVQTTSAATETTNTAVQNSTITDN      50
NKQTVTFLTTRQTVTHTQRALITETTTRRTPSQAELEALFAKIKMGGEGP     100
IGSTTTTTTTTSSRSRPPSLNGVSFRSTQPFKATASNAGKRSSTLVKTEQ     150
TTVTQKNGRTVTQHLETHRVDLKGSRPKATWASFASTANSSTSSYVSPYR     200
QKPSMAITCTSPNIKTPKTTSSTSSSSASSITSPPKPSSSVSSISSIFKS     250
APKQVDKPLSSTATPKPFISLGSSGGTKPKVTAVAQSQDAQGTISTSLGI     300
SKSSLTKNKLKPARVYIFNHERFDNKNEFRKGSAQDVKVLRATFEQLKCK     350
VEVITDATLVTIKKTVRMLQTKDFEDKSALVLVILSHGTRHDQIAAKDDD     400
YSLDDDVVFPILRNRTLKDKPKLIFVQACKGDCQLGGFMTDAAQPNGSPN     450
EILKCYSTYEGFVSFRTEDGTPFIQTLCEALNRSGKTSDIDTIMMNVRQV     500
VKMQSKDRQIPSVTSTLTSKYVFGDYI                             527
```

B

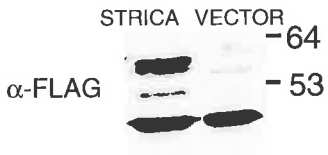

C

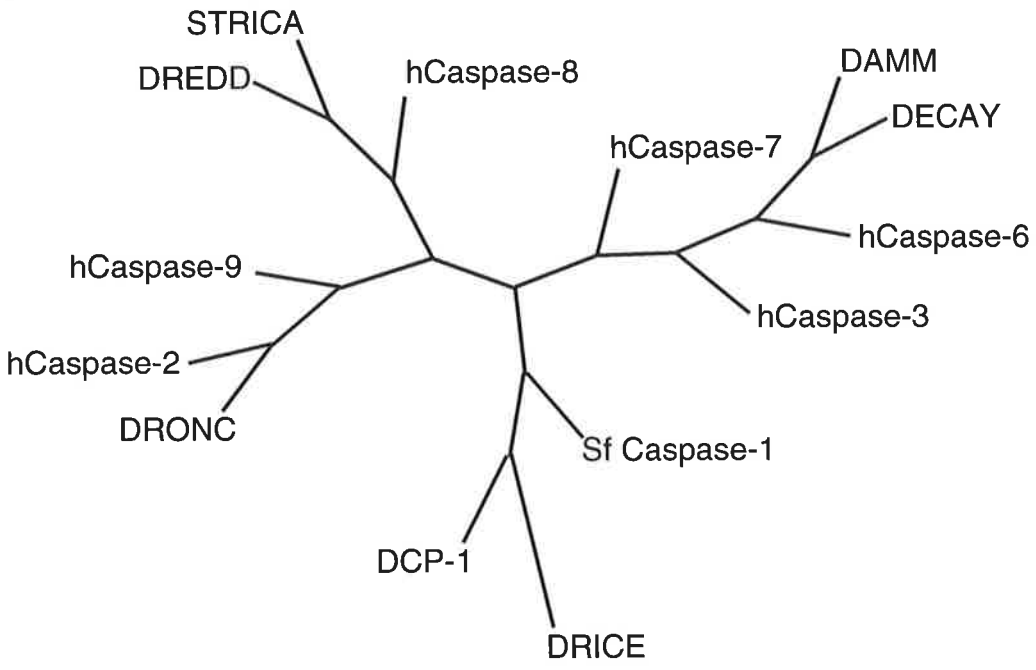

cysteine residue is identical in DAMM and STRICA. None of the other five fly caspases share this sequence.

Although a phylogenetic tree composed of the *Drosophila* caspases and several mammalian caspases places STRICA next to DREDD and Caspase-8, the prodomain of STRICA lacks a CARD or DED and, in fact, possesses no known protein-protein interaction domains. This prodomain remains unique amongst all known caspases. Of note are the numerous serine and threonine residues distributed throughout the putative prodomain (figure 3.2 A). It was this feature that led to the naming of STRICA (**S**er/**T**hr-**RI**ch **CA**spase).

3.3 Developmental expression of *strica*

Northern blot analysis of *strica* expression showed very weak bands of around 2.5 kb at several developmental stages (data not shown) suggesting that *strica* is expressed at low levels during development. To determine the expression pattern of *strica* throughout *Drosophila* development, total RNA was isolated from embryos, larvae, pupae and adult flies. Random-primed cDNAs were reverse-transcribed and used as templates in PCR reactions. *strica* is expressed uniformly in early embryos and first instar larvae. Expression is downregulated during second and third instar larval stages prior to upregulation in early pupae, a time where the developing fly is undergoing massive programmed cell death in order to histolyse tissues such as the midgut and salivary glands which are not present in adulthood (figure 3.3 A).

The expression pattern of *strica* during fly development was further analysed by *in situ* hybridisation to *Drosophila* embryos and larval tissues using a digoxigenin-labelled antisense mRNA probe (Figure 3.3 B). Because of the low expression of *strica*, tyramide amplification following hybridisation was used to detect *strica* mRNA expression. In early embryos, *strica* mRNA was present uniformly, but became more concentrated in some tissues later during embryogenesis (figure 3.3 B (a, c)). *strica* expression was clearly evident in the midgut and salivary glands from third instar larvae (e and g). As stated earlier, these tissues

Figure 3.3 Developmental expression of *strica*

A *strica* mRNA is expressed throughout *Drosophila* development. cDNA synthesised from total RNA was used as a template for PCR. The expected 393 bp *strica* product was detected in all stages of development. Expression is downregulated in late larval stages, before being upregulated in pupal stages and maintained to adulthood. The *Drosophila* housekeeping gene, ribosomal protein 49 (*rp49*) expressed ubiquitously throughout *Drosophila* development, was used as an internal control. **B** *In situ* analysis of *strica* expression during development. A *strica* antisense RNA probe labelled with digoxygenin was used to detect expression *in situ.* **a** Expression of *strica* in a stage 4 syncytial blastoderm shows remnants of maternally deposited mRNA. **b** and **c.** Germ band extended (stage 9-10) and germ band retracted (stage 13-14) with antisense *strica* probe. **d.** Germ band retracted (stage 13-14) with sense *strica* control probe. Late 3rd instar larval midgut with antisense *strica* probe (**e**), and negative control sense probe (**f**). Late 3rd instar larval salivary gland with antisense *strica* (**g**) and sense control probe (**h**). Adult ovaries (stage 10a and 10b) with sense *strica* probe (**i**) and nuclei stained with Hoechst DNA stain (**j**). Adult ovaries before (stage 10a) and after (stage 11/12) nurse cell cytoplasmic dumping (**k**). **l.** Hoechst staining of the ovaries shown in K. **m.** Adult ovaries stained with sense *strica* probe.

A

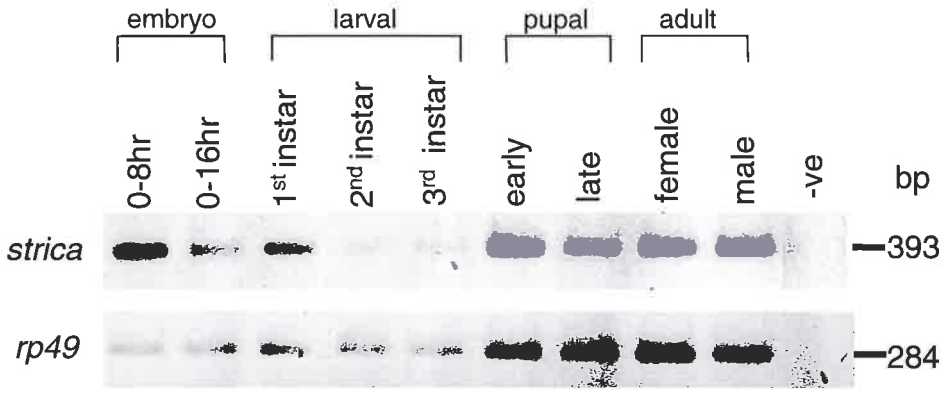
embryo
larval
pupal
adult
0-8hr
0-16hr
1st instar
2nd instar
3rd instar
early
late
female
male
-ve
bp
strica
393
rp49
284

B

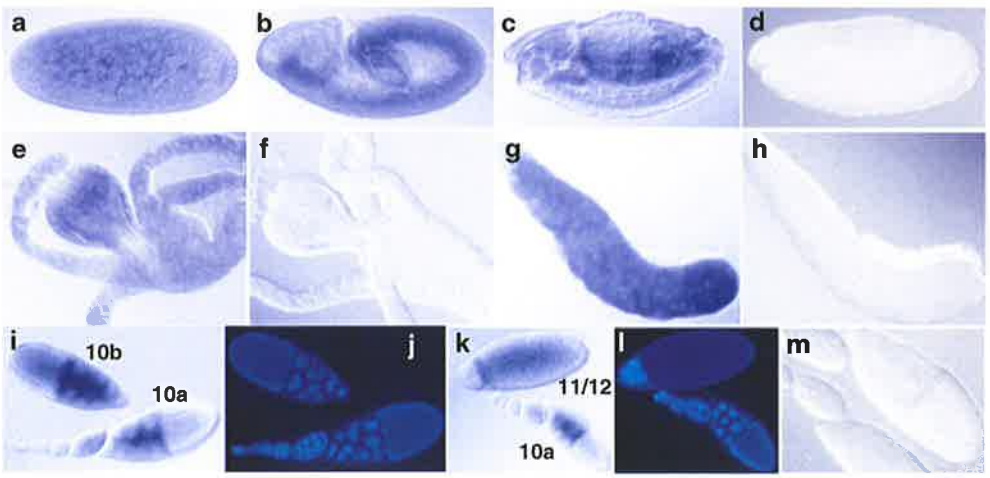
a
b
c
d
e
f
g
h
i
10b
10a
j
k
11/12
10a
l
m

are known to undergo massive cell death during larval to pupal metamorphosis and are completely removed by adulthood (Baehrecke, 2000, 2002). mRNA for other fly caspases, including *dronc* and *decay*, are known to accumulate in larval midgut and salivary glands before histolysis of these tissues (Dorstyn *et al.*, 1999a and 1999b). Relatively high levels of *strica* transcript were evident in the nurse cell compartment of stage 10a and 10b ovaries (figure 3.3 B (i)). At later stages, when nurse cells dump their cytoplasmic contents into the oocyte (Buszczak and Cooley, 2000) *strica* mRNA was clearly seen in the oocyte (k). These results indicate that the relatively high levels of *strica* RNA in early embryos (a; data not shown for pre-cellularised embryos) is likely to be derived maternally.

A burst of the steroid hormone ecdysone at the prepupal to pupal transition is responsible for the upregulation of a number of genes, including several known apoptotic regulators including *dronc*, *drice* and *dark*. *strica* has also been reported to be upregulated seven fold at the RNA level in response to ecdysone (Lee *et al.*, 2003). However, despite an increase in *strica* RNA during the early pupal stage (figure 3.3 A), no direct upregulation by ecdysone was confirmed (data not shown).

3.4 Localisation of STRICA in transfected cells

Most caspases reside in the cytoplasm of the cell with Caspase-2 and Caspase-12 as notable exceptions, localising to the nucleus and golgi, and endoplasmic reticulum respectively (Colussi *et al.*, 1998a; Mancini *et al.*, 2000; Nakagawa *et al.*, 2000). To determine the subcellular localisation of STRICA in cultured cells, immunofluorescence was performed in mammalian 293T cells and *Drosophila* SL2 cells. Cells were transiently transfected with expression constructs containing either wild-type STRICA or STRICA with its catalytic cysteine residue replaced with a glycine residue (C429G), tagged at the carboxy terminus with the FLAG epitope. Protein localisation was determined by staining with α-FLAG monoclonal antibody and α-mouseFITC. STRICA localised to the cytoplasm of the cell in a semi-diffuse fashion with complete exclusion of the nucleus (figure 3.4). In 293T

Figure 3.4 The subcellular localisation of STRICA in transfected cells

Localisation of STRICA in transfected cells. Constructs expressing FLAG-tagged STRICA or STRICA (C429G) were transfected into 293T cells (upper panels) and *Drosophila* SL2 cells (lower panels). For 293T cells, 24 hours post-transfection, cells were fixed and stained with α-FLAG antibody and analysed by fluorescence microscopy. For SL2 cells, STRICA expression was induced with 0.7mM $CuSO_4$ for 24 hours prior to fixation, immunostaining and visualisation. In both cell types, STRICA localisation is cytoplasmic.

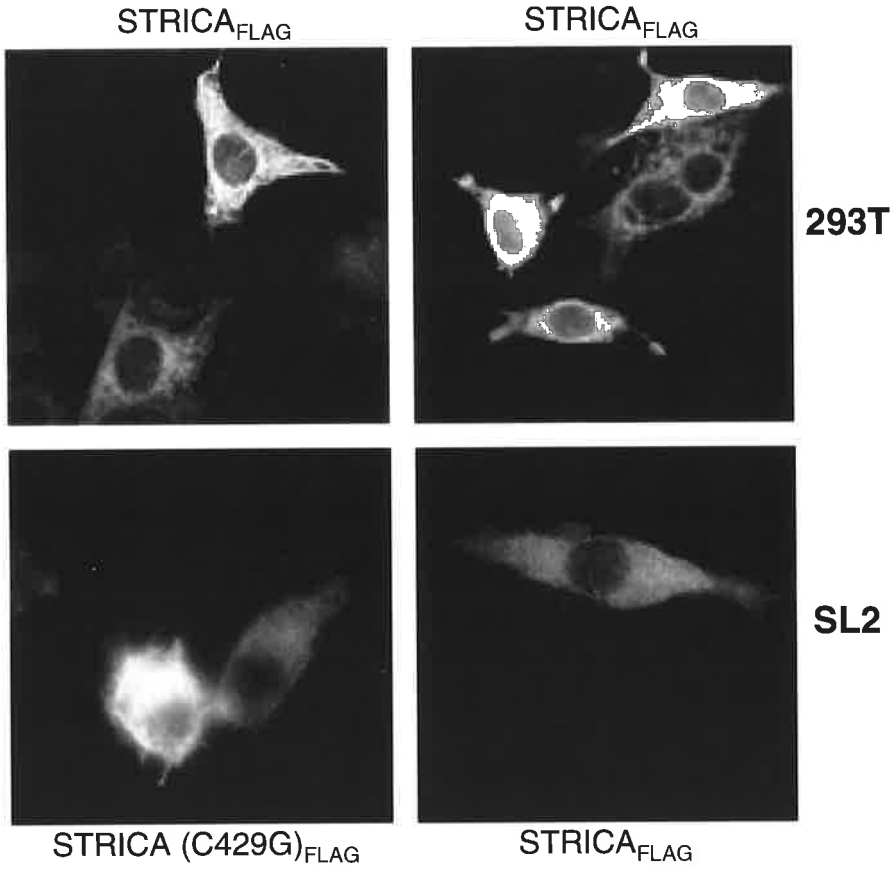
STRICA$_{FLAG}$
STRICA$_{FLAG}$
293T
SL2
STRICA (C429G)$_{FLAG}$
STRICA$_{FLAG}$

cells, STRICA appeared to be localised to the cytoskeleton, however, STRICA did not colocalise with actin fibres (data not shown).

3.5 The prodomain of STRICA does not oligomerise

Caspases with long prodomains are activated by proximity-induced autocatalytic processes (Kumar, 1999; Kumar and Colussi, 1999; Boatright *et al.*, 2003; Boatright and Salvesen, 2003; Degterev *et al.*, 2003). In this model, a CARD or DEDs in the prodomain mediate oligomerisation of procaspase molecules directly, or via specific adaptor molecules. In the case of mammalian Caspase-2, the CARD domain is sufficient for homodimerisation in yeast two-hybrid assays (Butt *et al.*, 1998; Colussi *et al.*, 1998b). Additionally, when fused to the downstream caspase, Caspase-3, the prodomain of Caspase-2 is able to constitutively activate Caspase-3 (Colussi *et al.*, 1998). The ability of the prodomain of Caspase-2 to oligomerise enables Caspase-2 to autoactivate when overexpressed in cell lines (Butt *et al.*, 1998).

Although STRICA does not contain a CARD domain, yeast two-hybrid constructs were made to test whether the long prodomain of STRICA could dimerise. Various STRICA constructs were generated in the yeast two-hybrid vectors pAS2.1 and pACT2. One construct expressed the Gal4 DNA binding domain (DBD) fused to the prodomain of STRICA, while the second construct encoded a Gal4 activation domain (AD)-prodomain fusion. Constructs encoding full-length, catalytically inactive STRICA were also tested. Each construct had a selectable marker to confirm expression of the proteins of interest in transformed yeast. Pairs of constructs were simultaneously transformed into the auxotrophic yeast strain, Hf7C, and plated onto medium lacking TRP and LEU to select for yeast colonies expressing both plasmids. To select for colonies expressing proteins capable of interaction, an aliquot of the same transformation mix was plated onto -TRP-LEU-HIS medium. All STRICA transformants were able to grow on -LEU/-TRP medium demonstrating that these cells were expressing both constructs, however no growth was observed on -LEU/-TRP/-HIS plates

(Table 3.1). Caspase-2 prodomain fusions and murine p53/SV40 Large T antigen served as positive controls. Interaction between both Caspase-2 prodomains brought both the Gal4 DBD and AD together, initiating expression of the HIS3 reporter on -LEU/-TRP/-HIS media. Similarly, an interaction between p53 and the SV40 Large T antigen allowed growth on medium lacking histidine. Despite demonstrating the use of this system to confirm an interaction between two proteins, yeast cells expressing STRICA prodomain fusion proteins were unable to activate gene expression and grow on -HIS plates. These results suggest that, unlike the Caspase-2 prodomain, the prodomain of STRICA does not have the ability to homodimerise.

Gal4DBD construct in vector pAS2.1	**Gal4AD construct in vector pACT2**	**Growth on -LEU-TRP**	**Growth on -LEU-TRP-HIS**
Empty vector	Empty vector	+	-
Caspase-2 prodomain	Caspase-2 prodomain	+	+
p53	SV40 Large T antigen	+	+
p53	Empty vector	+	-
STRICA(C429G)	STRICA(C429G)	+	-
STRICA(C429G)	STRICA ΔPD	+	-
STRICA(C429G)	STRICA prodomain	+	-
STRICA prodomain	STRICA prodomain	+	-

Table 3.1 The prodomain of STRICA is not an oligomerisation domain.

Various STRICA constructs were expressed in the yeast two-hybrid vectors pAS2.1, which carries a TRP1 nutritrional marker gene, and pACT2, which carries a LEU2 marker gene. Hf7C competent yeast cells, auxotrophic for TRP, LEU and HIS, were transformed with pairs of constructs and plated onto selection medium as indicated. Positive interactors were able to grow on medium lacking HIS.

3.6 Ectopic expression of STRICA induces apoptosis in SL2 cells

In vivo, caspases exist as inactive zymogens and remain dormant in healthy cells until an apoptotic signal is received. However, when overexpressed in cultured cells, many caspases are able to induce apoptosis (Kumar and Lavin, 1996; Thornberry and Lazebnik, 1998; Nicholson, 1999). Initiator caspases are known to autoprocess when overexpressed, thereby causing cell death (Degterev *et al.*, 2003). To assess the cell killing ability of STRICA, *Drosophila* SL2 cells (Schneider, 1972) were transfected with a copper-inducible plasmid (pRMHa3) expressing either wild type STRICA or STRICA (C429G), together with a heat shock-inducible LacZ reporter construct (pCaSpeR-LacZ). 48 hours after induction of protein expression with copper sulphate and heat shocking at 37°C, cells were stained for β-galactosidase activity. Cell survival was calculated as the percentage of transfected (β-gal positive) cells in the copper sulphate-treated population relative to the percentage of transfected cells in the untreated population. All calculations were normalised against the 100% cell survival of vector-transfected cells. At 48 hours following induction of protein expression, around 50% of cells transfected with the wild-type STRICA construct were lost when compared to cells transfected with vector alone or STRICA (C429G) (figure 3.5).

IAPs function to suppress the activity of caspases in both their dormant and active states (section 1.5.2). In *Drosophila*, the role of IAPs is critical for cell survival (Wang, S.L *et al.*, 1999; Hay 2000). In particular, loss of DIAP1 in cultured cells by RNAi depletion results in unrestrained caspase-dependent cell death (Rodriguez *et al.*, 2002; Muro *et al.*, 2002). Another *Drosophila* IAP, DIAP2 plays a more enigmatic role that remains to be fully elucidated. To determine whether apoptosis induced by STRICA overexpression in cell lines is suppressed by *Drosophila* IAPs and the viral inhibitor of apoptosis, p35, STRICA was coexpressed with DIAP1, DIAP2 and p35 expression constructs, together with pCaSpeR-LacZ in *Drosophila* SL2 cells. DIAP1 effectively inhibited STRICA activity in these cells, while DIAP2 and p35 inhibited STRICA activity to a lesser extent as demonstrated by this assay (figure 3.5).

Figure 3.5 Ectopic expression of STRICA in cultured cells induces apoptosis

Overexpression of STRICA in cultured SL2 cells induces cell death. *Drosophila* SL2 cells were cotransfected with empty vector, pRMHa3-STRICA$_{FLAG}$, or STRICA (C429G)$_{FLAG}$ together with a LacZ reporter construct. Loss of cells was determined by the ratio of blue cells in copper-induced transfectants to the number of blue cells in uninduced populations. Where indicated, STRICA expression constructs were cotransfected with DIAP1, DIAP2 and p35 expression constructs. Wildtype STRICA expression results in a 50% loss of cells, whereas STRICA (C429G) does not induce significant apoptosis. The results, shown as average percentages ± SEM, were derived from three independent experiments.

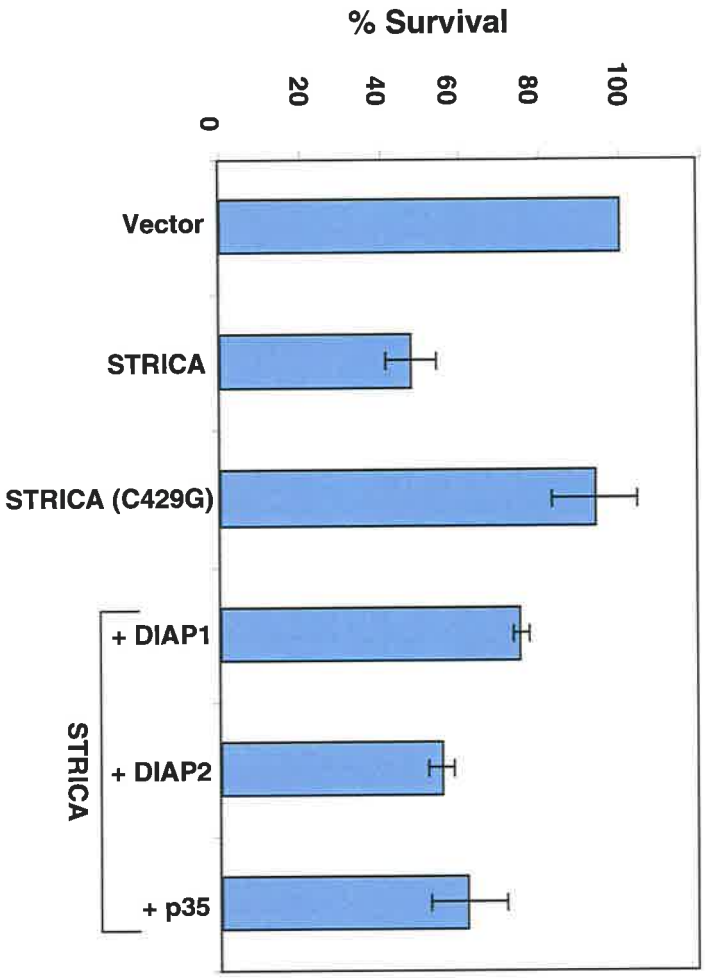
% Survival
0
20
40
60
80
100
Vector
STRICA
STRICA (C429G)
+ DIAP1
+ DIAP2
+ p35
STRICA

3.7 Cell death induced STRICA in 293T cells is morphologically similar to apoptosis

Apoptotic cell death was originally discovered based on the presence of morphological characteristics distinct from necrotic cell death (Kerr *et al.*, 1972). To establish that cell death induced by STRICA is consistent with apoptosis, 293T cells were co-transfected with pcDNA3-$_{FLAG}$STRICA and pEF-β-gal and stained for β-galactosidase activity with X-gal 24 hours later. Cells overexpressing STRICA were identified by the expression and activity of β-galactosidase and were assessed by light microscopy. Cells overexpressing STRICA displayed morphologies consistent with apoptosis including cytoplasmic shrinkage and plasma membrane blebbing (figure 3.6). Cells eventually detached completely and were lost. Therefore, cell death induced by STRICA occurs through the activity of the highly conserved apoptotic machinery in cells accompanied by common features of apoptosis.

3.8 STRICA stability is not affected by the proteasome inhibitor MG132

Full-length STRICA is difficult to detect, even when overexpressed in cell lines. A PEST domain in the prodomain of STRICA is predicted by WWW PESTfind (European Molecular Biology Network) with a score of +9.73, where a score above +5 is considered significant. PEST domains cause protein instability, raising the possibility that STRICA is rapidly degraded via the proteasomal degradation pathway (Rechsteiner and Rogers, 1996). To determine whether STRICA could be stabilised by inhibiting the proteasomal degradation pathway, COS cells were transfected in duplicate with pcDNA3 constructs expressing wildtype STRICA, STRICA (C429G), or STRICA ΔPD. The duplicate transfectants were treated with 50μM of the proteosome inhibitor, MG132 for 4 hours. Full length, catalytically active STRICA was barely detectable when immunoblotted with α-FLAG monoclonal antibody, whereas STRICA (C429G) was easily detected and expressed at high levels (figure 3.7 A). Based on this observation, it was concluded that the inability to detect high levels of STRICA protein is due to apoptosis induced in cells expressing STRICA. Cell death was due

Figure 3.6 Morphology of transfected cells expressing STRICA

293T cells were transfected with empty pcDNA3 vector or pcDNA3-STRICA, in a 3:1 ratio with a β-galactosidase expression construct. 18 hours post-transfection, cells were fixed and stained with X-gal. The morphology of blue cells was analysed by light microscopy. Compared with viable cells expressing empty pcDNA3 vector, cells expressing STRICA undergo programmed cell death and display the morphological features associated with apoptosis including cell shrinkage and membrane blebbing (indicated by arrows). Cells induced to die by STRICA overexpression detach from the dish and therefore fewer cells are observed. Cells were visualized under 10X (top panel) and 20X (lower panel) magnification as shown.

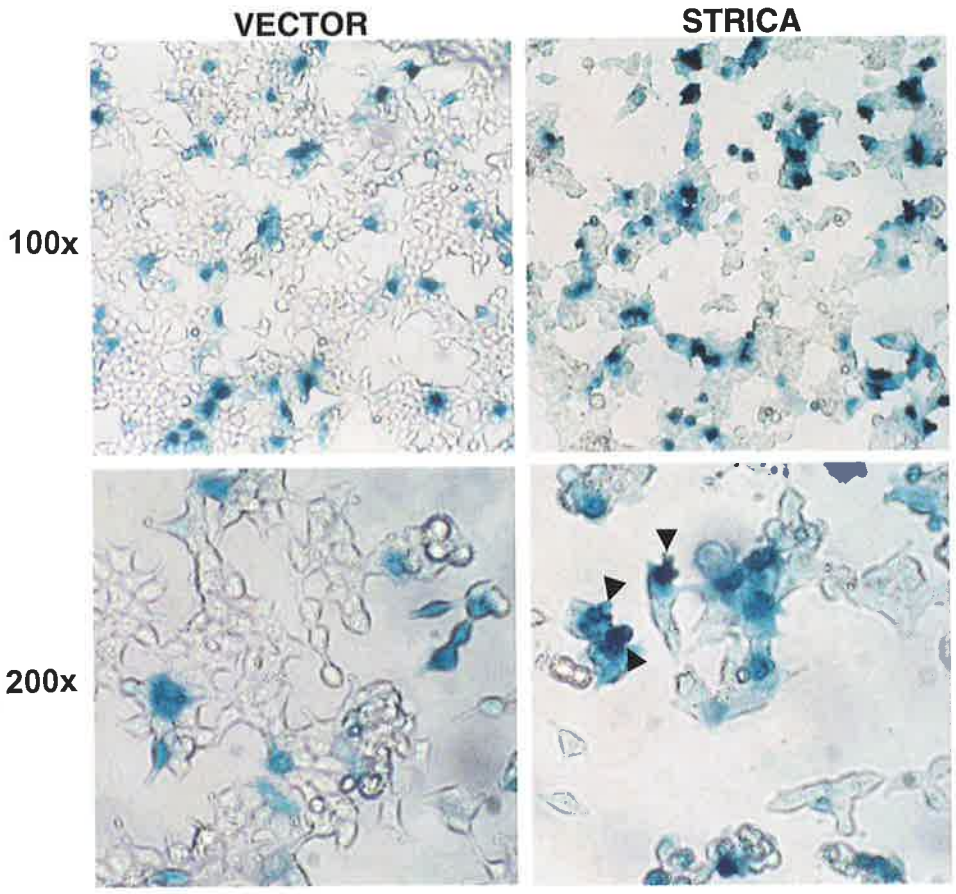
VECTOR
STRICA
100x
200x

Figure 3.7 STRICA protein is difficult to detect due to apoptosis

A To determine whether the inability to detect full-length STRICA protein is due to protein stability, pcDNA3-STRICA$_{FLAG}$, pcDNA3-STRICA (C429G) $_{FLAG}$ and pcDNA3-STRICA ΔPD$_{FLAG}$ were expressed in duplicate in COS cells. 24 hours post-transfection, cells were either left untreated, or treated with 50μM of the proteasome inhibitor, MG132, for 4 hours. MG132 had no effect on STRICA stability. Catalytically inactive STRICA (C429G) is expressed at high levels, demonstrating that the inability to detect STRICA is due to cell death induced by STRICA overexpression in cells. **B** Consistent with A, inhibition of STRICA-induced cell death in COS cells by coexpression with DIAP1 stabilises STRICA to some extent. COS cells were transfected with constructs as indicated. 24 hours following transfection, cells were harvested, resuspended in protein load buffer and samples run on a 10% SDS-PAGE gel. All STRICA constructs are C-terminally FLAG-tagged while DIAP1 is tagged with MYC at the C-terminus. A smaller STRICA product is observed when the wildtype construct is overexpressed, that migrates at the same rate as STRICA ΔPD. DIAP1 expression is shown in the middle panel by blotting with α-MYC antibody. Full-length DIAP1 and a smaller migrating cleavage product are detected by α-MYC Western blotting (lane 5). β-Actin was detected using an anti-β-Actin antibody and was used as a loading control. Non-specific (NS) bands are indicated.

A

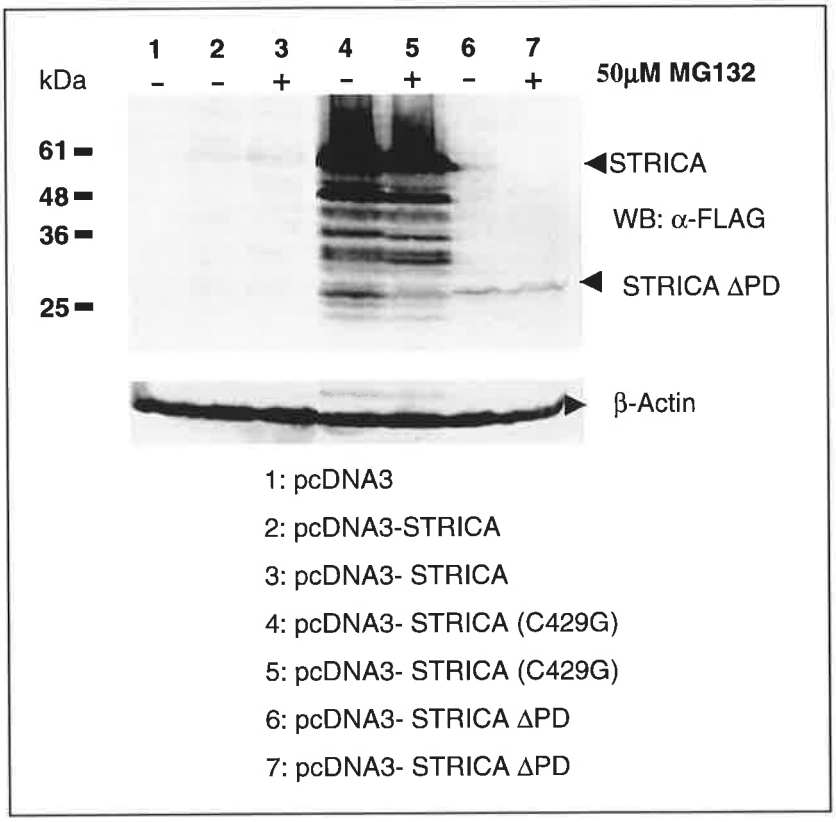
1 2 3 4 5 6 7
kDa
- - + - + - +
50μM MG132
61
48
36
25
STRICA
WB: α-FLAG
STRICA ΔPD
β-Actin
1: pcDNA3
2: pcDNA3-STRICA
3: pcDNA3- STRICA
4: pcDNA3- STRICA (C429G)
5: pcDNA3- STRICA (C429G)
6: pcDNA3- STRICA ΔPD
7: pcDNA3- STRICA ΔPD

B

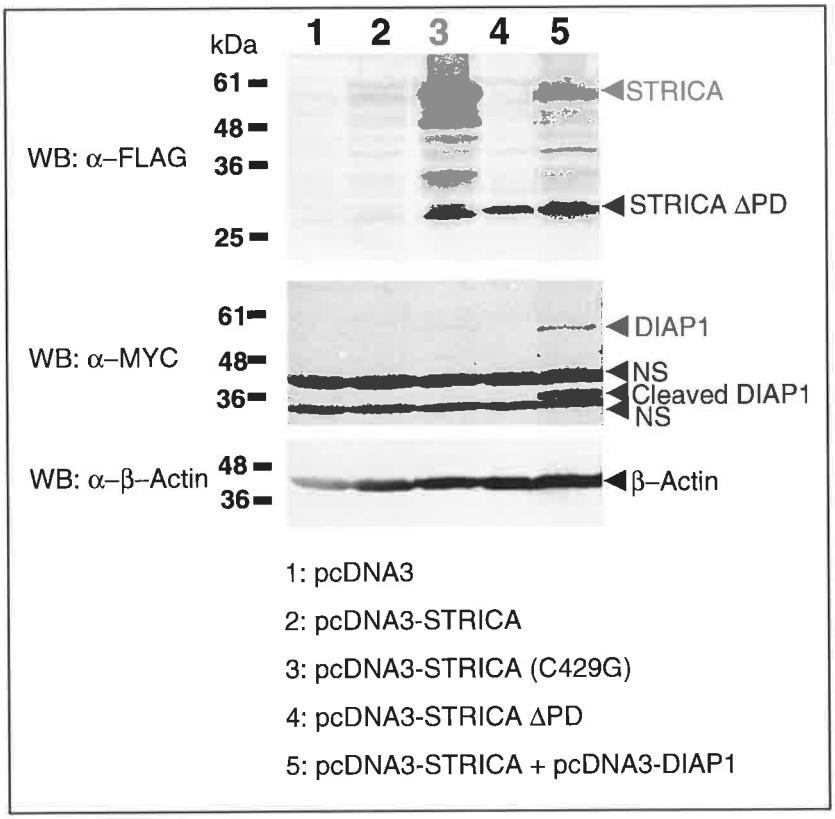
kDa
1 2 3 4 5
61
48
36
25
WB: α–FLAG
STRICA
STRICA ΔPD
WB: α–MYC
DIAP1
NS
Cleaved DIAP1
NS
WB: α–β–Actin
β–Actin
1: pcDNA3
2: pcDNA3-STRICA
3: pcDNA3-STRICA (C429G)
4: pcDNA3-STRICA ΔPD
5: pcDNA3-STRICA + pcDNA3-DIAP1

to STRICA's catalytic activity, since mutation of the catalytic cysteine residue renders STRICA incapable of inducing apoptosis (figure 3.5). Moreover, wildtype STRICA was detected in COS cells when coexpressed with the apoptosis inhibitor, DIAP1 (figure 3.7 B).

3.9 STRICA is autoprocessed between the prodomain and large subunit

Many initiator caspases are able to autoprocess when brought together by adaptor molecules or through oligomerisation (Weber and Vincenz, 2001; Tibbetts *et al.*, 2003). Coexpression of STRICA with DIAP1 prevents cell death and therefore makes it possible to detect STRICA in cells (figure 3.7 B lane 5). Full-length STRICA and a processed band were detected by SDS-PAGE when overexpressed in COS cells together with DIAP1 (figure 3.8). In contrast, overexpression of STRICA (C429G) resulted in the accumulation of the full-length molecule and the absence of the smaller processed band. The putative caspase processing site, KQVD presented as a possible cleavage site between the prodomain and large subunit. The STRICA ΔPD construct expresses a protein from this site to the C-terminus. Comigration of the processed STRICA fragment with the putative ΔPD mutant suggested that STRICA was cleaved between the prodomain and large subunit at this potential site, and that this processing required its own catalytic activity (figure 3.8). STRICA (S119G) is a putative phosphorylation mutant (discussed in chapter 5). The catalytic cysteine residue is present in STRICA (S119G).

3.10 Catalytically active STRICA cleaves DIAP1

Overexpression of DIAP1 together with STRICA in COS cells revealed two migrating bands corresponding to full-length DIAP1 and a smaller-migrating species (figure 3.7 B lane 5 and figure 3.9). MYC-tagged DIAP1 was coexpressed with either empty pcDNA3 vector, wildtype (wt) STRICA, STRICA (C429G) or STRICA ΔPD. Full-length DIAP1 accumulated in cells expressing STRICA (C429G), compared with cells expressing wildtype STRICA, STRICA (S119G) or STRICA ΔPD where the active site is preserved. This demonstrated that

Figure 3.8 Autoprocessing of STRICA in cultured cells

Overexpression of STRICA in COS cells, together with DIAP1 to prevent apoptosis and protein degradation, demonstrates a smaller migrating band of the same size as STRICA lacking the prodomain. STRICA is tagged at the C-terminus with FLAG. Processing to remove the prodomain of STRICA requires STRICA's own active site, as this smaller band is not detected when STRICA (C429G) is overexpressed.

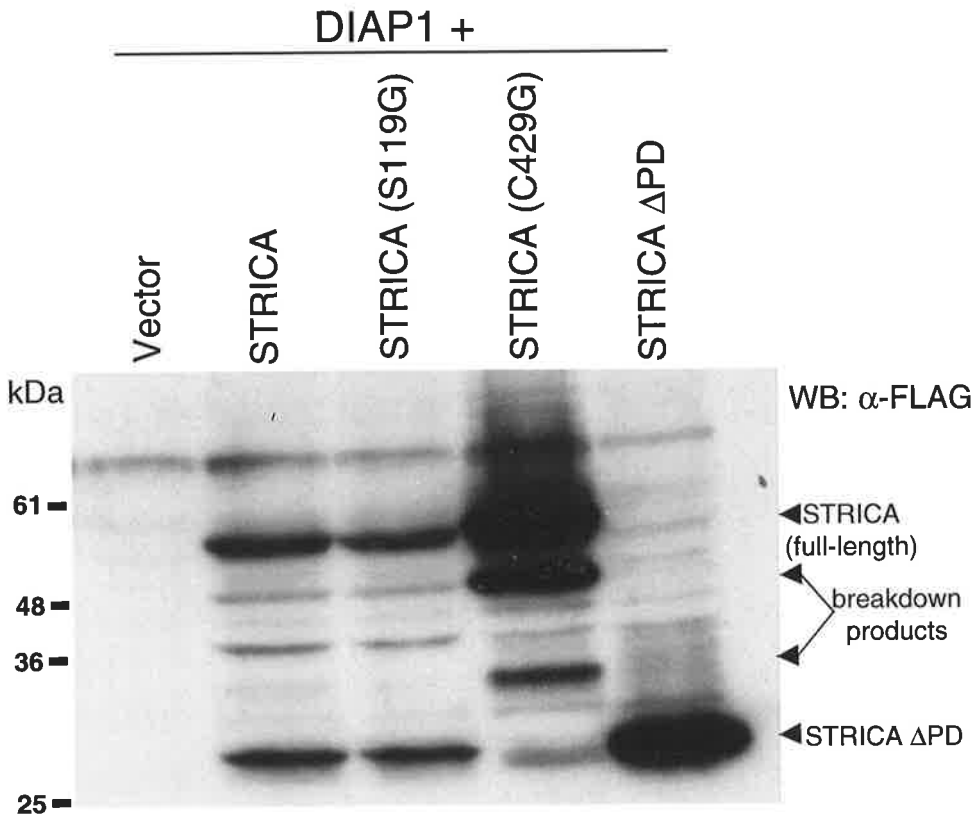
DIAP1 +
Vector
STRICA
STRICA (S119G)
STRICA (C429G)
STRICA ΔPD
kDa
61
48
36
25
WB: α-FLAG
STRICA
(full-length)
breakdown
products
STRICA ΔPD

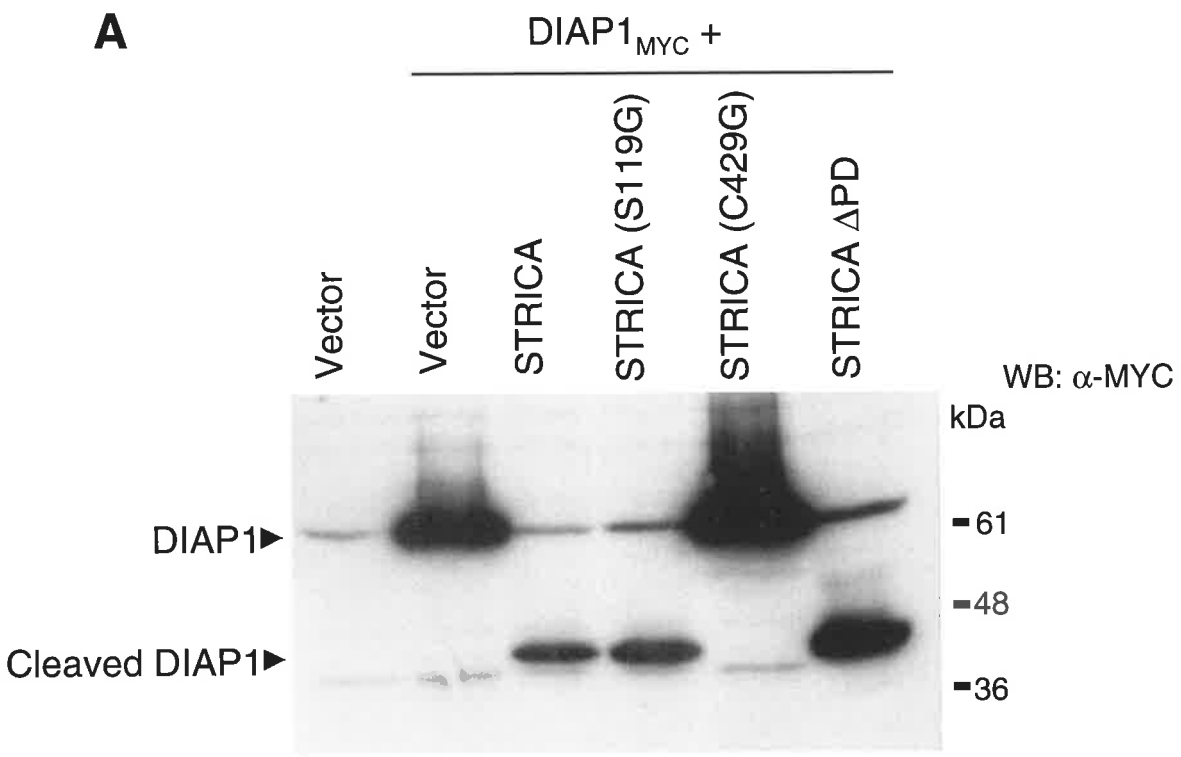
A
DIAP1MYC +
Vector
Vector
STRICA
STRICA (S119G)
STRICA (C429G)
STRICA ΔPD
WB: α-MYC
kDa
DIAP1►
Cleaved DIAP1►
61
48
36


B
35S-DIAP1 +
GST
STRICA ΔPD #1
STRICA ΔPD #3
kDa
DIAP1►
Cleavage product 1 ►
Cleavage product 2 ►
Cleavage product 3
Cleavage product 4►
63
49
37
26
19
15

Figure 3.9 STRICA cleaves DIAP1

A Coexpression of MYC-tagged DIAP1 with catalytically active STRICA in COS cells, results in the processing of full-length DIAP1 to produce a smaller migrating product. Coexpression with STRICA ΔPD results in the same processed band and depletion of full-length protein. However, DIAP1 remains intact when coexpressed with catalytically inactive STRICA (C429G), implicating the activity of STRICA in the cleavage of DIAP1. **B** *In vitro* translated (IVT) ^{35}S-methionine-labelled DIAP1 is processed by recombinant STRICA ΔPD. Bacterial lysates expressing either GST alone or GST-STRICA ΔPD were incubated with IVT DIAP1. Several DIAP1 cleavage products are generated by recombinant GST-STRICA ΔPD but not by GST alone. #1 and #3 represent two individual bacterial clones expressing GST-STRICA ΔPD. Cleavage product 1 migrates similarly to the cleavage product shown in A. The molecular weights of cleavage products 1 and 4 are consistent with cleavage by STRICA at a single site. Two other processed bands are also observed (cleavage products 1 and 2). The doublet running below the 49kDa marker is non-specific.

DIAP1 was cleaved to a smaller peptide only when the caspase activity of STRICA was overexpressed in the cell (figure 3.9 A). Furthermore, recombinant STRICA ΔPD expressed in bacterial cells as a GST fusion protein, generates DIAP1 cleavage products when incubated with ^{35}S-methinone-labelled DIAP1 (figure 3.9 B), demonstrating that processing of DIAP1 by STRICA is direct. One of the cleavage fragments is consistent in size to the product observed in transfected cells, demonstrating that cleavage of DIAP1 occurs at the same site in both transiently transfected cells, and in *in vitro* cleavage experiments.

3.11 Discussion

Here, I have reported the identification and preliminary characterisation of the newest, and final, member of the *Drosophila* family of caspases, STRICA. STRICA was identified by a database homology search, and cloned from a *Drosophila* larval cDNA library. The resulting 527 amino acid polypeptide contains all the residues conserved throughout the caspase superfamily as well as a long amino-terminal prodomain rich in serine and threonine residues.

STRICA is expressed throughout *Drosophila* development at relatively low levels, and is detected in tissues that are known to undergo developmental apoptosis. STRICA localises to the cytoplasm in transfected cells and induces cell death when overexpressed in SL2 cells and 293T cells. 293T cells expressing STRICA display the morphological features of apoptosis including cell shrinkage and plasma membrane blebbing. Despite the report that *strica* is slightly upregulated in response to the steroid hormone ecdysone (Yee *et al.*, 2002), exogenous treatment of larval midguts and salivary glands with ecdysone failed to show any significant upregulation of *strica* mRNA (data not shown). However this does not rule out the possibility that *strica* is developmentally upregulated by ecdysone under physiological conditions.

Many upstream caspases autoprocess when overexpresed in cells. Although processing of STRICA between the large and small subunits has not been detected, even upon induction of apoptosis (data not shown), a smaller migrating fragment of STRICA migrates together with a putative minus prodomain mutant of STRICA, suggesting that overexpression of STRICA in cultured cells results in the processing of the prodomain. It is possible that further cleavage between the large and small subunits is not required for STRICA function, once the prodomain is removed. Processing of the prodomain appears to be autocatalytic, as overexpression of the inactive mutant of STRICA fails to produce the same truncated product.

Although the role of STRICA's novel prodomain is not well elucidated, it is unable to mediate dimerisation of STRICA procaspase molecules when expressed as yeast two hybrid

fusion proteins. Given the lack of homology of this domain to other known prodomains that contain various protein-protein interaction motifs, the role of the prodomain of STRICA is an interesting area for further investigation, which may reveal novel mechanisms of caspase activation and regulation. The inability of the prodomain of STRICA to dimerise suggests that STRICA activation may require interaction with an adaptor molecule. The lack of any known protein-protein interaction motifs makes the identification of candidate adaptor molecules difficult. A yeast two-hybrid screen using STRICA (C429G) as bait was carried out, screening 1.2 x 10^6 yeast clones carrying inserts from a *Drosophila* 21hr embryo cDNA library. However, no potential interactors were identified by this approach (data not shown). This does not rule out the possibility that adaptor molecules for STRICA exist, perhaps only interacting transiently, to induce caspase activation. Given the ability of STRICA to autoprocess between the prodomain and large subunits, it is possible that using the catalytically inactive version of STRICA selected against interactions that depend on such processing. Alternatively, other mechanisms or post-translational modifications may be required for STRICA activation.

STRICA induces apoptosis in cells when overexpressed. As a result, STRICA is difficult to detect in transient transfection assays. The prodomain of STRICA possesses a putative PEST domain, identified by homology searching, that renders proteins highly unstable and targets them for degradation, usually via the proteasome pathway (Rechsteiner and Rogers, 1996). Indeed, STRICA ΔPD is detected more easily than full-length STRICA suggesting that the prodomain contributes to the instability of STRICA. However, incubation of transfected cells with the proteasome inhibitor, MG132, has no effect on STRICA stability suggesting that STRICA may not be targeted for proteasomal degradation. Moreover, catalytically inactive STRICA accumulates to high levels in cells, despite the presence of the prodomain and the putative PEST domain, further demonstrating that the inability to detect full-length STRICA is due to STRICA-induced apoptosis. Consistent with this, suppression

of cell death by coexpression of STRICA with DIAP1 allows the detection of STRICA by Western blotting.

Of interest, is the potential processing of DIAP1 by STRICA. When coexpressed in cultured cells, DIAP1 is detected as full-length protein, and a smaller migrating band of approximately 37kDa. The appearance of processed DIAP1 is only observed when coexpressed with catalytically active STRICA, whether full-length or ΔPD, and is absent when coexpressed with a single amino acid substitution in the QACKG active site of STRICA. Additionally, incubation of *in vitro* translated DIAP1 with bacterial lysates expressing GST-STRICA ΔPD confirms that STRICA directly cleaves DIAP1 to generate several processed fragments. Cleavage product 1 (figure 3.9 B) migrates similarly to the DIAP1 cleavage product observed in transiently transfected cells overexpressing DIAP1 and STRICA (figure 3.9 A).

There are several potential caspase cleavage sites in DIAP1. Two of these are EQED and EALD. The former possible cleavage site is towards the C-terminus of the BIR1 domain, while the latter site is between BIR1 and BIR2. DRONC cleaves DIAP1 at the VPQE sequence between the BIR and BIR2 domains (Yan *et al.*, 2004). The substrate specificity of STRICA has not been determined due to the high insolubility of bacterially expressed STRICA ΔPD and inactivity on synthetic fluorogenic substrates (data not shown). Although cleavage following an aspartate residue is probable, cleavage after glutamate cannot be ruled out. Despite these difficulties, the putative autoprocessed site between the prodomain and large subunit is KQVD and may represent the preferred consensus for substrate cleavage by STRICA. The observed cleavage products are consistent with potential processing by STRICA at EQED and VPQE, however further investigation is required to determine the exact cleavage sites.

As mentioned above, DRONC cleaves DIAP1 at glutamate 205 *in vitro* (Yan *et al.*, 2004). Such cleavage results in two DIAP1 fragments, the BIR1 domain, and the BIR2-RING domains. *Drosophila* cells reportedly exhibit this processing of DIAP1 by DRONC

constitutively (cited as personal communication by Yan *et al.* 2004). Given the multifunctional nature of DIAP1, specific cleavage events may play crucial regulatory roles in the regulation of DIAP1 and possible feedback on apoptosis signalling pathways in the fly. With this in mind, cleavage of DIAP1 by STRICA is an interesting area for further investigation. While direct processing of DIAP1 by STRICA is presented in this chapter, the site(s) of cleavage remain to be determined. The putative cleavage event may remove the BIR1 domain completely, or disrupt its function by processing within the domain itself. Individual BIR domains in DIAP1 have recently been characterised. The BIR1 domain of DIAP1 was shown to suppress the downstream, effector caspase DRICE (Zachariou *et al.*, 2003). Perhaps the processing of DIAP1 by STRICA serves to amplify cell death by removing the inhibition of DIAP1 over downstream caspases. When significant pools of STRICA molecules are activated, DIAP1 inhibition of apoptosis may be overcome by DIAP1 processing. Given the likelihood that STRICA and DRONC function in different apoptotic pathways, cleavage of DIAP1 by DRONC and STRICA may occur in different temporal and/or spatial contexts.

The processing of an IAP by a caspase to produce smaller migrating bands is not unique to *Drosophila*. In apoptotic cells, proteolytic fragments of XIAP have been reported (Deveraux *et al.*, 1999). Cleavage occurs in the linker region between BIR2 and BIR3. Processing by recombinant Caspase-3, -6, -7 and -8 has been reported. While each fragment retains the ability to suppress caspase activity, caspase cleavage of XIAP is likely to be a marker for late apoptosis rather than producing individual inhibitory units (Liston *et al.*, 2003). cIAP1 has also been reported to be cleaved by Caspase-3, resulting in a proapoptotic fragment (Clem *et al.*, 2001). The physiological relevance of IAP cleavage by caspases requires further investigation. However, it possibly occurs following caspase activation to remove any anti-apoptotic activity ensuring rapid, unhindered apoptosis.

In summary, this chapter outlines the initial characterisation of STRICA, the seventh and final member of the *Drosophila* caspase family. With the identification of STRICA, the

Drosophila genome encodes three long prodomain caspases, DRONC, DREDD and STRICA, and four caspases, DCP-1, DRICE, DECAY and DAMM, similar to mammalian effector caspases (figure 3.10). Results in this chapter demonstrate that STRICA functions as a caspase and potently induces cell death when overexpressed in cultured cells. While processing of pro-STRICA between the large and small catalytic subunits has not been detected, overexpression of STRICA, in the presence of DIAP1 to suppress cell death, results in the appearance of a fragment that migrates with a putative minus prodomain mutant of STRICA. The catalytic activity of STRICA is also associated with a proteolytic cleavage product of DIAP1. Initial experiments demonstrating the processing of DIAP1 by STRICA presented in this chapter provide a foundation for further investigation. Establishing whether or not this event occurs in *Drosophila* cells is essential. Given that recombinant STRICA cleaves *in vitro* translated DIAP1 directly, the exact cleavage site(s) in DIAP1 need be determined by mutagenesis or protein sequencing. The physiological relevance of such processing is an intriguing area for further research. Characterisation of STRICA by genetic interaction studies is presented in the following chapters.

Figure 3.10 The *Drosophila* caspase family

A schematic representation of the seven members of the *Drosophila* caspase family. Three caspases, including STRICA, have long prodomains while four lack a long prodomain. While DRONC and DREDD contain protein-protein interaction motifs, CARD and DEDs respectively, the prodomain of STRICA lacks any known motifs.

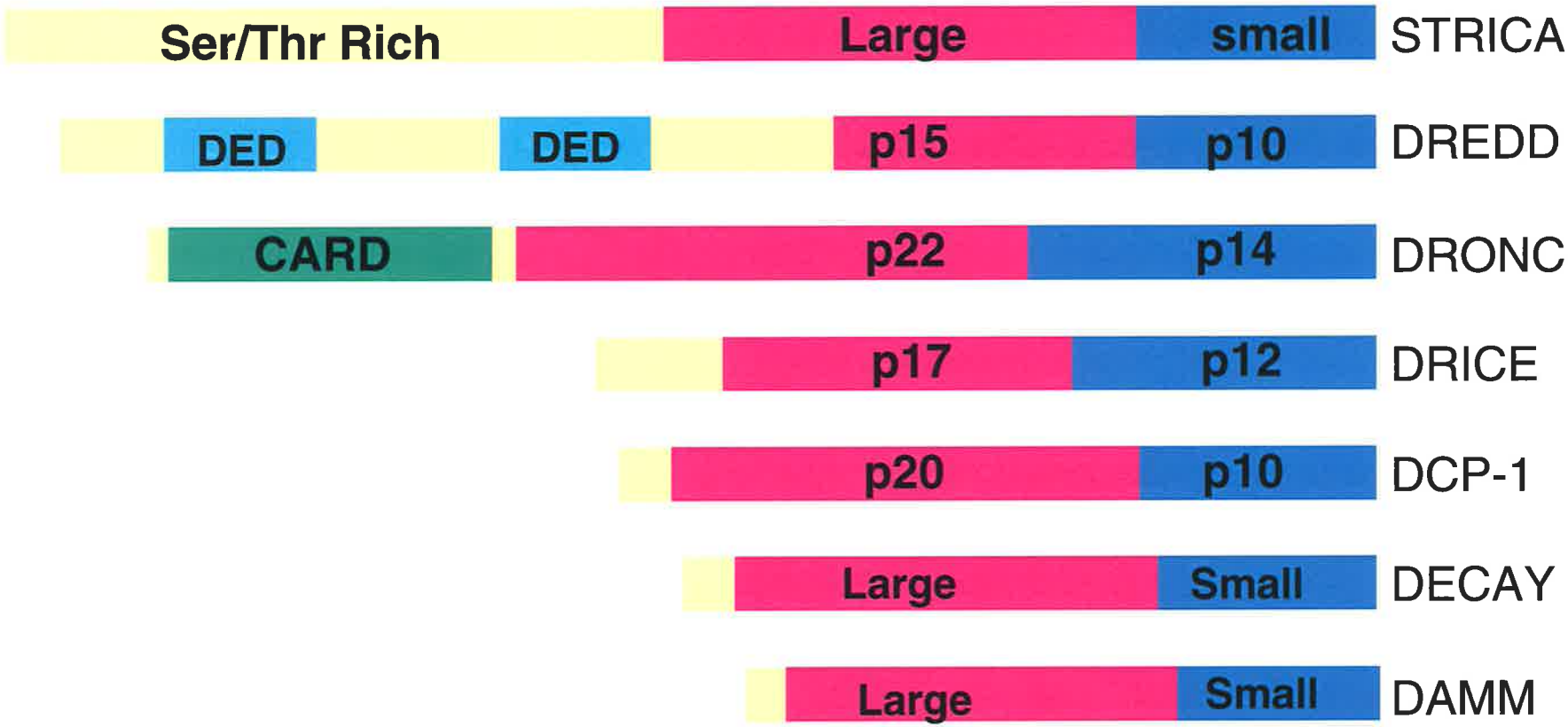
Ser/Thr Rich
Large
small
STRICA
DED
DED
p15
p10
DREDD
CARD
p22
p14
DRONC
p17
p12
DRICE
p20
p10
DCP-1
Large
Small
DECAY
Large
Small
DAMM

Chapter 4

Genetic Interaction Studies Between STRICA and Cell Death Molecules

4.1 Introduction

Drosophila melanogaster is a model organism well suited for the study of proteins in signalling pathways. The *Drosophila* compound eye is composed of 750 ommatidia positioned within a hexagonal lattice (figure 4.1 A). Each ommatidium consists of eight photoreceptor cells, four cone cells and two pigment cells. The appropriate arrangement of cells in this highly organised structure is dependent on normal developmental cell death (Rusconi *et al.*, 2000; Brachmann and Cagan, 2003). Disruptions to apoptosis can cause severely abnormal phenotypes, making this structure ideal for the study of ectopically expressed cell death molecules. Given that the fly eye is not required for viability, it can be used to observe the effects of overexpressing genes of interest involved in pathways of cell death, proliferation and differentiation. Additionally, the ease with which flies carrying various transgenes are crossed to generate flies expressing two different proteins of interest allows for the elucidation of gene products that function in the same genetic pathway.

The main apoptotic pathway in *Drosophila* functions through activation of the upstream caspase DRONC. The cell death activator, REAPER, removes DIAP1 inhibition over DRONC, allowing for DARK-dependent DRONC activation and the subsequent processing and activation of the downstream caspase, DRICE (sections 1.9.1 and 1.11.1). This pathway appears to be the major road to cell death in the fly, where DRONC and DARK are essential for apoptosis, and DIAP1 is necessary for cell survival (Hay, 2000).

The aim of this chapter was to elucidate the *in vivo* pathway in which STRICA functions, using the *GMR-Gal4* system and RNAi. Results presented here confirm the role of DIAP1 as an inhibitor of apoptosis in *Drosophila*, which physically interacts with STRICA. Moreover, STRICA induces ectopic cell death in the fly eye that is suppressed by DIAP1 and p35, and partially suppressed by DIAP2, placing these molecules in the same genetic pathway. Interestingly results from both RNAi experiments and *in vivo* genetic interaction studies suggest that STRICA-induced apoptosis is distinct from the major REAPER/DRONC/DARK pathway in flies.

4.2 Overexpression of STRICA in the *Drosophila* eye induces apoptosis

The glass minimal reporter (GMR) protein specifically drives expression of genes in the eye. A *Drosophila melanogaster* line carrying a *GMR-strica* transgene balanced by a curly wing (Cyo) chromosome exhibited ectopic cell death as seen by significant loss of pigment cells when maintained at 25°C. Homozygous flies carrying two transgene copies had a more severely ablated eye phenotype with a highly reduced eye size and almost complete loss of pigment cells (figure 4.1 B) compared to a wildtype eye (figure 4.1 A). Females consistently exhibited a slightly more severe phenotype.

To determine the effect of various transgenes and mutants on STRICA-induced cell death *in vivo*, *GMR-strica* flies were crossed to various transgenic lines and the eyes of the resulting progeny analysed for suppression or enhancement of the STRICA eye phenotype as described below.

4.3 STRICA physically associates with DIAP1 and DIAP2

Given the ability of DIAP1 and DIAP2 to inhibit cell death induced by STRICA in transient transfection death assays (figure 3.5), immunoprecipitation studies were performed to determine whether a direct interaction mediates this inhibition. FLAG-tagged versions of STRICA (C429G), or STRICA ΔPD, were coexpressed in 293T cells with DIAP1 or DIAP2. Both DIAP1 and DIAP2 coimmunoprecipitated with STRICA (figure 4.2 A and B). The prodomain of STRICA was not required for this interaction since STRICA ΔPD immunoprecipitated with DIAP1 (figure 4.2 C). The established interaction between DRONC and DIAP1 was performed as a positive interaction control (figure 4.2 A and B).

Figure 4.1 STRICA induces apoptosis in the *Drosophila* eye

A An example of a wildtype *Drosophila* compound eye. **B** Flies carrying one copy of the *strica* transgene (*strica/+*) display loss of red pigment cells compared to wildtype. *GMR-strica* homozygotes (*strica/strica*) demonstrate a more severely ablated eye phenotype with further loss of pigment cells and a small eye phenotype.

A

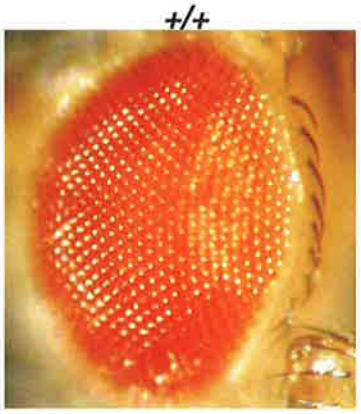

B

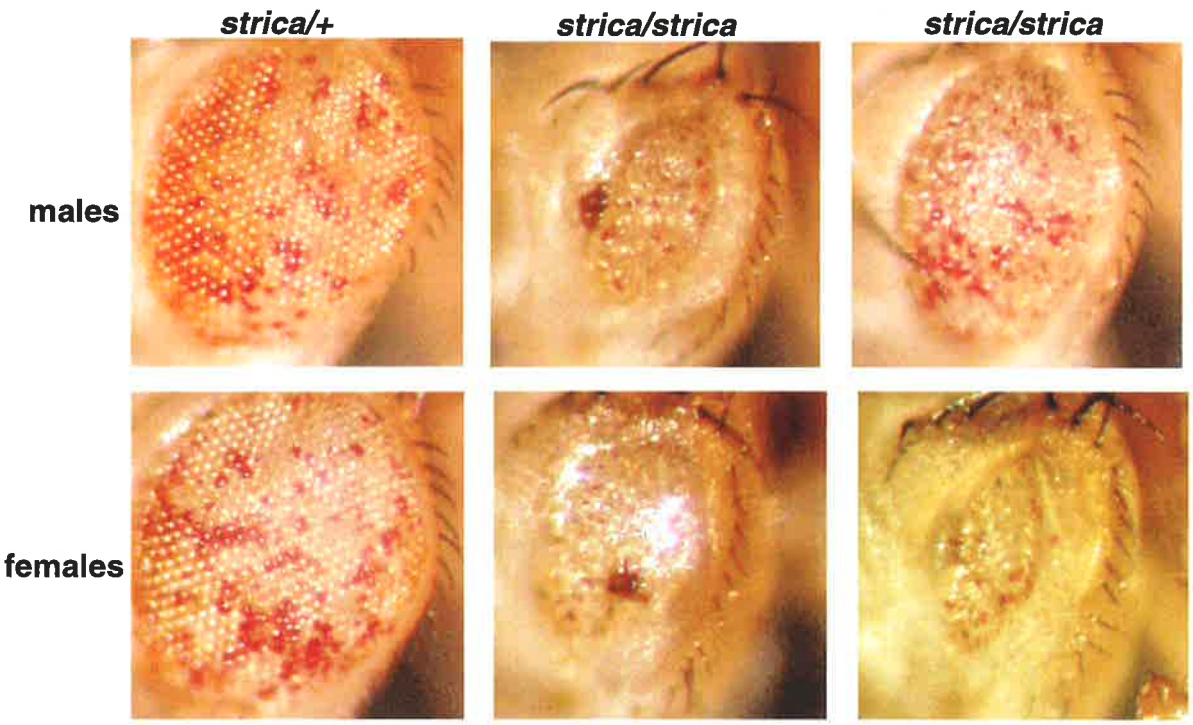

Figure 4.2 STRICA physically interacts with DIAP1 and DIAP2

293T cells were cotransfected with various tagged cDNAs in the pcDNA3 expression vector. FLAG-tagged STRICA or STRICA minus prodomain (MPD) were cotransfected with either MYC-tagged DIAP1 or HA-tagged DIAP2. Both DIAP1 and DIAP2 are detected in lysates imunoprecipitated with an α-FLAG monoclonal antibody (**A** and **B**). STRICA and STRICA-MPD (minus prodomain) are detected in lysates immunoprecipitated with α-MYC (**C**). In a control experiment, HA-tagged DRONC coimmunoprecipitates with DIAP1, as expected (**A** and **B**). Expression of each construct was confirmed by immunoprecipitating with the appropriate antibody, followed by immunoblotting with the same antibody. All STRICA constructs used in these experiments contained the C429G mutation.

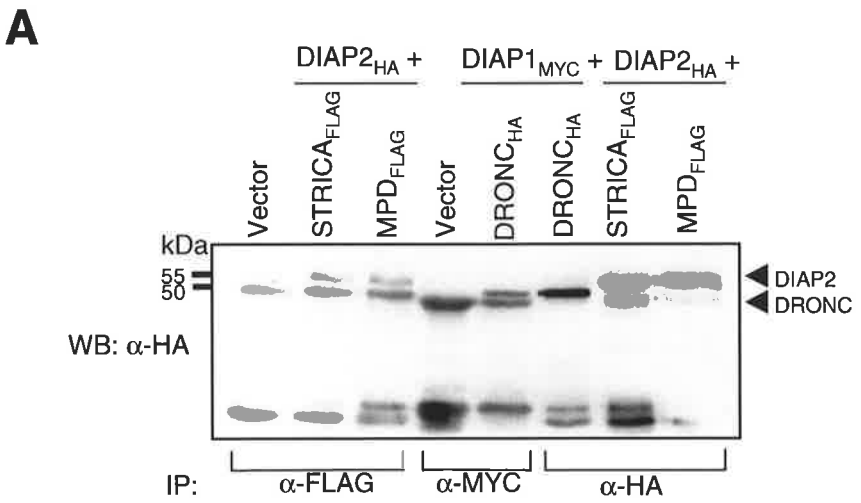
A
DIAP2HA +
DIAP1MYC + DIAP2HA +
Vector
STRICAFLAG
MPDFLAG
Vector
DRONCHA
DRONCHA
STRICAFLAG
MPDFLAG
kDa
55
50
DIAP2
DRONC
WB: α-HA
IP:
α-FLAG
α-MYC
α-HA

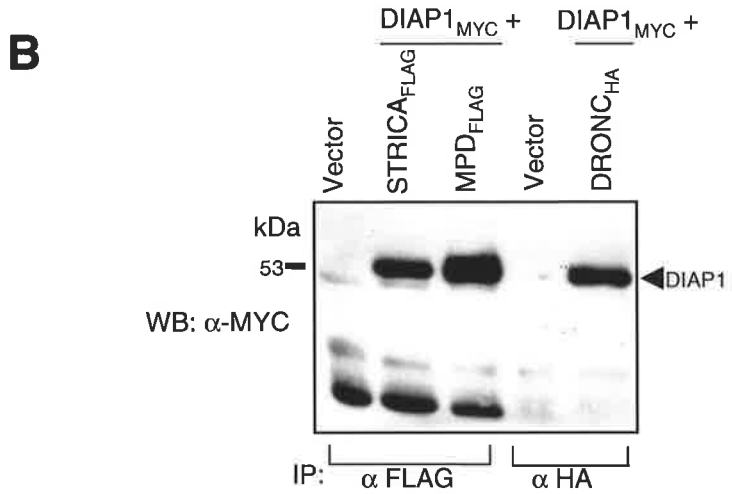
B
DIAP1MYC +
DIAP1MYC +
Vector
STRICAFLAG
MPDFLAG
Vector
DRONCHA
kDa
53
DIAP1
WB: α-MYC
IP:
α FLAG
α HA

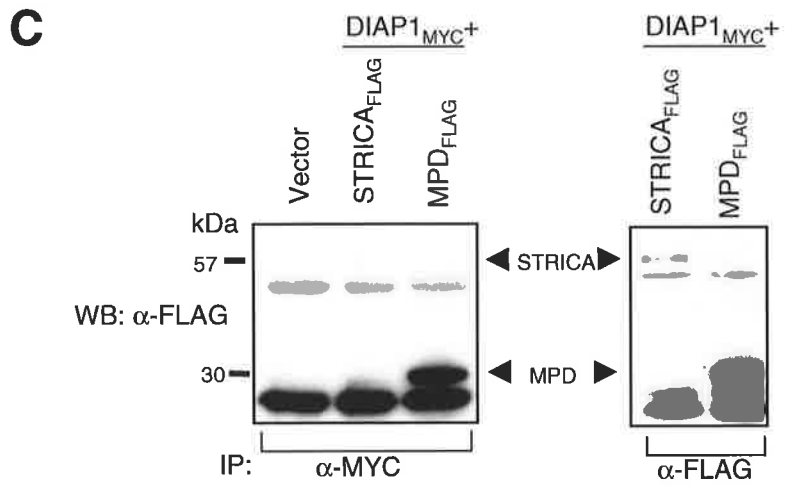
C
DIAP1MYC+
DIAP1MYC+
Vector
STRICAFLAG
MPDFLAG
STRICAFLAG
MPDFLAG
kDa
57
STRICA
WB: α-FLAG
30
MPD
IP:
α-MYC
α-FLAG

4.4 STRICA genetically interacts with DIAP1

As shown above, DIAP1 physically interacts with STRICA in transiently transfected cells and inhibits the activity of STRICA in overexpression death assays in *Drosophila* cells (figure 3.5). To confirm this interaction *in vivo*, flies carrying the *GMR-strica* transgene were crossed with flies overexpressing DIAP1. The *diap1* transgene is carried on the X chromosome. The loss of pigment cells due to ectopically expressed STRICA was inhibited when these flies also carried the *diap1* transgene. The eyes of such progeny were restored to normal, confirming that DIAP1 efficiently suppresses STRICA-induced cell death *in vivo* (figure 4.3). Consistent with this observation, heterozygosity at the *thread* locus enhanced the phenotype of GMR-*strica* heterozygotes (figure 4.4). Thus, halving the dosage of endogenous *diap1* further relieves the suppression of DIAP1 over STRICA, and enhances STRICA-induced apoptosis.

4.5 STRICA is partially inhibited by DIAP2 in the *Drosophila* eye

As shown above, STRICA physically interacts with DIAP2 (figure 4.2), although DIAP2 is less efficient in the suppression of STRICA-induced apoptosis in cell death assays (figure 3.5). To determine whether DIAP2 is able to inhibit STRICA *in vivo*, *GMR-strica* flies were crossed to *GMR-diap2* flies and analysed for suppression of the eye phenotype. Compared to parental *GMR-strica* flies, *strica/diap2* progeny displayed significant restoration of normal pigment cells in the eye, although complete suppression was not observed (figure 4.5). Thus, DIAP2 suppresses STRICA-induced apoptosis in the *Drosophila* eye, albeit less efficiently than DIAP1.

4.6 p35 suppresses STRICA-induced cell death *in vivo*

p35 is a viral inhibitor of apoptosis which functions as a universal caspase inhibitor in a vast number of species and cell types (Clem *et al.,* 1991; Bump *et al.,* 1995; Xue and Horvitz, 1995). Suppression by p35 is therefore considered to demonstrate the involvement

Figure 4.3 STRICA-induced cell death is suppressed by DIAP1

To determine whether DIAP1-mediated suppression of STRICA-induced apoptosis occurs *in vivo*, *GMR-strica/+* flies were crossed with flies ectopically expressing DIAP1 on the X chromosome (*GMR-diap1/+*). Loss of pigment cells caused by STRICA overexpression is completely inhibited by DIAP1 overexpression, demonstrating that DIAP1 inhibits STRICA activity *in vivo*. Female progeny carrying both the *GMR-strica* and *GMR-diap1* transgenes (*strica/diap1*) were compared to males carrying only *GMR-strica* (*strica/Y*).

Parental *strica/+*

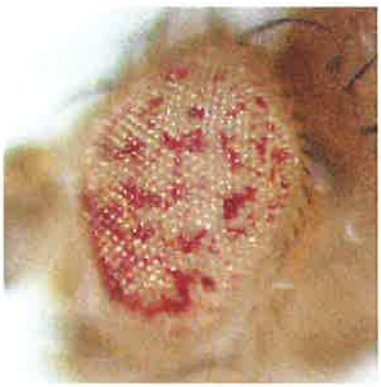

strica/Y

strica/diap1

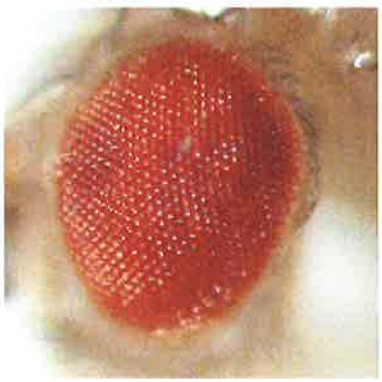

diap1/+

Figure 4.4 Halving the dose of endogenous *diap1* enhances the STRICA phenotype

thread5 is a DIAP1 loss-of-function mutant. *GMR-strica* flies were crossed to *thread5/+* flies where the endogenous levels of *diap1* are halved. Enhancement of the STRICA phenotype is observed in *strica/thread5* progeny

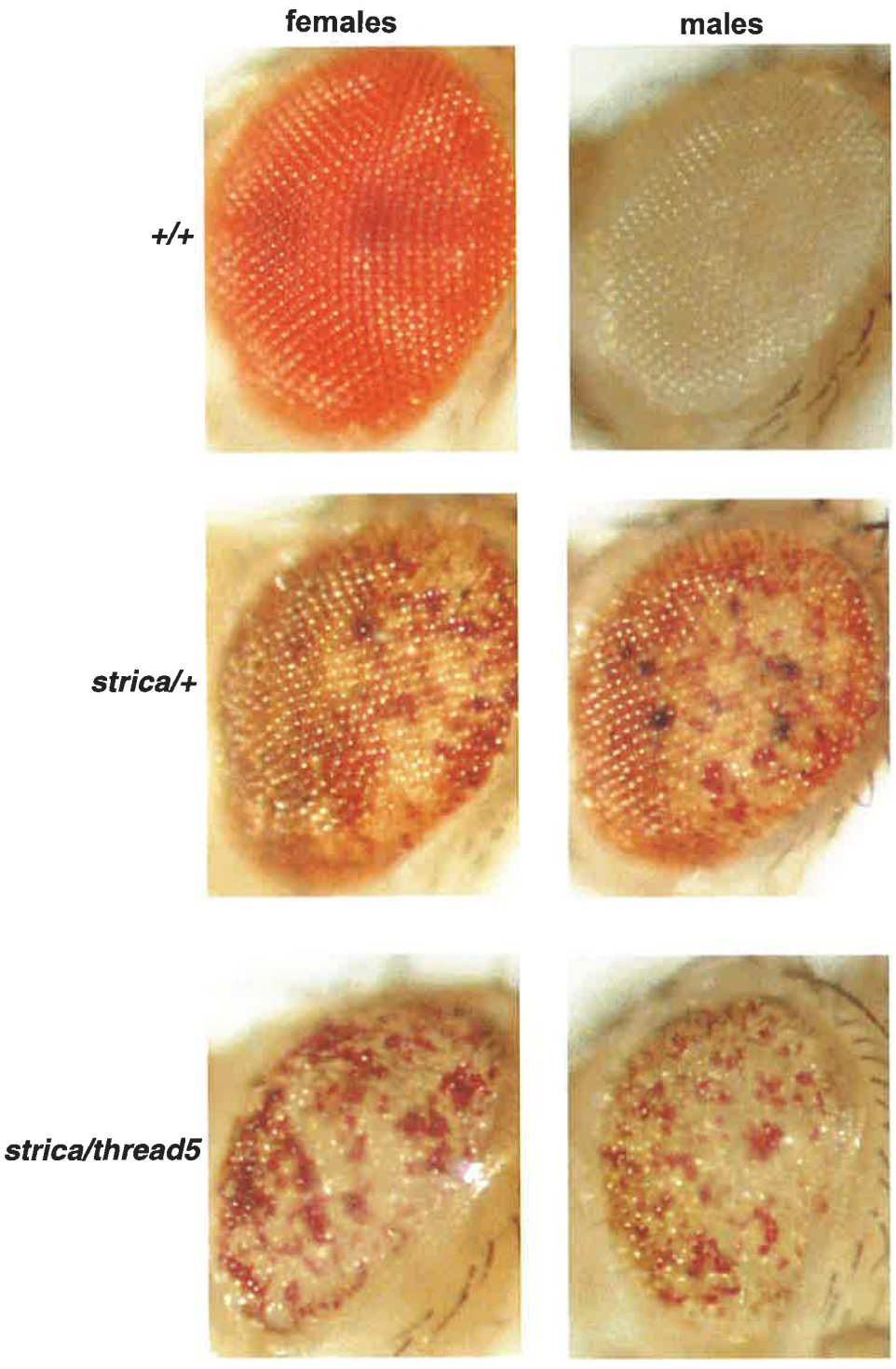
females
males
+/+
strica/+
strica/thread5

Figure 4.5 DIAP2 partially suppresses STRICA-induced cell death in the eye

Compared with DIAP1, DIAP2 inhibits STRICA-induced apoptosis less efficiently in cell death assays. STRICA and DIAP2 physically interact and when *GMR-strica/+* are crossed with flies overexpressing DIAP2 (*GMR-diap2/+*), the cell death phenotype of *GMR-strica/+* is partially suppressed. *strica/diap2* progeny demonstrate a greater number of pigment cells with fewer pigment cell deaths occurring. Thus, DIAP2 suppresses STRICA-induced cell death in the eye, to some extent.

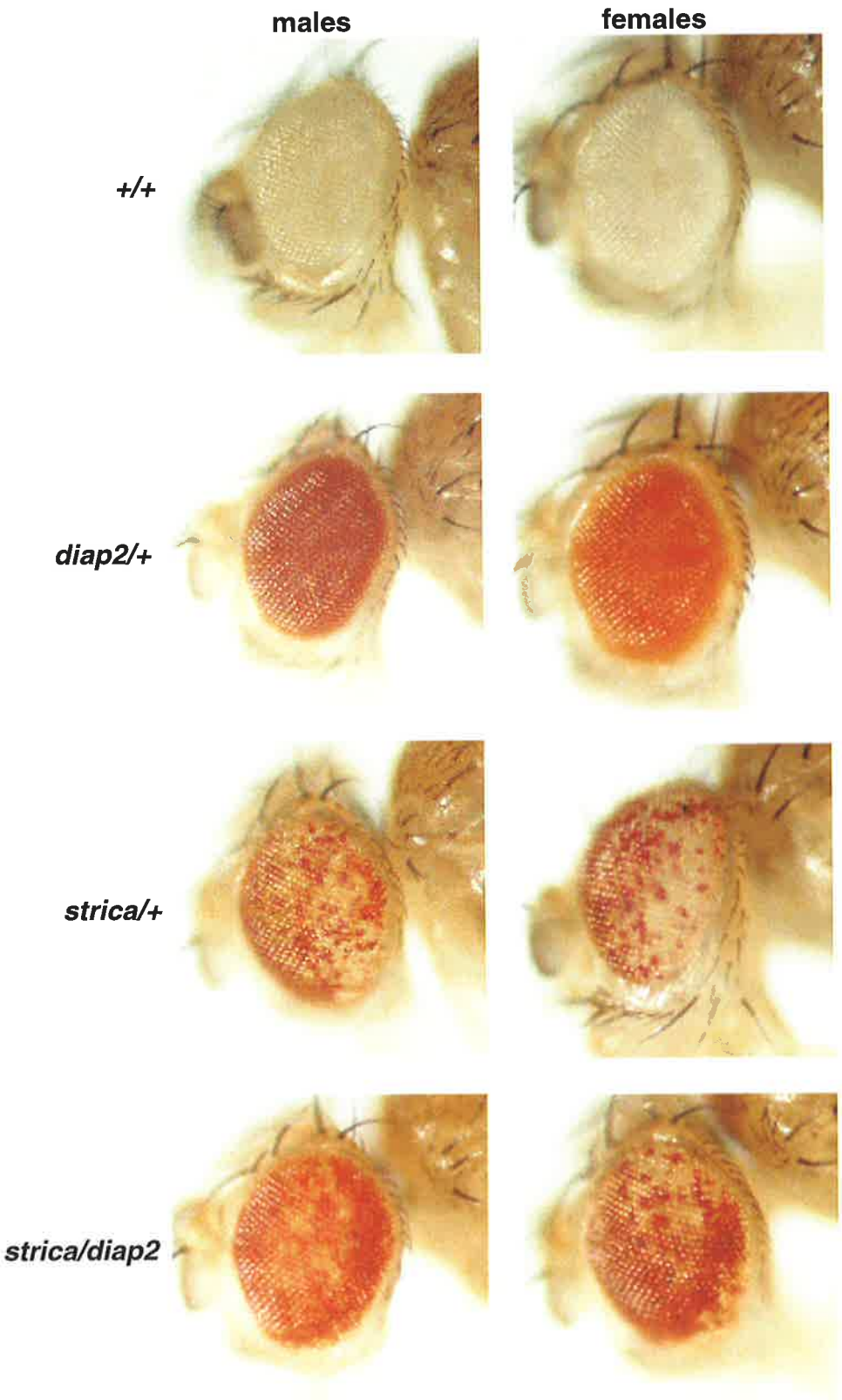
males
females
+/+
diap2/+
strica/+
strica/diap2

of caspases in programmed cell death triggered by various stimuli. To determine whether p35 is able to suppress STRICA-induced apoptosis *in vivo*, transgenic flies overexpressing p35 in the eye were crossed to *GMR-strica* flies. Progeny from this cross developed eyes of normal size and pigment demonstrating that STRICA is a p35-inhibitable caspase (figure 4.6).

4.7 BUFFY does not suppress apoptosis induced by STRICA

BUFFY, one of two Bcl-2 homologues in *Drosophila*, has been reported as a prosurvival molecule, playing a role in embryonic cell survival (Quinn *et al.*, 2003). Overexpression of BUFFY in the fly eye rescues the apoptotic phenotype induced by overexpression of the proapoptotic protein, DEBCL (Quinn *et al.*, 2003). To assess whether BUFFY could suppress STRICA-induced cell death, flies ectopically expressing BUFFY in the eye were crossed to *GMR-strica* flies. Results indicate that BUFFY has no effect on STRICA-induced cell death (figure 4.7) indicating that BUFFY and STRICA do not function in the same genetic pathway.

4.8 Deficiency of the *reaper*, *hid* and *grim* locus has no effect on STRICA-induced death

REAPER, HID and GRIM are potent inducers of apoptosis in *Drosophila*. These molecules activate cell death by binding to DIAP1, thereby relieving the inhibition DIAP1 exerts over caspases (section 1.9.1). A transgenic line carrying a deficiency of *reaper*, *hid* and *grim*, *Df(3)H99*, was crossed to flies carrying the *GMR-strica* transgene to determine whether STRICA requires the activity of the H99 gene products for activation. No suppression of the STRICA phenotype was observed when the dosage of *reaper*, *grim* and *hid* was halved, suggesting that STRICA-induced cell death is not affected by the levels of the H99 genes (figure 4.8).

Figure 4.6 STRICA-induced cell death is inhibited by p35 in the *Drosophila* compound eye

The viral pan caspase inhibitor, p35, is an efficient inhibitor of apoptosis induced by most caspases. Complete restoration of the *Drosophila* compound eye is observed when flies overexpressing STRICA (*strica/+*) also overexpress p35 (*strica/p35*), demonstrating that STRICA is a p35-inhibitable caspase.

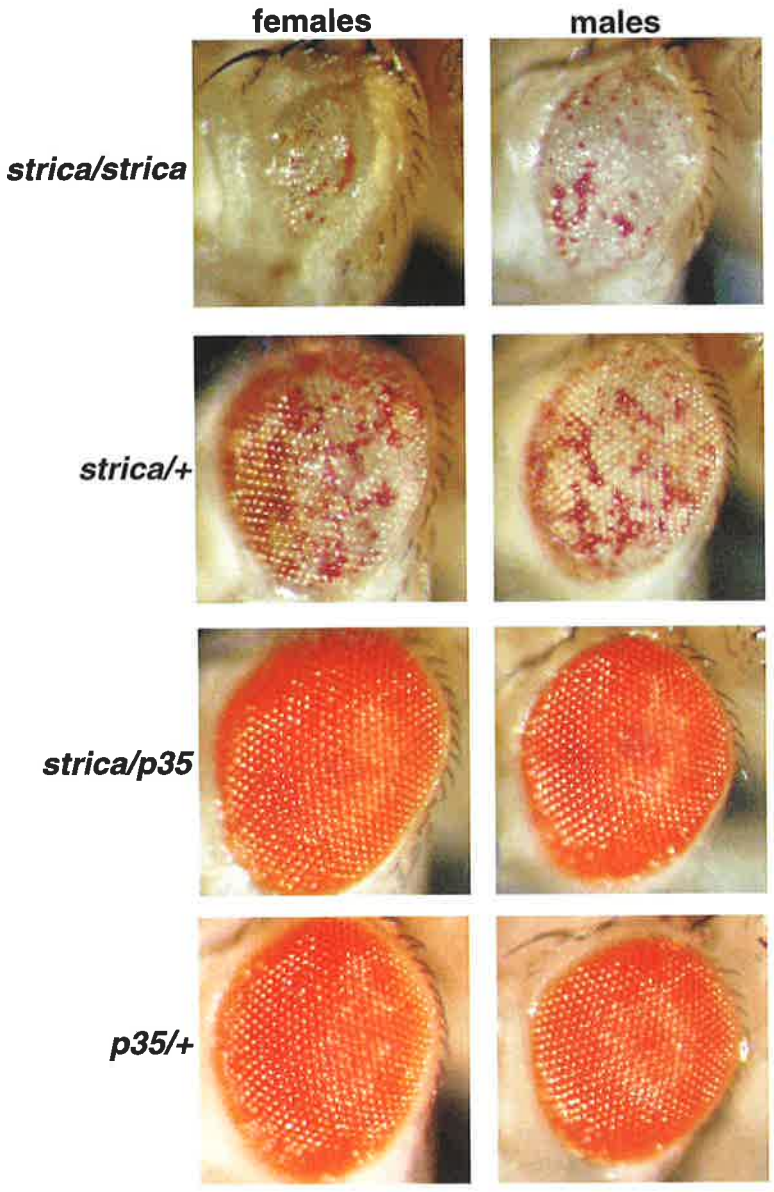
females
males
strica/strica
strica/+
strica/p35
p35/+

Figure 4.7 The STRICA eye ablation phenotype is not affected by ectopically expressed BUFFY

GMR-strica/+ flies were crossed to flies overexpressing BUFFY in the eye (*GMR-Gal4, UAS-buffy/+).* No suppression of the STRICA-induced ablation of pigment cells is observed, demonstrating that STRICA and BUFFY function in independent pathways in *Drosophila.*

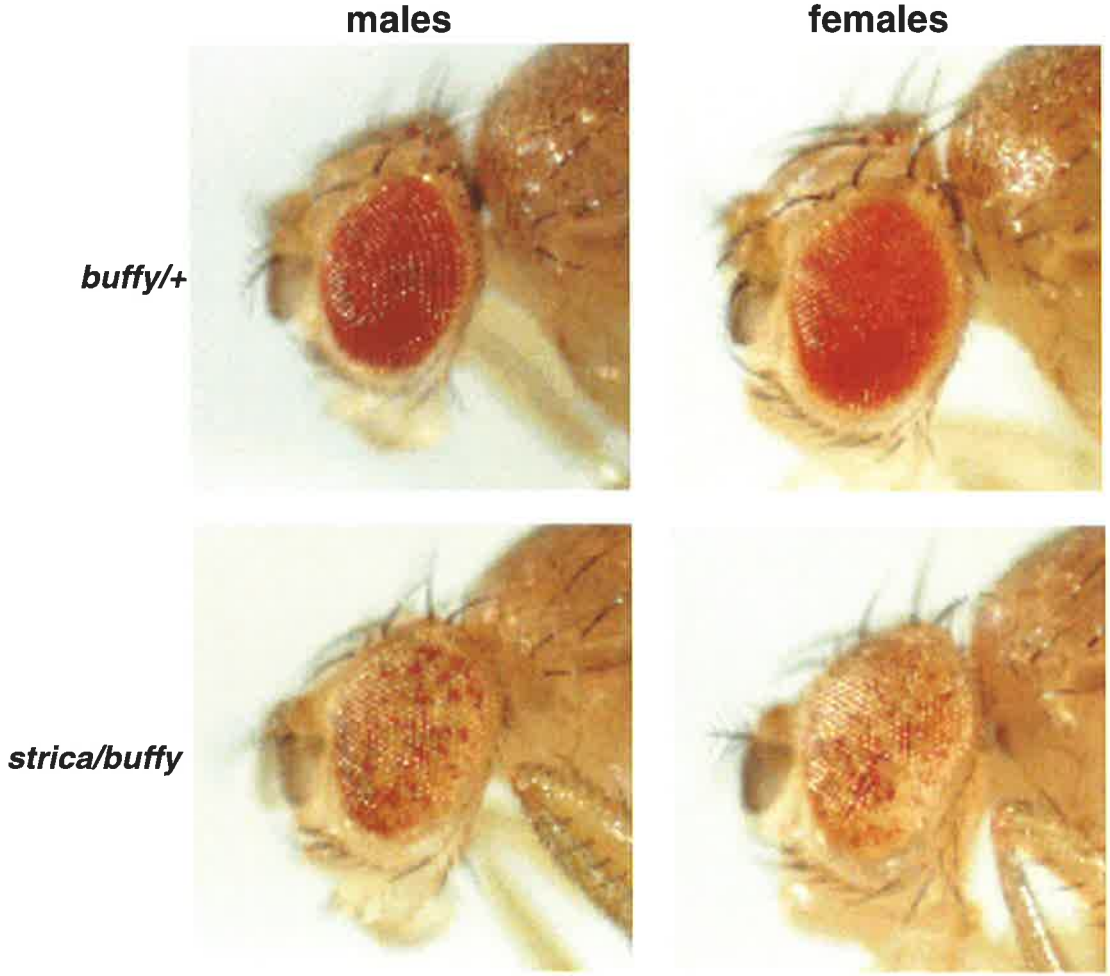
males
females
buffy/+
strica/buffy

Figure 4.8 STRICA-induced cell death in the fly is not affected by halving the dosage of *reaper*, *hid* and *grim*

GMR-strica/+ flies demonstrate loss of pigment cells due to ectopic overexpression of STRICA. These flies were crossed with *Df(3L)H99/+* flies that contain a deficiency in the H99 genes, *reaper*, *hid* and *grim*. Halving the dosage of endogenous levels of these death activators has no effect on the STRICA eye ablation phenotype, demonstrating that STRICA-induced apoptosis is insensitive to levels of REAPER, HID and GRIM.

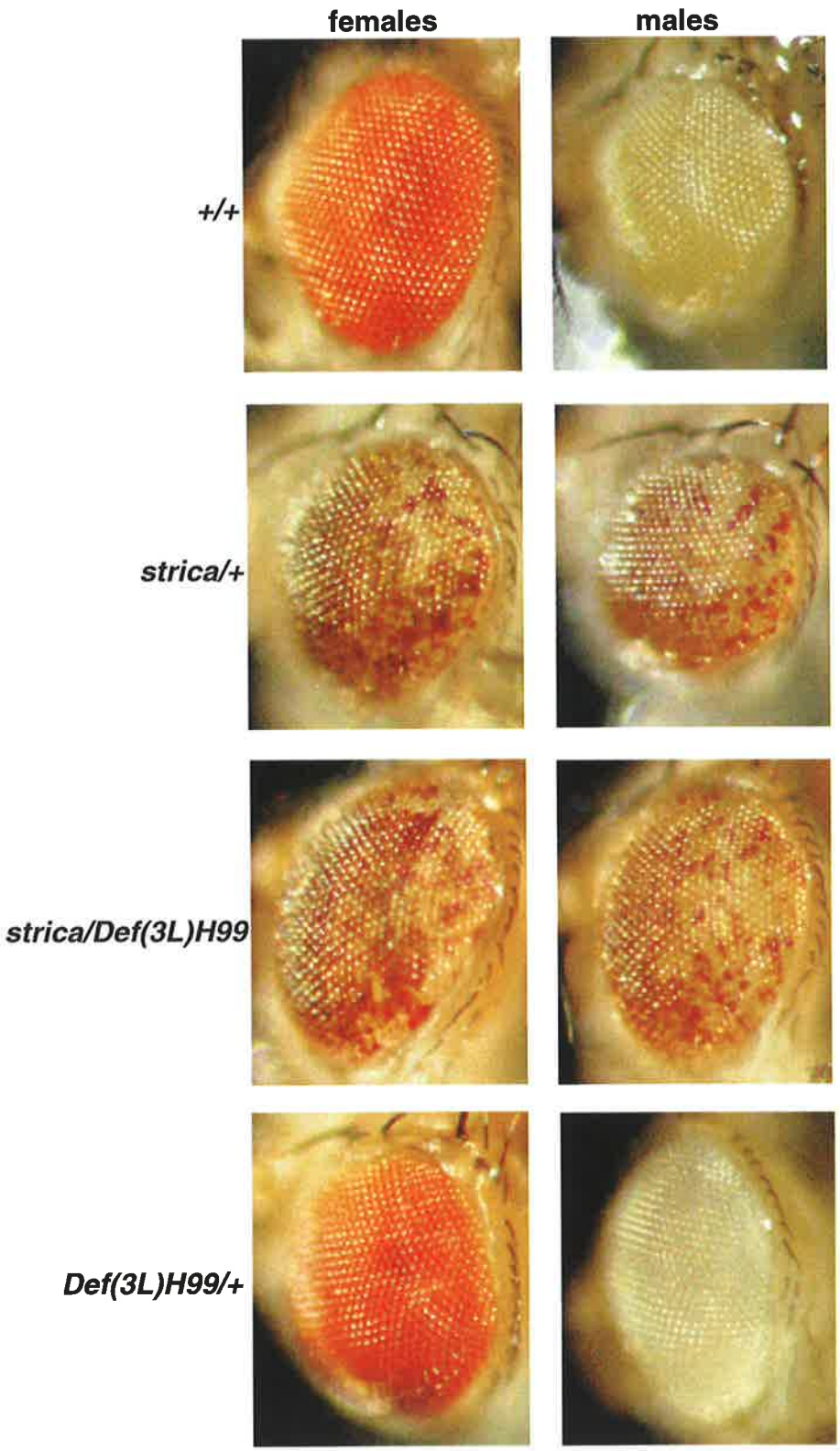
females
males
+/+
strica/+
strica/Def(3L)H99
Def(3L)H99/+

4.9 *strica* RNAi fails to protect BG2 cells from cycloheximide-induced apoptosis

RNA interference (RNAi) is a powerful technique for ablating the function of a protein and delineating complex signalling pathways by targeting specific transcripts for degradation (Clemens *et al.,* 2000). The *Drosophila* system is particularly amenable to this technique as large double-stranded RNA molecules can be taken up by cells in culture and broken down to small interfering RNAs (siRNAs) by the cell's machinery (Hammond *et al.,* 2000; Caplen *et al.,* 2000). These siRNAs then specifically target the complementary mRNA molecules for degradation. In *Drosophila*, amplification of the RNAi process also occurs, making the knockdown of specific transcripts highly efficient (Lipardi *et al.*, 2001).

Using RNAi, the roles of various components of the apoptotic pathway in *Drosophila* have been elucidated (Clemens *et al.,* 2000). Depletion of the *diap1* transcript rapidly causes extensive cell death in *Drosophila* S2 cells due to unrestrained caspase activity, even in the absence of a death-inducing stimulus (Rodriguez *et al.*, 2002; Muro *et al.,* 2002). Ablating the caspase *dronc* in the ecdysone-responsive cell line, *l(2)*mbn, desensitises these cells to apoptosis induced by the steroid hormone ecdysone (Cakouros *et al.,* 2002).

BG2-c2 cells are an insulin-dependent neuronal cell line derived from *Drosophila* embryos (Ui-Tei *et al.,* 2000). This cell line was used to analyse the role of STRICA in programmed cell death using RNAi. The efficacy of this approach was confirmed using *dark* and *dronc* dsRNAs as positive controls. dsRNA was made using STRICA ΔPD as a template. Cells were treated with dsRNA and mRNA knockdown confirmed by RT-PCR analysis (data not shown). In each case, significant knockdown of endogenous transcript levels was achieved.

Cycloheximide (CHX) is a rapid inducer of cell death. Cells depleted for each transcript were treated with 25μg/ml CHX for 4-5 hours. Four hours after treatment, greater than 30% of the cells either left untreated, or treated with control dsRNA were non-viable as scored by a trypan blue dye-exclusion assay (figure 4.9 A). In contrast, cells depleted of either *dronc* or *dark* were protected against CHX-induced apoptosis. Despite downregulation

of the *strica* transcript, loss of STRICA in BG2 cells was insufficient to protect cells against death induced by cycloheximide. After five hours of treatment, most cells had undergone apoptosis and were clearly seen as small rounded apoptotic cells compared to healthy, viable cells in which *dronc* or *dark* were ablated (figure 4.9 B). Therefore, while DRONC and DARK are essential for cell death induced by cycloheximide, STRICA function is dispensable for apoptosis triggered by this stimulus in BG2 cells.

Figure 4.9 STRICA activity is dispensable for CHX-induced apoptosis in BG2 cells

BG2 cells were depleted for *strica*, *dark* or *dronc* by RNAi. Following RNAi, cells were treated with 25μg/ml of the cytotoxic drug, cycloheximide (CHX) for 4-5 hours. **A** At 4 hours following treatment, cells were harvested and stained with trypan blue to calculate the percentage of dead cells in the population. A small percentage (<10%) of cells treated with *dark* or *dronc* dsRNA undergo apoptosis, while cells left untreated, or treated with a control mouse dsRNA (*bp5A*) or *strica* dsRNA, exhibit 30-40% cell death. Results represent three individual treatments over two independent experiments. Error bars represent ± SEM. **B** At 5 hours following CHX treatment, cells treated with dsRNAs as indicated were visualised by light microscopy and digitally photographed. Cells treated with *dark* or *dronc*, or a combination of dsRNAs, are seen as healthy cells still attached to the dish. In contrast, cells treated with *strica* or *bp5A* dsRNA, show a rounded, shrinking morphology and detach from the dish. The control dsRNA used in these experiments, *bp5A*, is a mouse protein not involved in PCD.

A

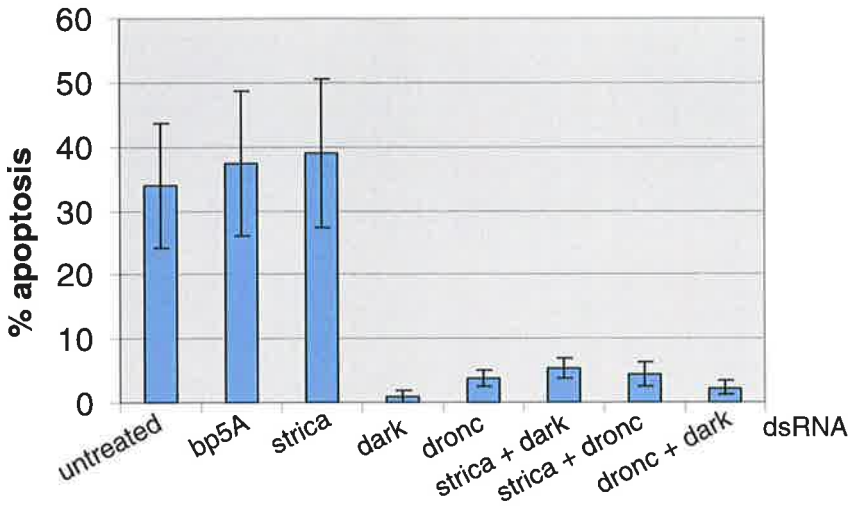
60
50
40
30
20
10
0
% apoptosis
untreated
bp5A
strica
dark
dronc
strica + dark
strica + dronc
dronc + dark
dsRNA

B

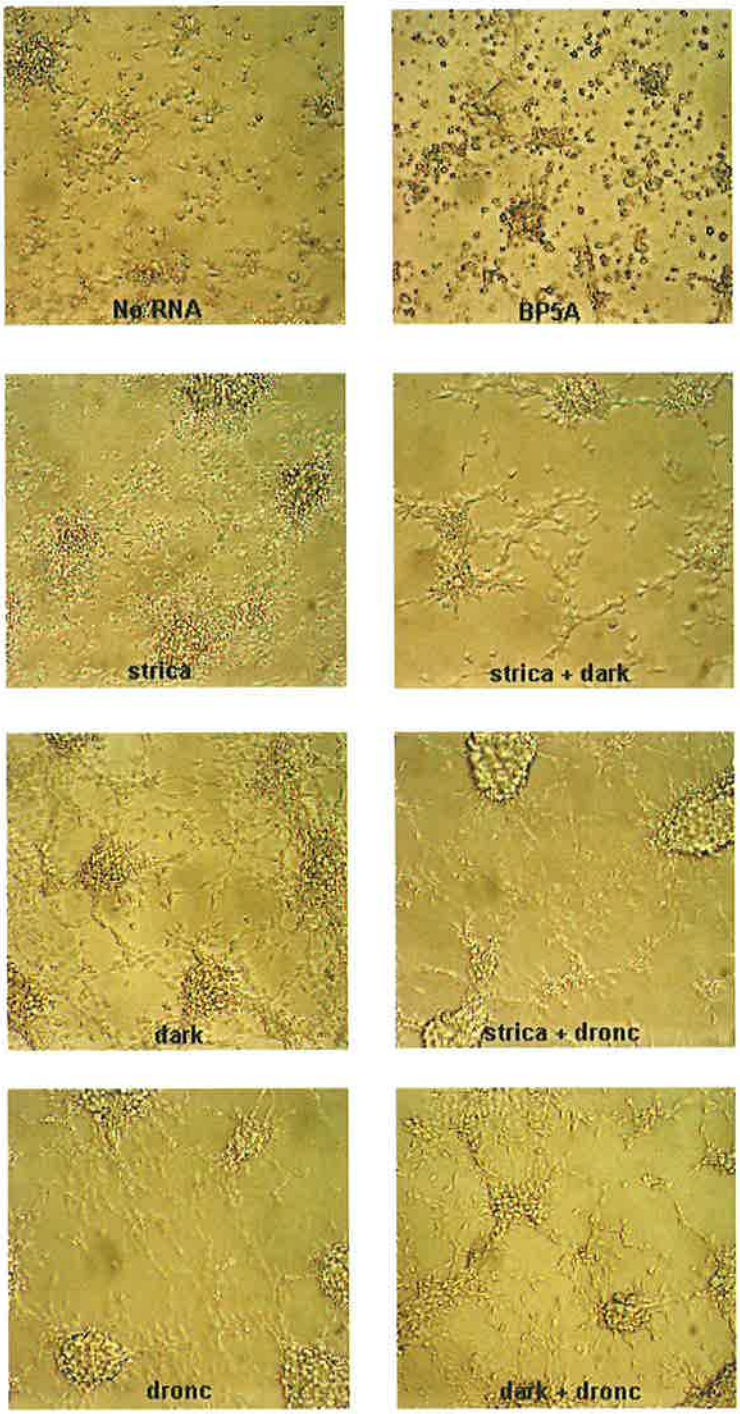
No RNA
BP5A
strica
strica + dark
dark
strica + dronc
dronc
dark + dronc

4.11 Discussion

The results presented in this chapter further elucidate the role of STRICA in *Drosophila* apoptosis, using an *in vivo* system. DIAP1 is essential for cell survival in the fly (section 1.11.1). Data presented here demonstrates that DIAP1 is an efficient inhibitor of apoptosis induced by STRICA overexpression *in vivo*. DIAP1 and DIAP2 are both capable of interacting physically with STRICA when coexpressed in BG2 cells, however, DIAP1 is able to completely restore the eye phenotype induced by STRICA, whereas suppression by DIAP2 is incomplete. The role of DIAP1 has been well defined in the apoptotic pathway whereas the function of DIAP2 is less clear. The physiological relevance for the interaction between DIAP2 and STRICA is not known, however exploring this further may shed light on the role of these two proteins in cellular signalling pathways. DIAP2 interacts with the DPP receptor, thick veins, in *Drosophila* (Oeda *et al.,* 1998). It is possible that STRICA, like DIAP2, functions in some other signalling pathway besides apoptosis.

The pan caspase inhibitor, p35, also suppresses STRICA-induced cell death in the eye, while the Bcl-2 homologue, BUFFY, has no effect. Moreover, STRICA activity is insensitive to levels of REAPER, HID and GRIM, as halving the dosage of these potent cell death activators does not suppress STRICA-induced apoptosis in the fly eye. RNAi ablation of *strica* in BG2 is insufficient to protect cells against apoptosis induced by cycloheximide, whereas depletion of either *dronc* or *dark* renders cells resistant to the same trigger. These results confirm the model for apoptosis in *Drosophila* in which DRONC plays the key role in inducing programmed cell death, in a manner dependent upon the activity of the adaptor molecule DARK. It appears that STRICA activity is unlikely to be required in cells where DRONC and DARK play crucial roles in the initiation of apoptosis. STRICA may, therefore, function in an alternative pathway, or respond to different stimuli.

The critical role of DIAP1 in apoptosis in *Drosophila* is supported by results presented in this chapter. While REAPER, HID and GRIM activate the DRONC pathway of cell death, other signalling pathways, independent of REAPER, HID and GRIM, exist and still require

the function of DIAP1 for survival (Wang, S.L *et al.*, 1999). Regardless of the pathway, DIAP1 is able to efficiently inhibit STRICA-induced cell death. DIAP1 is, therefore, a common inhibitory factor that transcends different apoptotic pathways by inhibiting various caspases, and is crucial for cell survival in the fly.

In conclusion, STRICA induces apoptosis when overexpressed in the *Drosophila* compound eye. STRICA-induced cell death is completely inhibited by p35 and DIAP1, partially suppressed by DIAP2, and not affected by halving the dosage of REAPER, HID and GRIM, or by overexpression of BUFFY. RNAi results suggest that STRICA may function in a pathway distinct from DRONC and DARK. The unique nature of the STRICA prodomain raises the possibility that STRICA is regulated either by a novel protein-protein interaction motif, or perhaps by phosphorylation. The possibility that STRICA functions in a serine/threonine kinase phosphorylation pathway is further explored in the next chapter.

Chapter 5

STRICA is a Potential Substrate for the Serine/Threonine kinase, DAKT

5.1 Introduction

Apart from the major cellular pathways that lead to caspase-activation and cell death, other molecules with diverse functions have been shown to impinge upon the apoptotic signalling cascade. In mammals, the phosphatidylinositol 3-kinase (PI3-K) pathway activates a serine threonine kinase, AKT/PKB. Activation of PI3-K has a protective effect on the cell while inhibition of PI3-K has the reverse effect and leads to cell death (Kennedy *et al.,* 1997; Dudek *et al.,* 1997). Protein Kinase B (PKB)/AKT, is the downstream effector activated in response to stimulation of the PI3-K signalling cascade (Datta *et al.*, 1999).

AKT is implicated in cell and organ growth, and cell survival, and functions as part of the PI3-K pathway in response to various extracellular factors such as insulin, cytokines and growth factors. PI3-K is recruited to the plasma membrane in response to such signals, where it phosphorylates phosphatidylinositol 3,4-bisphosphate (PIP_2), converting it to phosphatidylinositol 3,4,5-bisphosphate ($PIP_{3)}$ (Cantrell *et al.*, 2001). Membrane-bound PIP_3 then recruits AKT from the cytosol through a pleckstrin homology (PH) domain-dependent interaction, which is phosphorylated by Phosphoinositide dependent protein kinase (PDK1) at two sites (Alessi *et al.,* 2001). This process is negatively regulated by PTEN (the phosphatase and tensin homologue on chromosome 10) which dephosphorylates PIP_3. The PH domain of AKT is important not only for recruitment to the plasma membrane, but also for keeping AKT in the cytosol through intramolecular inhibition (Calleja *et al.*, 2003). Once activated, AKT phosphorylates a number of downstream substrates, by recognising the consensus motif R-x-R-x-x-S/T-F/L (Alessi *et al.,* 1996). The mammalian PI3-K/PTEN/AKT pathway is summarised in figure 5.1.

There are three mammalian isoforms of AKT, encoded by a single gene. The AKT family of proteins are characterised by a central kinase domain, which phosphorylates serine and threonine targets, an N-terminal pleckstrin homology (PH) domain required for membrane targeting, and a C-terminal hydrophobic and proline-rich domain. AKT homologues have been isolated from diverse species including *Drosophila melanogaster* and

Figure 5.1 The mammalian PI3-K/PTEN/AKT pathway of cell survival

In mammals, stimulation of membrane bound receptors by survival factors lead to the recruitment of PI3-K to the plasma membrane. Following PI3-K compartmentalisation, PI3-K phosphorylates phosphatidylinositol 3,4-bisphosphate (PIP_2), converting it to phosphatidylinositol 3,4,5-bisphosphate (PIP_3). Membrane-bound PIP_3 then recruits AKT from the cytosol through PH domain-dependent interaction, which is phosphorylated at two residues by 3-phosphoinositide-dependent protein kinase (PDK1). This process is negatively regulated by PTEN which dephosphorylates PIP_3. Once activated, AKT phosphorylates a number of downstream substrates, by recognising the consensus motif R-x-R-x-x-S/T-F/L. Among the substrates involved in apoptosis are Forkhead transcription factor (FKH) and the proapoptotic Bcl-2 homologue, Bad. Phosphorylation of FKH mediates interaction with 14-3-3, preventing the translocation of FKH to the nucleus and the transcriptional activation of genes such as FasL. Phosphorylation of Bad also results in the binding of Bad by 14-3-3, preventing Bad from heterodimerising with the prosurvival protein Bcl-X_L and triggering mitochondrial-mediatied apoptosis.

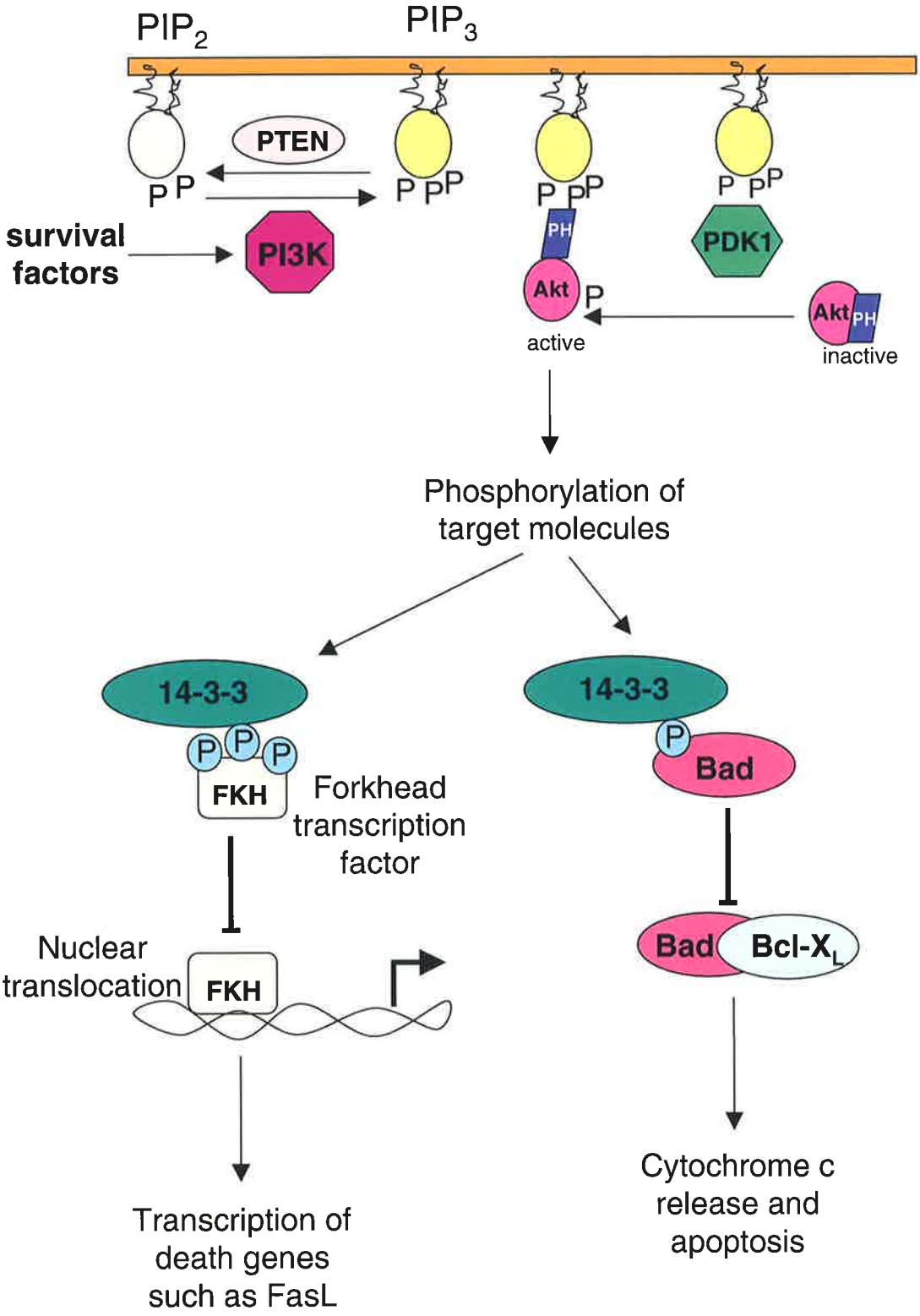
PIP2
PIP3
PTEN
P P
P PP
P PP
P PP
survival factors
PI3K
PH
Akt
P
active
PDK1
Akt PH
inactive
Phosphorylation of target molecules
14-3-3
P P P
FKH
Forkhead transcription factor
Nuclear translocation
FKH
Transcription of death genes such as FasL
14-3-3
P
Bad
Bad Bcl-XL
Cytochrome c release and apoptosis

C. elegans, indicating the fundamental importance of this molecule. *Drosophila* homologues for the main components of the PI3-K pathway are listed in figure 5.2.

The downstream targets of AKT implicated in the prosurvival function of the kinase include Bad, Caspase-9 and the Forkhead transcription factor (Downward *et al.,* 1999; Cardone *et al.,* 1998; Brunet *et al.,* 1999). In the case of Bad, phosphorylation allows the binding of Bad by 14-3-3, preventing the heterodimerisation of Bad with Bcl-X_L. This allows Bcl-X_L to exert its prosurvival function in the cell (Downward *et al.,* 1999 and figure 5.1). The Forkhead transcription factor (FKH) is recruited to the cytosol upon phosphorylation by AKT, through interaction with 14-3-3, thereby preventing it from upregulating proapoptotic molecules such as Fas ligand (Brunet *et al.,* 1999 and figure 5.1). Phosphorylation of Caspase-9 by AKT is somewhat controversial. The site of phosphorylation in mouse Caspase-9 (Cardone *et al.,* 1998) is not conserved among other mammalian species such as human, shedding doubt on the functional significance of such an event. AKT has been implicated in a number of human conditions including ovarian cancer and diabetes (Testa and Bellacosa, 2001; Huisamen, 2003; Hanada *et al.*, 2004).

Cell survival signalling through the PI3-K/PTEN/AKT pathway is conserved in *Drosophila melanogaster.* Staveley *et al.* (1998) identified a larval lethal mutant, *l(3) 89B q1*, that could be rescued by DAKT expression. This 'q' mutant was found to encode a point mutation in the kinase domain of DAKT resulting in complete loss of kinase activity. Loss of DAKT kinase activity *in vivo* results in increased embryonic apoptosis that is suppressed by the pan caspase inhibitor p35 suggesting that this cell death is caspase-dependent (Staveley *et al.,* 1998). This implicates DAKT as a prosurvival molecule that functions to suppress caspase-dependent cell death in *Drosophila.* Interestingly, the apoptotic phenotype associated with loss of DAKT function in embryos is not suppressed by deletion of the H99 region of genomic DNA, encoding apoptosis activators, REAPER, GRIM and HID. This suggests that the p35-inhibitable caspase activity associated with DAKT abrogation is insensitive to levels of REAPER, GRIM and HID.

Figure 5.2 *Drosophila* PI3-K/PTEN/AKT homologues

The PI3-K/PTEN/AKT survival signalling pathway is conserved in *Drosophila*, with homologues for PI3-K, PTEN, PDK-1 and AKT present in the fly. The function for each signalling molecule is described.

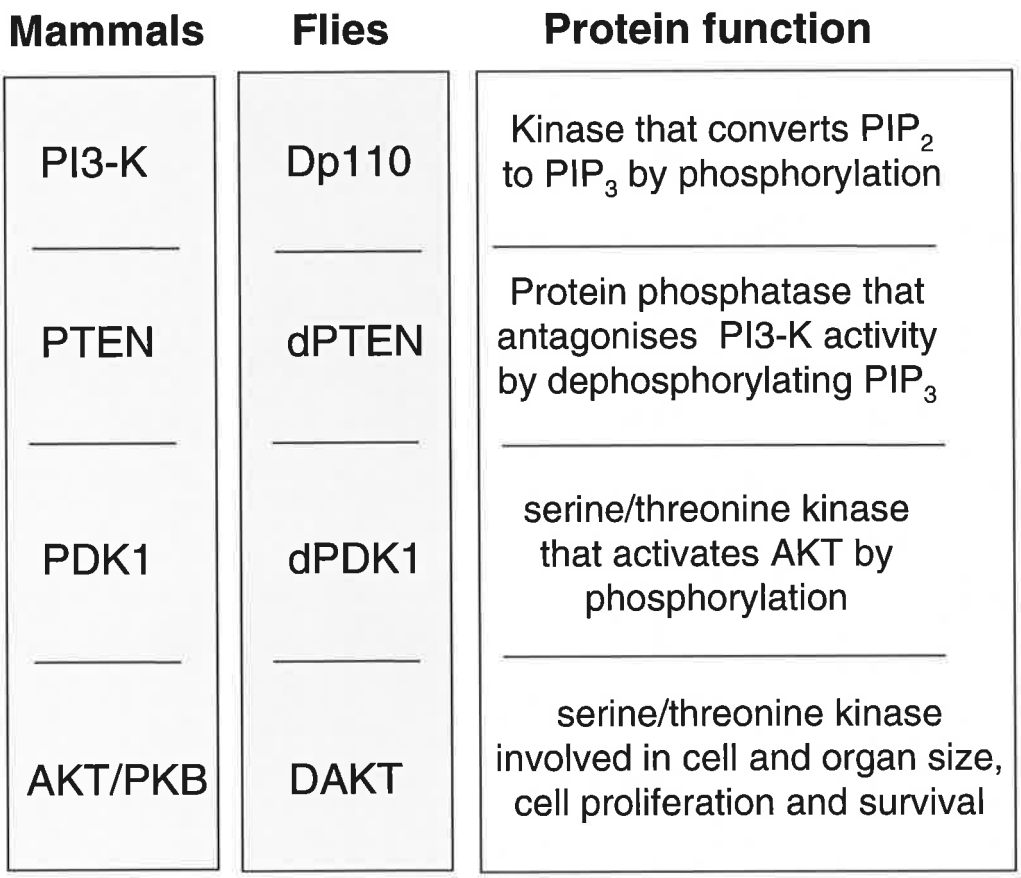
Mammals
Flies
Protein function
PI3-K
Dp110
Kinase that converts PIP_2 to PIP_3 by phosphorylation
PTEN
dPTEN
Protein phosphatase that antagonises PI3-K activity by dephosphorylating PIP_3
PDK1
dPDK1
serine/threonine kinase that activates AKT by phosphorylation
AKT/PKB
DAKT
serine/threonine kinase involved in cell and organ size, cell proliferation and survival

AKT is normally phosphorylated and activated by PDK-1 (Franke *et al.*, 2003). The *Drosophila* homologue of PDK-1 is implicated in cell growth and organ size in *Drosophila* and enhances the bulgy eye phenotype of DAKT overexpression in the fly eye (Cho *et al.*, 2001).

Given the vast number of serine and threonine residues in the prodomain of STRICA, the aim of the experiments described in this chapter was to identify possible phosphorylation sites and determine whether STRICA activity could be affected by a serine-threonine kinase. A potential AKT phosphorylation consensus motif was identified in the STRICA prodomain using SCANSITE (Lawlor and Alessi, 2001; Obata *et al.*, 2000; Yaffe *et al.*, 2001) under high stringency, raising the possbility that STRICA may be regulated by DAKT. Here, data is presented to confirm the function of dPTEN and DAKT in *Drosophila*. The small eye phenotype resulting from dPTEN overexpression is suppressed by DIAP1 and partially by DIAP2, as well as the caspase inhibitor p35, suggesting the role of a caspase downstream of dPTEN activity. DAKT has a prosurvival effect when coexpressed with STRICA in cultured cells. *In vivo*, DAKT partially suppresses STRICA-induced cell death in the fly eye, while the loss-of-function q mutant mildly enhances STRICA-induced cell death in the eye.

5.2 The PI3-kinase pathway is conserved in *Drosophila*

For the purpose of this study, the role of DAKT and dPTEN in the regulation of apoptosis in *Drosophila* was explored. Flies carrying the *UAS-dakt*, *UAS-pkb* or *UAS-dpten* transgene were crossed to a *GMR-Gal4* driver line to drive expression of these genes in the compound eye. As previously published (Verdu *et al.*, 1999), overexpression of DAKT resulted in an enlarged eye phenotype (figure 5.3 A). Mammalian AKT (PKB) produced a similar phenotype, although less pronounced, when ectopically expressed in the eye (figure 5.3 B). Conversely, overexpression of the negative regulator of DAKT, dPTEN, induced apoptosis causing a small eye phenotype (figure 5.3 A). Fly stocks carrying both the transgene and the *GMR-Gal4* driver balanced over the selectable phenotypic marker, curly wings (Cyo), were established, as described in section 2.14.8 (figure 5.4). Flies expressing dPTEN in the eye were selected by the small eye phenotype caused by dPTEN overexpresion. Flies expressing DAKT or PKB in the eye were more difficult to distinguish from wildtype and were selected by looking for an increase in protein expression in the eye by Western blotting. PKB was HA tagged and an overexpression line was isolated by Western blotting with α-HA antibody (figure 5.4 B). α-DAKT, a commercial antibody that cross-reacts with *Drosophila*, was used to identify DAKT overexpressing lines (figure 5.4 C).

5.3 The dPTEN small eye phenotype is suppressed by caspase inhibitors

For the purpose of this study, initial experiments were carried out to confirm previously published results. To establish that the small eye phenotype induced by dPTEN was due to caspase-dependent apoptosis, *GMRGal4-UASdPTEN/Cyo* flies were crossed to flies carrying a transgene expressing either p35, DIAP1 or DIAP2. The small eye phenotype was rescued by coexpression with p35 (figure 5.5 A) and DIAP1 (figure 5.5 B), and partially suppressed by DIAP2 (figure 5.5 C), demonstrating that caspase activity downstream of

Figure 5.3 Ectopic expression of DAKT, dPTEN and PKB in the *Drosophila* eye

A Overexpression of DAKT and dPTEN in the *Drosophila* compound eye. *UAS-dakt* and *UAS-dpten* flies were crossed to flies carrying the *GMR-Gal4* driver to overexpress each protein in the eye. The eyes of progeny with genotypes *GMR-Gal4/+*, *GMR-Gal4/UAS-dakt* and *GMR-Gal4/UAS-dpten* are shown in males and females as indicated. Two different magnifications are presented. Eyes are different in each case. Compared with GMR-Gal4 alone, overexpression of DAKT results in enlarged eyes. Conversely, overexpression of dPTEN gives rise to flies with a small eye phenotype. **B** Mammalian AKT/PKB was overexpressed as above by crossing the *GMR-Gal4* driver line to *UAS-pkb* flies. Progeny with genotypes *GMR-Gal4/+* and *GMR-Gal4/UAS-pkb* are shown. Like DAKT, PKB overexpression causes an enlarged eye phenotype.

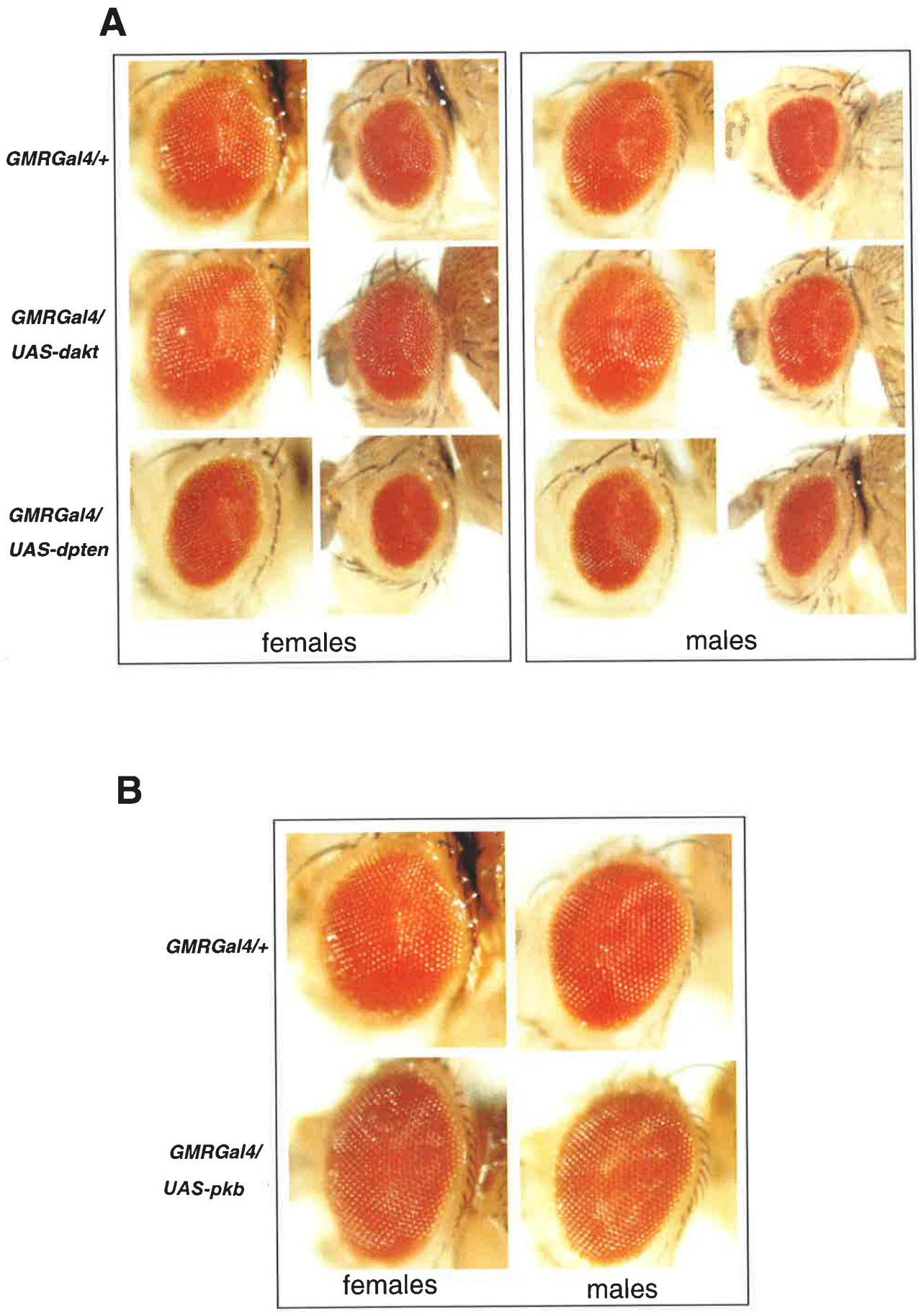
A
GMRGal4/+
GMRGal4/
UAS-dakt
GMRGal4/
UAS-dpten
females
males
B
GMRGal4/+
GMRGal4/
UAS-pkb
females
males

Figure 5.4 Expression of PKB, DAKT and dPTEN in balanced *Drosophila* lines

Transgenic lines expressing PKB, DAKT and dPTEN in the eye balanced with a curly wing (Cyo) marker chromosome were established as described in Materials and Methods section 2.14.8. Progeny of crosses described in figure 5.3 were crossed with a *Df(2)rougheye/Cyo* double balancer fly stock. Two *GMRGal4-UASdpten/Cyo* lines were established. Line 2 was used for further crosses described later. Of three potential lines, one (line 2) was found to express PKB by Western blotting (**B**). A commercial AKT antibody that cross-reacts with *Drosophila* AKT was used to detect lines overexpressing DAKT. A non-specific band (NS) in was used as a loading control. Four lines were identified (**C**) and two, lines 4 and 5, were used in subsequent crosses. Representative phenotypes are presented in **A**.

A

GMR-Gal4/Cyo

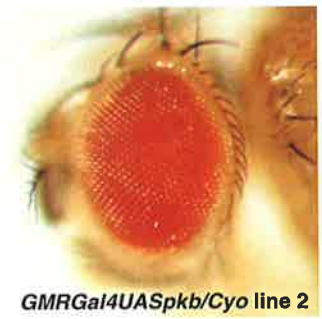

GMRGal4UASpkb/Cyo line 2

GMRGal4-UASdakt/Cyo line 5

GMRGal4-UASdpten/Cyo line 2

B

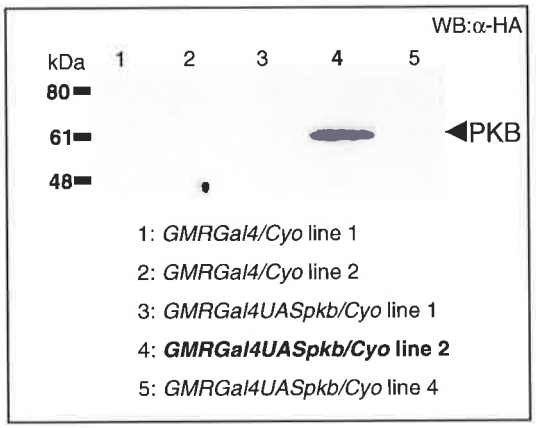

1: *GMRGal4/Cyo* line 1

2: *GMRGal4/Cyo* line 2

3: *GMRGal4UASpkb/Cyo* line 1

4: ***GMRGal4UASpkb/Cyo* line 2**

5: *GMRGal4UASpkb/Cyo* line 4

C

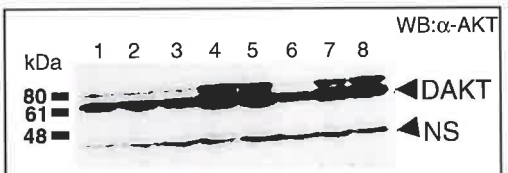

1: *GMRGal4/Cyo* line 1

2: *GMRGal4/Cyo* line 2

3: *GMRGal4-UASdakt/Cyo* line 1

4: *GMRGal4-UASdakt/Cyo* line 4

5: ***GMRGal4-UASdakt*/Cyo line 5**

6: *GMRGal4-UASdakt/Cyo* line 6

7: *GMRGal4-UASdakt/Cyo* line 8

8: *GMRGal4-UASdakt/Cyo* line 9

Figure 5.5 dPTEN-induced cell death is suppressed by p35, DIAP1 and DIAP2 in the fly eye

GMRGal4-UASdpten/Cyo flies were crossed to flies carrying a *GMR-p35* transgene. Progeny were analysed for suppression of the small eye phenotype induced by overexpression of dPTEN. Significant suppression is observed in *GMRGal4-UASdpten/GMR-p35* progeny (**A**). *GMRGal4-UASdpten* flies were crossed with flies carrying *GMR-diap1* on the X chromosome. Progeny were analysed for suppression of the dPTEN small eye phenotype. Males (*dpten/Y*) were compared to females (*dpten/diap1*). Significant restoration of eye size is observed in flies expressing both dPTEN and DIAP1 (**B**). The small eye phenotype of *GMRGal4-UASdpten* flies is partially suppressed by one copy of a DIAP2 overexpression transgene (*GMR-diap2*). Complete restoration is not observed (**C**).

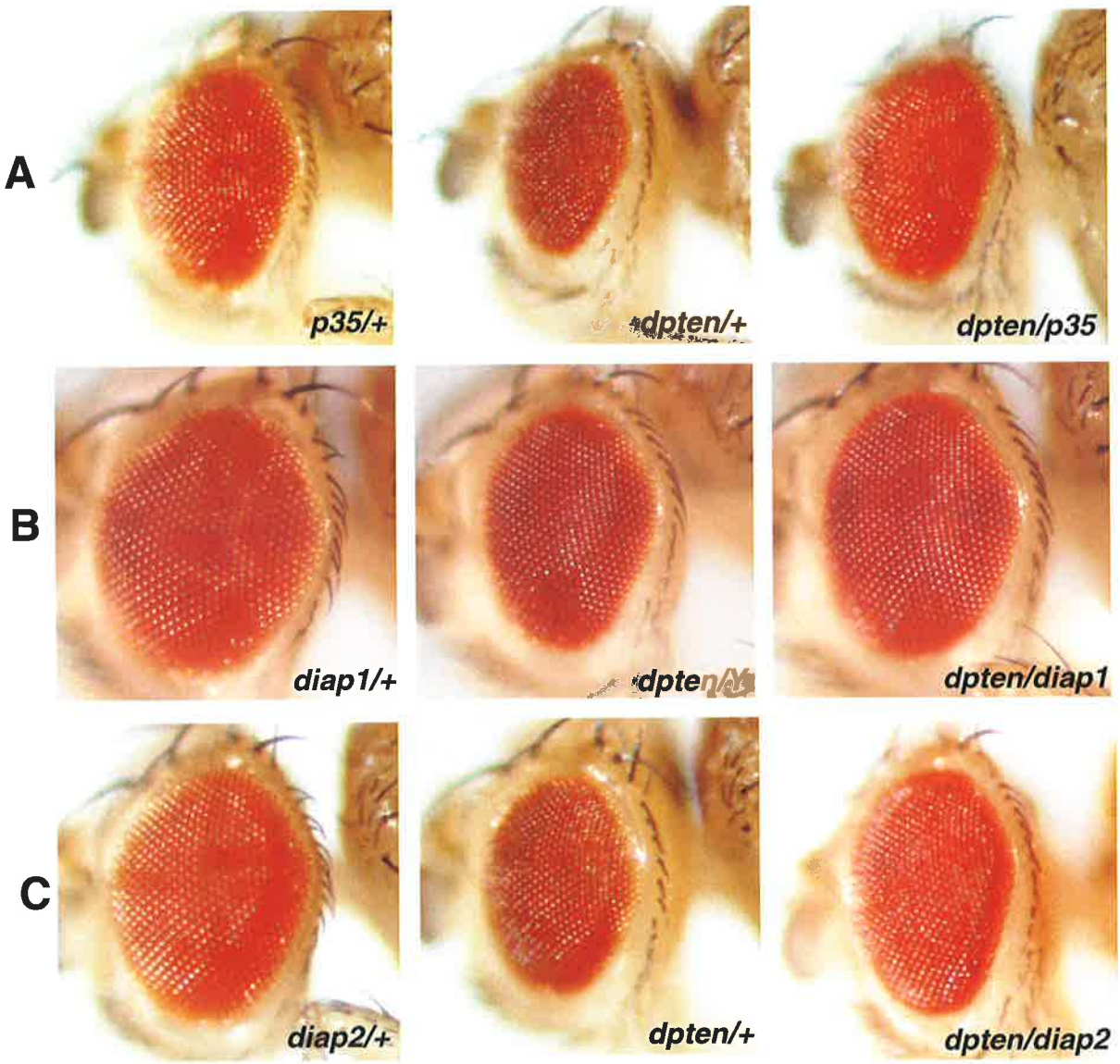
A
p35/+
dpten/+
dpten/p35
B
diap1/+
dpten/+
dpten/diap1
C
diap2/+
dpten/+
dpten/diap2

dPTEN signalling contributes to the small eye phenotype resulting from ectopic dPTEN expression.

5.4 dPTEN is suppressed by DAKT in the *Drosophila* eye

DAKT functions downstream of dPTEN in the PI3-K pathway. As expected, coexpression of dPTEN with DAKT suppressed the small eye phenotype caused by overexpression of dPTEN, favouring an enlarged, bulgy eye phenotype (figure 5.6). This demonstrates that the *GMRGal4-UASdakt* flies generated in this study, are expressing sufficient levels of DAKT to suppress the dPTEN phenotype.

5.5 The prodomain of STRICA contains a putative AKT phosphorylation site

STRICA was named based on the presence of a large number of serine and threonine residues in its prodomain (Ser/Thr RIch Caspase). This feature raises the possibility that STRICA is phosphorylated by a serine/threonine kinase and may therefore be regulated by phosphorylation. A search for potential phosphorylation sites detected a consensus phosphorylation motif for AKT. A program developed by Yaffe *et al.*, (2001) was used to search the primary sequence of STRICA for AKT phosphorylation motifs under high stringency. A consensus site was detected where the putative phosphorylated serine residue is serine 119 in the prodomain (figure 5.7).

5.6 DAKT suppresses STRICA-induced cell death in cultured cells

STRICA induces apoptosis when overexpressed in cultured cells. STRICA was coexpressed in COS cells with DAKT or DIAP1. STRICA induced apoptosis in 50% of cells that was inhibited by both DIAP1 and DAKT (figure 5.8 A). A STRICA mutant, where the potentially phosphorylated serine residue was substituted with glycine, induced apoptosis to levels comparable to wildtype. Apoptosis induced by STRICA (S119G) was not significantly suppressed by DAKT, suggesting that DAKT may regulate STRICA by phosphorylation at

Figure 5.6 dPTEN genetically interacts with DAKT in the *Drosophila* eye

Overexpression of DAKT suppresses the small eye phenotype induced by dPTEN overexpression. Eyes from *GMRGal4-UASdpten/GMRGal4-UASdakt* progeny are enlarged with disruption to ommatidia.

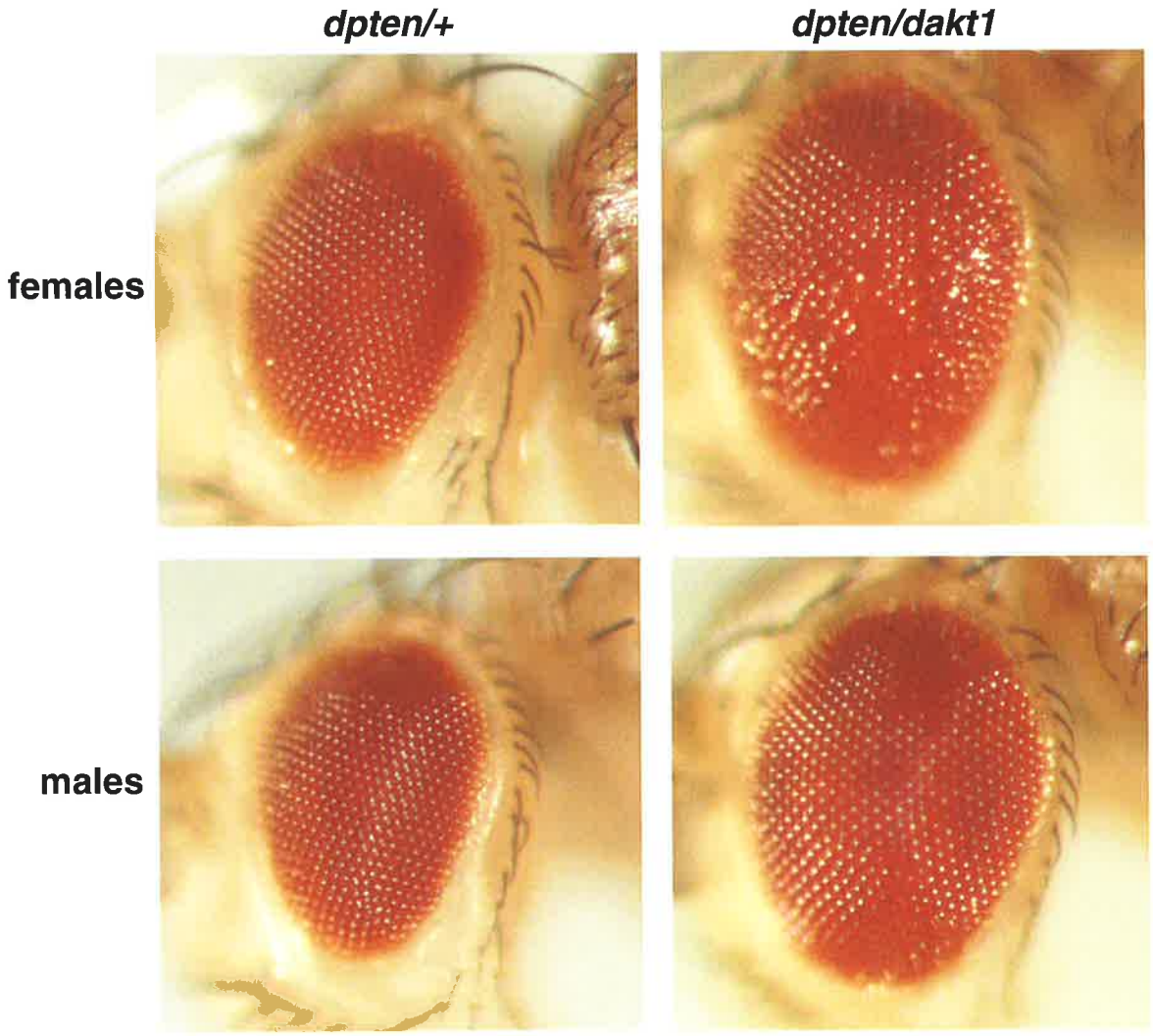
dpten/+
dpten/dakt1
females
males

Figure 5.7 Prediction of an AKT phosphorylation motif in the prodomain of STRICA

The amino acid sequence of full-length STRICA was analysed for potential AKT phosphorylation sites using a programme developed by Yaffe *et al.* (described in Lawlor and Alessi, 2001). High stringency hits fall within the top 0.2% of all aligned potential AKT phosphorylation sites. A potential phosphorylation site in STRICA was detected using this programme (http://cansite.bidmc.harvard.edu/cantley85.phtml). The sequence in STRICA conforms to the RxRxxS/T-F/L consensus, with serine 119 predicted to be targeted for phosphorylation by AKT. This prediction scores within the top 0.096%, making it an attractive putative AKT phosphorylation site.

Motif Scan Graphic Results: STRICA

Description: User-entered sequence
Motifs scanned: Akt_Kin
Stringency: High
Show domains: Yes

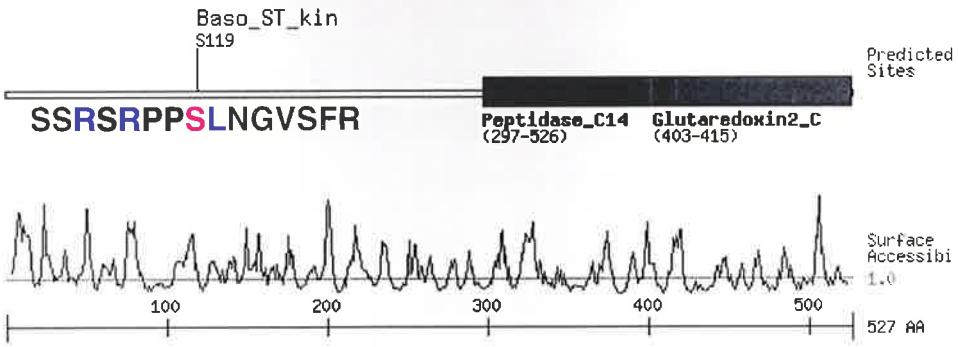

Basophilic serine/threonine kinase group (Baso_ST_kin)
Akt Kinase Gene Card AKT1

Site	Score	Percentile	Sequence	SA
S119	0.2726	0.096 %	SSRSRPPSLNGVSFR	1.001

AKT consensus: RxRxxS/T-F/L

Figure 5.8 DAKT suppresses STRICA-induced cell death in cultured cells

A COS7 cells were transiently transfected with pcDNA3 construct as indicated. STRICA induces apoptosis in over 50% of cells, as determined by this death assay (described in Materials and Methods section 2.10.1). Coexpression of STRICA with DAKT suppresses apoptosis by half. DIAP1 also shows suppression of STRICA-induced cell death. STRICA (C429G) does not induce cell death in cells, whereas STRICA ΔPD and a putative AKT phosphorylation mutant (STRICA (S119G)), induce apoptosis. DAKT has a lesser effect on apoptosis induced by STRICA (S119G). Results are representative of two independent experiments with error bars indicating ±SD. **B** COS cells transiently transfected with constructs expressing the proteins as indicated were harvested and analysed at the protein level by Western blotting. All STRICA constructs are C-terminally FLAG tagged and DAKT is C-terminally MYC tagged. STRICA and STRICA (S119G) are barely detectable (lanes 1 and 2), whereas STRICA (C429G) is expressed at high levels due to lack of induced cell death. Coexpression with DAKT suppresses cell death, enabling full-length STRICA and STRICA (S119G) to be detected. The blot was stripped and re-probed to confirm DAKT expression. Some remaining STRICA (C429G) signals are also seen. A nonspecific cross-reacting band is indicated (NS).

A

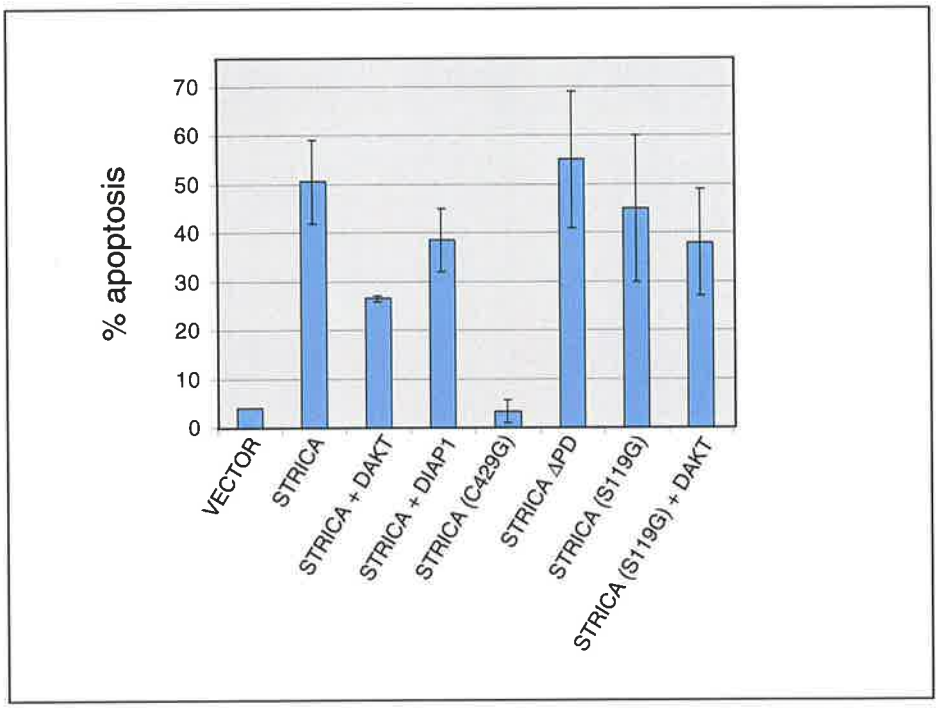
% apoptosis
70
60
50
40
30
20
10
0
VECTOR
STRICA
STRICA + DAKT
STRICA + DIAP1
STRICA (C429G)
STRICA ΔPD
STRICA (S119G)
STRICA (S119G) + DAKT

B

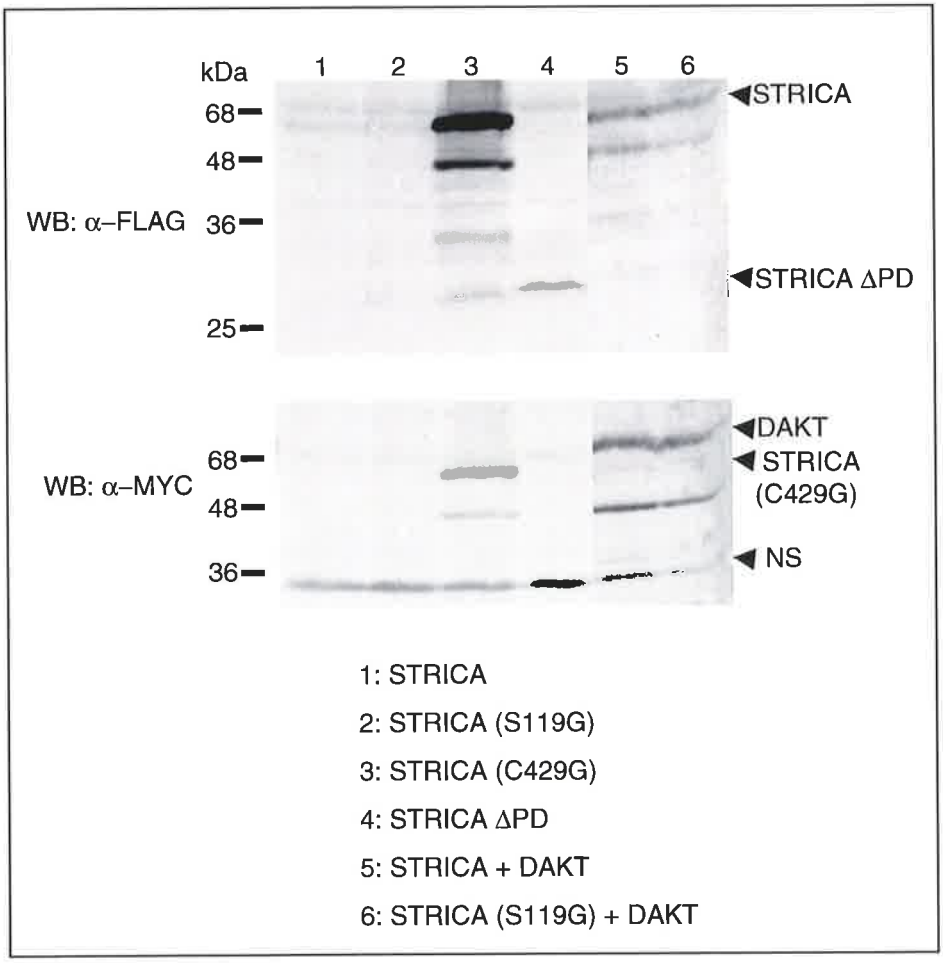
kDa
1
2
3
4
5
6
68
48
36
25
WB: α–FLAG
STRICA
STRICA ΔPD
WB: α–MYC
68
48
36
DAKT
STRICA
(C429G)
NS
1: STRICA
2: STRICA (S119G)
3: STRICA (C429G)
4: STRICA ΔPD
5: STRICA + DAKT
6: STRICA (S119G) + DAKT

this site. Overexpression of STRICA in COS cells induces cell death, making detection of full-length STRICA protein difficult. Coexpression of DAKT with STRICA allowed for the detection of STRICA protein in COS cells by suppressing STRICA-induced cell death (figure 5.8 B).

5.7 STRICA-induced cell death is partially suppressed by DAKT in the *Drosophila* eye

GMR-strica flies were crossed to *GMRGal4-UASdakt* flies to determine whether overexpression of DAKT is capable of suppressing STRICA-induced cell death *in vivo*. While DAKT does not completely restore the loss of pigment cells due to STRICA-induced apoptosis in the eye, an increase in the number of pigment cells was observed in the progeny of flies generated by crossing *GMR-strica* flies to two DAKT overexpression lines, 4 and 5 (figure 5.9 A and B). Overexpression of mammalian AKT/PKB had no effect on STRICA in the eye (figure 5.9 C). Furthermore, flies carrying one copy of the *GMR-strica* transgene, and heterozygous for the DAKT kinase inactive mutant (q), demonstrated a slight enhancement of the STRICA-induced apoptotic phenotype (figure 5.10). Taken together, these results demonstrate that DAKT overexpression has an effect on ectopic STRICA-induced apoptosis, indicating that DAKT contributes, at least in part, to the regulation of STRICA activity.

Figure 5.9 STRICA-induced cell death is partially suppressed by DAKT in the fly eye

GMR-strica flies were crossed with *GMRGal4-UASdakt* flies and the resulting progeny assessed for suppression of the STRICA-induced apoptotic phenotype. Expression of STRICA in the eye causes loss of pigment cells due to ectopic cell death. Coexpression with DAKT demonstrates a slight suppression of the STRICA phenotype, with an increase in red pigment cells observed. Some eyes coexpressing DAKT also show loss of ommatidia organisation with areas exhibiting a bulgy phenotype. Progeny of *GMR-strica* flies crossed to *GMRGal4-UASdakt* line 5 (**A**) and line 4 (**B**) are shown. No significant increase in pigment cells is observed in flies coexpressing STRICA and PKB (**C**).

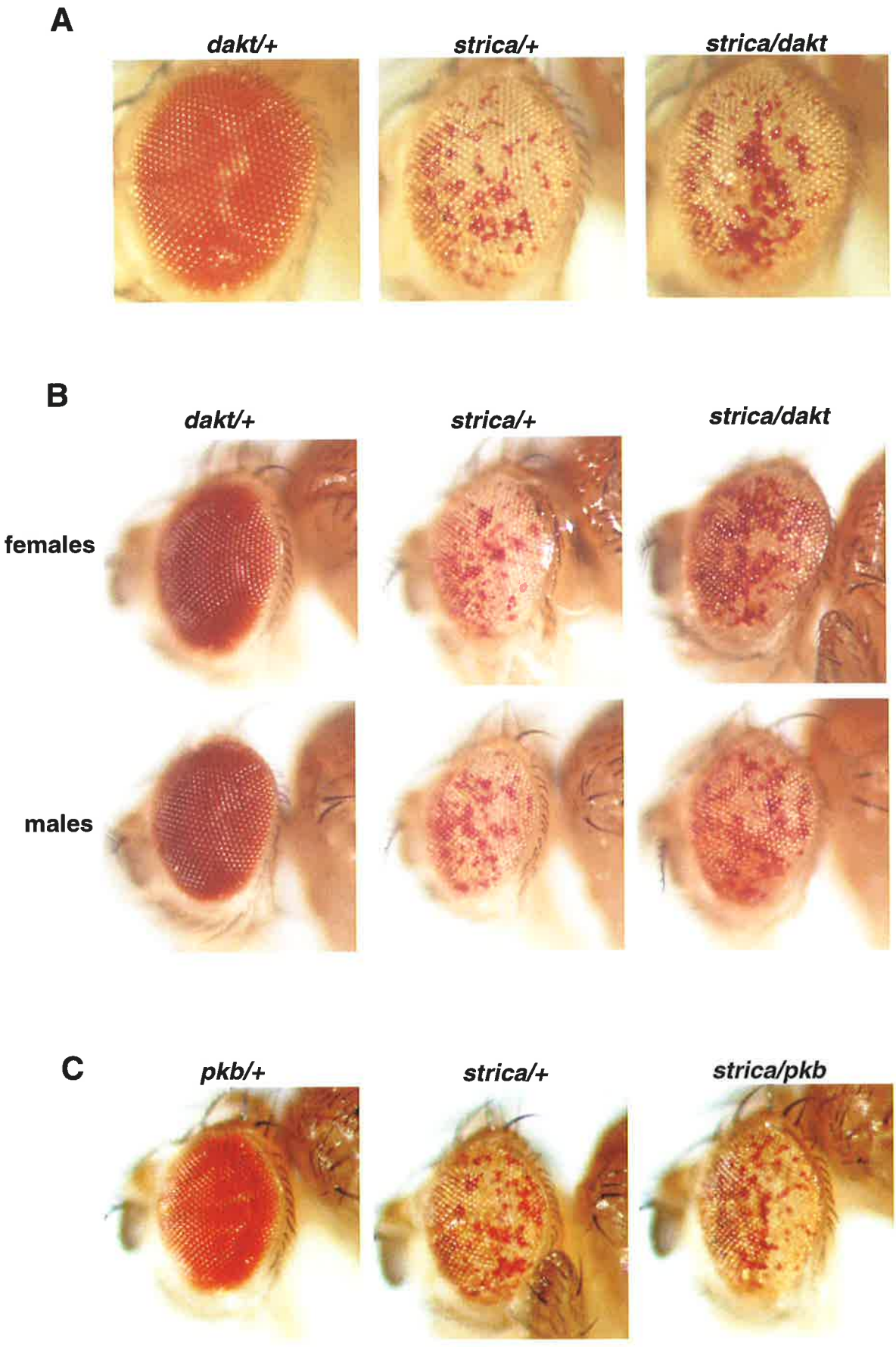
A
dakt/+
strica/+
strica/dakt
B
dakt/+
strica/+
strica/dakt
females
males
C
pkb/+
strica/+
strica/pkb

Figure 5.10 Halving the dosage of kinase-active DAKT has a subtle effect on STRICA-induced apoptosis

Dakt1 q1/Tm3Sb flies carry a point mutation that renders DAKT kinase-inactive. To determine whether halving the dose of wildtype *dakt* has an effect on STRICA-induced cell death in the eye, *Dakt1 q1/Tm3Sb* flies were crossed with *GMR-strica/Cyo* flies. *strica/+* progeny demonstrate the usual loss of pigment cells caused by ectopic STRICA expression. In many cases, slight enhancement of this phenotype was observed in *strica/q* flies, however the subtlety of this effect was sometimes difficult to detect. Results from two independent crosses are presented.

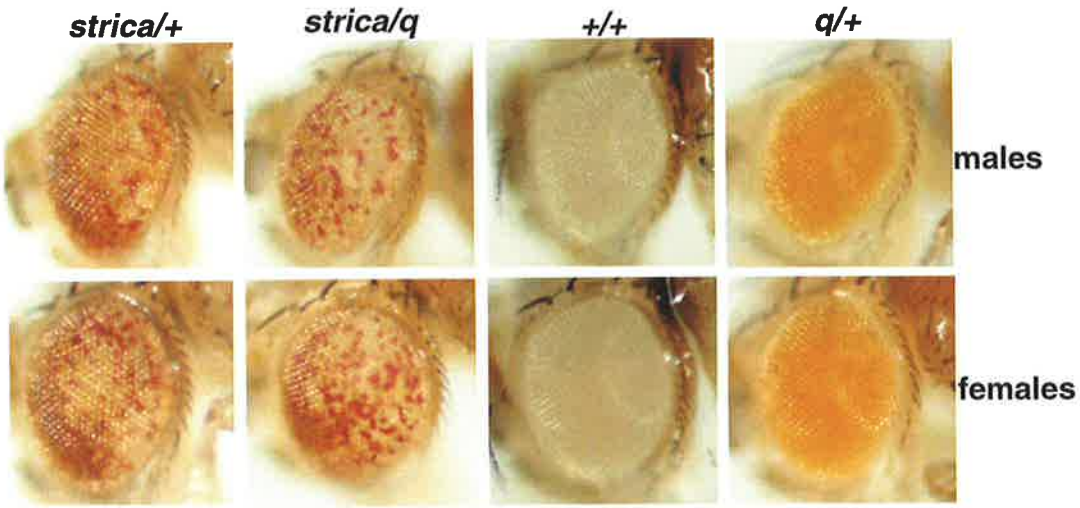
strica/+
strica/q
+/+
q/+
males
females

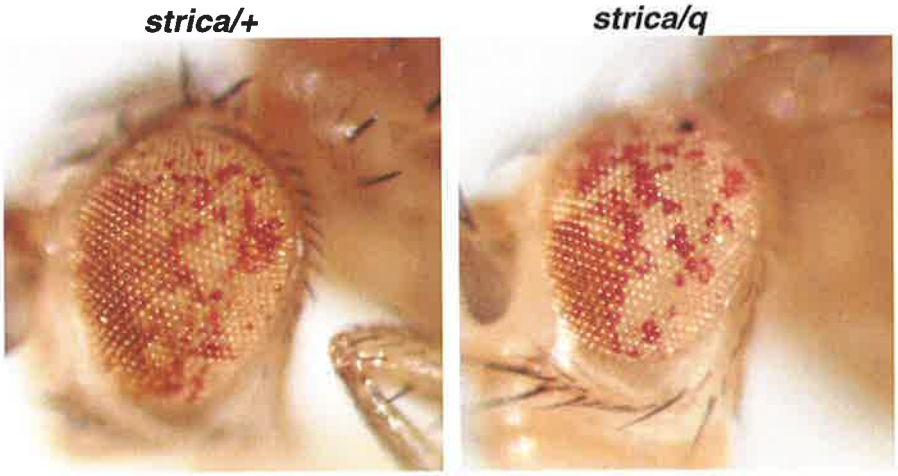
strica/+
strica/q

5.8 Discussion

Here I have presented data that suggest STRICA may function in a serine/threonine kinase pathway in *Drosophila*. In mammals, AKT/PKB functions in diverse cellular processes including cell cycle progression, cell and organ size, differentiation and cell survival (Franke *et al.*, 2003). In *Drosophila*, the PI3-K signalling pathway is conserved and is initiated by signalling through the insulin receptor, CHICO (insulin-receptor substrate (IRS)) and Dp110 (PI3-K) (Goberdhan *et al.*, 1999; Scanga *et al.*, 2000; Clancy *et al.*, 2001).

The function of DAKT is dependent on the stage of *Drosophila* development. While dPTEN has been reported to induce apoptosis when ectopically expressed during a range of developmental stages, DAKT reportedly only plays a role in cell survival during embyrogenesis (Staveley *et al.*, 1998; Scanga *et al.*, 2000). dPTEN overexpression in the fly eye shows a small, rough eye phenotype that is suppressed by p35 (Huang *et al.*, 1999). Furthermore, *GMR-Gal4/UASdpten* third instar larval eye discs exhibit substantially increased cell death. dPTEN antagonises Dp110, the *Drosophila* PI3-K homologue, and its upstream activator, CHICO (Goberdhan *et al.*, 1999).

The kinase that activates AKT, PDK-1, has a homologue in *Drosophila*, dPDK-1. In flies, *dPDK-1* deficiency results in embryonic lethality with an apoptotic phenotype (Cho *et al.*, 2001). Conversely, the same authors report that overexpression of dPDK-1 increased cell and organ size, in a PI3-K-dependent manner.

Interestingly, unlike dPTEN and Dp110, DAKT has been reported to play a role in the regulation of cell size alone during eye development (Verdu *et al.*, 1999; Scanga *et al.*, 2000). However DAKT overexpression is sufficient to suppress the loss of cell number induced by dPTEN and Dp110 (Scanga *et al.*, 2000). During embryogenesis, on the other hand, evidence suggests that the Dp110/dPTEN/DAKT pathway plays a role in cell survival (Scanga *et al.*, 2000).

Here I have reported that the *Drosophila* caspase STRICA contains an AKT phosphorylation site in the prodomain, detected using a high-stringency homology search

(Lawlor and Alessi, 2001; Obata *et al.*, 2000; Yaffe *et al.*, 2001). *Drosophila* lines kindly provided by Prof. Manoukian were used to establish fly stocks expressing dPTEN, DAKT and PKB ectopically in the fly eye, using the UAS, GMR-Gal4 system. Consistent with previously published data, overexpression of dPTEN results in a small eye phenotype that is suppressed by p35, DIAP1, and partially by DIAP2, confirming a role for dPTEN in caspase-dependent cell death. Overexpression of DAKT also suppresses dPTEN-induced apoptosis in the eye, placing DAKT downstream of dPTEN in the PI3-K pathway.

DAKT partially suppresses STRICA-induced apoptosis in the eye, and in cell death assays. However, suppression *in vivo* is only slight. Furthermore, STRICA-induced cell death is not significantly affected by halving the dosage of functional, kinase-active DAKT, or by overexpression of mammalian PKB. This suggests that, unlike DIAP1 that maintains constant inhibition over caspases in healthy cells, the effect of DAKT may be more specific to both temporal and spatial factors. Although PKB has no effect on STRICA-induced cell death *in vivo*, there is no known mammalian homologue for STRICA to date, raising the possibility that the function of STRICA is specific to apoptosis in the fly and may therefore only be recognised by species-specific signalling proteins.

If DAKT functions to prevent STRICA activation, it is possible that STRICA overexpression overcomes DAKT inhibition to a large extent, given the ability of STRICA to autoprocess. Processing of the prodomain of STRICA removes the AKT phosphorylation site and conceivably renders STRICA insensitive to DAKT. Furthermore STRICA is detected in transiently transfected cultured cells when coexpressed with DAKT, demonstrating the prosurvival function of this molecule. However, the putative serine phosphorylation mutant of STRICA (S119G), can still induce apoptosis when overexpressed in cells, and is difficult to detect in transfected cells. Both wildtype STRICA and STRICA (S119G) autoprocess between the prodomain and large subunits when overexpressed (figure 3.8). It is, therefore, not surprising that apoptosis is induced by both molecules, given that the putative AKT phosphorylation motif is removed when the prodomain is processed, and this may overcome

any inhibition resulting from phosphorylation at this site. It is possible that the increase in protein detected may be due to indirect suppression of cell death rather than direct suppression of STRICA activity.

Phosphorylation of targets by DAKT results in a diverse range of effects, including targeting to the proteasomal degradation pathway. In the case of STRICA, mutation of the putative phosphorylated serine residue does not increase STRICA stability, suggesting that if DAKT phosphorylates STRICA, it is unlikely to affect protein stability. Perhaps phosphorylation of STRICA is required for interaction with an inhibitory molecule, preventing STRICA activation.

The role of the Dp110/dPTEN/DAKT pathway of cell survival in *Drosophila* is well established, and given that cell death events caused by loss of DAKT function or overexpression of dPTEN are caspase-dependent, STRICA is a good candidate for initiation of cell death downstream of insulin signalling. STRICA is the only *Drosophila* caspase that contains a putative AKT phosphorylation site, however it must be emphasised that site predictions are speculative and need to be functionally confirmed. It should also be emphasised that the experiments presented in this chapter were performed by overexpressing STRICA ectopically, and subtle effects may be overcome under these conditions. Further understanding of the physiological signifance of the relationship between STRICA and DAKT requires the isolation and analysis of *strica* null mutants.

Although data presented here cannot, with certainty, conclude a functional relationship between STRICA and DAKT, these results strongly suggest that STRICA functions in the PI3-K/DAKT signalling pathway in the fly. Given the presence of a strong AKT phosphorylation motif, and the suppression of STRICA by DAKT *in vivo*, this alternative pathway would be an interesting area for further investigation.

Chapter 6

Analysis of the Differential Intracellular Localisation of BUFFY and DEBCL

6.1 Introduction

In mammals, two major pathways exist to initiate apoptosis in response to different stimuli. The binding of extracellular ligands to their membrane-bound receptors triggers the extrinsic pathway, and begins a cascade of protein recruitment and caspase activation (section 1.6.1). Cells respond to stimuli such as UV irradiation and cytotoxic drug exposure by initiating the intrinsic apoptotic pathway. In this case, the integrity of the mitochondrial outer membrane is compromised, leading to organelle rupture and the release of several small, death-inducing molecules including Smac/Diablo, HtrA2 and cytochrome c (section 1.6.2). Once released, the latter molecule binds to the WD40 repeats of the large CED-4-like adaptor molecule, Apaf-1, causing a conformational change. Apaf-1, now in an open configuration, recruits Procaspase-9 molecules and in the presence of dATP, forms a high molecular weight complex known as the apoptosome. Structurally, the apoptosome is a highly efficient 'death wheel' that allows the continual processing and activation of Caspase-9, and the subsequent activation of Caspase-3 (section 1.4).

The Bcl-2 family of proteins share one to four Bcl-2 homology (BH) domains. The prosurvival faction of this family are characterised by BH1-BH4 domains and act as guardians of the mitochondria to maintain the integrity of these organelles and prevent the release of cytochrome c (section 1.7). The opposing, BH3-only proapoptotic members like Bad, Bik, Bim, Noxa and Puma, respond to death stimuli in different cell types and induce cell death in a Bax/Bak-dependent manner (section 1.7.1). The presence of a C-terminal hydrophobic membrane anchor (MA) in most of the Bcl-2 family members mediates the intracellular localisation of these proteins to membranes of the mitochondria, ER and nuclear envelope. Although the precise mode of action that leads to cytochrome c release is still under scrutiny, it is considered to involve sequestration of the prosurvival members by BH3-only proteins and the formation of Bax and Bak oligomers that form channels on the mitochorndrial outer membrane through which cytochrome c can pass (Cory *et al.*, 2003).

The C-terminal membrane anchor is critical for the correct localisation and function of both prosurvival and proapoptotic Bcl-2 homologues (section 1.7.2). Kaufmann *et al.* (2003) have recently described the fundamental basis for the differential intracellular localisation of Bcl-2 and Bcl-X_L. Bcl-2 has long been known to localise to membranes of the mitochondria, ER and nuclear envelope (Krajewski *et al.*, 1993; Lithgow *et al.*, 1994). Using site-directed mutagenesis, Kaufmann *et al.* identified multiple positively charged residues flanking the membrane anchor of Bcl-X_L that are absent in Bcl-2. The authors suggest that in the absence of such a strong positive charge, Bcl-2 is able to localise to other membranes as well as mitochondria.

Drosophila have two Bcl-2 homologues, BUFFY and DEBCL. At the commencement of this study, DEBCL was the first cloned Bcl-2 homologue in *Drosophila* and was characterised as a proapototic protein by several independent groups (Colussi *et al.,* 2000; Brachmann *et al.*, 2000; Igaki *et al.,* 2000). A second Bcl-2 homologue was cloned in our laboratory and was shown to have a prosurvival function in transgenic flies (Quinn *et al.,* 2003). The studies in this chapter aimed to carry out a comparative study to assess the differential localisation of BUFFY and DEBCL, and to further characterise the function of BUFFY in cultured cells. Results presented here suggest that transmembrane domain (TMB)-flanking residues in DEBCL, homologous to Bcl-X_L, are required for the targeting of DEBCL to mitochondria. C-terminal positively charged residues present in DEBCL are absent in BUFFY, which localises to the ER in cell lines. The TMB in both molecules is required for the correct targeting of these proteins.

EGFP was fused to DEBCL, BUFFY and various mutants targeting the putative mitochondrial outer membrane (MOM)-targeting sequence in DEBCL. While DEBCL mutants mislocalise similarly to Bcl-X_L, some differences exist between BUFFY and Bcl-2 suggesting that perhaps a different mechanism is used for the intracellular localisation of BUFFY. Interestingly, a putative nuclear localisation signal (NLS) was identified in the N-terminal region of BUFFY. Data are presented to demonstrate that this NLS is functional.

Abbreviations for transmembrane domain (TMB) and membrane anchor (MA) are used interchangeably to describe the C-terminal hydrophobic tails of BUFFY, DEBCL, Bcl-X_L and Bcl-2.

6.2 BUFFY and DEBCL physically interact

The mode of action of the Bcl-2 family of proteins is thought to depend upon the formation of proapoptotic dimers on the mitochondrial outer membrane, causing cytochrome c release and caspase activation, and the prevention of homodimer formation by the prosurvival Bcl-2 homologues (section 1.7). Prosurvival Bcl-2 homologues commonly have a BH4 domain in addition to the BH1-3 domains shared by their proapoptotic counterparts. Alignment of the protein sequences of BUFFY and DEBCL showed a high degree of homology between these two proteins. Both BUFFY and DEBCL are most similar to the proapoptotic Bcl-2 homologue in mammals, Bok (figure 6.1).

DEBCL has been shown to interact with mammalian prosurvival Bcl-2 homologues (Colussi *et al.,* 2000) and associates physically with BUFFY in mammalian cells (Quinn *et al.,* 2003). To determine whether BUFFY and DEBCL physically interact in insect cells, constructs expressing HA-tagged DEBCL and FLAG-tagged BUFFY were co-transfected into *Drosophila* BG2 cells. DEBCL and BUFFY coimmunoprecipitated in these cells. Interestingly, individual BH3 domain mutations in DEBCL did not alter the interaction between these two proteins (figure 6.2 A). Coexpression of EGFP-BUFFY and $_{HA}$DEBCL in NIH3T3 cells demonstrated that these two molecules colocalise when overexpressed in cells (figure 6.2 B). Expression was similar to that of BUFFY alone (section 6.4) suggesting that DEBCL localisation was altered by coexpression with BUFFY.

6.3 BUFFY and DEBCL induce cell death in cultured cells

Insect constructs expressing BUFFY, DEBCL and various mutants were transfected into BG2 cells together with the reporter plasmid pIE-LacZ. To determine the effect of BUFFY overexpression on cell viability, transfected cells were fixed and stained with X-gal. A fixed number of fields of view were scored in each case and the number of β-galactosidase

Figure 6.1 Amino acid alignment of BUFFY, DEBCL and Bok

The two Bcl-2 homologues in *Drosophila*, BUFFY and DEBCL, are most similar to the mammalian proapoptotic Bcl-2 homologue, Bok. The amino acid alignment shows the conserved Bcl-2 homology (BH) domains, BH1-BH3, and the C-terminal hydrophobic membrane anchor (MA) characteristic of these molecules. Identical residues shared by all molecules are highlighted in black and similar residues in grey.

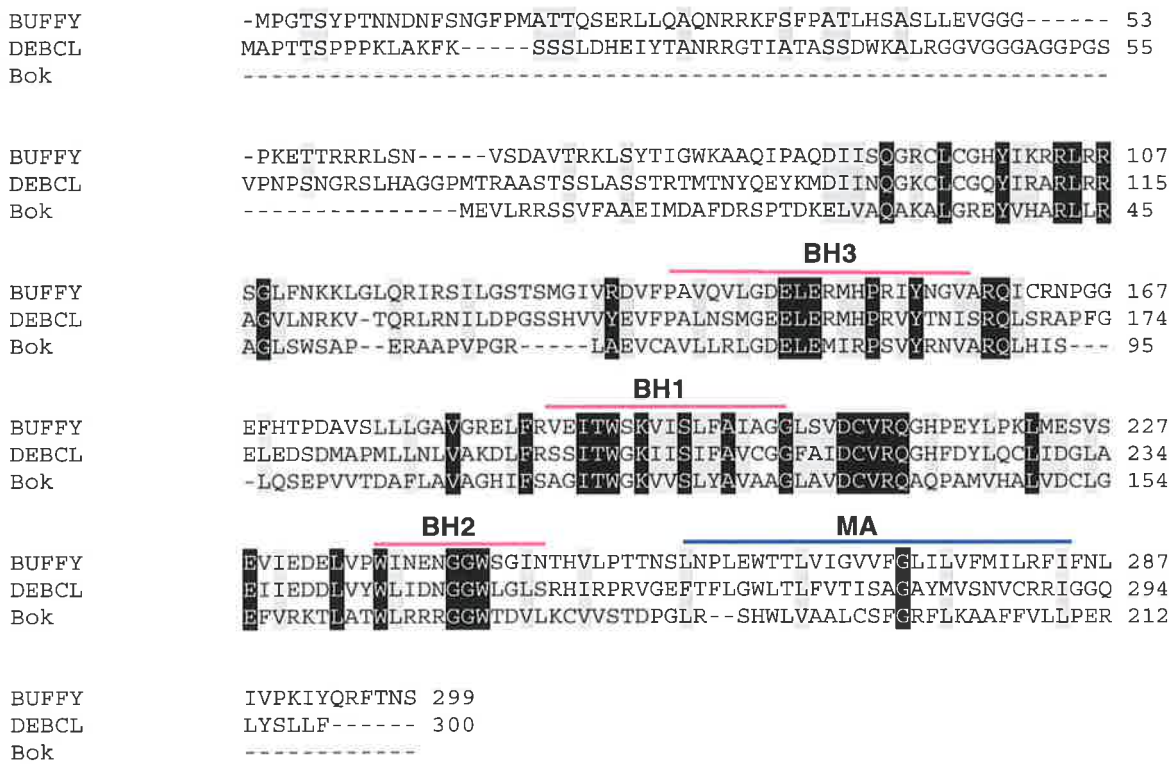
BUFFY -MPGTSYPTNNDNFSNGFPMATTQSERLLQAQNRRKFSFPATLHSASLLEVGGG------ 53
DEBCL MAPTTSPPPKLAKFK-----SSSLDHEIYTANRRGTIATASSDWKALRGGVGGGAGGPGS 55
Bok ----------
BUFFY -PKETTRRRLSN-----VSDAVTRKLSYTIGWKAAQIPAQDIISQGRCLCGHYIKRRLRR 107
DEBCL VPNPSNGRSLHAGGPMTRAASTSSLASSTRTMTNYQEYKMDIINQGKCLCGQYIRARLRR 115
Bok ---------------MEVLRRSSVFAAEIMDAFDRSPTDKELVAQAKALGREYVHARLLR 45
BH3
BUFFY SGLFNKKLGLQRIRSILGSTSMGIVRDVFPAVQVLGDELERMHPRIYNGVARQICRNPGG 167
DEBCL AGVLNRKV-TQRLRNILDPGSSHVVYEVFPALNSMGEELERMHPRVYTNISRQLSRAPFG 174
Bok AGLSWSAP--ERAAPVPGR-----LAEVCAVLLRLGDELEMIRPSVYRNVARQLHIS--- 95
BH1
BUFFY EFHTPDAVSLLLGAVGRELFRVEITWSKVISLFAIAGGLSVDCVRQGHPEYLPKLMESVS 227
DEBCL ELEDSDMAPMLLNLVAKDLFRSSITWGKIISIFAVCGGFAIDCVRQGHFDYLQCLIDGLA 234
Bok -LQSEPVVTDAFLAVAGHIFSAGITWGKVVSLYAVAAGLAVDCVRQAQPAMVHALVDCLG 154
BH2
MA
BUFFY EVIEDELVPWINENGGWSGINTHVLPTTNSLNPLEWTTLVIGVVFGLILVFMILRFIFNL 287
DEBCL EIIEDDLVYWLIDNGGWLGLSRHIRPRVGEFTFLGWLTLFVTISAGAYMVSNVCRRIGGQ 294
Bok EFVRKTLATWLRRRGGWTDVLKCVVSTDPGLR--SHWLVAALCSFGRFLKAAFFVLLPER 212
BUFFY IVPKIYQRFTNS 299
DEBCL LYSLLF------ 300
Bok ------------

Figure 6.2 BUFFY and DEBCL interact

A HA-tagged DEBCL and FLAG-tagged BUFFY were coexpressed in *Drosophila* BG2 cells. Expression was confirmed by direct Western blotting of lysates prior to immunoprecipitation (bottom two panels). Various mutants were also tested for interaction. Two individual amino acid substitutions in the BH3 domain of DEBCL, L/G and E/G, are indicated. mBUFFY denotes a mutant version of BUFFY in which the BH3 domain possesses three amino acid changes. mBUFFY is not expressed well in this experiment. Immunoprecipitation with α-HA antibody and Western blotting with α-FLAG detects BUFFY in immunocomplexes with DEBCL and both DEBCL BH3 domains mutants, but not with vector alone. Immunoprecipitation with α-FLAG followed by α-HA immunoblotting pulls down DEBCL with both wildtype BUFFY and mBUFFY. IgG bands are indicated. **B.** BUFFY and DEBCL colocalise in NIH3T3 cells. EGFP-BUFFY was coexpressed with $_{HA}$DEBCL in NIH3T3 cells. Cells were stained for DEBCL expression with α-HA, followed by α-rat Alexa Fluor® 568**.** Fluorescence was analysed by microscopy and captured digitally.

A

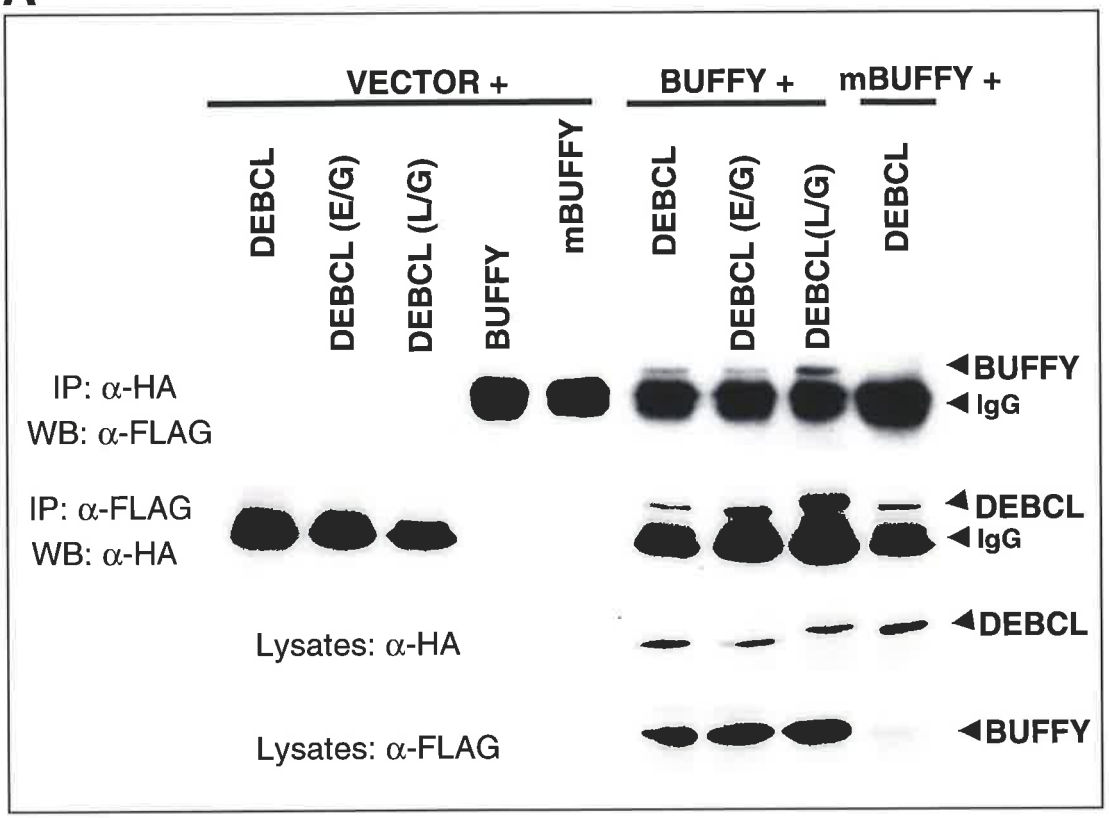
VECTOR +
BUFFY +
mBUFFY +
DEBCL
DEBCL (E/G)
DEBCL (L/G)
BUFFY
mBUFFY
DEBCL
DEBCL (E/G)
DEBCL(L/G)
DEBCL
IP: α-HA
WB: α-FLAG
BUFFY
IgG
IP: α-FLAG
WB: α-HA
DEBCL
IgG
Lysates: α-HA
DEBCL
Lysates: α-FLAG
BUFFY

B

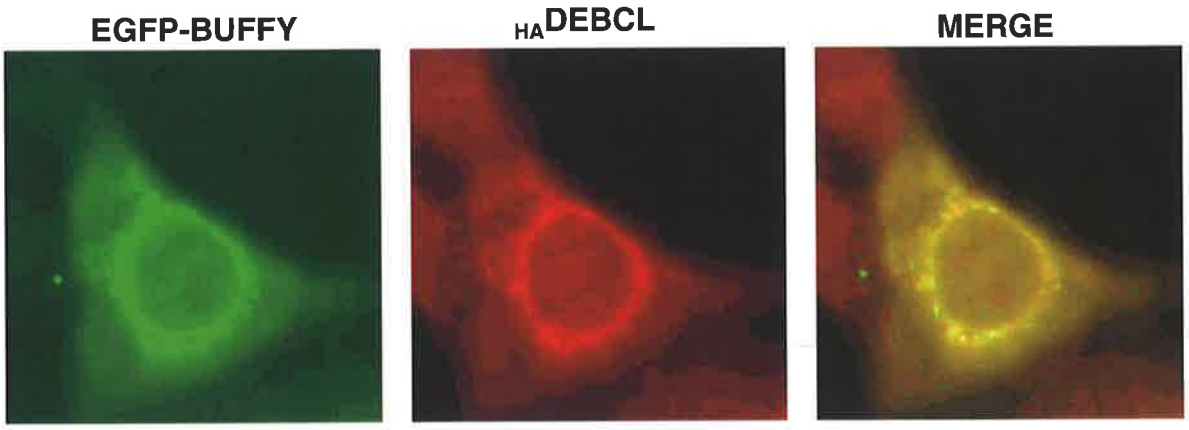
EGFP-BUFFY
HADEBCL
MERGE

positive (β-gal$^+$) cells were counted. Cell survival was calculated by comparing the number of β-gal$^+$ cells in test transfections, with the number scored for the vector control. As expected, DEBCL was able to induce cell death efficiently. Surprisingly, BUFFY also induced cell death in BG2 cells to a similar extent as DEBCL. Coexpression of both BUFFY and DEBCL in the same cells enhanced the cell killing effect (figure 6.3 A). Overexpression of a mutant version of BUFFY lacking the hydrophobic membrane anchor had no effect on cell viability whereas a BH3 domain mutant still induced apoptosis. This result demonstrates that the membrane anchor is required for BUFFY proapoptotic activity, probably indirectly by targeting the protein to the correct site of action. The enhancement of cell death when both DEBCL and BUFFY were coexpressed in cells suggests that these two molecules may act in concert.

To test whether cell death induced by BUFFY and DEBCL can be suppressed by treatment with zVAD-fmk, the death assay described above was repeated, and cells treated with the caspase inhibitor. Cell death induced by DEBCL was suppressed by treatment with zVAD-fmk (figure 6.3 B), whereas BUFFY-induced cell death was only slightly suppressed. Interestingly, overexpression of both BUFFY and DEBCL rendered cells insensitive to zVAD-fmk treatment.

6.4 BUFFY localises to the endoplasmic reticulum in transfected cells

To determine the intracellular localisation of BUFFY in transfected cells, pcDNA3-$_{HA}$BUFFY was expressed in COS cells. 24 hours after transfection, cells were immunostained prior to analysis by confocal microscopy (figure 6.4 A). Cells expressing BUFFY demonstrated intense perinuclear staining with punctate staining in the cytoplasm, that colocalised with the ER marker, Calnexin. Expression of $_{FLAG}$BUFFY in BG2 and SL2 insect cells followed by staining with α-FLAG and α-mouseFITC demonstrated the same perinuclear localisation (figure 6.4 B).

Figure 6.3 BUFFY and DEBCL induce cell death when overexpressed in cultured cells

A BG2 cells were transfected with 0.5μg pIE-LacZ reporter plasmid, together with 1.5μg of each construct as indicated. 24 hours later, cells were fixed and stained with X-gal as described in section 2.10.2. BUFFY and mBUFFY induce cell death significantly. In contrast, cell death is not induced by a BUFFY mutant lacking the C-terminal transmembrane anchor (ΔMA). DEBCL similarly induces apoptosis. Coexpression of both BUFFY and DEBCL increases the already potent cell death induced by each molecule alone. Results were gathered from three independent experiments performed in duplicate. Error bars represent ±SEM. **B** Death assays were performed as described above. Duplicate transfectants were treated with 50μM zVAD-fmk for 4 hours following transfection. DEBCL-induced cell death is significantly suppressed by zVAD-fmk, while only slight inhibition of BUFFY-induced death is observed. zVAD-fmk has little effect on cell death induced by coexpression of both BUFFY and DEBCL. Results obtained from two independent experiments performed in duplicate are respresented as colums ±SD.

A

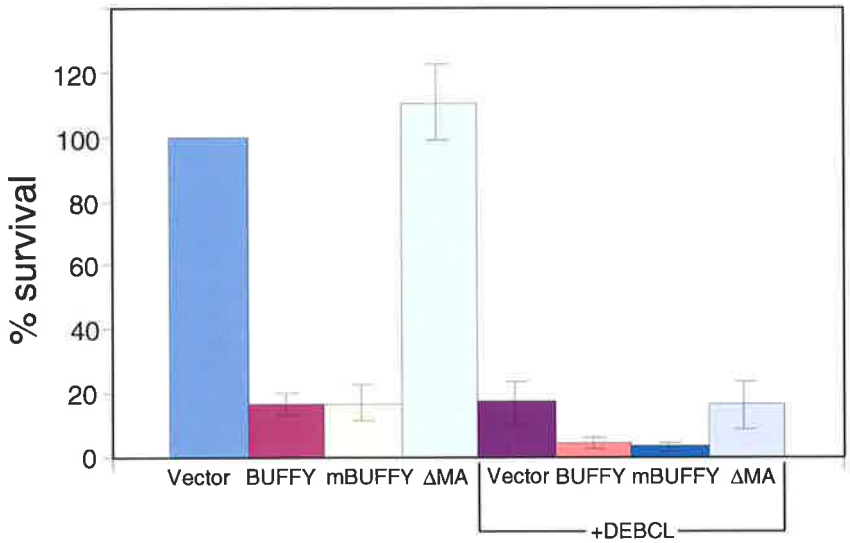
% survival
120
100
80
60
40
20
0
Vector
BUFFY
mBUFFY
ΔMA
Vector
BUFFY
mBUFFY
ΔMA
+DEBCL

B

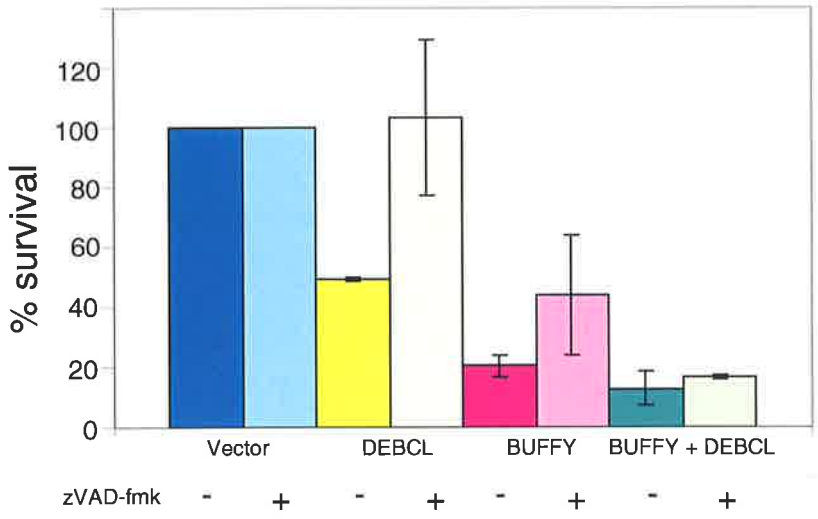
% survival
120
100
80
60
40
20
0
Vector
DEBCL
BUFFY
BUFFY + DEBCL
zVAD-fmk
-
+
-
+
-
+
-
+

Figure 6.4 BUFFY localises to the ER in transfected cells

A and **B** COS cells were transfected with pcDNA3-$_{HA}$BUFFY (section 2.8.1), fixed 24 hours later and incubated with α-HA antibody and α-mouseTXR as described in section 2.9. The ER was visualised by staining with α-Calnexin, followed by fluorescence with α-rabbit Alexa Fluor® 488. Cells were analysed by confocal microscopy (**A**). BUFFY colocalises with Calnexin in COS cells, demonstrating that BUFFY localises to the ER.

B Expression of transfected $_{FLAG}$BUFFY is shown in two insect lines, BG2 (top panel) and SL2 (bottom panel). Cells were transfected as described in section 2.8.2 and immunostained with α-FLAG as above. Nuclei were stained with Hoechst, demonstrating the absence of BUFFY in the nucleus.

A

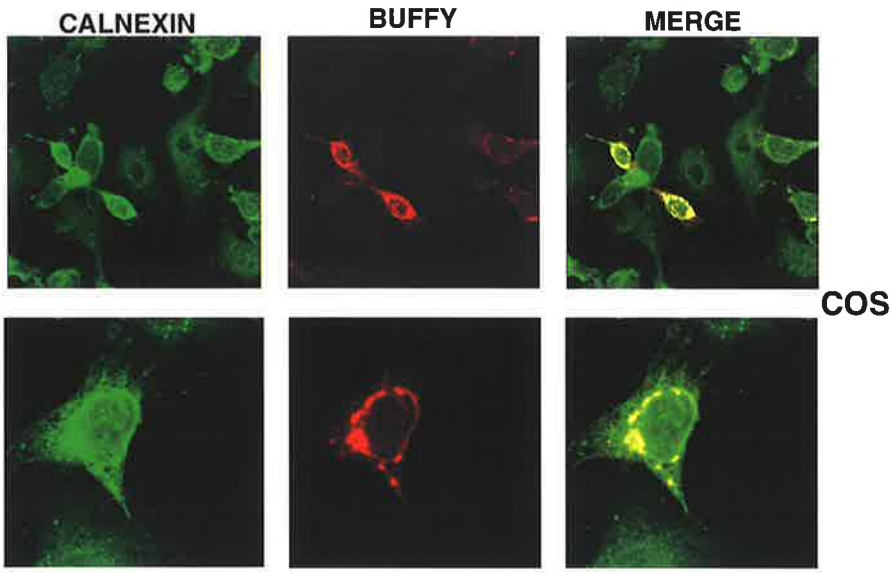

B

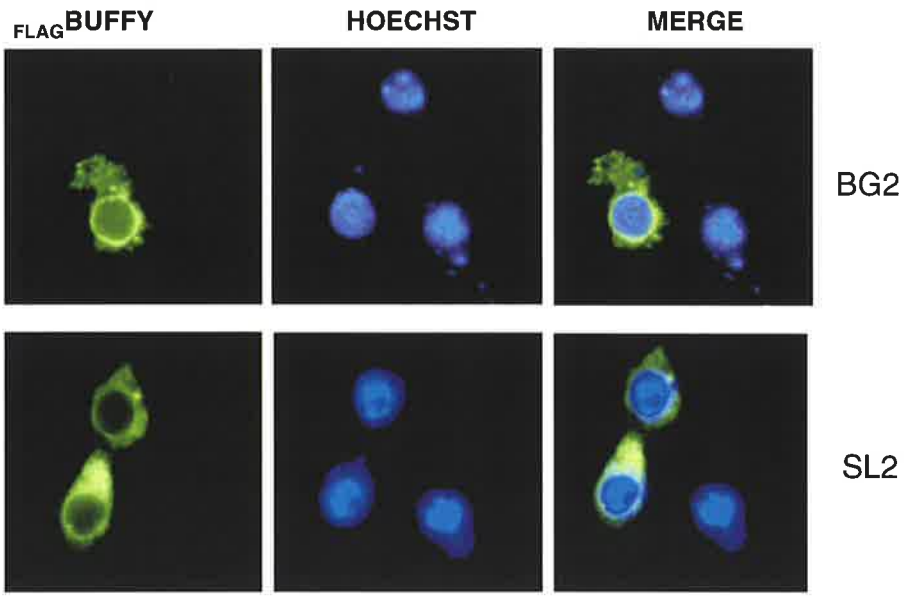

6.5 The transmembrane anchor is essential for BUFFY localisation

To demonstrate the importance of the C-terminal hydrophobic membrane anchor for the correct localisation of BUFFY, this domain was removed (BUFFYΔMA). pIE constructs expressing either full-length $_{FLAG}$BUFFY or $_{FLAG}$BUFFYΔMA were transfected into BG2 cells and stained with α-FLAG and α-mouseFITC antibodies. In contrast to the perinuclear and punctate cytoplasmic staining of wildtype $_{FLAG}$BUFFY, $_{FLAG}$BUFFYΔMA failed to localise to intracellular membranes and accumulated in the nucleus (figure 6.5 A). Crude fractionation of BG2 cells expressing $_{FLAG}$BUFFY or $_{FLAG}$BUFFYΔMA showed a shift in the fractions containing wildtype and truncated BUFFY (figure 6.5 B). Expression of EGFP-BUFFYΔMA in NIH3T3 cells and staining the ER with Calnexin clearly demonstrated the disruption of the normal ER localisation of BUFFY by removal of the membrane anchor (figure 6.5 C).

6.6 BUFFY contains a functional Nuclear Localisation Signal

To determine whether BUFFYΔMA accumulates in the nucleus by passive diffusion or by active targeting, the protein sequence of BUFFY was studied for the presence of a nuclear localisation signal (NLS). A string of five basic residues with an internal leucine residue presented as a possible NLS (figure 6.6 A). The first 118 amino acids of BUFFY, containing this putative NLS were fused to EGFP, subcloned into the pIE insect expression vector and transfected into SL2 cells (mutants presented schematically in figure 6.6 A). In this cell line, EGFP alone localised throughout the cell with a large proportion present in the nucleus. However, fusion of EGFP to aa1-118 of BUFFY (BUFFY1-118EGFP) eliminated the cytoplasmic EGFP fraction and shifted the localisation entirely to the nucleus, suggesting that this N-terminal region of BUFFY contains a functional NLS (figure 6.6 B).

To further investigate this possibility, BUFFY1-118 was also fused to the C-terminal region of the cytoplasmic caspase, STRICA. STRICA was chosen because it is known to localise to the cytoplasm, and restriction sites were compatible for construction of an in-frame

Figure 6.5 BUFFY localisation requires the C-terminal membrane anchor

A BG2 cells were transfected with either pIE-$_{FLAG}$BUFFY or pIE-$_{FLAG}$BUFFYΔMA. 24 hours post-transfection, cells were stained with α-FLAG and α-mouseFITC. Deletion of the membrane anchor completely disrupts the localisation of BUFFY, and results in protein accumulation in the nucleus. **B** Crude fractions were prepared from transfected BG2 cells. BUFFY is expressed at lower levels than BUFFYΔMA due to BUFFY-induced apoptosis. P1 represents the pellet fraction containing undisrupted cells and nuclei. The heavy membrane (HM) fraction contains mitochondria and intact golgi, the light membrane (LM) fraction contains ER and golgi membranes and S-100 is the soluble fraction of the cell. While BUFFY is shown to be ER-localised, it associates with the HM in crude fractions. BUFFYΔMA demonstrates a different fractionation pattern with a high proportion of the protein in the nuclei (P1) fraction as well as some association with the LM fraction.

C Confocal images demonstrate the exclusive nuclear localisation of EGFP-BUFFYΔMA in NIH3T3 cells.

A

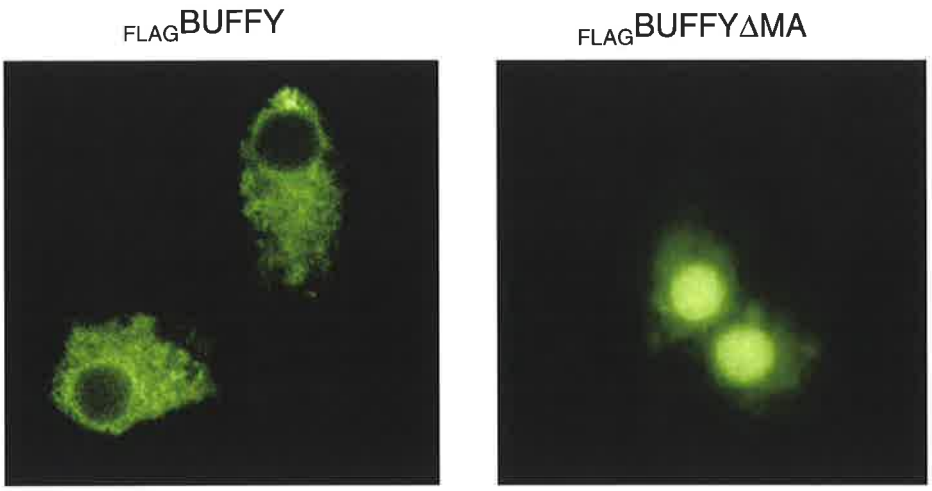
FLAGBUFFY
FLAGBUFFYΔMA

B

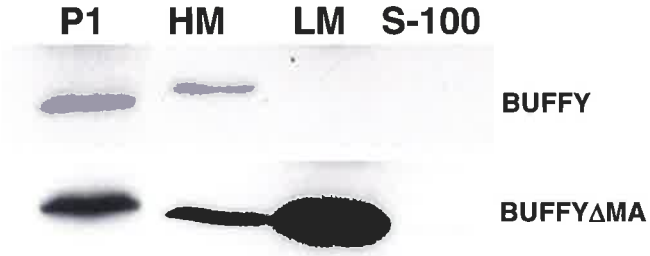
P1
HM
LM
S-100
BUFFY
BUFFYΔMA

C

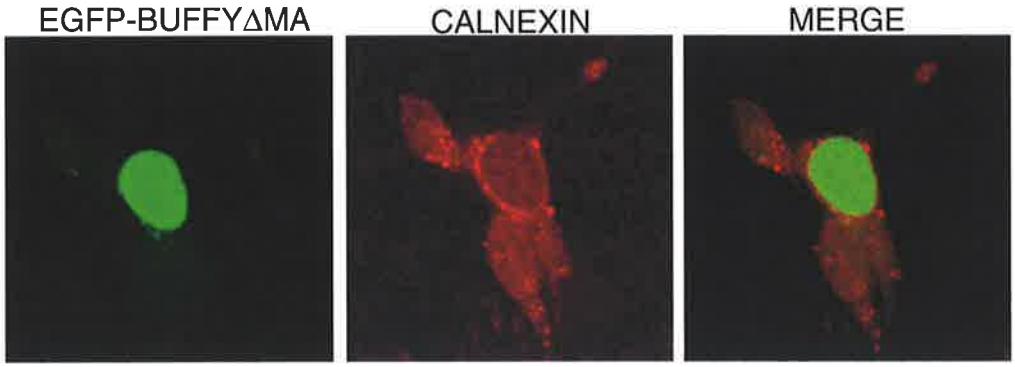
EGFP-BUFFYΔMA
CALNEXIN
MERGE

Figure 6.6 The N-terminal 118 amino acids of BUFFY can target protein to the nucleus

A Shematic representation of constructs used to demonstrate the ability of the N-terminal 118 amino acids of BUFFY to target heterologous proteins to the nucleus. All constructs were cloned in the pIE1.4 insect vector as described in Materials and Methods (section 2.5.3). Full-length, wildtype BUFFY is shown at the top. Wildtype sequence, KRRLRR, was mutated to AAALRR as indicated. With the exception of EGFP and Buf1-118EGFP, all constructs were tagged with FLAG epitope at the N-terminus. **B** SL2 cells were transfected with pIE-EGFP or pIE-Buf1-118EGFP as indicated. A significant proportion of EGFP localises to the nucleus, with a fraction present in the cytosol, diffusely localised. Fusion of the N-terminal 118 amino acids of BUFFY to EGFP eliminates the cytosolic proportion of EGFP, localising exclusively to the nucleus. **C** A fusion between the N-terminal 118 amino acids of BUFFY with the C terminal region of STRICA was expressed in *Drosophila* SL2 cells. The putative nuclear localisation signal (NLS) within this region was mutated in this fusion molecule and also expressed in cells. Mutation of the NLS results in diffuse localisation throughout the cell (bottom panel), compared with the limited cytosolic localisation in the wildtype NLS fusion (top panel). **D** The constructs expressed in C were also expressed in BG2 cells and nuclei stained with Hoechst to demonstrate the loss of nuclear localisation by mutation of the NLS.

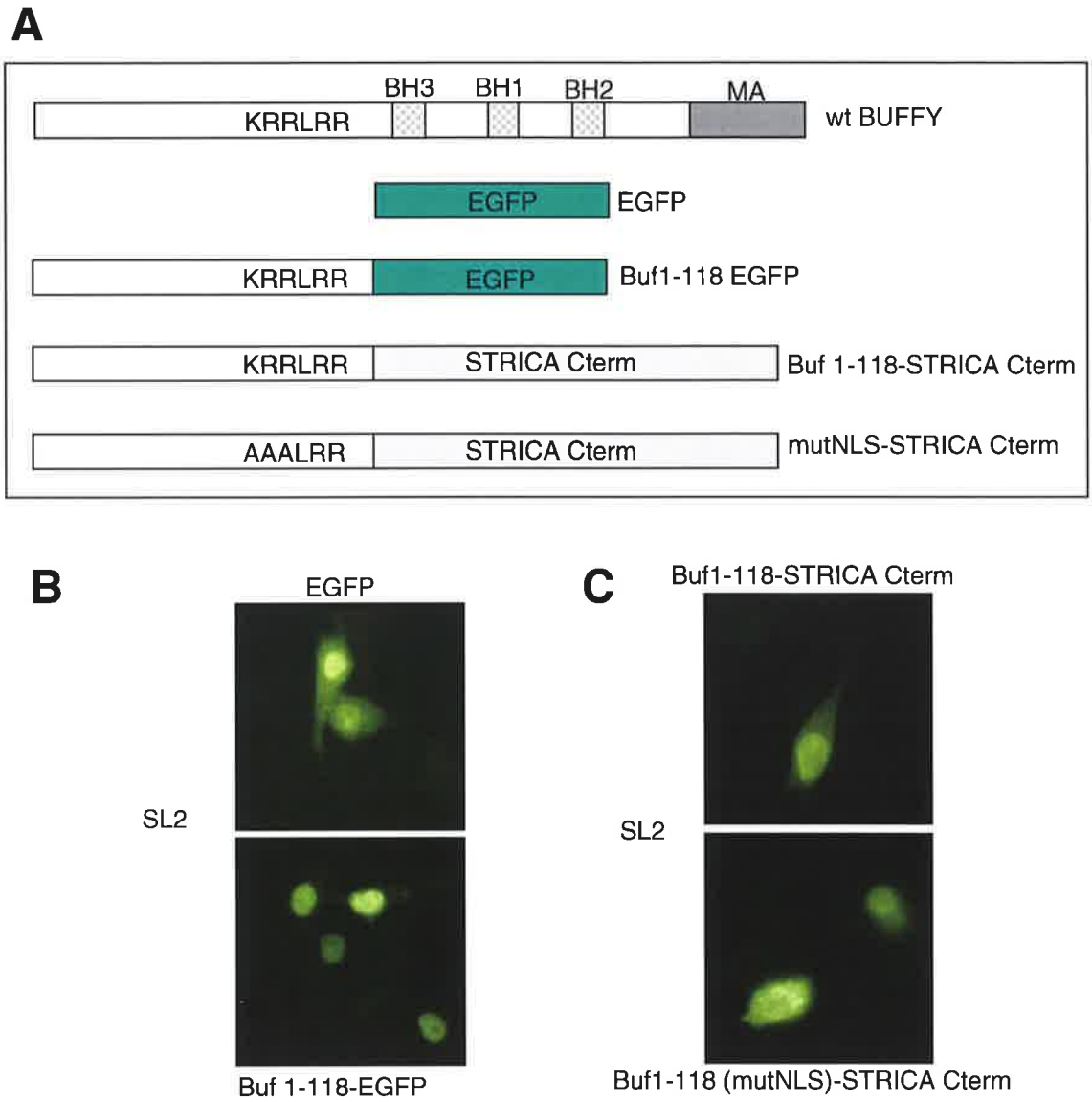
A
BH3
BH1
BH2
MA
KRRLRR
wt BUFFY
EGFP
EGFP
KRRLRR
EGFP
Buf1-118 EGFP
KRRLRR
STRICA Cterm
Buf 1-118-STRICA Cterm
AAALRR
STRICA Cterm
mutNLS-STRICA Cterm
B
EGFP
SL2
Buf 1-118-EGFP
C
Buf1-118-STRICA Cterm
SL2
Buf1-118 (mutNLS)-STRICA Cterm
D
FLAG
HOECHST
MERGE
Buf1-118
STRICA
Cterm
mutNLS-
STRICA
Cterm

fusion protein. This chimeric molecule localised predominantly to the nucleus in both BG2 and SL2 insect cell lines. However, mutation of three of the basic residues in the putative NLS to alanine (KRRLRR to AAALRR) caused a shift in localisation spreading into the cytosol (figure 6.6 C and 6.6 D).

In NIH3T3 cells, EGFP-BUFFYΔMA localised exclusively to the nucleus in a similar fashion to localisation in insect cells. When the putative NLS was mutated in EGFP-BUFFYΔMA (shown schematically in figure 6.7 A), the localisation was significantly disrupted (figure 6.7 B). Together, these results suggest that BUFFY contains a functional NLS in the N-terminal region of the protein that is able to target BUFFYΔMA to the nucleus. This raises the possibility that in some contexts, post-translational modifications may result in the targeting of BUFFY to the nucleus.

6.7 DEBCL contains a MOM-targeting sequence while BUFFY does not

A study carried out by Kaufmann *et al.* (2003) identified residues flanking the C-terminal transmembrane domain (TMB) in Bcl-X_L that are required for targeting Bcl-X_L to the mitochondrial outer membrane (MOM). Comparison between the MOM-targeting sequence of Bcl-X_L with other known mitochondrially-targeted proteins led Kaufmann *et al.* to identify a consensus for MOM targeting. The consensus for mitochondrial outer membrane-targeting is $\mathbf{B}x_{0\text{-}9}\mathbf{B}x_{0\text{-}2}$ TMB $x_{0\text{-}1}\mathbf{B}x_{0\text{-}6}\mathbf{B}$ where B is a basic residue such as arginine (R) or lysine (K) and TMB represents the transmembrane domain (figure 6.8 A). In the absence of such a targeting sequence, transmembrane domain-containing proteins distribute to other membranes including the ER.

As shown in figure 6.4, BUFFY localises to the ER in transiently transfected cells. In contrast, DEBCL has been shown to be localised to the MOM (Igaki *et al.*, 2000). Analysis of the C-terminal residues in BUFFY and DEBCL led to the commencement of a comparative study to determine whether similar charges are responsible for the differential localisation of BUFFY and DEBCL. Comparison of DEBCL with Bcl-X_L showed that the X domain

Figure 6.7 The putative NLS in BUFFY is functional

A Schematic representation of the BUFFY constructs for expression in NIH3T3 cells. EGFP-BUFFYΔMA differs from EGFP-BUFFYΔMA (mutNLS) by 3 amino acid substitutions in the putative N-terminal NLS in BUFFY. **B** EGFP-BUFFYΔMA in NIH3T3 cells localises exclusively to the nucleus. Mutation of the NLS in EGFP-BUFFYΔMA (mutNLS) still has a fraction of protein present in the nucleus but expression shifts to include the cytoplasm of the cell, demonstrating that the amino acid changes prevent the targeting of protein to the nucleus.

A

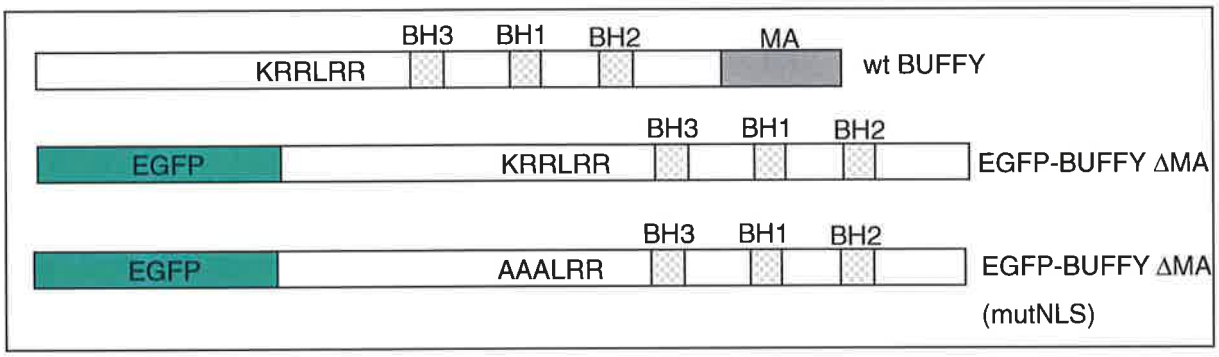

B

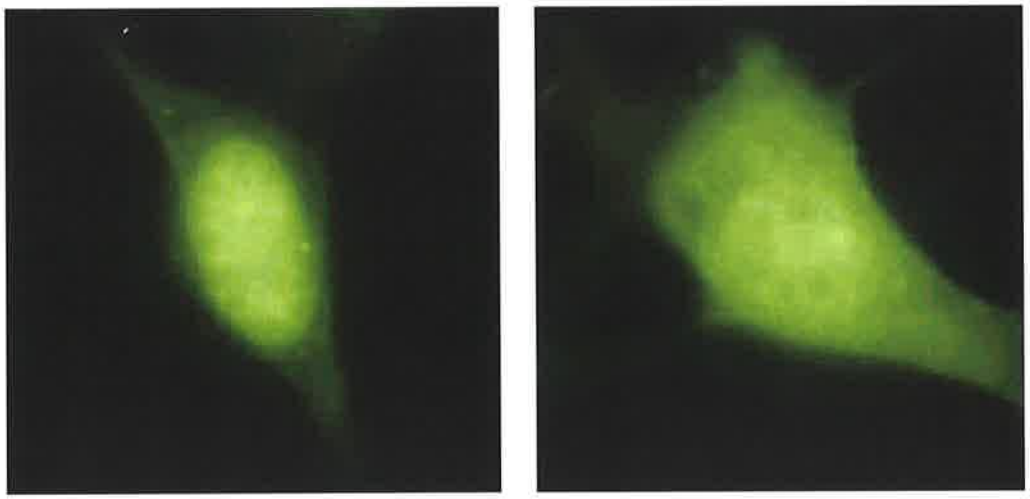

EGFP-BUFFY ΔMA

EGFP-BUFFY ΔMA (mutNLS)

Figure 6.8 Comparison of the C-terminal transmembrane domains of Bcl-X_L, Bcl-2, DEBCL and BUFFY.

Results published by Kaufmann *et al.* (2003), identified various amino acid differences in the transmembrane flanking regions of Bcl-X_L and Bcl-2 reponsible for the differential intracellular targeting of these two Bcl-2 homologues. The X domain describes the region in Bcl- X_L that possesses various positive charges absent in Bcl-2. The corresponding region in Bcl-2 is denoted as the X/2 domain. The basic (B) domain in Bcl- X_L represents the two basic charges at the C-terminal end of the transmembrane domain (TMB). The consensus for mitochondrial outer membrane (MOM)-targeting is shown in the boxed section. Analysis of the amino acid sequences in BUFFY and DEBCL show that DEBCL contains residues required for MOM-targeting while these residues are lacking in BUFFY.

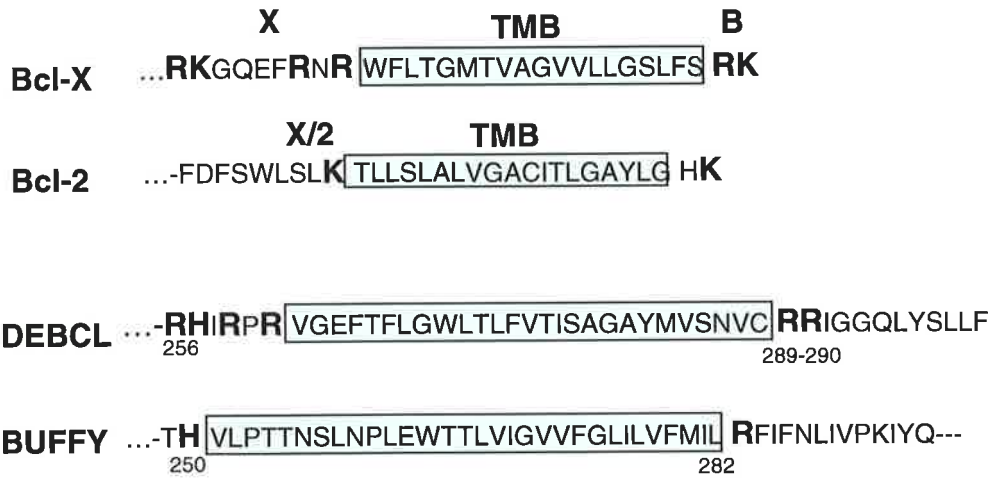

Consensus for MOM-targeted proteins

$BX_{0-9}BX_{0-2}$ **TMB** $X_{0-1}BX_{0-6}B$

conforms to the consensus, with two positively charged arginine residues in both proteins, N-terminal to the hydrophobic TMB (figure 6.8). Additionally, Bcl- X_L and DEBCL each possess a double positive charge at the C terminus of the membrane anchor. Bcl-2 and BUFFY, on the other hand, lack such strong positive charges (figure 6.8) allowing for localisation to other intracellular membranes. Thus, at the amino acid level, the residues required for MOM-targeting are conserved between Bcl- X_L and DEBCL, and are lacking in Bcl-2 and BUFFY.

6.8 EGFP-BUFFY and EGFP-DEBCL localise appropriately in cultured cells

In order to carry out a comparative study, *buffy* and *debcl* were cloned into pEGFP-c2 vector, fusing EGFP to the N-terminus of each protein. The presence of a tag at the C-terminus of membrane anchor-containing proteins is unsuitable, resulting in protein mislocalisation, even with short tags such as FLAG (Kaufmann *et al.*, 2003). A series of mutants were subsequently made by site-directed PCR mutagenesis (presented schematically in figure 6.9 A). Various Bcl-X_L and Bcl-2 constructs, including several mutants, were used as comparative controls (figure 6.9 B). NIH3T3 cells were selected for this study for several reasons: firstly, these cells are strongly adherent and remain attached to glass coverslips throughout the washing steps of immunostaining. Secondly, NIH3T3 cells are flat, with a large cytoplasmic area, well suited for the assessment of intracellular organelle structures. Lastly, by comparison with insect cells, NIH3T3 cells are transfected with ease and are much larger in size, allowing for increased resolution by microscopy.

Cells on coverslips were transfected with pEGFP-BUFFY or pEGFP-DEBCL. 24 hours later, cells were fixed and costained with α-Calnexin antibody as described in Materials and Methods (section 2.9). As expected, EGFP-BUFFY colocalised with Calnexin (figure 6.10 A) and EGFP-DEBCL colocalised with Mitotracker Red (figure 6.10 B) confirming that DEBCL is targeted to the MOM while BUFFY localises to the nuclear envelope and ER membranes.

Figure 6.9 Expression constructs for a comparative study of the differential localisation of BUFFY and DEBCL.

Schematic representation of constructs used. **A** Wildtype, full-length BUFFY and DEBCL were cloned into pEGFPc2. Various mutants were made by site-directed PCR mutagenesis as indicated. **B** Various constructs provided by Prof. Christoph Borner are shown. Basic residues are shown in bold and mutant residues are underlined.

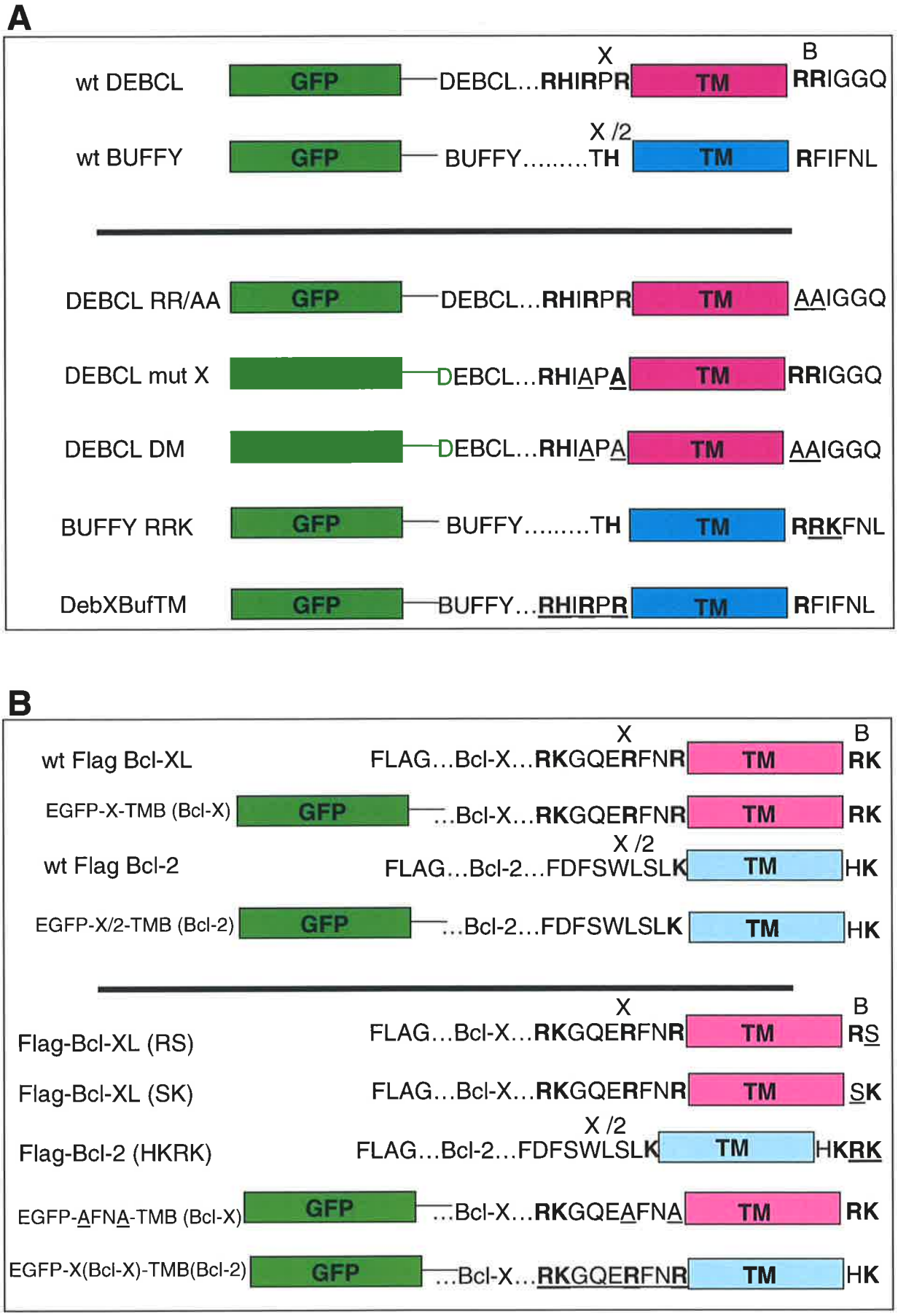
A
X
B
wt DEBCL
GFP
DEBCL…RHIRPR
TM
RRIGGQ
X /2
wt BUFFY
GFP
BUFFY……TH
TM
RFIFNL
DEBCL RR/AA
GFP
DEBCL…RHIRPR
TM
AAIGGQ
DEBCL mut X
DEBCL…RHIAPA
TM
RRIGGQ
DEBCL DM
DEBCL…RHIAPA
TM
AAIGGQ
BUFFY RRK
GFP
BUFFY……TH
TM
RRKFNL
DebXBufTM
GFP
BUFFY…RHIRPR
TM
RFIFNL
B
X
B
wt Flag Bcl-XL
FLAG…Bcl-X…RKGQERFNR
TM
RK
EGFP-X-TMB (Bcl-X)
GFP
…Bcl-X…RKGQERFNR
TM
RK
X /2
wt Flag Bcl-2
FLAG…Bcl-2…FDFSWLSLK
TM
HK
EGFP-X/2-TMB (Bcl-2)
GFP
…Bcl-2…FDFSWLSLK
TM
HK
X
B
Flag-Bcl-XL (RS)
FLAG…Bcl-X…RKGQERFNR
TM
RS
Flag-Bcl-XL (SK)
FLAG…Bcl-X…RKGQERFNR
TM
SK
X /2
Flag-Bcl-2 (HKRK)
FLAG…Bcl-2…FDFSWLSLK
TM
HKRK
EGFP-AFNA-TMB (Bcl-X)
GFP
…Bcl-X…RKGQEAFNA
TM
RK
EGFP-X(Bcl-X)-TMB(Bcl-2)
GFP
…Bcl-X…RKGQERFNR
TM
HK

Figure 6.10 Expression of EGFP-BUFFY and EGFP-DEBCL in NIH3T3 cells

NIH3T3 cells were transfected with either EGFP-BUFFY (**A**) or EGFP-DEBCL (**B**) EGFP-BUFFY-expressing cells were costained with Calnexin, demonstrating that BUFFY localises to the ER in transfected NIH3T3 cells (**A**). EGFP-DEBCL-expressing cells were costained with Mitotracker Red, demonstrating that DEBCL localises to mitochondria in transfected cells (**B**).

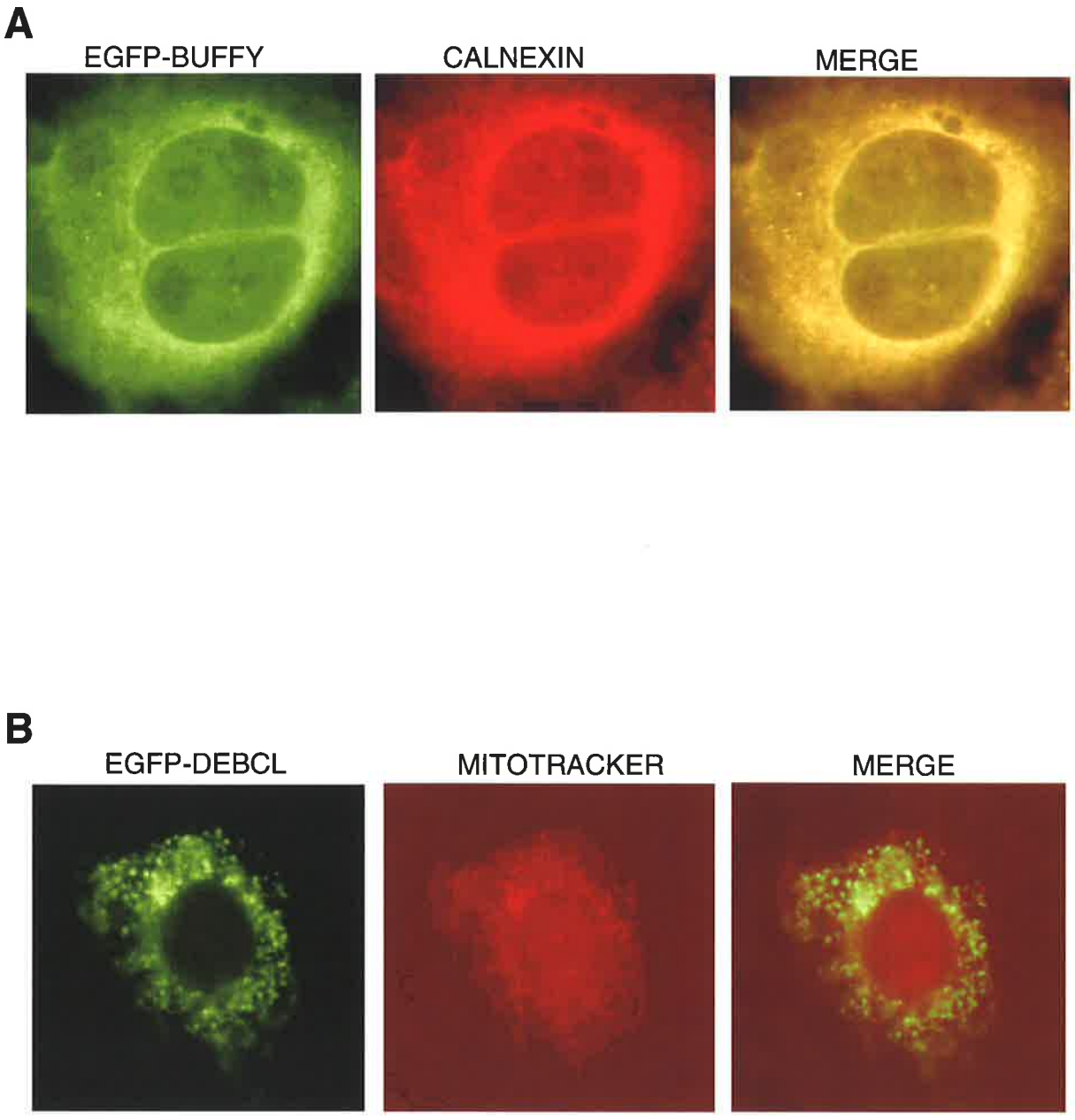
A
EGFP-BUFFY
CALNEXIN
MERGE
B
EGFP-DEBCL
MITOTRACKER
MERGE

6.9 Positive charges flanking the TMB of DEBCL are required for MOM-targeting

To test whether Bcl-X_L control constructs localise in NIH3T3 cells according to reported data (Kaufmann *et al.,* 2003), constructs were transfected into cells. The minimal region required for targeting to the MOM included the X domain and TMB. pEGFP-X-TMB(Bcl-X_L) effectively targeted to mitochondria and colocalised with cytochrome c (figure 6.11 A). Of the four arginine residues in the X domain of Bcl-X_L, the two closest to the TMB were shown to be sufficient for MOM targeting (Kaufmann *et al.,* 2003). Mutation of these two basic residues in the X domain of Bcl-X_L to alanine (EGFP-AFNA-TMB(Bcl-X_L)) resulted in loss of MOM targeting (Kaufmann *et al.*, 2003). However, using NIH3T3 cells, this mutant construct did not significantly mislocalise the protein, with most expressing cells costaining with cytochrome c (figure 6.11 B). On the other hand, mutation of the C-terminal-most arginine residues (B domain) had a profound effect on Bcl-X_L localisation. In this case, mutation of one or the other arginine residues in a FLAG-tagged version of Bcl-X_L resulted in diffuse cytoplasmic staining and perinuclear localisation similar to Bcl-2 (figure 6.11 C). Thus, the C-terminal B domain, containing two positive charges in Bcl-X_L, plays a crucial role in targeting Bcl-X_L to mitochondrial membranes, whereas positive charges in the X domain have lesser effect.

Expression of EGFP-DEBCL and staining for cytochrome c demonstrates that EGFP-DEBCL is mitochondrially localised (figure 6.12 A). Mutation of two positively charged arginine residues to alanines in the X domain of DEBCL (EGFP-DEBCL mut X) did not significantly disrupt the localisation of the protein (figure 6.12 B), whereas some disruption was observed in a mutant version where the two C-terminal arginines were mutated (EGFP-DEBCL RR/AA [figure 6.12 C]). Despite each of these mutant versions of DEBCL having little effect on the mitochondrial localisation of the molecule, mutation of both the X domain and C-terminal charges (EGFP-DEBCL DM, where DM stands for double mutant), resulted in a more diffuse localisation pattern with an increase in perinuclear staining, compared with

Figure 6.11 Expression of various Bcl-X_L proteins in NIH3T3 cells

Various control constructs were obtained from Prof. Christoph Borner. The minimal region required for localisation of Bcl- X_L to the mitochondrial outer membrane was found to be X-TMB(Bcl-X_L) as shown scematically in figure 6.8. NIH3T3 cells were transfected with the indicated constructs. In the case of EGFP fusion proteins, cells were fixed and the mitochondria stained with an antibody against native cytochrome c and α-mouse Alexa Fluor®568 (red). FLAG-tagged constructs were immunostained with α-FLAG and α-mouse Alexa Fluor®488. EGFP-X-TMB(Bcl-X_L) localises to mitochondria, as shown by colocalisation with cytochrome c (**A**). Mutation of two basic charges to alanines in the X domain of Bcl-X_L does not significantly alter the localisation of Bcl-X_L in NIH3T3 cells (**B**). In contrast, C-terminal mutations drastically alter the localisation of Bcl-X_L compared to wildtype, with perinuclear localisation and diffuse cytoplasmic localisation observed (**C**). The Alexa Fluor ® 488 green is outside of the printing gamut and was substituted with a reproducible green in C only.

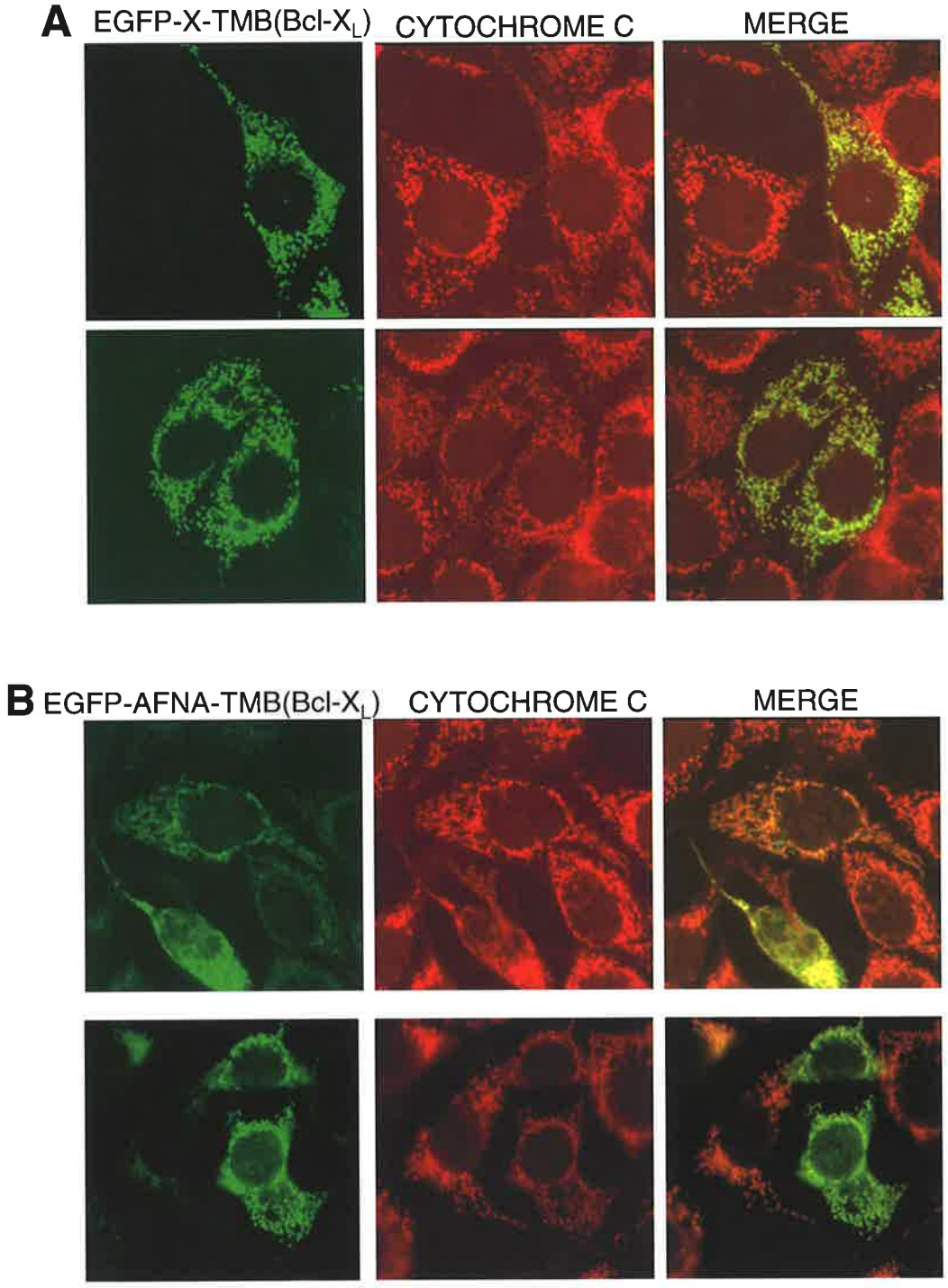
A
EGFP-X-TMB(Bcl-X$_L$)
CYTOCHROME C
MERGE
B
EGFP-AFNA-TMB(Bcl-X$_L$)
CYTOCHROME C
MERGE
C
FLAG-Bcl-X$_L$
FLAG- Bcl-X$_L$ (RS)
FLAG- Bcl-X$_L$ (SK)

Figure 6.12 Localisation of EGFP-DEBCL and mutants in NIH3T3 cells

NIH3T3 cells were transfected with pEGFP-DEBCL and stained with α-cytochrome c 24 hours later, demonstrating that DEBCL localises to mitochondria (**A**). Various DEBCL mutants were expressed as EGFP fusions in NIH3T3 cells and costained with cytochrome c. Mutation of two arginine residues to alanines in the DEBCL X domain (DEBCL mutX) does not strongly affect localisation with most of the protein still costaining with cytochrome c (**B**). DEBCL RR/AA exhibits slight mislocalisation with an increase in perinuclear localisation and more diffuse cytoplasmic staining (**C**). DEBCL DM (double mutant) possesses both mutX and RR/AA mutations and has a more severe effect on protein localisation (**D**), demonstrating that basic residues at either end of the TMB contribute to MOM-targeting of DEBCL in transfected cells.

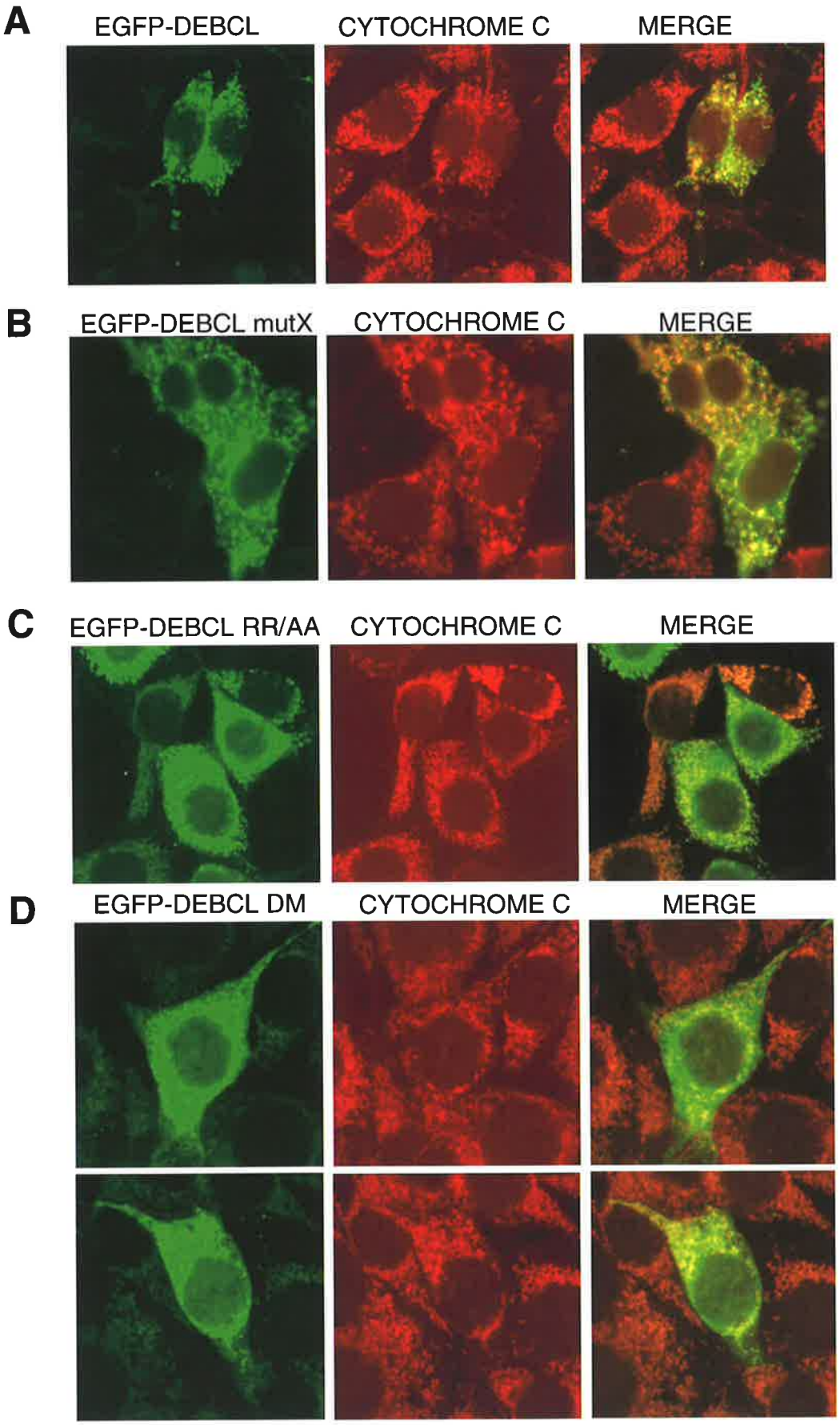
A
EGFP-DEBCL
CYTOCHROME C
MERGE
B
EGFP-DEBCL mutX
CYTOCHROME C
MERGE
C
EGFP-DEBCL RR/AA
CYTOCHROME C
MERGE
D
EGFP-DEBCL DM
CYTOCHROME C
MERGE

wildtype DEBCL (figure 6.12 D). This demonstrates that both the X domain and B domain contribute to DEBCL mitochondrial localisation.

6.10 Increasing C-terminal basicity in BUFFY alters its intracellular localisation

Bcl-2 has been shown to localise to membranes of the nuclear envelope and endoplasmic reticulum in addition to the mitochondrial outer membrane (Lithgow *et al.*, 1994). Control constructs were analysed together with novel BUFFY mutants constructed for the purpose of this study. A construct expressing EGFP fused to half of the X domain (X/2) and TMB of Bcl-2 (EGFP-X/2-TMB(Bcl-2)) was expressed in NIH3T3 cells and costained for expression of the ER-specific marker, Calnexin. Although EGFP-X/2-TMB(Bcl-2) significantly colocalised with Calnexin and displayed perinuclear localisation consistent with the nuclear envelope, a significant proportion of expressed protein was observed in the cytoplasm in a punctate manner remininscent of mitochondria (figure 6.13 A). Replacement of the X/2 domain of Bcl-2 with the X domain of Bcl-X_L, disrupted the perinuclear staining observed in the wildtype, and increased the MOM-targeting of the protein (figure 6.13 B). Perinuclear staining was also lost when the C-terminal basicity of Bcl-2 was increased by the addition of arginine and lysine residues (figure 6.13 C), confirming the importance of a strong basic charge for mitochondrial localisation, the lack of which allows protein localisation to the nuclear envelope and ER.

Similar mutants were generated for BUFFY. EGFP-BUFFY largely colocalises with Calnexin in transfected NIH3T3 cells (figure 6.14 A). Increasing the basicity C-terminal to the membrane anchor had some effect on the perinuclear localisation of BUFFY, however an increase in the amount of diffuse cytoplasmic protein in the cell was observed (figure 6.14 B). Additionally, some cells exhibited diffuse staining throughout the cell, suggesting that the ability to target to membranes was lost entirely. Insertion of the X domain of DEBCL N-terminal to the transmembrane domain of BUFFY did not drastically alter protein localisation, however an increase in the punctate cytoplasmic localisation was observed (figure 6.14 C).

Figure 6.13 Expression of Bcl-2 controls in NIH3T3 cells

EGFP fused to X/2-TMB(Bcl-2) demonstrates perinuclear staining and colocalises with Calnexin. However a proportion of the fusion protein appears to localise to mitochondria and does not colocalise with Calnexin in the cytosol (**A**). Insertion of the X domain of Bcl-X_L results in a more pronounced pattern of mitochondrial localisation (**B**). Compared with a FLAG-Bcl-2 control, increasing the basicity at the C-terminal flank of the TMB of Bcl-2 (FLAG-Bcl-2 (HKRK) results in loss of perinuclear staining, similar to Bcl-X_L (**C**). For printing purposes, the EGFP and Alexa Fluor® 488 green was substituted with a reproducible green in B and C.

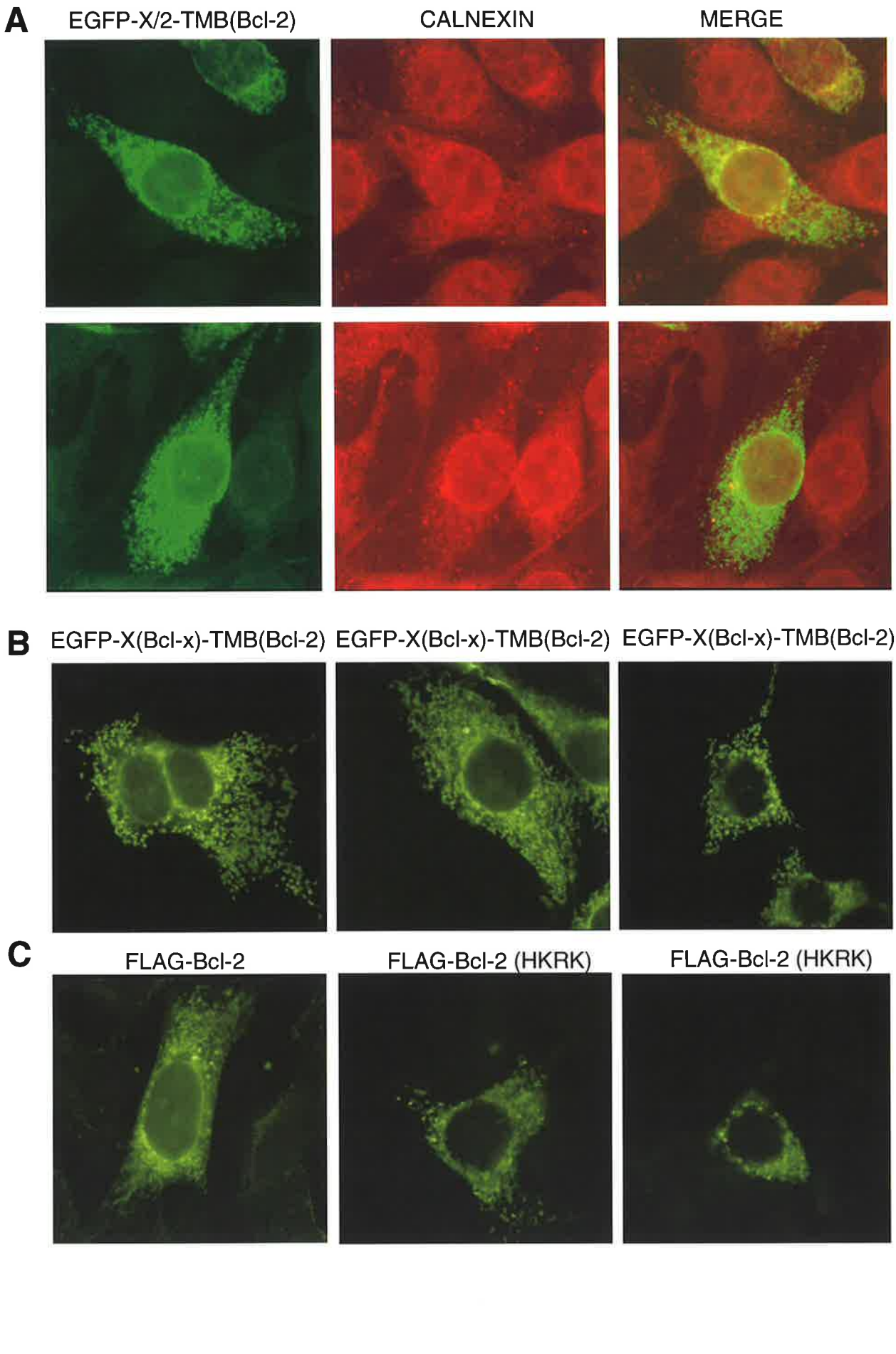
A
EGFP-X/2-TMB(Bcl-2)
CALNEXIN
MERGE
B
EGFP-X(Bcl-x)-TMB(Bcl-2)
EGFP-X(Bcl-x)-TMB(Bcl-2)
EGFP-X(Bcl-x)-TMB(Bcl-2)
C
FLAG-Bcl-2
FLAG-Bcl-2 (HKRK)
FLAG-Bcl-2 (HKRK)

Figure 6.14 Expression of BUFFY and mutants in NIH3T3 cells

EGFP-BUFFY colocalises with Calnexin in transfected cells (**A**). Increasing the basic charge at the end of the membrane anchor (EGFP-BUFFY RRK) increases the cytoplasmic localisation of the protein, while some cells mislocalise completely and accumulate protein in the nucleus (**B**). Insertion of the X domain of DEBCL has a moderate effect on BUFFY localisation. Perinuclear staining is preserved while punctate staining in the cytoplasm, indicative of mitochondrial localisation, increases (**C**). Confocal images are shown in C.

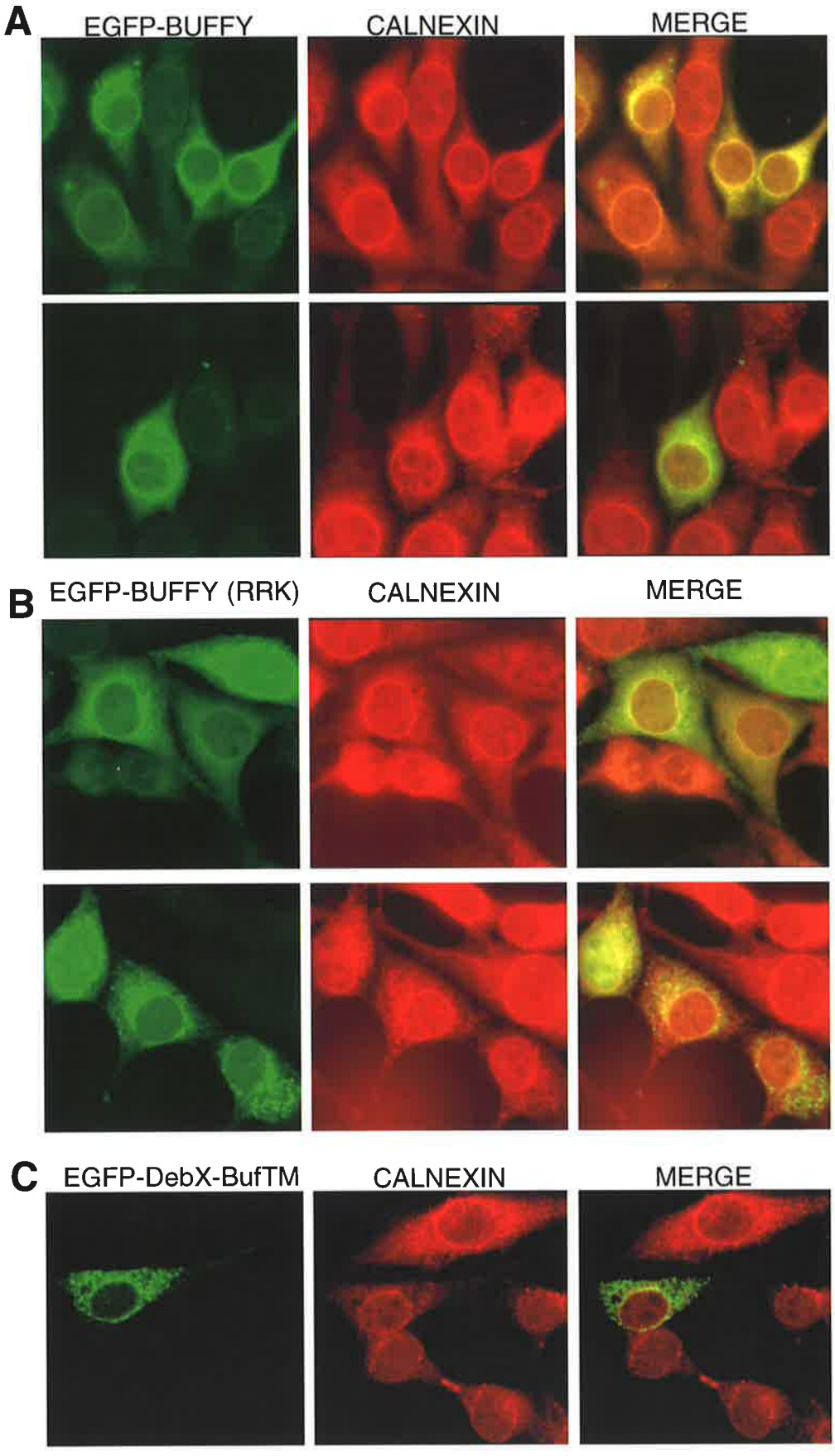
A
EGFP-BUFFY
CALNEXIN
MERGE
B
EGFP-BUFFY (RRK)
CALNEXIN
MERGE
C
EGFP-DebX-BufTM
CALNEXIN
MERGE

6.11 Discussion

At the commencement of this thesis, two Bcl-2 homologues had been identified in *Drosophila*, DEBCL and BUFFY (Igaki and Miura, 2003). DEBCL was characterised as a proapoptotic protein while the function of BUFFY remained to be investigated. The primary sequence of both BUFFY and DEBCL is most closely related to the proapoptotic mammalian Bcl-2 homologue Bok (figure 6.1). Despite findings that suggest that BUFFY is a prosurvival protein (Quinn *et al.,* 2003), the roles of both *Drosophila* Bcl-2 homologues remain to be fully elucidated.

The mammalian Bcl-2 family has over 20 members spanning three different groups, as discussed in section 1.7. In contrast, the *Drosophila* genome possesses only two Bcl-2 homologues (section 1.11.2). It is conceivable that, rather than functioning towards cell death or survival exclusively, BUFFY and DEBCL may function in both contexts, depending on a range of cellular cues and factors. Indeed, DEBCL reportedly protects cells from apoptosis induced by some death insults but not others (Brachmann *et al.,* 2000). Results presented in this chapter demonstrate that BUFFY overexpression in cultured *Drosophila* cells efficiently induces cell death, similar to DEBCL overexpression. This is in contrast to Bcl-2 that protects cells against apoptosis induced by various stimuli such as growth factor withdrawal, UV-irradiation and cytotoxic drug treatment when expressed in cell lines (Tsujimoto *et al.*, 1989; Allsop *et al.*, 1993; Vaux *et al.*, 1993; Walton *et al.*, 1993). Interestingly, BUFFY-induced cell death is not significantly inhibited by the caspase inhibitor, zVAD-fmk whereas DEBCL-induced cell death is. This may indicate a role for BUFFY in caspase-independent apoptosis. Despite localising to different cellular compartments when expressed individually, BUFFY and DEBCL colocalise in cells overexpressing both molecules, in a pattern reminiscent of the ER. Consistent with this, BUFFY and DEBCL physically interact when coexpressed in BG2 cells and apoptosis is enhanced by expression of both molecules in BG2 cell death assays. Interestingly, two individual amino acid substitutions in the BH3 domain of DEBCL do not affect the association between BUFFY and DEBCL. Given the high degree of identity between these two molecules, it is possible that other domains are involved. Further

mutational analyses are required to determine the basis for the interaction between BUFFY and DEBCL.

Attempts to determine whether BUFFY plays a role in cell survival by RNAi were hampered by technical difficulties. Endogenous *buffy* transcript was difficult to detect in *Drosophila* BG2 and SL2 cells making it impossible to demonstrate message knockdown. Limited findings, however, did not indicate a prosurvival role for BUFFY in cultured cells.

Given difficulties with RNAi experiments, as well as the induction of cell death by BUFFY and data pertaining to BUFFY as the prosurvival Bcl-2 homologue in the fly by Quinn *et al.* (2003), aims for the project shifted to assess the cellular localisation of BUFFY and DEBCL. Initial experiments demonstrated the importance of the hydrophobic membrane anchor at the C terminus of BUFFY, shared by most Bcl-2 homologues. Results presented here demonstrate the importance of the membrane anchor for the localisation and function of BUFFY. Deletion of the membrane anchor renders BUFFY inactive in cell death assays and causes drastic mislocalisation of the protein in both insect and mammalian cells, with protein accumulation observed in the nucleus. Sequence analysis revealed a stretch of basic charges that could serve as a nuclear localisation signal (NLS). However, given that deletion of the membrane anchor (BUFFYΔMA) results in a 30kDa protein small enough for passive entry into the nucleus, the functionality of the putative NLS required testing. Preliminary experiments fusing the N-terminal 118 amino acids of BUFFY, containing the putative NLS, to heterologous proteins such as EGFP and N-terminally truncated STRICA suggest that this stretch of basicity can contribute to nuclear localisation. Experiments were somewhat hampered by the partial nuclear localisation of EGFP alone in both insect and mammalian NIH3T3 cells, however, results presented in this chapter clearly demonstrate that this putative NLS is indeed functional. The physiological significance of this remains to be determined. It may serve as a regulatory mechanism whereby post-translational modifications cause the nuclear targeting of BUFFY, sequestering it away from its site of action.

A study by Kaufmann *et al.* (2003) identified differences in the C-terminal amino acid sequences of Bcl-X_L, a MOM-targeted molecule, and Bcl-2, that localises to membranes of the ER and nuclear envelope in addition to mitochondria. Given the conservation of such residues in DEBCL and the absence of these in BUFFY, the aim of this comparative study was to identify the basis for the differential localisation of BUFFY and DEBCL.

The findings of this comparative study investigating the role of various residues in the differential localisation of BUFFY and DEBCL, demonstrate that specific amino acids flanking the hydrophobic transmembrane anchor are required, in addition to the membrane anchor itself, for correct intracellular targeting. DEBCL shares similar residues with Bcl-X_L and both of these molecules are targeted to the MOM. Data presented in this chapter demonstrate that the strong positive charges at the C-terminus play an important role in MOM-targeting, whereas arginine residues in the X domain, while contributing to mitochondrial localisation, play a less significant role. Localisation of the Bcl-X_L controls is consistant with the results obtained for DEBCL, although somewhat different to originally published data (Kaufmann *et al.,* 2003). Specifically, while mutation of the C-terminal charges has a drastic effect on Bcl-X_L localisation, as published, mutations in the X domain have little effect on MOM-targeting, in NIH3T3 cells (figure 6.16 B). Correct mitochondrial targeting of DEBCL depends on both the two ariginines in the X domain, as well as the two arginines in the B domain. Mutation of the X domain alone does not significantly mislocalise EGFP-DEBCL, while the B domain mutations (RR/AA) have a more marked effect. Most disruptive, however, is the effect of both mutations on EGFP-DEBCL. Significant mislocalisation was observed in EGFP-DEBCL DM, with loss of the punctate cytoplasmic staining characteristic of mitochondria, favouring a more diffuse cytoplasmic staining. EGFP-DEBCL DM did not colocalise with cytochrome c in transfected cells and exhibit an increase in localisation around the nucleus, further demonstrating loss of normal localisation. It should be noted that while the corresponding X domain mutations in Bcl-X_L reportedly mislocalise, no significant difference was observed using this control in the experiments

presented in this chapter. Although the X domain and B domain are required for the correct localisation of DEBCL, other residues are likely to be required as well as the TMB itself, since the EGFP-DEBCL mutants do not adopt a classic ER pattern of staining.

In the case of BUFFY, ER-localisation is somewhat disrupted by insertion of the X domain of DEBCL C-terminal to the BUFFY TMB. More pronounced, however, is the effect of increasing the basicity at the C-terminal end of the TMB from RF to RRK, with some cells displaying a complete loss of normal localisation, with diffuse staining throughout the cell. While an increase in basicity at the C terminus in BUFFY does not result in a drastic shift to MOM-targeting, exact colocalisation with Calnexin is lost, demonstrating the importance of more neutral amino acids for ER localisation. While the wildtype EGFP-X/2-Bcl-2 control does not exactly costain with Calnexin in NIH3T3 cells, increasing the basicity at either transmembrane flank increases the mitochondrial targeting of the molecule.

Thus, data presented in this chapter demonstrate that C-terminal basicity following the transmembrane domains of BUFFY and DEBCL plays a role in the differential localisation of these molecules. Positive charges at the N-terminal flank also contribute to the correct intracellular localisation of the proteins, however the TMB itself and other residues are likely to be required for targeting to the MOM or other organelle membranes. It should be noted that in each case, some cells appeared unaffected by various mutations. Levels of protein expression may be a factor in determining localisation in these experiments.

Chapter 7

General Discussion

At the commencement of the studies described in this thesis, the mechanisms of apoptosis in *Drosophila* were relatively poorly understood. Early in 2000, the *Drosophila* genome project was completed and the entire annotated sequence was available. At that time, five caspases had been cloned and characterised. Two of these, DRONC and DREDD, possessed long prodomains containing a CARD and DEDs respectively. STRICA was identified by database homology searching and cloned by PCR using a combination of EST clone and cDNA library DNA as templates.

The primary sequence of STRICA contains a QACKG, shared only with the *Drosophila* caspase, DAMM, and possesses all the residues conserved throughout the caspase family. The unique nature of the long prodomain of STRICA is immediately obvious. Homology searches fail to detect any known protein-protein interaction domains. Additionally, the prodomain of STRICA bears no similarity with the prodomains of other caspases. Of note are the vast number of serine and threonine residues present, that led to the naming of STRICA (**S**erine/**T**hreonine-**RI**ch **C**aspase).

Chapters 3 and 4 of this thesis present initial characterization experiments that confirm the function of STRICA as a caspase. Like most caspases, STRICA is a cytoplasmic protein, capable of inducing apoptosis when overexpressed in cell lines. Furthermore, STRICA induces apoptosis when ectopically expressed in the *Drosophila* eye, as seen by loss of pigment cells. Homozygous *GMR-strica* flies exhibit a more severe phenotype with almost complete loss of pigment cells and a severe small, rough eye phenotype. STRICA-induced cell death is suppressed by the pan caspase inhibitor, p35 in cell death assays as well as *in vivo* in the fly eye. STRICA interacts physically and genetically with both DIAP1 and DIAP2, although suppression by DIAP1 is most efficient and completely suppresses the cell death phenotype induced by STRICA overexpression in the *Drosophila* compound eye.

The induction of apoptosis by STRICA when overexpressed in cells renders it difficult to detect protein by Western blotting. Coexpression with the IAP molecule, DIAP1, suppresses STRICA-induced cell death, allowing for protein detection. Under these

conditions, a processed band associated with overexpression of STRICA, but not the catalytically inactive C429G mutant is detected, that migrates at the same rate as a putative minus prodomain mutant, strongly suggesting that STRICA is able to autoprocess when overexpressed.

An RNAi experiment in *Drosophila* BG2 cells suggests that STRICA activity is dispensable in cells where DRONC and DARK are present to initiate the cell death pathway. In contrast to DRONC, depletion of *strica* does not protect BG2 cells from CHX-induced apoptosis. Furthermore, unlike DRONC, STRICA is not sensitive to the dosage of the H99 death activators, REAPER, HID and GRIM, further raising the possibility that STRICA functions in an alternative cellular pathway.

The catalytic activity of STRICA is also associated with a processed fragment of DIAP1 in transfected cells, and is reproduced *in vitro* by recominant GST-STRICA ΔPD. Furthermore, recombinant GST-STRICA ΔPD generates several DIAP1 cleavage products *in vitro*, demonstrating that STRICA directly processes DIAP1. Mammalian IAPs have previously been reported to be caspase substrates, but it has only recently been reported that a *Drosophila* IAP is processed by a caspase. Specifically, DRONC cleaves DIAP1 following a glutamate residue, resulting in two fragments containing the BIR1, and BIR2-RING domains respectively (Yan *et al.*, 2004). Given the critical role for DIAP1 in cell survival, processing of this molecule may mark late-stage apoptosis, where it is cleaved and inactivated by activated caspases including DRONC and STRICA to allow apoptosis to proceed unhindered. The direct processing of DIAP1 by STRICA requires further analysis, including the identification of the cleavage sites within DIAP1. Given that the substrate specificity of STRICA is not known, the sites at which STRICA processes DIAP1 may shed light on STRICA's preferred substrate consensus. RNAi data suggests that STRICA activity may not be required in cells where DRONC and DARK are present to initiate apoptosis. Therefore, cleavage of DIAP1 by STRICA may function to regulate DIAP1 is an alternative pathway.

A putative AKT phosphorylation site was detected in STRICA. Given that negative regulation of the *Drosophila* AKT homologue, DAKT, by dPTEN results in caspase-dependent apoptosis, STRICA is a good candidate for functioning downstream of dPTEN in this kinase signalling pathway. While STRICA-induced cell death is suppressed by DAKT in mammalian cell death assays, and *in vivo* in the *Drosophila* eye to some extent, further investigation is required to determine the physiological significance of this observation. Inhibition of STRICA-induced cell death will need to be confirmed in *Drosophila* cells. Moreover, direct phosophorylation of STRICA by DAKT should be determined. The inability to detect full-length STRICA protein in the absence of a cell death inhibitor made this technically difficult. It would also be interesting to determine whether DAKT and STRICA physically interact. The effect of phosphorylation, if confirmed, would be an interesting area for further study. Perhaps phosphorylation maintains STRICA in an inactive conformation, requiring adaptor binding for activation. Alternatively, phosphorylation may be a prerequisite for interaction with a binding partner that prevents activation and cell death. It is also possible that the suppression of STRICA-induced cell death by DAKT presented in this thesis is due to suppression of a downstream caspase by DAKT, or the indirect result of DAKT phosphorylation of another target molecule. For this reason, it is essential to confirm direct phosphorylation of STRICA by DAKT.

The report that DAKT functions only in the regulation of cell size in the *Drosophila* eye, while playing a role in cell survival during embyrogenesis suggests that the role of STRICA in the PI3-K/dPTEN/DAKT pathway may be stage-specific. Furthermore, overexpression experiments, while valuble, may make functional conclusions difficult. Perhaps investigating the relationship between STRICA and DAKT in the fly embryo may shed more light on this putative genetic interaction. It would be interesting to determine whether *strica* ablation in the embryo by RNAi is sufficient to prevent cell death caused by loss of *dakt* or overexpression of dPTEN.

Identifying interactors for STRICA is important for understanding the role of this caspase in apoptosis or alternative cellular pathways. With this in mind, a yeast two-hybrid screen of a *Drosophila* embryonic cDNA library was carried out. Although all the control experiments gave expected results, no potential interactors were identified in a screen of 1.2 x 10^6 clones. There are several possibilities for this negative finding. Firstly, STRICA may interact with an adaptor in a transient manner making it unable to be detected by a yeast two-hybrid screen where weak, transient signals are often undetected. Secondly, protein-protein interactions depend upon correct folding and post-translational modifications, such as phosphorylation, of the proteins involved. If STRICA fused to the Gal4 DNA-binding domain was misfolded when expressed in yeast, or had not undergone modification, interaction with potential binding partners may be abrogated. Finally, if the binding partner is not well represented by the cDNA library or if the insert is incomplete, interaction will not be detected. Therefore, limitations of the yeast two-hybrid screen may have contributed to the inability to isolate putative interactors for STRICA.

The final results chapter, chapter 6, investigated the fundamental basis for the differential localisation of BUFFY and DEBCL. The ability of Bcl-2 to localise not only to mitochondria but also to membranes of the ER and nuclear envelope (Krajewski *et al.*, 1993; Lithgow *et al.*, 1994) has triggered interest in the role of the ER in apoptosis (Breckenridge *et al.*, 2003). In healthy cells, the ER is involved in protein folding, modification and sorting and maintaining Ca^{2+} homeostasis. Aberrations to the normal function of the ER trigger a number of responses to allow the cell to recover. The unfolded protein response (UPR) is activated to upregulate ER chaperones and block protein synthesis (Travers *et al.*, 2000). Targeting of Bcl-2 to either mitochondria or the ER using heterologous targeting sequences have shown that ER-localised Bcl-2 inhibits apoptosis induced by Myc but not etoposide in Rat-1 cells, whereas the wildtype Bcl-2 can inhibit against both stimuli (Lee *et al.*, 1999; Annis *et al.*, 2001). ER-targeted Bcl-2 conferred protection against radiation-induced

apoptosis, whereas both mitochondrial and ER-localised Bcl-2 cannot suppress receptor-mediated cell death induced by TRAIL or CD95 (Rudner *et al.*, 2001). The differential activity of mitochondrial and ER-targeted Bcl-2 highlights the physiological significance of intracellular targeting for the control of apoptosis in response to different death triggers (Zhu *et al.*, 1996).

The crosstalk between the ER and mitochondria is demonstrated in embryonic fibroblasts from Bax/Bak double deficient mice. These cells are resistant to ER stress-induced apoptosis caused by disrupted calcium homeostasis or accumulation of unfolded proteins (Wei *et al.*, 2001; Zong *et al.*, 2001) indicating that mitochondria may play a role in the execution of apoptosis triggered through the ER, or suggesting an as yet unidentified role for Bax and Bak in ER-mediated cell death. Indeed, Zong *et al.* (2003) suggest that Bax and Bak may function directly at the ER.

In *Drosophila*, the proapoptotic Bcl-2 protein, DEBCL, localises to mitochondria, while BUFFY, is targeted to the ER and nuclear membrane. DEBCL shares a number of positive arginine residues with Bcl-X_L, that function to target the protein to the mitochondrial outer membrane (MOM). In contrast, Bcl-2 localises to the ER and nuclear envelope, in addition to mitochondria, due to the lack of positively charged residues flanking the transmembrane domain (TMB) (Kaufmann *et al.*, 2003). Results of a comparative study were presented in chapter 6. Initial experiments established that BUFFY localises to the ER in transfected mammalian and insect cells, dependent on the TMB. BUFFY lacking the membrane anchor (BUFFYΔMA) is shown to accumulate in the nucleus, and renders BUFFY inactive in death assays, where it has a negative effect on cell viability. EGFP fusion constructs expressing BUFFY and DEBCL were shown to localise to the ER and mitochondria respectively, as shown by costaining with Calnexin and cytochrome c. Based on results obtained for various mutant versions of BUFFY and DEBCL targeting specific residues flanking the TMB, it can be concluded that MOM-targeting of DEBCL requires two arginine residues in the X domain, and two arginines in the B domain at the C-terminal end of

the TMB. Conversely, while insertion of the X domain of DEBCL N-terminal to the TMB in BUFFY results in a moderate mislocalisation of the protein, this mutation is insufficient to cause MOM-targeting of BUFFY. Increasing the basicity at the C-terminal TMB flank also has a slight effect on BUFFY localisation, but it does not target exclusively to mitochondria. This data demonstrates that while charges at either end of the TMB contribute to the appropriate targeting of BUFFY and DEBCL, additional residues, possibly in the TMB itself, are likely to also be required.

The relationship between BUFFY and DEBCL is an interesting one. Overexpression of both molecules in cells demonstrates that they colocalise in a pattern reminiscent of the ER, suggesting that BUFFY may recruit DEBCL to the ER. BUFFY and DEBCL interact in cultured mammalian cells (Quinn *et al.*, 2003) as well as in insect cells (presented in chapter 6), suggesting that the function of these two molecules is affected by each other. The intracellular localisation of BUFFY and DEBCL, as with other Bcl-2 homologues, is likely to be critical for their appropriate function. Both BUFFY and DEBCL exhibit proapoptotic activity when overexpressed in cultured cells, however cells expressing BUFFY together with DEBCL are insensitive to caspase inhibition by zVAD-fmk, raising the possbibility that a caspase-independent pathway of cell death may be employed.

In summary, results presented in this thesis describe the cloning and characterisation of a novel *Drosophila* caspase, STRICA. The unique nature of STRICA suggests that this caspase may be regulated by novel mechanisms and may function in a pathway independent of the major apoptotic pathway in the fly. The cleavage of DIAP1 by STRICA presented in this thesis should be investigated further and provides valuable insight into the relationship between these two opposing molecules. The putative phosphorylation of STRICA by DAKT is also an intriguing area for further investigation and may provide unique insights into the function of a caspase in a receptor-mediated kinase signalling pathway.

The differential localisation of BUFFY and DEBCL was analysed and presented in this thesis and demonstrates an interesting relationship between the only two Bcl-2 homologues in the fly. Appropriate localisation is likely to hold the key to understanding the function of these molecules in programmed cell death in the fly and may affect their function in apoptosis or survival. Studies described in this thesis contribute to the understanding of apoptosis in *Drosophila* and provide a framework for further characterisation of the unique caspase, STRICA, and the Bcl-2 homologues, BUFFY and DEBCL.

Bibliography

Bibliography

Acehan, D., Jiang, X., Morgan, D. G., Heuser, J. E., Wang, X., and Akey, C. W. (2002). Three-dimensional structure of the apoptosome: implications for assembly, procaspase-9 binding, and activation. Mol Cell *9*, 423-432.

Akgul, C., Moulding, D. A., White, M. R., and Edwards, S. W. (2000). *In vivo* localisation and stability of human Mcl-1 using green fluorescent protein (GFP) fusion proteins. FEBS Lett *478*, 72-76.

Alessi, D. R., Caudwell, F. B., Andjelkovic, M., Hemmings, B. A., and Cohen, P. (1996). Molecular basis for the substrate specificity of protein kinase B; comparison with MAPKAP kinase-1 and p70 S6 kinase. FEBS Lett *399*, 333-338.

Alessi, D. R. (2001). Discovery of PDK1, one of the missing links in insulin signal transduction. Colworth Medal Lecture. Biochem Soc Trans *29*, 1-14.

Allsop, T. E., Wyatt, S., Paterson, H. F., and Davies, A. M. (1993). The proto-oncogene *bcl-2* can selectively rescue neurotrophic factor-dependent neurons from apoptosis. Cell *73*, 295-307.

Ambrosini, G., Adida, C., and Altieri, D. C. (1997). A novel anti-apoptosis gene, *survivin*, expressed in cancer and lymphoma. Nat Med *3*, 917-921.

Annis, M. G., Zamzami, N., Zhu, W., Penn, L. Z., Kroemer, G., Leber, B., and Andrews, D. W. (2001). Endoplasmic reticulum localized Bcl-2 prevents apoptosis when redistribution of cytochrome c is a late event. Oncogene *20*, 1939-1952.

Antonsson, B., Montessuit, S., Lauper, S., Eskes, R., and Martinou, J. C. (2000). Bax oligomerization is required for channel-forming activity in liposomes and to trigger cytochrome c release from mitochondria. Biochem J *345 Pt 2*, 271-278.

Antonsson, B., Montessuit, S., Sanchez, B., and Martinou, J. C. (2001). Bax is present as a high molecular weight oligomer/complex in the mitochondrial membrane of apoptotic cells. J Biol Chem *276*, 11615-11623.

Baehrecke, E. H. (2000). Steroid regulation of programmed cell death during *Drosophila* development. Cell Death Differ *7*, 1057-1062.

Baehrecke, E. H. (2002). How death shapes life during development. Nat Rev Mol Cell Biol *3*, 779-787.

Barnhart, B. C., Lee, J. C., Alappat, E. C., and Peter, M. E. (2003). The death effector domain protein family. Oncogene *22*, 8634-8644.

Bergeron, L., Perez, G. I., Macdonald, G., Shi, L., Sun, Y., Jurisicova, A., Varmuza, S., Latham, K. E., Flaws, J. A., Salter, J. C. M., Hara, H., Moskowitz, M. A., Li, E., Greenberg, A., Tilly, J. L. and Yuan, J. (1998). Defects in regulation of apoptosis in caspase-2-deficient mice. Genes Dev *12*, 1304-1314.

Bergmann, A., Agapite, J., McCall, K., and Steller, H. (1998). The *Drosophila* gene hid is a direct molecular target of Ras-dependent survival signaling. Cell *95*, 331-341.

Bertin, J., Armstrong, R. C., Ottilie, S., Martin, D. A., Wang, Y., Banks, S., Wang, G. H., Senkevich, T. G., Alnemri, E. S., Moss, B., *et al.* (1997). Death effector domain-containing herpesvirus and poxvirus proteins inhibit both Fas- and TNFR1-induced apoptosis. Proc Natl Acad Sci U S A *94*, 1172-1176.

Birnbaum, M. J., Clem, R. J., and Miller, L. K. (1994). An apoptosis-inhibiting gene from a nuclear polyhedrosis virus encoding a polypeptide with Cys/His sequence motifs. J Virol *68*, 2521-2528.

Boatright, K. M., Renatus, M., Scott, F. L., Sperandio, S., Shin, H., Pedersen, I. M., Ricci, J. E., Edris, W. A., Sutherlin, D. P., Green, D. R., and Salvesen, G. S. (2003). A unified model for apical caspase activation. Mol Cell *11*, 529-541.

Boatright, K. M., and Salvesen, G. S. (2003). Mechanisms of caspase activation. Curr Opin Cell Biol *15*, 725-731.

Bodmer, J. L., Holler, N., Reynard, S., Vinciguerra, P., Schneider, P., Juo, P., Blenis, J., and Tschopp, J. (2000). TRAIL receptor-2 signals apoptosis through FADD and Caspase-8. Nat Cell Biol *2*, 241-243.

Bouillet, P., Metcalf, D., Huang, D. C., Tarlinton, D. M., Kay, T. W., Kontgen, F., Adams, J. M., and Strasser, A. (1999). Proapoptotic Bcl-2 relative Bim required for certain apoptotic responses, leukocyte homeostasis, and to preclude autoimmunity. Science *286*, 1735-1738.

Brand, A.H. and Perrimon, N. (1993). Targeted gene expression as a means of altering cell fates and generating dominant phenotypes. Development *118*, 401-415.

Bouillet, P., Purton, J. F., Godfrey, D. I., Zhang, L. C., Coultas, L., Puthalakath, H., Pellegrini, M., Cory, S., Adams, J. M., and Strasser, A. (2002). BH3-only Bcl-2 family member Bim is required for apoptosis of autoreactive thymocytes. Nature *415*, 922-926.

Brachmann, C. B., Jassim, O. W., Wachsmuth, B. D., and Cagan, R. L. (2000). The *Drosophila* bcl-2 family member dBorg-1 functions in the apoptotic response to UV-irradiation. Curr Biol *10*, 547-550.

Brachmann, C. B., and Cagan, R. L. (2003). Patterning the fly eye: the role of apoptosis. Trends Genet *19*, 91-96.

Breckenridge, D. G., Germain, M., Mathai, J. P., Nguyen, M., and Shore, G. C. (2003). Regulation of apoptosis by endoplasmic reticulum pathways. Oncogene *22*, 8608-8618.

Brodsky, M. H., Nordstrom, W., Tsang, G., Kwan, E., Rubin, G. M., and Abrams, J. M. (2000). *Drosophila* p53 binds a damage response element at the *reaper* locus. Cell *101*, 103-113.

Brunet, A., Bonni, A., Zigmond, M. J., Lin, M. Z., Juo, P., Hu, L. S., Anderson, M. J., Arden, K. C., Blenis, J., and Greenberg, M. E. (1999). Akt promotes cell survival by phosphorylating and inhibiting Forkhead transcription factor. Cell *96*, 857-868.

Bump, N. J., Hackett, M., Hugunin, M., Seshagiri, S., Brady, K., Chen, P., Ferenz, C., Franklin, S., Ghayur, T., Li, P., and et al. (1995). Inhibition of ICE family proteases by baculovirus antiapoptotic protein p35. Science *269*, 1885-1888.

Buszczak, M., and Cooley, L. (2000). Eggs to die for: cell death during *Drosophila* oogenesis. Cell Death Differ *7*, 1071-1074.

Butt, A. J., Harvey, N. L., Parasivam, G., and Kumar, S. (1998). Dimerization and autoprocessing of the Nedd2 (Caspase-2) precursor requires both the prodomain and the carboxyl-terminal regions. J Biol Chem *273*, 6763-6768.

Calleja, V., Ameer-Beg, S. M., Vojnovic, B., Woscholski, R., Downward, J., and Larijani, B. (2003). Monitoring conformational changes of proteins in cells by fluorescence lifetime imaging microscopy. Biochem J *372*, 33-40.

Cakouros, D., Daish, T., Martin, D., Baehrecke, E. H., and Kumar, S. (2002). Ecdysone-induced expression of the caspase DRONC during hormone-dependent programmed cell death in *Drosophila* is regulated by Broad-Complex. J Cell Biol *157*, 985-995.

Cakouros, D., Daish, T. J., and Kumar, S. (2004). Ecdysone receptor directly binds the promoter of the *Drosophila* caspase *dronc*, regulating its expression in specific tissues. J Cell Biol *165*, 631-640.

Cantrell, D. A. (2001). Phosphoinositide 3-kinase signalling pathways. J Cell Sci *114*, 1439-1445.

Caplen, N. J., Fleenor, J., Fire, A., and Morgan, R. A. (2000). dsRNA-mediated gene silencing in cultured *Drosophila* cells: a tissue culture model for the analysis of RNA interference. Gene *252*, 95-105.

Cardone, M. H., Roy, N., Stennicke, H. R., Salvesen, G. S., Franke, T. F., Stanbridge, E., Frisch, S., and Reed, J. C. (1998). Regulation of the cell death protease Caspase-9 by phosphorylation. Science *282*, 1318-1321.

Chai, J., Du, C., Wu, J. W., Kyin, S., Wang, X., and Shi, Y. (2000). Structural and biochemical basis of apoptotic activation by Smac/DIABLO. Nature *406*, 855-862.

Chai, J., Shiozaki, E., Srinivasula, S. M., Wu, Q., Datta, P., Alnemri, E. S., Shi, Y., and Dataa, P. (2001). Structural basis of Caspase-7 inhibition by XIAP. Cell *104*, 769-780.

Chai, J., Yan, N., Huh, J. R., Wu, J. W., Li, W., Hay, B. A., and Shi, Y. (2003). Molecular mechanism of Reaper-Grim-Hid-mediated suppression of DIAP1-dependent Dronc ubiquitination. Nat Struct Biol *10*, 892-898.

Chan, H. Y., and Bonini, N. M. (2000). *Drosophila* models of human neurodegenerative disease. Cell Death Differ *7*, 1075-1080.

Chen, P., Nordstrom, W., Gish, B., and Abrams, J. M. (1996). *grim*, a novel cell death gene in *Drosophila*. Genes Dev *10*, 1773-1782.

Chen, P., Rodriguez, A., Erskine, R., Thach, T., and Abrams, J. M. (1998). DREDD, a novel effector of the apoptosis activators REAPER, GRIM, and HID in *Drosophila*. Dev Biol *201*, 202-216.

Cheng, E. H., Wei, M. C., Weiler, S., Flavell, R. A., Mak, T. W., Lindsten, T., and Korsmeyer, S. J. (2001). BCL-2, BCL-X_L sequester BH3 domain-only molecules preventing BAX- and BAK-mediated mitochondrial apoptosis. Mol Cell *8*, 705-711.

Chinnaiyan, A. M., Chaudhary, D., O'Rourke, K., Koonin, E. V., and Dixit, V. M. (1997a). Role of CED-4 in the activation of CED-3. Nature *388*, 728-729.

Chinnaiyan, A. M., O'Rourke, K., Lane, B. R., and Dixit, V. M. (1997b). Interaction of CED-4 with CED-3 and CED-9: a molecular framework for cell death. Science *275*, 1122-1126.

Cho, K. S., Lee, J. H., Kim, S., Kim, D., Koh, H., Lee, J., Kim, C., Kim, J., and Chung, J. (2001). *Drosophila* phosphoinositide-dependent kinase-1 regulates apoptosis and growth via the phosphoinositide 3-kinase-dependent signaling pathway. Proc Natl Acad Sci U S A *98*, 6144-6149.

Christich, A., Kauppila, S., Chen, P., Sogame, N., Ho, S. I., and Abrams, J. M. (2002). The damage-responsive *Drosophila* gene *sickle* encodes a novel IAP binding protein similar to but distinct from *reaper*, *grim*, and *hid*. Curr Biol *12*, 137-140.

Chun, H. J., Zheng, L., Ahmad, M., Wang, J., Speirs, C. K., Siegel, R. M., Dale, J. K., Puck, J., Davis, J., Hall, C. G., *et al.* (2002). Pleiotropic defects in lymphocyte activation caused by caspase-8 mutations lead to human immunodeficiency. Nature *419*, 395-399.

Clancy, D. J., Gems, D., Harshman, L. G., Oldham, S., Stocker, H., Hafen, E., Leevers, S. J., and Partridge, L. (2001). Extension of life-span by loss of CHICO, a Drosophila insulin receptor substrate protein. Science *292*, 104-106.

Claveria, C., Albar, J. P., Serrano, A., Buesa, J. M., Barbero, J. L., Martinez, A. C., and Torres, M. (1998). *Drosophila* grim induces apoptosis in mammalian cells. EMBO J *17*, 7199-7208.

Clem, R. J., Fechheimer, M., and Miller, L. K. (1991). Prevention of apoptosis by a baculovirus gene during infection of insect cells. Science *254*, 1388-1390.

Clem, R. J., and Miller, L. K. (1994). Control of programmed cell death by the baculovirus genes *p35* and *iap*. Mol Cell Biol *14*, 5212-5222.

Clem, R. J., Sheu, T. T., Richter, B. W., He, W. W., Thornberry, N. A., Duckett, C. S., and Hardwick, J. M. (2001). c-IAP1 is cleaved by caspases to produce a proapoptotic C-terminal fragment. J Biol Chem *276*, 7602-7608.

Clemens, J. C., Worby, C. A., Simonson-Leff, N., Muda, M., Maehama, T., Hemmings, B. A., and Dixon, J. E. (2000). Use of double-stranded RNA interference in *Drosophila* cell lines to dissect signal transduction pathways. Proc Natl Acad Sci U S A *97*, 6499-6503.

Colussi, P. A., Harvey, N. L., and Kumar, S. (1998a). Prodomain-dependent nuclear localization of the caspase-2 (Nedd2) precursor. A novel function for a caspase prodomain. J Biol Chem *273*, 24535-24542.

Colussi, P. A., Harvey, N. L., Shearwin-Whyatt, L. M., and Kumar, S. (1998b). Conversion of procaspase-3 to an autoactivating caspase by fusion to the caspase-2 prodomain. J Biol Chem *273*, 26566-26570.

Colussi, P. A., Quinn, L. M., Huang, D. C., Coombe, M., Read, S. H., Richardson, H., and Kumar, S. (2000). Debcl, a proapoptotic Bcl-2 homologue, is a component of the *Drosophila melanogaster* cell death machinery. J Cell Biol *148*, 703-714.

Conradt, B., and Horvitz, H. R. (1998). The C. elegans protein EGL-1 is required for programmed cell death and interacts with the Bcl-2-like protein CED-9. Cell *93*, 519-529.

Cory, S., Huang, D. C., and Adams, J. M. (2003). The Bcl-2 family: roles in cell survival and oncogenesis. Oncogene *22*, 8590-8607.

Crook, N. E., Clem, R. J., and Miller, L. K. (1993). An apoptosis-inhibiting baculovirus gene with a zinc finger-like motif. J Virol *67*, 2168-2174.

Datta, S. R., Dudek, H., Tao, X., Masters, S., Fu, H., Gotoh, Y., and Greenberg, M. E. (1997). Akt phosphorylation of BAD couples survival signals to the cell-intrinsic death machinery. Cell *91*, 231-241.

Datta, S. R., Brunet, A., and Greenberg, M. E. (1999). Cellular survival: a play in three Akts. Genes Dev *13*, 2905-2927.

Datta, S. R., Katsov, A., Hu, L., Petros, A., Fesik, S. W., Yaffe, M. B., and Greenberg, M. E. (2000). 14-3-3 proteins and survival kinases cooperate to inactivate BAD by BH3 domain phosphorylation. Mol Cell *6*, 41-51.

Deckwerth, T. L., Elliott, J. L., Knudson, C. M., Johnson, E. M., Jr., Snider, W. D., and Korsmeyer, S. J. (1996). BAX is required for neuronal death after trophic factor deprivation and during development. Neuron *17*, 401-411.

Degterev, A., Boyce, M., and Yuan, J. (2003). A decade of caspases. Oncogene *22*, 8543-8567.

Deveraux, Q. L., Roy, N., Stennicke, H. R., Van Arsdale, T., Zhou, Q., Srinivasula, S. M., Alnemri, E. S., Salvesen, G. S., and Reed, J. C. (1998). IAPs block apoptotic events induced by caspase-8 and cytochrome c by direct inhibition of distinct caspases. EMBO J *17*, 2215-2223.

Deveraux, Q. L., Leo, E., Stennicke, H. R., Welsh, K., Salvesen, G. S., and Reed, J. C. (1999). Cleavage of human inhibitor of apoptosis protein XIAP results in fragments with distinct specificities for caspases. EMBO J *18*, 5242-5251.

Dijkers, P. F., Medema, R. H., Lammers, J. W., Koenderman, L., and Coffer, P. J. (2000). Expression of the proapoptotic Bcl-2 family member Bim is regulated by the forkhead transcription factor FKHR-L1. Curr Biol *10*, 1201-1204.

Ditzel, M., Wilson, R., Tenev, T., Zachariou, A., Paul, A., Deas, E., and Meier, P. (2003). Degradation of DIAP1 by the N-end rule pathway is essential for regulating apoptosis. Nat Cell Biol *5*, 467-473.

Dorstyn, L., Colussi, P. A., Quinn, L. M., Richardson, H., and Kumar, S. (1999a). DRONC, an ecdysone-inducible *Drosophila* caspase. Proc Natl Acad Sci U S A *96*, 4307-4312.

Dorstyn, L., Read, S. H., Quinn, L. M., Richardson, H., and Kumar, S. (1999b). DECAY, a novel *Drosophila* caspase related to mammalian caspase-3 and caspase-7. J Biol Chem *274*, 30778-30783.

Dorstyn, L., Read, S., Cakouros, D., Huh, J. R., Hay, B. A., and Kumar, S. (2002). The role of cytochrome c in caspase activation in *Drosophila melanogaster* cells. J Cell Biol *156*, 1089-1098.

Doumanis, J., Quinn, L., Richardson, H., and Kumar, S. (2001). STRICA, a novel *Drosophila melanogaster* caspase with an unusual serine/threonine-rich prodomain, interacts with DIAP1 and DIAP2. Cell Death Differ *8*(4), 387-94

Downward, J. (1999). How BAD phosphorylation is good for survival. Nat Cell Biol *1*, E33-35.

Du, C., Fang, M., Li, Y., Li, L., and Wang, X. (2000). Smac, a mitochondrial protein that promotes cytochrome c-dependent caspase activation by eliminating IAP inhibition. Cell *102*, 33-42.

Duckett, C. S., Nava, V. E., Gedrich, R. W., Clem, R. J., Van Dongen, J. L., Gilfillan, M. C., Shiels, H., Hardwick, J. M., and Thompson, C. B. (1996). A conserved family of cellular genes related to the baculovirus *iap* gene and encoding apoptosis inhibitors. EMBO J *15*, 2685-2694.

Dudek, H., Datta, S. R., Franke, T. F., Birnbaum, M. J., Yao, R., Cooper, G. M., Segal, R. A., Kaplan, D. R., and Greenberg, M. E. (1997). Regulation of neuronal survival by the serine-threonine protein kinase Akt. Science *275*, 661-665.

Ekert, P. G., Silke, J., and Vaux, D. L. (1999). Caspase inhibitors. Cell Death Differ *6*, 1081-1086.

Ekert, P. G., Silke, J., Hawkins, C. J., Verhagen, A. M., and Vaux, D. L. (2001). DIABLO promotes apoptosis by removing MIHA/XIAP from processed caspase 9. J Cell Biol *152*, 483-490.

Ellis, H. M., and Horvitz, H. R. (1986). Genetic control of programmed cell death in the nematode C. elegans. Cell *44*, 817-829.

Elrod-Erickson, M., Mishra, S., and Schneider, D. (2000). Interactions between the cellular and humoral immune responses in *Drosophila*. Curr Biol *10*, 781-784.

Enari, M., Hug, H., and Nagata, S. (1995). Involvement of an ICE-like protease in Fas-mediated apoptosis. Nature *375*, 78-81.

European Molecular Biology Network. WWW PESTfind Analysis. http://at.embnet.org/embnet/tools/bio/PESTfind/

Fadok, V. A., Voelker, D. R., Campbell, P. A., Cohen, J. J., Bratton, D. L., and Henson, P. M. (1992). Exposure of phosphatidylserine on the surface of apoptotic lymphocytes triggers specific recognition and removal by macrophages. J Immunol *148*, 2207-2216.

Fernandes-Alnemri, T., Litwack, G., and Alnemri, E. S. (1994). CPP32, a novel human apoptotic protein with homology to Caenorhabditis elegans cell death protein Ced-3 and mammalian interleukin-1 beta-converting enzyme. J Biol Chem *269*, 30761-30764.

Fisher, A. J., Cruz, W., Zoog, S. J., Schneider, C. L., and Friesen, P. D. (1999). Crystal structure of baculovirus P35: role of a novel reactive site loop in apoptotic caspase inhibition. EMBO J *18*, 2031-2039.

Franke, T. F., Hornik, C. P., Segev, L., Shostak, G. A., and Sugimoto, C. (2003). PI3K/Akt and apoptosis: size matters. Oncogene *22*, 8983-8998.

Fraser, A. G., and Evan, G. I. (1997). Identification of a *Drosophila melanogaster* ICE/CED-3-related protease, drICE. EMBO J *16*, 2805-2813.

Fraser, A. G., McCarthy, N. J., and Evan, G. I. (1997). drICE is an essential caspase required for apoptotic activity in *Drosophila* cells. EMBO J *16*, 6192-6199.

Fraser, A. G., James, C., Evan, G. I., and Hengartner, M. O. (1999). *Caenorhabditis elegans* inhibitor of apoptosis protein (IAP) homologue BIR-1 plays a conserved role in cytokinesis. Curr Biol *9*, 292-301.

Goldstein, J. C., Waterhouse, N. J., Juin, P., Evan, G. I., and Green, D. R. (2000). The coordinate release of cytochrome c during apoptosis is rapid, complete and kinetically invariant. Nat Cell Biol *2*, 156-162.

Glucksmann, A. (1951). Local factors in the histogenesis of hypertrophic scars. Br J Plast Surg *4*, 88-103.

Goberdhan, D. C., Paricio, N., Goodman, E. C., Mlodzik, M., and Wilson, C. (1999). *Drosophila* tumor suppressor PTEN controls cell size and number by antagonizing the Chico/PI3-kinase signaling pathway. Genes Dev *13*, 3244-3258.

Goyal, L., McCall, K., Agapite, J., Hartwieg, E., and Steller, H. (2000). Induction of apoptosis by *Drosophila reaper*, *hid* and *grim* through inhibition of IAP function. EMBO J *19*, 589-597.

Green, D. R., and Evan, G. I. (2002). A matter of life and death. Cancer Cell *1*, 19-30.

Grether, M. E., Abrams, J. M., Agapite, J., White, K., and Steller, H. (1995). The *head involution defective* gene of *Drosophila melanogaster* functions in programmed cell death. Genes Dev *9*, 1694-1708.

Haining, W. N., Carboy-Newcomb, C., Wei, C. L., and Steller, H. (1999). The proapoptotic function of *Drosophila* Hid is conserved in mammalian cells. Proc Natl Acad Sci U S A *96*, 4936-4941.

Hakem, R., Hakem, A., Duncan, G. S., Henderson, J. T., Woo, M., Soengas, M. S., Elia, A., de la Pompa, J. L., Kagi, D., Khoo, W., *et al.* (1998). Differential requirement for caspase 9 in apoptotic pathways *in vivo*. Cell *94*, 339-352.

Hamasaki, A., Sendo, F., Nakayama, K., Ishida, N., Negishi, I., and Hatakeyama, S. (1998). Accelerated neutrophil apoptosis in mice lacking A1-a, a subtype of the *bcl-2*-related *A1* gene. J Exp Med *188*, 1985-1992.

Hammond, S. M., Bernstein, E., Beach, D., and Hannon, G. J. (2000). An RNA-directed nuclease mediates post-transcriptional gene silencing in *Drosophila* cells. Nature *404*, 293-296.

Han, J., Flemington, C., Houghton, A. B., Gu, Z., Zambetti, G. P., Lutz, R. J., Zhu, L., and Chittenden, T. (2001). Expression of bbc3, a proapoptotic BH3-only gene, is regulated by diverse cell death and survival signals. Proc Natl Acad Sci U S A *98*, 11318-11323.

Hanada, M., Feng, J., and Hemmings, B. A. (2004). Structure, regulation and function of PKB/AKT--a major therapeutic target. Biochim Biophys Acta *1697*, 3-16.

Harada, H., Becknell, B., Wilm, M., Mann, M., Huang, L. J., Taylor, S. S., Scott, J. D., and Korsmeyer, S. J. (1999). Phosphorylation and inactivation of BAD by mitochondria-anchored protein kinase A. Mol Cell *3*, 413-422.

Harvey, N. L., Daish, T., Mills, K., Dorstyn, L., Quinn, L. M., Read, S. H., Richardson, H., and Kumar, S. (2001). Characterisation of the *Drosophila* caspase, DAMM. J Biol Chem *276*, 25342-25350.

Hawkins, C. J., Yoo, S. J., Peterson, E. P., Wang, S. L., Vernooy, S. Y., and Hay, B. A. (2000). The *Drosophila* caspase DRONC cleaves following glutamate or aspartate and is regulated by DIAP1, HID, and GRIM. J Biol Chem *275*, 27084-27093.

Hay, B. A., Wassarman, D. A., and Rubin, G. M. (1995). *Drosophila* homologs of baculovirus inhibitor of apoptosis proteins function to block cell death. Cell *83*, 1253-1262.

Hay, B. A. (2000). Understanding IAP function and regulation: a view from *Drosophila*. Cell Death Differ *7*, 1045-1056.

Hays, R., Wickline, L., and Cagan, R. (2002). Morgue mediates apoptosis in the *Drosophila melanogaster* retina by promoting degradation of DIAP1. Nat Cell Biol *4*, 425-431.

Hengartner, M. O., Ellis, R. E., and Horvitz, H. R. (1992). *Caenorhabditis elegans* gene *ced-9* protects cells from programmed cell death. Nature *356*, 494-499.

Hengartner, M. O., and Horvitz, H. R. (1994a). C. elegans cell survival gene *ced-9* encodes a functional homolog of the mammalian proto-oncogene *bcl-2*. Cell *76*, 665-676.

Hengartner, M. O., and Horvitz, H. R. (1994b). Activation of C. elegans cell death protein CED-9 by an amino-acid substitution in a domain conserved in Bcl-2. Nature *369*, 318-320.

Hildeman, D. A., Zhu, Y., Mitchell, T. C., Bouillet, P., Strasser, A., Kappler, J., and Marrack, P. (2002). Activated T cell death *in vivo* mediated by proapoptotic bcl-2 family member bim. Immunity *16*, 759-767.

Hinds, M. G., Norton, R. S., Vaux, D. L., and Day, C. L. (1999). Solution structure of a baculoviral inhibitor of apoptosis (IAP) repeat. Nat Struct Biol *6*, 648-651.

Hinds, M. G., Lackmann, M., Skea, G. L., Harrison, P. J., Huang, D. C., and Day, C. L. (2003). The structure of Bcl-w reveals a role for the C-terminal residues in modulating biological activity. EMBO J *22*, 1497-1507.

Hofmann, E. R., Milstein, S., Boulton, S. J., Ye, M., Hofmann, J. J., Stergiou, L., Gartner, A., Vidal, M., and Hengartner, M. O. (2002). *Caenorhabditis elegans* HUS-1 is a DNA damage checkpoint protein required for genome stability and EGL-1-mediated apoptosis. Curr Biol *12*, 1908-1918.

Holcik, M., Thompson, C. S., Yaraghi, Z., Lefebvre, C. A., MacKenzie, A. E., and Korneluk, R. G. (2000). The hippocampal neurons of neuronal apoptosis inhibitory protein 1 (NAIP1)-deleted mice display increased vulnerability to kainic acid-induced injury. Proc Natl Acad Sci U S A *97*, 2286-2290.

Howard, A. D., Kostura, M. J., Thornberry, N., Ding, G. J., Limjuco, G., Weidner, J., Salley, J. P., Hogquist, K. A., Chaplin, D. D., Mumford, R. A., and et al. (1991). IL-1-converting enzyme requires aspartic acid residues for processing of the IL-1 beta precursor at two distinct sites and does not cleave 31-kDa IL-1 alpha. J Immunol *147*, 2964-2969.

Hsu, Y. T., Wolter, K. G., and Youle, R. J. (1997). Cytosol-to-membrane redistribution of Bax and Bcl-X_L during apoptosis. Proc Natl Acad Sci U S A *94*, 3668-3672.

Hu, S., Vincenz, C., Buller, M., and Dixit, V. M. (1997). A novel family of viral death effector domain-containing molecules that inhibit both CD-95- and tumor necrosis factor receptor-1-induced apoptosis. J Biol Chem *272*, 9621-9624.

Hu, S., and Yang, X. (2000). dFADD, a novel death domain-containing adapter protein for the *Drosophila* caspase DREDD. J Biol Chem *275*, 30761-30764.

Hu, Y., Ding, L., Spencer, D. M., and Nunez, G. (1998). WD-40 repeat region regulates Apaf-1 self-association and procaspase-9 activation. J Biol Chem *273*, 33489-33494.

Hu, Y., Benedict, M. A., Ding, L., and Nunez, G. (1999). Role of cytochrome c and dATP/ATP hydrolysis in Apaf-1-mediated caspase-9 activation and apoptosis. EMBO J *18*, 3586-3595.

Huang, H., Potter, C. J., Tao, W., Li, D. M., Brogiolo, W., Hafen, E., Sun, H., and Xu, T. (1999). PTEN affects cell size, cell proliferation and apoptosis during *Drosophila* eye development. Development *126*, 5365-5372.

Huang, H., Joazeiro, C. A., Bonfoco, E., Kamada, S., Leverson, J. D., and Hunter, T. (2000). The inhibitor of apoptosis, cIAP2, functions as a ubiquitin-protein ligase and promotes in vitro monoubiquitination of caspases 3 and 7. J Biol Chem *275*, 26661-26664.

Huang, Y., Park, Y. C., Rich, R. L., Segal, D., Myszka, D. G., and Wu, H. (2001). Structural basis of caspase inhibition by XIAP: differential roles of the linker versus the BIR domain. Cell *104*, 781-790.

Huang, Y., Rich, R. L., Myszka, D. G., and Wu, H. (2003). Requirement of both the second and third BIR domains for the relief of X-linked inhibitor of apoptosis protein (XIAP)-mediated caspase inhibition by Smac. J Biol Chem *278*, 49517-49522.

Huh, J. R., Vernooy, S. Y., Yu, H., Yan, N., Shi, Y., Guo, M., and Hay, B. A. (2004). Multiple apoptotic caspase cascades are required in nonapoptotic roles for *Drosophila* spermatid individualization. PLoS Biol *2*, E15.

Huisamen, B. (2003). Protein kinase B in the diabetic heart. Mol Cell Biochem *249*, 31-38.

Hugunin, M., Quintal, L. J., Mankovich, J. A., and Ghayur, T. (1996). Protease activity of in vitro transcribed and translated *Caenorhabditis elegans* cell death gene (ced-3) product. J Biol Chem *271*, 3517-3522.

Igaki, T., Kanuka, H., Inohara, N., Sawamoto, K., Nunez, G., Okano, H., and Miura, M. (2000). Drob-1, a *Drosophila* member of the Bcl-2/CED-9 family that promotes cell death. Proc Natl Acad Sci U S A *97*, 662-667.

Igaki, T., Kanda, H., Yamamoto-Goto, Y., Kanuka, H., Kuranaga, E., Aigaki, T., and Miura, M. (2002a). Eiger, a TNF superfamily ligand that triggers the *Drosophila* JNK pathway. EMBO J *21*, 3009-3018.

Igaki, T., Yamamoto-Goto, Y., Tokushige, N., Kanda, H., and Miura, M. (2002b). Down-regulation of DIAP1 triggers a novel *Drosophila* cell death pathway mediated by DARK and DRONC. J Biol Chem *277*, 23103-23106.

Igaki, T., and Miura, M. (2004). Role of Bcl-2 family members in invertebrates. Biochim Biophys Acta *1644*, 73-81.

Imler, J. L., and Hoffmann, J. A. (2000). Signaling mechanisms in the antimicrobial host defense of *Drosophila*. Curr Opin Microbiol *3*, 16-22.

Irmler, M., Thome, M., Hahne, M., Schneider, P., Hofmann, K., Steiner, V., Bodmer, J. L., Schroter, M., Burns, K., Mattmann, C., *et al.* (1997). Inhibition of death receptor signals by cellular FLIP. Nature *388*, 190-195.

James, C., Gschmeissner, S., Fraser, A., and Evan, G. I. (1997). CED-4 induces chromatin condensation in *Schizosaccharomyces pombe* and is inhibited by direct physical association with CED-9. Curr Biol *7*, 246-252.

Jones, G., Jones, D., Zhou, L., Steller, H., and Chu, Y. (2000). Deterin, a new inhibitor of apoptosis from *Drosophila melanogaster*. J Biol Chem *275*, 22157-22165.

Juo, P., Kuo, C. J., Yuan, J., and Blenis, J. (1998). Essential requirement for Caspase-8/FLICE in the initiation of the Fas-induced apoptotic cascade. Curr Biol *8*, 1001-1008.

Kang, S. J., Wang, S., Hara, H., Peterson, E. P., Namura, S., Amin-Hanjani, S., Huang, Z., Srinivasan, A., Tomaselli, K. J., Thornberry, N. A., *et al.* (2000). Dual role of Caspase-11 in mediating activation of Caspase-1 and Caspase-3 under pathological conditions. J Cell Biol *149*, 613-622.

Kaiser, W. J., Vucic, D., and Miller, L. K. (1998). The *Drosophila* inhibitor of apoptosis D-IAP1 suppresses cell death induced by the caspase drICE. FEBS Lett *440*, 243-248.

Kanda, H., Igaki, T., Kanuka, H., Yagi, T., and Miura, M. (2002). Wengen, a member of the *Drosophila* tumor necrosis factor receptor superfamily, is required for Eiger signaling. J Biol Chem *277*, 28372-28375.

Kanuka, H., Sawamoto, K., Inohara, N., Matsuno, K., Okano, H., and Miura, M. (1999). Control of the cell death pathway by Dapaf-1, a *Drosophila* Apaf-1/CED-4-related caspase activator. Mol Cell *4*, 757-769.

Kasof, G. M., and Gomes, B. C. (2001). Livin, a novel inhibitor of apoptosis protein family member. J Biol Chem *276*, 3238-3246.

Kataoka, T., Holler, N., Micheau, O., Martinon, F., Tinel, A., Hofmann, K., and Tschopp, J. (2001). Bcl-rambo, a novel Bcl-2 homologue that induces apoptosis via its unique C-terminal extension. J Biol Chem *276*, 19548-19554.

Kaufmann, S. H., and Gores, G. J. (2000). Apoptosis in cancer: cause and cure. Bioessays *22*, 1007-1017.

Kaufmann, T., Schlipf, S., Sanz, J., Neubert, K., Stein, R., and Borner, C. (2003). Characterization of the signal that directs Bcl-X_L, but not Bcl-2, to the mitochondrial outer membrane. J Cell Biol *160*, 53-64.

Kauppila, S., Maaty, W. S., Chen, P., Tomar, R. S., Eby, M. T., Chapo, J., Chew, S., Rathore, N., Zachariah, S., Sinha, S. K., *et al.* (2003). Eiger and its receptor, Wengen, comprise a TNF-like system in *Drosophila*. Oncogene *22*, 4860-4867.

Kennedy, S. G., Wagner, A. J., Conzen, S. D., Jordan, J., Bellacosa, A., Tsichlis, P. N., and Hay, N. (1997). The PI 3-kinase/Akt signaling pathway delivers an anti-apoptotic signal. Genes Dev *11*, 701-713.

Kerr, J. F., Wyllie, A. H., and Currie, A. R. (1972). Apoptosis: a basic biological phenomenon with wide-ranging implications in tissue kinetics. Br J Cancer *26*, 239-257.

Khush, R. S., and Lemaitre, B. (2000). Genes that fight infection: what the *Drosophila* genome says about animal immunity. Trends Genet *16*, 442-449.

Kirchhoff, S., Muller, W. W., Li-Weber, M., and Krammer, P. H. (2000). Up-regulation of c-FLIPshort and reduction of activation-induced cell death in CD28-costimulated human T cells. Eur J Immunol *30*, 2765-2774.

Knudson, C. M., Tung, K. S., Tourtellotte, W. G., Brown, G. A., and Korsmeyer, S. J. (1995). Bax-deficient mice with lymphoid hyperplasia and male germ cell death. Science *270*, 96-99.

Knudson, C. M., and Korsmeyer, S. J. (1997). Bcl-2 and Bax function independently to regulate cell death. Nat Genet *16*, 358-363.

Kobayashi, K., Hatano, M., Otaki, M., Ogasawara, T., and Tokuhisa, T. (1999). Expression of a murine homologue of the inhibitor of apoptosis protein is related to cell proliferation. Proc Natl Acad Sci U S A *96*, 1457-1462.

Krajewski, S., Tanaka, S., Takayama, S., Schibler, M. J., Fenton, W., and Reed, J. C. (1993). Investigation of the subcellular distribution of the Bcl-2 oncoprotein: residence in the nuclear envelope, endoplasmic reticulum, and outer mitochondrial membranes. Cancer Res *53*, 4701-4714.

Krueger, A., Schmitz, I., Baumann, S., Krammer, P. H., and Kirchhoff, S. (2001). Cellular FLICE-inhibitory protein splice variants inhibit different steps of Caspase-8 activation at the CD95 death-inducing signaling complex. J Biol Chem *276*, 20633-20640.

Kuida, K., Zheng, T. S., Na, S., Kuan, C., Yang, D., Karasuyama, H., Rakic, P., and Flavell, R. A. (1996). Decreased apoptosis in the brain and premature lethality in CPP32-deficient mice. Nature *384*, 368-372.

Kuida, K., Haydar, T. F., Kuan, C. Y., Gu, Y., Taya, C., Karasuyama, H., Su, M. S., Rakic, P., and Flavell, R. A. (1998). Reduced apoptosis and cytochrome c-mediated caspase activation in mice lacking caspase 9. Cell *94*, 325-337.

Kumar, S., Tomooka, Y., and Noda, M. (1992). Identification of a set of genes with developmentally down-regulated expression in the mouse brain. Biochem Biophys Res Commun *185*, 1155-1161.

Kumar, S., Kinoshita, M., Noda, M., Copeland, N. G., and Jenkins, N. A. (1994). Induction of apoptosis by the mouse Nedd2 gene, which encodes a protein similar to the product of the *Caenorhabditis elegans* cell death gene *ced-3* and the mammalian IL-1 beta-converting enzyme. Genes Dev *8*, 1613-1626.

Kumar, S. (1995). Inhibition of apoptosis by the expression of antisense Nedd2. FEBS Lett *368*, 69-72.

Kumar S. and Lavin M.F. (1996) The ICE family of cysteine proteases as effectors of cell death. Cell Death Differ. *3*, 255-267

Kumar, S., Kinoshita, M., and Noda, M. (1997). Characterization of a mammalian cell death gene Nedd2. Leukemia *11 Suppl 3*, 385-386.

Kumar, S. (1999). Mechanisms mediating caspase activation in cell death. Cell Death Differ *6*, 1060-1066.

Kumar, S., and Colussi, P. A. (1999). Prodomains--adaptors--oligomerization: the pursuit of caspase activation in apoptosis. Trends Biochem Sci *24*, 1-4.

Kumar, S., and Doumanis, J. (2000). The fly caspases. Cell Death Differ *7*(11), 1039-44

Kurada, P., and White, K. (1998). Ras promotes cell survival in *Drosophila* by downregulating *hid* expression. Cell *95*, 319-329.

Lagace, M., Xuan, J. Y., Young, S. S., McRoberts, C., Maier, J., Rajcan-Separovic, E., and Korneluk, R. G. (2001). Genomic organization of the X-linked inhibitor of apoptosis and identification of a novel testis-specific transcript. Genomics *77*, 181-188.

Lassus, P., Opitz-Araya, X., and Lazebnik, Y. (2002). Requirement for caspase-2 in stress-induced apoptosis before mitochondrial permeabilization. Science *297*, 1352-1354.

Laundrie, B., Peterson, J. S., Baum, J. S., Chang, J. C., Fileppo, D., Thompson, S. R., and McCall, K. (2003). Germline cell death is inhibited by P-element insertions disrupting the *dcp-1/pita* nested gene pair in *Drosophila*. Genetics *165*, 1881-1888.

Lawlor, M. A., and Alessi, D. R. (2001). PKB/Akt: a key mediator of cell proliferation, survival and insulin responses? J Cell Sci *114*, 2903-2910.

Lee, C. Y., Cooksey, B. A., and Baehrecke, E. H. (2002a). Steroid regulation of midgut cell death during *Drosophila* development. Dev Biol *250*, 101-111.

Lee, C. Y., Simon, C. R., Woodard, C. T., and Baehrecke, E. H. (2002b). Genetic mechanism for the stage- and tissue-specific regulation of steroid triggered programmed cell death in *Drosophila*. Dev Biol *252*, 138-148.

Lee, C. Y., Clough, E. A., Yellon, P., Teslovich, T. M., Stephan, D. A., and Baehrecke, E. H. (2003). Genome-wide analyses of steroid- and radiation-triggered programmed cell death in *Drosophila*. Curr Biol *13*, 350-357.

Lee, S. T., Hoeflich, K. P., Wasfy, G. W., Woodgett, J. R., Leber, B., Andrews, D. W., Hedley, D. W., and Penn, L. Z. (1999). Bcl-2 targeted to the endoplasmic reticulum can inhibit apoptosis induced by Myc but not etoposide in Rat-1 fibroblasts. Oncogene *18*, 3520-3528.

Lefebvre, S., Burglen, L., Reboullet, S., Clermont, O., Burlet, P., Viollet, L., Benichou, B., Cruaud, C., Millasseau, P., Zeviani, M., and et al. (1995). Identification and characterization of a spinal muscular atrophy-determining gene. Cell *80*, 155-165.

Leulier, F., Rodriguez, A., Khush, R. S., Abrams, J. M., and Lemaitre, B. (2000). The *Drosophila* caspase Dredd is required to resist gram-negative bacterial infection. EMBO Rep *1*, 353-358.

Li, F., and Altieri, D. C. (1999). The cancer antiapoptosis mouse survivin gene: characterization of locus and transcriptional requirements of basal and cell cycle-dependent expression. Cancer Res *59*, 3143-3151.

Li, H., Zhu, H., Xu, C. J., and Yuan, J. (1998). Cleavage of BID by caspase 8 mediates the mitochondrial damage in the Fas pathway of apoptosis. Cell *94*, 491-501.

Li, K., Li, Y., Shelton, J. M., Richardson, J. A., Spencer, E., Chen, Z. J., Wang, X., and Williams, R. S. (2000). Cytochrome c deficiency causes embryonic lethality and attenuates stress-induced apoptosis. Cell *101*, 389-399.

Li, P., Allen, H., Banerjee, S., Franklin, S., Herzog, L., Johnston, C., McDowell, J., Paskind, M., Rodman, L., Salfeld, J., and et al. (1995). Mice deficient in IL-1 beta-converting enzyme are defective in production of mature IL-1 beta and resistant to endotoxic shock. Cell *80*, 401-411.

Li, P., Nijhawan, D., Budihardjo, I., Srinivasula, S. M., Ahmad, M., Alnemri, E. S., and Wang, X. (1997). Cytochrome c and dATP-dependent formation of Apaf-1/caspase-9 complex initiates an apoptotic protease cascade. Cell *91*, 479-489.

Lin, J. H., Deng, G., Huang, Q., and Morser, J. (2000). KIAP, a novel member of the inhibitor of apoptosis protein family. Biochem Biophys Res Commun *279*, 820-831.

Lindsten, T., Ross, A. J., King, A., Zong, W. X., Rathmell, J. C., Shiels, H. A., Ulrich, E., Waymire, K. G., Mahar, P., Frauwirth, K., *et al.* (2000). The combined functions of proapoptotic Bcl-2 family members bak and bax are essential for normal development of multiple tissues. Mol Cell *6*, 1389-1399.

Lipardi, C., Wei, Q., and Paterson, B. M. (2001). RNAi as random degradative PCR: siRNA primers convert mRNA into dsRNAs that are degraded to generate new siRNAs. Cell *107*, 297-307.

Liston, P., Roy, N., Tamai, K., Lefebvre, C., Baird, S., Cherton-Horvat, G., Farahani, R., McLean, M., Ikeda, J. E., MacKenzie, A., and Korneluk, R. G. (1996). Suppression of apoptosis in mammalian cells by NAIP and a related family of IAP genes. Nature *379*, 349-353.

Liston, P., Fong, W. G., and Korneluk, R. G. (2003). The inhibitors of apoptosis: there is more to life than Bcl2. Oncogene *22*, 8568-8580.

Lithgow, T., van Driel, R., Bertram, J. F., and Strasser, A. (1994). The protein product of the oncogene bcl-2 is a component of the nuclear envelope, the endoplasmic reticulum, and the outer mitochondrial membrane. Cell Growth Differ *5*, 411-417.

Liu, Q., Fischer, U., Wang, F., and Dreyfuss, G. (1997). The spinal muscular atrophy disease gene product, SMN, and its associated protein SIP1 are in a complex with spliceosomal snRNP proteins. Cell *90*, 1013-1021.

Liu, X., Kim, C. N., Yang, J., Jemmerson, R., and Wang, X. (1996). Induction of apoptotic program in cell-free extracts: requirement for dATP and cytochrome c. Cell *86*, 147-157.

Liu, Z., Sun, C., Olejniczak, E. T., Meadows, R. P., Betz, S. F., Oost, T., Herrmann, J., Wu, J. C., and Fesik, S. W. (2000). Structural basis for binding of Smac/DIABLO to the XIAP BIR3 domain. Nature *408*, 1004-1008.

Lockshin, R. A., and Williams, C. M. (1965). Programmed cell death. IV. The influence of drugs on the breakdown of the intersegmental muscles of silkmoths. J Insect Physiol *11*, 803-809.

Los, M., Van de Craen, M., Penning, L. C., Schenk, H., Westendorp, M., Baeuerle, P. A., Droge, W., Krammer, P. H., Fiers, W., and Schulze-Osthoff, K. (1995). Requirement of an ICE/CED-3 protease for Fas/APO-1-mediated apoptosis. Nature *375*, 81-83.

Luo, X., Budihardjo, I., Zou, H., Slaughter, C., and Wang, X. (1998). Bid, a Bcl2 interacting protein, mediates cytochrome c release from mitochondria in response to activation of cell surface death receptors. Cell *94*, 481-490.

Mancini, M., Machamer, C. E., Roy, S., Nicholson, D. W., Thornberry, N. A., Casciola-Rosen, L. A., and Rosen, A. (2000). Caspase-2 is localized at the Golgi complex and cleaves golgin-160 during apoptosis. J Cell Biol *149*, 603-612.

Maniatis, T., Sambrook , J. and Fritsch, E.F. (1989) Molecular cloning: A laboratory manual (2^{nd} edition)

Margolin, N., Raybuck, S. A., Wilson, K. P., Chen, W., Fox, T., Gu, Y., and Livingston, D. J. (1997). Substrate and inhibitor specificity of interleukin-1 beta-converting enzyme and related caspases. J Biol Chem *272*, 7223-7228.

Marsden, V. S., O'Connor, L., O'Reilly, L. A., Silke, J., Metcalf, D., Ekert, P. G., Huang, D. C., Cecconi, F., Kuida, K., Tomaselli, K. J., *et al.* (2002). Apoptosis initiated by Bcl-2-regulated caspase activation independently of the cytochrome c/Apaf-1/caspase-9 apoptosome. Nature *419*, 634-637.

Martin, D. A., Zheng, L., Siegel, R. M., Huang, B., Fisher, G. H., Wang, J., Jackson, C. E., Puck, J. M., Dale, J., Straus, S. E., *et al.* (1999). Defective CD95/APO-1/Fas signal complex formation in the human autoimmune lymphoproliferative syndrome, type Ia. Proc Natl Acad Sci U S A *96*, 4552-4557.

Martin, S. J., O'Brien, G. A., Nishioka, W. K., McGahon, A. J., Mahboubi, A., Saido, T. C., and Green, D. R. (1995). Proteolysis of fodrin (non-erythroid spectrin) during apoptosis. J Biol Chem *270*, 6425-6428.

Martins, L. M. (2002a). The serine protease Omi/HtrA2: a second mammalian protein with a Reaper-like function. Cell Death Differ *9*, 699-701.

Martins, L. M., Iaccarino, I., Tenev, T., Gschmeissner, S., Totty, N. F., Lemoine, N. R., Savopoulos, J., Gray, C. W., Creasy, C. L., Dingwall, C., and Downward, J. (2002b). The serine protease Omi/HtrA2 regulates apoptosis by binding XIAP through a reaper-like motif. J Biol Chem *277*, 439-444.

McCall, K., and Steller, H. (1998). Requirement for DCP-1 caspase during *Drosophila* oogenesis. Science *279*, 230-234.

Meier, P., Silke, J., Leevers, S. J., and Evan, G. I. (2000). The *Drosophila* caspase DRONC is regulated by DIAP1. EMBO J *19*, 598-611.

Mikhailov, V., Mikhailova, M., Pulkrabek, D. J., Dong, Z., Venkatachalam, M. A., and Saikumar, P. (2001). Bcl-2 prevents Bax oligomerization in the mitochondrial outer membrane. J Biol Chem *276*, 18361-18374.

Miller, T. M., Moulder, K. L., Knudson, C. M., Creedon, D. J., Deshmukh, M., Korsmeyer, S. J., and Johnson, E. M., Jr. (1997). Bax deletion further orders the cell death pathway in cerebellar granule cells and suggests a caspase-independent pathway to cell death. J Cell Biol *139*, 205-217.

Miura, M., Friedlander, R. M., and Yuan, J. (1995). Tumor necrosis factor-induced apoptosis is mediated by a CrmA-sensitive cell death pathway. Proc Natl Acad Sci U S A *92*, 8318-8322.

Moreno, E., Yan, M., and Basler, K. (2002). Evolution of TNF signaling mechanisms: JNK-dependent apoptosis triggered by Eiger, the *Drosophila* homolog of the TNF superfamily. Curr Biol *12*, 1263-1268.

Motoyama, N., Wang, F., Roth, K. A., Sawa, H., Nakayama, K., Negishi, I., Senju, S., Zhang, Q., Fujii, S., and et al. (1995). Massive cell death of immature hematopoietic cells and neurons in Bcl-x-deficient mice. Science *267*, 1506-1510.

Muro, I., Hay, B. A., and Clem, R. J. (2002). The *Drosophila* DIAP1 protein is required to prevent accumulation of a continuously generated, processed form of the apical caspase DRONC. J Biol Chem *277*, 49644-49650.

Murphy, K. M., Ranganathan, V., Farnsworth, M. L., Kavallaris, M., and Lock, R. B. (2000). Bcl-2 inhibits Bax translocation from cytosol to mitochondria during drug-induced apoptosis of human tumor cells. Cell Death Differ *7*, 102-111.

Muzio, M., Chinnaiyan, A. M., Kischkel, F. C., O'Rourke, K., Shevchenko, A., Ni, J., Scaffidi, C., Bretz, J. D., Zhang, M., Gentz, R., *et al.* (1996). FLICE, a novel FADD-homologous ICE/CED-3-like protease, is recruited to the CD95 (Fas/APO-1) death--inducing signaling complex. Cell *85*, 817-827.

Myers, E. W., Sutton, G. G., Delcher, A. L., Dew, I. M., Fasulo, D. P., Flanigan, M. J., Kravitz, S. A., Mobarry, C. M., Reinert, K. H., Remington, K. A., *et al.* (2000). A whole-genome assembly of *Drosophila*. Science *287*, 2196-2204.

Nakagawa, T., Zhu, H., Morishima, N., Li, E., Xu, J., Yankner, B. A., and Yuan, J. (2000). Caspase-12 mediates endoplasmic-reticulum-specific apoptosis and cytotoxicity by amyloid-beta. Nature *403*, 98-103.

Nakano, K., and Vousden, K. H. (2001). PUMA, a novel proapoptotic gene, is induced by p53. Mol Cell *7*, 683-694.

Nechushtan, A., Smith, C. L., Hsu, Y. T., and Youle, R. J. (1999). Conformation of the Bax C-terminus regulates subcellular location and cell death. EMBO J *18*, 2330-2341.

Nechushtan, A., Smith, C. L., Lamensdorf, I., Yoon, S. H., and Youle, R. J. (2001). Bax and Bak coalesce into novel mitochondria-associated clusters during apoptosis. J Cell Biol *153*, 1265-1276.

Nicholson, D. W. (1999). Caspase structure, proteolytic substrates, and function during apoptotic cell death. Cell Death Differ *6*, 1028-1042.

Obata, T., Yaffe, M. B., Leparc, G. G., Piro, E. T., Maegawa, H., Kashiwagi, A., Kikkawa, R., and Cantley, L. C. (2000). Peptide and protein library screening defines optimal substrate motifs for AKT/PKB. J Biol Chem *275*, 36108-36115.

Oda, E., Ohki, R., Murasawa, H., Nemoto, J., Shibue, T., Yamashita, T., Tokino, T., Taniguchi, T., and Tanaka, N. (2000). Noxa, a BH3-only member of the Bcl-2 family and candidate mediator of p53-induced apoptosis. Science *288*, 1053-1058.

Oeda, E., Oka, Y., Miyazono, K., and Kawabata, M. (1998). Interaction of *Drosophila* inhibitors of apoptosis with thick veins, a type I serine/threonine kinase receptor for decapentaplegic. J Biol Chem *273*, 9353-9356.

Okada, H., Suh, W. K., Jin, J., Woo, M., Du, C., Elia, A., Duncan, G. S., Wakeham, A., Itie, A., Lowe, S. W., *et al.* (2002). Generation and characterization of Smac/DIABLO-deficient mice. Mol Cell Biol *22*, 3509-3517.

Orrell, R. W., Habgood, J. J., de Belleroche, J. S., and Lane, R. J. (1997). The relationship of spinal muscular atrophy to motor neuron disease: investigation of SMN and NAIP gene deletions in sporadic and familial ALS. J Neurol Sci *145*, 55-61.

Paroni, G., Henderson, C., Schneider, C., and Brancolini, C. (2002). Caspase-2 can trigger cytochrome c release and apoptosis from the nucleus. J Biol Chem *277*, 15147-15161.

Perez, G. I., Robles, R., Knudson, C. M., Flaws, J. A., Korsmeyer, S. J., and Tilly, J. L. (1999). Prolongation of ovarian lifespan into advanced chronological age by Bax-deficiency. Nat Genet *21*, 200-203.

Peterson, C., Carney, G. E., Taylor, B. J., and White, K. (2002). reaper is required for neuroblast apoptosis during *Drosophila* development. Development *129*, 1467-1476.

Peterson, J. S., Barkett, M., and McCall, K. (2003). Stage-specific regulation of caspase activity in *Drosophila* oogenesis. Dev Biol *260*, 113-123.

Petros, A. M., Medek, A., Nettesheim, D. G., Kim, D. H., Yoon, H. S., Swift, K., Matayoshi, E. D., Oltersdorf, T., and Fesik, S. W. (2001). Solution structure of the antiapoptotic protein Bcl-2. Proc Natl Acad Sci U S A *98*, 3012-3017.

Print, C. G., Loveland, K. L., Gibson, L., Meehan, T., Stylianou, A., Wreford, N., de Kretser, D., Metcalf, D., Kontgen, F., Adams, J. M., and Cory, S. (1998). Apoptosis regulator bcl-w is essential for spermatogenesis but appears otherwise redundant. Proc Natl Acad Sci U S A *95*, 12424-12431.

Pronk, G. J., Ramer, K., Amiri, P., and Williams, L. T. (1996). Requirement of an ICE-like protease for induction of apoptosis and ceramide generation by REAPER. Science *271*, 808-810.

Puthalakath, H., Huang, D. C., O'Reilly, L. A., King, S. M., and Strasser, A. (1999). The proapoptotic activity of the Bcl-2 family member Bim is regulated by interaction with the dynein motor complex. Mol Cell *3*, 287-296.

Puthalakath, H., Villunger, A., O'Reilly, L. A., Beaumont, J. G., Coultas, L., Cheney, R. E., Huang, D. C., and Strasser, A. (2001). Bmf: a proapoptotic BH3-only protein regulated by interaction with the myosin V actin motor complex, activated by anoikis. Science *293*, 1829-1832.

Richardson, H., O'Keefe, L.V., Marty, T. and Saint, R. (1995) Ectopic cyclin E expression induces premature entry into S phase and disrupts pattern formation in the *Drosophila* eye imaginal disc. Development *121*, 3371-79

Puthalakath, H., and Strasser, A. (2002). Keeping killers on a tight leash: transcriptional and post-translational control of the proapoptotic activity of BH3-only proteins. Cell Death Differ *9*, 505-512.

Qin, H., Srinivasula, S. M., Wu, G., Fernandes-Alnemri, T., Alnemri, E. S., and Shi, Y. (1999). Structural basis of procaspase-9 recruitment by the apoptotic protease-activating factor 1. Nature *399*, 549-557.

Quinn, L. M., Dorstyn, L., Mills, K., Colussi, P. A., Chen, P., Coombe, M., Abrams, J., Kumar, S., and Richardson, H. (2000). An essential role for the caspase DRONC in developmentally programmed cell death in *Drosophila*. J Biol Chem *275*, 40416-40424.

Quinn, L., Coombe, M., Mills, K., Daish, T., Colussi, P., Kumar, S., and Richardson, H. (2003). Buffy, a *Drosophila* Bcl-2 protein, has anti-apoptotic and cell cycle inhibitory functions. EMBO J *22*, 3568-3579.

Ray, C. A., Black, R. A., Kronheim, S. R., Greenstreet, T. A., Sleath, P. R., Salvesen, G. S., and Pickup, D. J. (1992). Viral inhibition of inflammation: cowpox virus encodes an inhibitor of the interleukin-1 beta converting enzyme. Cell *69*, 597-604.

Rechsteiner, M., and Rogers, S. W. (1996). PEST sequences and regulation by proteolysis. Trends Biochem Sci *21*, 267-271.

Renatus, M., Zhou, Q., Stennicke, H. R., Snipas, S. J., Turk, D., Bankston, L. A., Liddington, R. C., and Salvesen, G. S. (2000). Crystal structure of the apoptotic suppressor CrmA in its cleaved form. Structure Fold Des *8*, 789-797.

Richter, B. W., Mir, S. S., Eiben, L. J., Lewis, J., Reffey, S. B., Frattini, A., Tian, L., Frank, S., Youle, R. J., Nelson, D. L., *et al.* (2001). Molecular cloning of ILP-2, a novel member of the inhibitor of apoptosis protein family. Mol Cell Biol *21*, 4292-4301.

Riedl, S. J., Renatus, M., Snipas, S. J., and Salvesen, G. S. (2001). Mechanism-based inactivation of caspases by the apoptotic suppressor p35. Biochemistry *40*, 13274-13280.

Rinkenberger, J. L., Horning, S., Klocke, B., Roth, K., and Korsmeyer, S. J. (2000). Mcl-1 deficiency results in peri-implantation embryonic lethality. Genes Dev *14*, 23-27.

Robertson, J. D., Enoksson, M., Suomela, M., Zhivotovsky, B., and Orrenius, S. (2002). Caspase-2 acts upstream of mitochondria to promote cytochrome c release during etoposide-induced apoptosis. J Biol Chem *277*, 29803-29809.

Rodriguez, A., Oliver, H., Zou, H., Chen, P., Wang, X., and Abrams, J. M. (1999). Dark is a *Drosophila* homologue of Apaf-1/CED-4 and functions in an evolutionarily conserved death pathway. Nat Cell Biol *1*, 272-279.

Rodriguez, A., Chen, P., Oliver, H., and Abrams, J. M. (2002). Unrestrained caspase-dependent cell death caused by loss of Diap1 function requires the *Drosophila* Apaf-1 homolog, Dark. EMBO J *21*, 2189-2197.

Ross, A. J., Waymire, K. G., Moss, J. E., Parlow, A. F., Skinner, M. K., Russell, L. D., and MacGregor, G. R. (1998). Testicular degeneration in Bcl-w-deficient mice. Nat Genet *18*, 251-256.

Rothe, M., Pan, M. G., Henzel, W. J., Ayres, T. M., and Goeddel, D. V. (1995). The TNFR2-TRAF signaling complex contains two novel proteins related to baculoviral inhibitor of apoptosis proteins. Cell *83*, 1243-1252.

Roucou, X., Montessuit, S., Antonsson, B., and Martinou, J. C. (2002a). Bax oligomerization in mitochondrial membranes requires tBid (caspase-8-cleaved Bid) and a mitochondrial protein. Biochem J *368*, 915-921.

Roucou, X., Rostovtseva, T., Montessuit, S., Martinou, J. C., and Antonsson, B. (2002b). Bid induces cytochrome c-impermeable Bax channels in liposomes. Biochem J *363*, 547-552.

Roy, N., Mahadevan, M. S., McLean, M., Shutler, G., Yaraghi, Z., Farahani, R., Baird, S., Besner-Johnston, A., Lefebvre, C., Kang, X., and et al. (1995). The gene for neuronal apoptosis inhibitory protein is partially deleted in individuals with spinal muscular atrophy. Cell *80*, 167-178.

Roy, N., Deveraux, Q. L., Takahashi, R., Salvesen, G. S., and Reed, J. C. (1997). The c-IAP-1 and c-IAP-2 proteins are direct inhibitors of specific caspases. EMBO J *16*, 6914-6925.

Rubin, G. M., Yandell, M. D., Wortman, J. R., Gabor Miklos, G. L., Nelson, C. R., Hariharan, I. K., Fortini, M. E., Li, P. W., Apweiler, R., Fleischmann, W., *et al.* (2000). Comparative genomics of the eukaryotes. Science *287*, 2204-2215.

Rudner, J., Lepple-Wienhues, A., Budach, W., Berschauer, J., Friedrich, B., Wesselborg, S., Schulze-Osthoff, K., and Belka, C. (2001). Wild-type, mitochondrial and ER-restricted Bcl-2 inhibit DNA damage-induced apoptosis but do not affect death receptor-induced apoptosis. J Cell Sci *114*, 4161-4172.

Rusconi, J. C., Hays, R., and Cagan, R. L. (2000). Programmed cell death and patterning in *Drosophila*. Cell Death Differ *7*, 1063-1070.

Ryoo, H. D., Bergmann, A., Gonen, H., Ciechanover, A., and Steller, H. (2002). Regulation of *Drosophila* IAP1 degradation and apoptosis by reaper and ubcD1. Nat Cell Biol *4*, 432-438.

Saito, M., Korsmeyer, S. J., and Schlesinger, P. H. (2000). BAX-dependent transport of cytochrome c reconstituted in pure liposomes. Nat Cell Biol *2*, 553-555.

Sax, J. K., Fei, P., Murphy, M. E., Bernhard, E., Korsmeyer, S. J., and El-Deiry, W. S. (2002). BID regulation by p53 contributes to chemosensitivity. Nat Cell Biol *4*, 842-849.

Scanga, S. E., Ruel, L., Binari, R. C., Snow, B., Stambolic, V., Bouchard, D., Peters, M., Calvieri, B., Mak, T. W., Woodgett, J. R., and Manoukian, A. S. (2000). The conserved PI3'K/PTEN/Akt signaling pathway regulates both cell size and survival in *Drosophila*. Oncogene *19*, 3971-3977.

Schinzel, A., Kaufmann, T., and Borner, C. (2004). Bcl-2 family members: intracellular targeting, membrane-insertion, and changes in subcellular localization. Biochim Biophys Acta *1644*, 95-105.

Schneider, I. (1972). Cell lines derived from late embryonic stages of *Drosophila melanogaster*. J Embryol Exp Morphol *27*, 353-365.

Seshagiri, S., and Miller, L. K. (1997). *Caenorhabditis elegans* CED-4 stimulates CED-3 processing and CED-3-induced apoptosis. Curr Biol *7*, 455-460.

Shaham, S., and Horvitz, H. R. (1996). An alternatively spliced *C. elegans ced-4* RNA encodes a novel cell death inhibitor. Cell *86*, 201-208.

Shearwin-Whyatt, L., Baliga, B., Doumanis, J., and Kumar, S. (2001). Chimeric caspase molecules with potent cell killing activity in apoptosis-resistant cells. Biochem Biophys Res Commun *282*, 1114-1119.

Shimizu, S., Narita, M., and Tsujimoto, Y. (1999). Bcl-2 family proteins regulate the release of apoptogenic cytochrome c by the mitochondrial channel VDAC. Nature *399*, 483-487.

Shimizu, S., Matsuoka, Y., Shinohara, Y., Yoneda, Y., and Tsujimoto, Y. (2001). Essential role of voltage-dependent anion channel in various forms of apoptosis in mammalian cells. J Cell Biol *152*, 237-250.

Shinjyo, T., Kuribara, R., Inukai, T., Hosoi, H., Kinoshita, T., Miyajima, A., Houghton, P. J., Look, A. T., Ozawa, K., and Inaba, T. (2001). Downregulation of Bim, a proapoptotic relative of Bcl-2, is a pivotal step in cytokine-initiated survival signaling in murine hematopoietic progenitors. Mol Cell Biol *21*, 854-864.

Shiozaki, E. N., Chai, J., Rigotti, D. J., Riedl, S. J., Li, P., Srinivasula, S. M., Alnemri, E. S., Fairman, R., and Shi, Y. (2003). Mechanism of XIAP-mediated inhibition of caspase-9. Mol Cell *11*, 519-527.

Silke, J., and Vaux, D. L. (2001). Two kinds of BIR-containing protein - inhibitors of apoptosis, or required for mitosis. J Cell Sci *114*, 1821-1827.

Song, Z., McCall, K., and Steller, H. (1997). DCP-1, a *Drosophila* cell death protease essential for development. Science *275*, 536-540.

Spector, M. S., Desnoyers, S., Hoeppner, D. J., and Hengartner, M. O. (1997). Interaction between the *C. elegans* cell-death regulators CED-9 and CED-4. Nature *385*, 653-656.

Spiess, C., Beil, A., and Ehrmann, M. (1999). A temperature-dependent switch from chaperone to protease in a widely conserved heat shock protein. Cell *97*, 339-347.

Sprick, M. R., Weigand, M. A., Rieser, E., Rauch, C. T., Juo, P., Blenis, J., Krammer, P. H., and Walczak, H. (2000). FADD/MORT1 and caspase-8 are recruited to TRAIL receptors 1 and 2 and are essential for apoptosis mediated by TRAIL receptor 2. Immunity *12*, 599-609.

Srinivasula, S. M., Ahmad, M., Fernandes-Alnemri, T., and Alnemri, E. S. (1998). Autoactivation of procaspase-9 by Apaf-1-mediated oligomerization. Mol Cell *1*, 949-957.

Srinivasula, S. M., Hegde, R., Saleh, A., Datta, P., Shiozaki, E., Chai, J., Lee, R. A., Robbins, P. D., Fernandes-Alnemri, T., Shi, Y., and Alnemri, E. S. (2001). A conserved XIAP-interaction motif in caspase-9 and Smac/DIABLO regulates caspase activity and apoptosis. Nature *410*, 112-116.

Srinivasula, S. M., Datta, P., Kobayashi, M., Wu, J. W., Fujioka, M., Hegde, R., Zhang, Z., Mukattash, R., Fernandes-Alnemri, T., Shi, Y., *et al.* (2002). sickle, a novel *Drosophila* death gene in the reaper/hid/grim region, encodes an IAP-inhibitory protein. Curr Biol *12*, 125-130.

Staveley, B. E., Ruel, L., Jin, J., Stambolic, V., Mastronardi, F. G., Heitzler, P., Woodgett, J. R., and Manoukian, A. S. (1998). Genetic analysis of protein kinase B (AKT) in *Drosophila*. Curr Biol *8*, 599-602.

Stennicke, H. R., and Salvesen, G. S. (1999). Catalytic properties of the caspases. Cell Death Differ *6*, 1054-1059.

Sulston, J. E., and Horvitz, H. R. (1977). Post-embryonic cell lineages of the nematode, *Caenorhabditis elegans*. Dev Biol *56*, 110-156.

Sun, C., Cai, M., Meadows, R. P., Xu, N., Gunasekera, A. H., Herrmann, J., Wu, J. C., and Fesik, S. W. (2000). NMR structure and mutagenesis of the third BIR domain of the inhibitor of apoptosis protein XIAP. J Biol Chem *275*, 33777-33781.

Suzuki, M., Youle, R. J., and Tjandra, N. (2000). Structure of Bax: coregulation of dimer formation and intracellular localization. Cell *103*, 645-654.

Suzuki, Y., Imai, Y., Nakayama, H., Takahashi, K., Takio, K., and Takahashi, R. (2001a). A serine protease, HtrA2, is released from the mitochondria and interacts with XIAP, inducing cell death. Mol Cell *8*, 613-621.

Suzuki, Y., Nakabayashi, Y., Nakata, K., Reed, J. C., and Takahashi, R. (2001b). X-linked inhibitor of apoptosis protein (XIAP) inhibits caspase-3 and -7 in distinct modes. J Biol Chem *276*, 27058-27063.

Takahashi, R., Deveraux, Q., Tamm, I., Welsh, K., Assa-Munt, N., Salvesen, G. S., and Reed, J. C. (1998). A single BIR domain of XIAP sufficient for inhibiting caspases. J Biol Chem *273*, 7787-7790.

Talanian, R. V., Quinlan, C., Trautz, S., Hackett, M. C., Mankovich, J. A., Banach, D., Ghayur, T., Brady, K. D., and Wong, W. W. (1997). Substrate specificities of caspase family proteases. J Biol Chem *272*, 9677-9682.

Tenev, T., Zachariou, A., Wilson, R., Paul, A., and Meier, P. (2002). Jafrac2 is an IAP antagonist that promotes cell death by liberating Dronc from DIAP1. EMBO J *21*, 5118-5129.

Testa, J. R., and Bellacosa, A. (2001). AKT plays a central role in tumorigenesis. Proc Natl Acad Sci U S A *98*, 10983-10985.

Thome, M., Schneider, P., Hofmann, K., Fickenscher, H., Meinl, E., Neipel, F., Mattmann, C., Burns, K., Bodmer, J. L., Schroter, M., *et al.* (1997). Viral FLICE-inhibitory proteins (FLIPs) prevent apoptosis induced by death receptors. Nature *386*, 517-521.

Thornberry, N. A., Bull, H. G., Calaycay, J. R., Chapman, K. T., Howard, A. D., Kostura, M. J., Miller, D. K., Molineaux, S. M., Weidner, J. R., Aunins, J., and et al. (1992). A novel heterodimeric cysteine protease is required for interleukin-1 beta processing in monocytes. Nature *356*, 768-774.

Thornberry, N. A., Rano, T. A., Peterson, E. P., Rasper, D. M., Timkey, T., Garcia-Calvo, M., Houtzager, V. M., Nordstrom, P. A., Roy, S., Vaillancourt, J. P., *et al.* (1997). A combinatorial approach defines specificities of members of the caspase family and granzyme B. Functional relationships established for key mediators of apoptosis. J Biol Chem *272*, 17907-17911.

Thornberry, N. A., and Lazebnik, Y. (1998). Caspases: enemies within. Science *281*, 1312-1316.

Tibbetts, M. D., Zheng, L., and Lenardo, M. J. (2003). The death effector domain protein family: regulators of cellular homeostasis. Nat Immunol *4*, 404-409.

Travers, K. J., Patil, C. K., Wodicka, L., Lockhart, D. J., Weissman, J. S., and Walter, P. (2000). Functional and genomic analyses reveal an essential coordination between the unfolded protein response and ER-associated degradation. Cell *101*, 249-258.

Tschopp, J., Thome, M., Hofmann, K., and Meinl, E. (1998). The fight of viruses against apoptosis. Curr Opin Genet Dev *8*, 82-87.

Tsujimoto, Y., Finger, L. R., Yunis, J., Nowell, P. C., and Croce, C. M. (1984). Cloning of the chromosome breakpoint of neoplastic B cells with the t(14;18) chromosome translocation. Science *226*, 1097-1099.

Tsujimoto, Y. (1989). Stress-resistance conferred by high level bcl-2α protein in human B lymphoblastoid cell. Oncogene *4*, 1331-1336

Ui-Tei, K., Nagano, M., Sato, S., and Miyata, Y. (2000). Calmodulin-dependent and -independent apoptosis in cell of a *Drosophila* neuronal cell line. Apoptosis *5*, 133-140.

Uren, A. G., Pakusch, M., Hawkins, C. J., Puls, K. L., and Vaux, D. L. (1996). Cloning and expression of apoptosis inhibitory protein homologs that function to inhibit apoptosis and/or bind tumor necrosis factor receptor-associated factors. Proc Natl Acad Sci U S A *93*, 4974-4978.

Uren, A. G., Beilharz, T., O'Connell, M. J., Bugg, S. J., van Driel, R., Vaux, D. L., and Lithgow, T. (1999). Role for yeast inhibitor of apoptosis (IAP)-like proteins in cell division. Proc Natl Acad Sci U S A *96*, 10170-10175.

Utz, P. J., and Anderson, P. (2000). Life and death decisions: regulation of apoptosis by proteolysis of signaling molecules. Cell Death Differ *7*, 589-602.

van Loo, G., Saelens, X., van Gurp, M., MacFarlane, M., Martin, S. J., and Vandenabeele, P. (2002). The role of mitochondrial factors in apoptosis: a Russian roulette with more than one bullet. Cell Death Differ *9*, 1031-1042.

van Gurp, M., Festjens, N., van Loo, G., Saelens, X., and Vandenabeele, P. (2003). Mitochondrial intermembrane proteins in cell death. Biochem Biophys Res Commun *304*, 487-497.

Varfolomeev, E. E., Schuchmann, M., Luria, V., Chiannilkulchai, N., Beckmann, J. S., Mett, I. L., Rebrikov, D., Brodianski, V. M., Kemper, O. C., Kollet, O., *et al.* (1998). Targeted disruption of the mouse Caspase 8 gene ablates cell death induction by the TNF receptors, Fas/Apo1, and DR3 and is lethal prenatally. Immunity *9*, 267-276.

Varshavsky, A. (2003). The N-end rule and regulation of apoptosis. Nat Cell Biol *5*, 373-376.

Vaux, D. L., Cory, S., and Adams, J. M. (1988). Bcl-2 gene promotes haemopoietic cell survival and cooperates with c-myc to immortalize pre-B cells. Nature *335*, 440-442.

Vaux, D. L., Weissman, I. L., and Kim, S. K. (1992). Prevention of programmed cell death in *Caenorhabditis elegans* by human bcl-2. Science *258*, 1955-1957.

Vaux, D. L. (1993). Toward an understanding of the molecular mechanisms of physiological cell death. Proc Natl Acad Sci U S A *90*, 786-789.

Veis, D. J., Sorenson, C. M., Shutter, J. R., and Korsmeyer, S. J. (1993). Bcl-2-deficient mice demonstrate fulminant lymphoid apoptosis, polycystic kidneys, and hypopigmented hair. Cell *75*, 229-240.

Verdu, J., Buratovich, M. A., Wilder, E. L., and Birnbaum, M. J. (1999). Cell-autonomous regulation of cell and organ growth in *Drosophila* by Akt/PKB. Nat Cell Biol *1*, 500-506.

Verhagen, A. M., Ekert, P. G., Pakusch, M., Silke, J., Connolly, L. M., Reid, G. E., Moritz, R. L., Simpson, R. J., and Vaux, D. L. (2000). Identification of DIABLO, a mammalian protein that promotes apoptosis by binding to and antagonizing IAP proteins. Cell *102*, 43-53.

Verhagen, A. M., Coulson, E. J., and Vaux, D. L. (2001). Inhibitor of apoptosis proteins and their relatives: IAPs and other BIRPs. Genome Biol *2*, REVIEWS3009.

Verhagen, A. M., and Vaux, D. L. (2002). Cell death regulation by the mammalian IAP antagonist Diablo/Smac. Apoptosis *7*, 163-166.

Vernooy, S. Y., Chow, V., Su, J., Verbrugghe, K., Yang, J., Cole, S., Olson, M. R., and Hay, B. A. (2002). *Drosophila* Bruce can potently suppress Rpr- and Grim-dependent but not Hid-dependent cell death. Curr Biol *12*, 1164-1168.

Vogt, C. (1842) Sdothum: Jent and Gassman, 130

Vucic, D., Kaiser, W. J., Harvey, A. J., and Miller, L. K. (1997). Inhibition of reaper-induced apoptosis by interaction with inhibitor of apoptosis proteins (IAPs). Proc Natl Acad Sci U S A *94*, 10183-10188.

Vucic, D., Kaiser, W. J., and Miller, L. K. (1998). Inhibitor of apoptosis proteins physically interact with and block apoptosis induced by *Drosophila* proteins HID and GRIM. Mol Cell Biol *18*, 3300-3309.

Vucic, D., Stennicke, H. R., Pisabarro, M. T., Salvesen, G. S., and Dixit, V. M. (2000). ML-IAP, a novel inhibitor of apoptosis that is preferentially expressed in human melanomas. Curr Biol *10*, 1359-1366.

Walton, M. I., Whysong, D., O'Connor, P. M., Hockenbery, D., Korsmeyer, S. J., and Kohn, K. W. (1993). Constitutive expression of human Bcl-2 modulates nitrogen mustard and camptothecin induced apoptosis. Cancer Res *53*, 1853-1861.

Wang, H. G., Pathan, N., Ethell, I. M., Krajewski, S., Yamaguchi, Y., Shibasaki, F., McKeon, F., Bobo, T., Franke, T. F., and Reed, J. C. (1999). Ca2+-induced apoptosis through calcineurin dephosphorylation of BAD. Science *284*, 339-343.

Wang, S. L., Hawkins, C. J., Yoo, S. J., Muller, H. A., and Hay, B. A. (1999). The *Drosophila* caspase inhibitor DIAP1 is essential for cell survival and is negatively regulated by HID. Cell *98*, 453-463.

Weber, C. H., and Vincenz, C. (2001). The death domain superfamily: a tale of two interfaces? Trends Biochem Sci *26*, 475-481.

Wei, M. C., Lindsten, T., Mootha, V. K., Weiler, S., Gross, A., Ashiya, M., Thompson, C. B., and Korsmeyer, S. J. (2000). tBID, a membrane-targeted death ligand, oligomerizes BAK to release cytochrome c. Genes Dev *14*, 2060-2071.

Wei, M. C., Zong, W. X., Cheng, E. H., Lindsten, T., Panoutsakopoulou, V., Ross, A. J., Roth, K. A., MacGregor, G. R., Thompson, C. B., and Korsmeyer, S. J. (2001). Proapoptotic BAX and BAK: a requisite gateway to mitochondrial dysfunction and death. Science *292*, 727-730.

White, K., Grether, M. E., Abrams, J. M., Young, L., Farrell, K., and Steller, H. (1994). Genetic control of programmed cell death in *Drosophila*. Science *264*, 677-683.

White, K., Tahaoglu, E., and Steller, H. (1996). Cell killing by the *Drosophila* gene *reaper*. Science *271*, 805-807.

White, F. A., Keller-Peck, C. R., Knudson, C. M., Korsmeyer, S. J., and Snider, W. D. (1998). Widespread elimination of naturally occurring neuronal death in Bax-deficient mice. J Neurosci *18*, 1428-1439.

Wilson, R., Goyal, L., Ditzel, M., Zachariou, A., Baker, D. A., Agapite, J., Steller, H., and Meier, P. (2002). The DIAP1 RING finger mediates ubiquitination of DRONC and is indispensable for regulating apoptosis. Nat Cell Biol *4*, 445-450.

Wing, J. P., Zhou, L., Schwartz, L. M., and Nambu, *J. R. (1998).* Distinct cell killing properties of the *Drosophila reaper, head involution defective*, and *grim* genes. Cell Death Differ *5*, 930-939.

Wing, J. P., Karres, J. S., Ogdahl, J. L., Zhou, L., Schwartz, L. M., and Nambu, J. R. (2002a). *Drosophila* sickle is a novel grim-reaper cell death activator. Curr Biol *12*, 131-135.

Wing, J. P., Schreader, B. A., Yokokura, T., Wang, Y., Andrews, P. S., Huseinovic, N., Dong, C. K., Ogdahl, J. L., Schwartz, L. M., White, K., and Nambu, J. R. (2002b). *Drosophila* Morgue is an F box/ubiquitin conjugase domain protein important for grim-reaper mediated apoptosis. Nat Cell Biol *4*, 451-456.

Wu, D., Wallen, H. D., and Nunez, G. (1997). Interaction and regulation of subcellular localization of CED-4 by CED-9. Science *275*, 1126-1129.

Wu, G., Chai, J., Suber, T. L., Wu, J. W., Du, C., Wang, X., and Shi, Y. (2000). Structural basis of IAP recognition by Smac/DIABLO. Nature *408*, 1008-1012.

Wu, J. W., Cocina, A. E., Chai, J., Hay, B. A., and Shi, Y. (2001). Structural analysis of a functional DIAP1 fragment bound to grim and hid peptides. Mol Cell *8*, 95-104.

Wyllie, A. H., Kerr, J. F., and Currie, A. R. (1980). Cell death: the significance of apoptosis. Int Rev Cytol *68*, 251-306.

Xu, G., Cirilli, M., Huang, Y., Rich, R. L., Myszka, D. G., and Wu, H. (2001). Covalent inhibition revealed by the crystal structure of the caspase-8/p35 complex. Nature *410*, 494-497.

Xue, D., Shaham, S., and Horvitz, H. R. (1996). The *Caenorhabditis elegans* cell-death protein CED-3 is a cysteine protease with substrate specificities similar to those of the human CPP32 protease. Genes Dev *10*, 1073-1083.

Xue, D., and Horvitz, H. R. (1997). *Caenorhabditis elegans* CED-9 protein is a bifunctional cell-death inhibitor. Nature *390*, 305-308.

Yaffe, M. B., Leparc, G. G., Lai, J., Obata, T., Volinia, S., and Cantley, L. C. (2001). A motif-based profile scanning approach for genome-wide prediction of signaling pathways. Nat Biotechnol *19*, 348-353.

Yamaguchi, K., Nagai, S., Ninomiya-Tsuji, J., Nishita, M., Tamai, K., Irie, K., Ueno, N., Nishida, E., Shibuya, H., and Matsumoto, K. (1999). XIAP, a cellular member of the inhibitor of apoptosis protein family, links the receptors to TAB1-TAK1 in the BMP signaling pathway. EMBO J *18*, 179-187.

Yan, N., Wu, J. W., Chai, J., Li, W., and Shi, Y. (2004). Molecular mechanisms of DrICE inhibition by DIAP1 and removal of inhibition by Reaper, Hid and Grim. Nat Struct Mol Biol *11*, 420-428.

Yang, X., Chang, H. Y., and Baltimore, D. (1998). Essential role of CED-4 oligomerization in CED-3 activation and apoptosis. Science *281*, 1355-1357.

Yeh, W. C., Pompa, J. L., McCurrach, M. E., Shu, H. B., Elia, A. J., Shahinian, A., Ng, M., Wakeham, A., Khoo, W., Mitchell, K., *et al.* (1998). FADD: essential for embryo development and signaling from some, but not all, inducers of apoptosis. Science *279*, 1954-1958.

Yeh, W. C., Itie, A., Elia, A. J., Ng, M., Shu, H. B., Wakeham, A., Mirtsos, C., Suzuki, N., Bonnard, M., Goeddel, D. V., and Mak, T. W. (2000). Requirement for Casper (c-FLIP) in regulation of death receptor-induced apoptosis and embryonic development. Immunity *12*, 633-642.

Yoo, S. J., Huh, J. R., Muro, I., Yu, H., Wang, L., Wang, S. L., Feldman, R. M., Clem, R. J., Muller, H. A., and Hay, B. A. (2002). Hid, Rpr and Grim negatively regulate DIAP1 levels through distinct mechanisms. Nat Cell Biol *4*, 416-424.

Yoon, H. J., and Carbon, J. (1999). Participation of Bir1p, a member of the inhibitor of apoptosis family, in yeast chromosome segregation events. Proc Natl Acad Sci U S A *96*, 13208-13213.

Yuan, J., and Horvitz, H. R. (1992). The *Caenorhabditis elegans* cell death gene *ced-4* encodes a novel protein and is expressed during the period of extensive programmed cell death. Development *116*, 309-320.

Yuan, J., Shaham, S., Ledoux, S., Ellis, H. M., and Horvitz, H. R. (1993). The *C. elegans* cell death gene *ced-3* encodes a protein similar to mammalian interleukin-1 beta-converting enzyme. Cell *75*, 641-652.

Zachariou, A., Tenev, T., Goyal, L., Agapite, J., Steller, H., and Meier, P. (2003). IAP-antagonists exhibit non-redundant modes of action through differential DIAP1 binding. EMBO J *22*, 6642-6652.

Zha, J., Harada, H., Yang, E., Jockel, J., and Korsmeyer, S. J. (1996). Serine phosphorylation of death agonist BAD in response to survival factor results in binding to 14-3-3 not BCL-X_L Cell *87*, 619-628.

Zha, J., Harada, H., Osipov, K., Jockel, J., Waksman, G., and Korsmeyer, S. J. (1997). BH3 domain of BAD is required for heterodimerization with BCL-X_L and proapoptotic activity. J Biol Chem *272*, 24101-24104.

Zhang, H., Huang, Q., Ke, N., Matsuyama, S., Hammock, B., Godzik, A., and Reed, J. C. (2000). *Drosophila* proapoptotic Bcl-2/Bax homologue reveals evolutionary conservation of cell death mechanisms. J Biol Chem *275*, 27303-27306.

Zhou, L., Song, Z., Tittel, J., and Steller, H. (1999). HAC-1, a *Drosophila* homolog of APAF-1 and CED-4 functions in developmental and radiation-induced apoptosis. Mol Cell *4*, 745-755.

Zhou, L., and Steller, H. (2003). Distinct pathways mediate UV-induced apoptosis in *Drosophila* embryos. Dev Cell *4*, 599-605.

Zhu, W., Cowie, A., Wasfy, G. W., Penn, L. Z., Leber, B., and Andrews, D. W. (1996). Bcl-2 mutants with restricted subcellular location reveal spatially distinct pathways for apoptosis in different cell types. EMBO J *15*, 4130-4141.

Zimmermann, K. C., Ricci, J. E., Droin, N. M., and Green, D. R. (2002). The role of ARK in stress-induced apoptosis in *Drosophila* cells. J Cell Biol *156*, 1077-1087.

Zong, W. X., Lindsten, T., Ross, A. J., MacGregor, G. R., and Thompson, C. B. (2001). BH3-only proteins that bind prosurvival Bcl-2 family members fail to induce apoptosis in the absence of Bax and Bak. Genes Dev *15*, 1481-1486.

Zou, H., Henzel, W. J., Liu, X., Lutschg, A., and Wang, X. (1997). Apaf-1, a human protein homologous to *C. elegans* CED-4, participates in cytochrome c-dependent activation of caspase-3. Cell *90*, 405-413.

Zou, H., Li, Y., Liu, X., and Wang, X. (1999). An APAF-1.cytochrome c multimeric complex is a functional apoptosome that activates procaspase-9. J Biol Chem *274*, 11549-11556.

Explanatory notes:

Chapter 4 results: Non-transgenic flies have white eyes. Flies carrying transgenic genes are red.

Chapter 3 results: varying levels of processed versus unprocessed STRICA are observed, due to different cell types used and the level of overexpression achieved.

Chapter 5: Processing of BUFFY and/or DEBCL has not been observed, although this possibility remains to be fully investigated and is an attractive hypothesis in the regulation their intracellular localisation and function.